The Biogeochemistry of Radioactively Contaminated Land

A thesis submitted to The University of Manchester for the degree of Doctor of Philosophy in the Faculty of Engineering and Physical Sciences

2012

Clare Louise Thorpe

School of Earth, Atmospheric and Environmental Sciences

Table of contents

List of tables

List of figures

Abbreviations

Abbreviation	Term
DECC	Department of Energy and Climate Change
DOE	Department of Energy
EDAX	Energy Dispersive X-ray Spectroscopy
EPSRC	Engineering and Physical Science Research Council
ESEM	Environmental Scanning Electron Microscope
EXAFS	Extended X-Ray Absorption Fine Structure
IC	Ion Chromatography
ICP-AES	Inductively Coupled Plasma – Atomic Emission Spectroscopy
IAES	International Atomic Energy Agency
INES	International Nuclear and Radiological Events Scale
mM	Millimolar (10^{-3})
µM	Micromolar (10^{-6})
nM	Nanomolar (10^{-9})
NERC	Natural Environmental Research Council
PCR	Polymerase Chain Reaction
16S rRNA	16S Ribosomal Ribonucleic Acid
SEAES	School of Earth, Atmospheric and Environmental Sciences
TEAPs	Terminal Electron Accepting Processes
TEM	Transmission Electron Microscopy
XANES	X-Ray Absorption Near Edge Structure
XAS	X-Ray Absorption Spectroscopy
XRD	X-Ray Diffraction
XRF	X-Ray Fluorescence

Abstract

A global legacy of radioactively contaminated land exists as a result of nuclear fuel cycle operations. Demonstration of the safe management of the UK nuclear legacy, including contaminated land, is important whilst the long term fate of legacy waste remains uncertain and the UK moves towards new nuclear power. One aspect of nuclear contaminated land research focuses on the immobilisation of intermediate and long lived radionuclides that are mobile in groundwater and are migrating in the environment. At Sellafield nuclear facility, UK, strontium-90 and technetium-99 are found as co-contaminants in groundwater alongside the most abundant non radioactive contaminant, nitrate. Their differing radiochemical behaviour and the presence of nitrate presents a challenge for remediation strategies. Bioremediation has the potential for *in-situ* immobilization of ^{99}Tc *via* reduction from mobile Tc(VII) to less mobile Tc(IV) concurrent with Fe(III) reduction. In this project bioreduction processes were investigated in sediment microcosms and model systems under variable pH and nitrate conditions and using microorganisms representative of the Sellafield site.

Sediment bioreduction occurred *via* stimulation of the natural microbial community. Denitrification resulted in a delay in the onset of metal reduction followed by a raised pH. At the mildly acidic pH of the natural sediments, a nitrate concentration of 100 mM caused bioreduction to stall. However, at pH 7, reduction of 100 mM nitrate resulted in a final pH > 9 and alkaline Fe(III) reduction. In bioreduced sediments, the microbial ecology was dominated by nitrate reducing microorganisms and Fe(III) reducing enrichment cultures were necessary to identify relevant alkaline Fe(III) reducing bacteria. Enrichment cultures isolated a novel alkali tolerant Fe(III) reducing *Serratia* sp. with a growth range of pH 4 to 9. Increased pH resulting from denitrification decreased the mobility of Sr^{2+} *via* increased sorption to mineral surfaces. X-ray absorption spectroscopy confirmed Sr^{2+} incorporation into carbonate mineral phases above pH 8.5. Model systems showed reductive removal of ^{99}Tc from solution by an Fe(II) bearing mineral assemblage at both pH 7 and 9. In contrast Sr^{2+} remained in solution at pH 7 and precipitated as $SrCO_3$ at pH > 8.5. This study for the first time demonstrates the effects of high nitrate on pH in Sellafield type sediments, alkaline Fe(III) reduction by a *Serratia* sp, the incorporation behaviour of Sr^{2+} during sediment bioreduction and the behaviour of Sr^{2+} and ^{99}Tc in novel Fe(II) mineral bearing model systems. These findings improve the understanding of radionuclide migration at contaminated sites and inform possible engineered bioremediation scenarios.

Declaration

No portion of the work referred to in the thesis has been submitted in support of an application for another degree or qualification of this or any other university or other institute of learning.

Copyright statement

Acknowledgements

Three and a half years of science has transformed my flowing, if a little meandering, musings into concise, if a little less interesting, scientific text. Here in my acknowledgments I take full advantage of the opportunity to revert to my former ways and use as many superfluous words as I wish.

I would like firstly to acknowledge 'the team' my supervisors Kath Morris, Jon Lloyd and Gareth Law for their leadership, patience and for introducing me to the existence of German steaks, Lancashire towels and custom made beds. I would also like to thank my occasional supervisors Sam Shaw, Ian Burke and all the super efficient technicians, Al Bewsher, Paul Lythgoe, David Ashley, John Waters, Katie Law and Chris Boothman who are the reason my research ran as smoothly as it did. There are too many in the Lloyd/Morris group to name but you know who you are and thanks for the beers, walks and hours listening to absolute 80s radio. I would also like to acknowledge Julian Cruickshank from Sellafield Ltd who, in addition to acquiring samples for me, provided encouragement and a constant reminder of why I started this work in the first place.

For help with data collection I thank the ESRF beamline (B-26) scientists, Sarah Wallace, Chris Hubbard, Adam Williamson, Diana Brookshaw and Jon Fellowes. This work was supported by a studentship from the Engineering and Physical Science Research Council (EPSRC) as part of the Decommissioning, Immobilisation and Management of Nuclear Waste for Disposal (DIAMOND) consortium: grant EP/F055412/1. We also acknowledge the support of the Natural Environment Research Council grant NE/H007768/1.

My parents deserve thanks for loan of their back room, Mum for spell checking and left over food and my Dad (Dr Thorpe the 1st) for supplying me with cups of tea whist warning me off academia. I want to thank my partner James who has the brains but not the attention span to complete a PhD. We've spent the last three and a half years 200 miles apart and I have discovered that my young persons' railcard and plug sockets on trains are both key to a healthy work/relationship balance.

There are also some people whose contribution to this work is more along the lines of 'distraction from' rather than 'help with' but nevertheless want to mention my little brother for attempting to keep chickens in his basement, my friend Tom for the Kinder

beer barrel challenge and other madness, Susi Q for toad in the hole and sane conversations and Dr Colette who makes sure that I am never short of something to look forward to and helps me escape the landlocked streets of Manchester.

For me at least sailing and science have proved complementary and for that reason I need to thank Heinz, Greet and the crew of the *Anna-Margaretha* for taking me on their voyage to Antarctica, *Osprey* and Alan from the British Kiel Yacht Club for getting me safe to St Petersburg complete with mast, Diggory and Liz from *Pegasus*, my crack racing team and friends '*the Captains Daughters*' for following me on each new adventure, Calvyn and the *Black Diamond* for always knowing where the rum is and James, Mark and everyone from the *John Laing* for good times on the 'big red throbber'. Finally, Jonny, Orla and *Pameta*, 80 years old and held together by paint and belief she has been the focus of many office daydreams. Through the final year of my PhD we have been fixing her up, on rare sunny northern evenings, in a yard off the Manchester ship canal and I think it is fitting that finishing this thesis coincides with her being fully seaworthy again and ready to head out to sea.

The Author

The author graduated from the University of Manchester in 2008 with a Masters degree in Earth Sciences (MEarthSci) from the School or Earth Atmospheric and Environmental Sciences and the MacKenzie and Guilford prize for best final mark in Earth Sciences.

Since October 2008 she has been working on the contents of this thesis firstly at the University of Leeds (October 2008- December 2009) and later transferring to the University of Manchester (January 2009 – March 2012).

Chapter 1: Project relevance and thesis structure

1.1 Project context and relevance

Nuclear activities over 70 years have left an extensive legacy of contaminated land around the world. Recent accidental release of radionuclides at the Fukushima nuclear power plant in Japan, 2011, serves as a reminder that this legacy is highly challenging and has the potential to affect society if mismanaged. In the UK, decommissioning of retired nuclear power plants and the onset of new nuclear power puts management of legacy waste at the forefront of political discussions. Solutions to the problems of decontamination and the disposal of legacy waste are a priority for convincing scientists and the public of the safety of new nuclear power. This project concerns contaminated land at nuclear facilities and in particular those radionuclides and non radioactive co-contaminants that are present and mobile in groundwater and therefore migrating through the subsurface. Among the strategies discussed for the immobilization of groundwater radionuclides 'bioremediation' has been widely investigated over the last 15 years (e.g. Lloyd and Macaskie, 1997; Lloyd, 2003; Istok et al., 2004; North et al., 2004; Burke et al., 2005; Lloyd and Renshaw, 2005a, 2005b; Edwards et al., 2007; Renshaw et al., 2007; Law et al., 2010). This project focuses on the role of microorganisms in controlling subsurface geochemical conditions and the mobility of problematic radionuclides. The findings have implications both for understanding the

migration of radionuclides in legacy contaminated land and informing the discussion regarding the migration of radionuclides from a future deep geological disposal facility.

1.2 Research objectives and approach

The objective of this research was to investigate the effect of sediment bioreduction on radioactive and non-radioactive co-contaminants in sediments representative of nuclear legacy sites. A multidisciplinary approach was used to explore the biogeochemistry of sediments representative of those contaminated with key problematic radionuclides ^{99}Tc and ^{90}Sr. Geochemical conditions were varied to address a range of scenarios including low pH, alkalinity and high nitrate concentrations. Past research supports the following hypotheses that form the basis for undertaking this research project:

- Tc(VII) can be immobilized in groundwater *via* reduction to Tc(IV) concurrent with microbial Fe(III) reduction in sediments.
- Elevated nitrate conditions (> 1 mM) can inhibit microbial Fe(III) reduction by competition as a more energetically favourable electron acceptor, especially at low pH where microbial metabolism is challenged.
- Bioreduction can affect sediment pH *via* the release of alkalinity and bicarbonate.
- Sr^{2+} becomes less mobile in sediment with increasing pH due to sorption and precipitation reactions.

Based on previous research the following broad research questions were formulated:

1) What are the effects of high nitrate concentrations on the reduction of metals and radionuclides in sediments with low and circumneutral pH?

2) What effects do changes in geochemistry during sediment bioreduction have on the mobility of non redox active radionuclides such as ^{90}Sr?

3) What are the effects of neutral and alkaline Fe(III) reduction on the mobility of key groundwater radionuclides, ^{99}Tc and Sr^{2+}?

Microcosm experiments were used to investigate bioreduction under a range of environmentally relevant conditions using sediments representative of the UK nuclear facility, Sellafield, and groundwater representative of the Sellafield region. In addition, model Fe(III) reducing systems were established using a microbial consortium enriched from Fe(III) reducing sediment microcosms. The geochemistry of these systems was assessed in detail using a range of analytical techniques including spectrophotometry, X-ray absorption spectroscopy (XAS), ion chromatography (IC), inductively coupled plasma – atomic emission spectroscopy (ICP-AES), X-ray diffraction (XRD), X-ray fluorescence spectroscopy (XRF), environmental scanning electron microscopy (ESEM), liquid scintillation counting (LSC) and sequential extractions. Microbial communities were analysed using molecular techniques (16S rRNA gene analysis).

1.3 Thesis structure

This thesis consists of a general introduction followed by four papers that have been published or prepared for publication and a summary chapter tying together the conclusions that can be drawn from the research. The methods used are more fully explained in appendices along with details of conference presentations relating to the work presented in this thesis.

Chapter 2 contains a general introduction outlining the current legacy of radioactively contaminated land and the biogeochemical processes that are the focus of this project. The main study site, Sellafield, UK, is described followed by an overview of the environmental behaviour of key problematic contaminants: nitrate, ^{90}Sr and ^{99}Tc, and a summary of previous research into biogeochemical processes at nuclear legacy sites. At the end of Chapter 2, the research hypotheses above are discussed in the context of the Sellafield site.

Chapter 3 consists of a paper entitled "The synergistic effects of high nitrate concentrations on sediment bioreduction" published in Geomicrobiology Journal, March, 2012. This work investigates the effect of varying nitrate concentration on bioreduction in acetate amended sediments representative of the Sellafield site. A microcosm approach was used to conduct detailed analysis of the sediment geochemistry and microbiology during bioreduction in the presence of nitrate.

Chapter 4 consists of a paper entitled "Alkaline Fe(III) reduction by a novel alkali-tolerant *Serratia* sp. isolated from surface sediments close to Sellafield nuclear facility, UK" published in FEMS Microbiology Letters, February, 2012. This paper characterises an unusual Fe(III) reducing bacteria isolated from Sellafield sediment and not previously reported as alkali tolerant.

Chapter 5 consists of a paper entitled "Strontium sorption and precipitation behaviour during bioreduction in nitrate impacted sediments" accepted for publication in Chemical Geology, available online March, 2012. This paper investigates the behaviour of Sr^{2+} during sediment bioreduction under varying pH and nitrate concentrations. A microcosm approach is combined with XAS analysis to determine Sr^{2+} speciation in key systems.

Chapter 6 consists of a paper entitled "Interactions of an Fe(III)-reducing microbial consortium with Sr^{2+} and ^{99}Tc under neutral and alkaline conditions" in preparation for submission to Applied Geochemistry in 2012. Here a model mineral system is used to investigate the effects of Fe(III) reduction on the mobility of key problematic radionuclides ^{99}Tc and ^{90}Sr.

Chapter 7 provides a summary of the work prepared for publication and highlights the key findings of this research. In addition, this chapter contains suggestions for future work.

1.4 Paper status and collaborator contributions

The papers presented in this thesis are multiple author contributions due to the multi-disciplinary approaches used to investigate the complex geochemical and microbiological systems. The role of individual authors is clarified below.

Chapter 3: The synergistic effects of high nitrate concentrations on sediment bioreduction, published in Geomicrobiology Journal, March, 2012.

C. L. Thorpe – principal author, performed all experimental work, concept development; K. Morris – initial concept, concept development, extensive manuscript review; G. T. W. Law – concept development, extensive manuscript review; I. T. Burke – concept development; J. R. Lloyd – concept development; C. Boothman – microbiological analysis; D. Ashley – technical assistance (IC); P. Lythgoe – technical assistance (XRF).

Chapter 4: Alkaline Fe(III) reduction by a novel alkali-tolerant *Serratia* sp. isolated from surface sediments close to Sellafield nuclear facility, UK, published in FEMS Microbiology Letters, February, 2012.

C. L. Thorpe – principal author, performed all experimental work, concept development; J. R. Lloyd – initial concept, extensive manuscript review; K. Morris – concept development, extensive manuscript review; C. Boothman – microbiological analysis; J. Waters – technical assistance (XRD).

Chapter 5: Strontium sorption and precipitation behaviour during bioreduction in nitrate impacted sediments, accepted for publication in Chemical Geology, available online March, 2012.

C. L. Thorpe – principal author, performed all experimental work, initial concept, concept development, XAS analysis; K. Morris – initial concept, concept development, extensive manuscript review; G. T. W. Law – concept development, manuscript review; I. T. Burke – concept development, aided XAS analysis, manuscript review; S. Shaw – concept development, aided XAS analysis, manuscript review; J. R. Lloyd – concept development, manuscript review; N.D. Bryan – assistance with geochemical modelling; P. Lythgoe – technical assistance (ICP-AES; XRF); A. Bewsher – technical assistance (IC); J. Waters – technical assistance (XRD); J. Fellows – technical assistance (ESEM).

Chapter 6: Interactions of an Fe(III)-reducing microbial consortium with Sr^{2+} and ^{99}Tc under neutral and alkaline conditions, prepared for submission to Applied Geochemistry.

C. L. Thorpe – principal author, performed all experimental work, initial concept, concept development; K. Morris – initial concept, concept development, extensive manuscript review; G. T. W. Law – concept development, manuscript review; J. R. Lloyd – concept development, manuscript review; P. Lythgoe – technical assistance (ICP-AES; XRF); A. Bewsher – technical assistance (IC); J. Waters – technical assistance (XRD).

1.5 References

Burke, I.T., Boothman, C., Lloyd, J.R., Mortimer, R.J.G., Livens, F.R., Morris, K. (2005). Effects of progressive anoxia on the solubility of technetium in sediments. *Environmental Science & Technology*, 39, 4109-4116.

Edwards, L., Kusel, K., Drake, H., Kostka, J.E. (2007). Electron flow in acidic subsurface sediments co-contaminated with nitrate and uranium. *Geochimica Et Cosmochimica Acta*, 71, 643-654.

Istok, J.D., Senko, J.M., Krumholz, L.R., Watson, D., Bogle, M.A., Peacock, A., Chang, Y.J., White, D.C. (2004). In situ bioreduction of technetium and uranium in a nitrate-contaminated aquifer. *Environmental Science & Technology*, 38, 468-475.

Law, G.T.W., Geissler, A., Boothman, C., Burke, I.T., Livens, F.R., Lloyd, J.R., Morris, K. (2010). Role of nitrate in conditioning aquifer sediments for technetium bioreduction. *Environmental Science & Technology*, 44, 150-155.

Lloyd, J.R., Renshaw, J.C. (2005a). Microbial transformations of radionuclides: Fundamental mechanisms and biogeochemical implications. *Metal Ions in Biological Systems*, 44, 205-240.

Lloyd, J.R., Renshaw, J.C. (2005b). Bioremediation of radioactive waste: radionuclide-microbe interactions in laboratory and field-scale studies. *Current Opinion in Biotechnology*, 16, 254-260.

Lloyd, J.R. (2003). Microbial reduction of metals and radionuclides. *FEMS Microbiology Reviews*, 27, 411-425.

Lloyd, J.R., Macaskie, L.E. (1997). Microbially-mediated reduction and removal of technetium from solution. *Research in Microbiology*, 148, 530-532.

North, N.N., Dollhopf, S.L., Petrie, L., Istok, J.D., Balkwill, D.L., Kostka, J.E. (2004). Change in bacterial community structure during in situ biostimulation of subsurface sediment cocontaminated with uranium and nitrate. *Applied and Environmental Microbiology*, 70, 4911-4920.

Renshaw, J.C., Lloyd, J.R., Livens, F.R. (2007). Microbial interactions with actinides and long-lived fission products. *Comptes Rendus Chimie*, 10, 1067-1077.

Chapter 2: Introduction and review of previous research

This chapter comprises a brief introduction to the world wide legacy of radioactively contaminated land with focus on several highly contaminated reprocessing facilities. There follows an overview of stable element and radionuclide biogeochemistry and a more detailed review of the environmental behaviour of key groundwater contaminants at the Sellafield site: technetium-99 (^{99}Tc), strontium-90 (^{90}Sr) and nitrate. The chapter

concludes with a short review of 'bioremediation' as a remediation technique for radioactively contaminated land and the goals of this research.

2.1 The nuclear fuel cycle

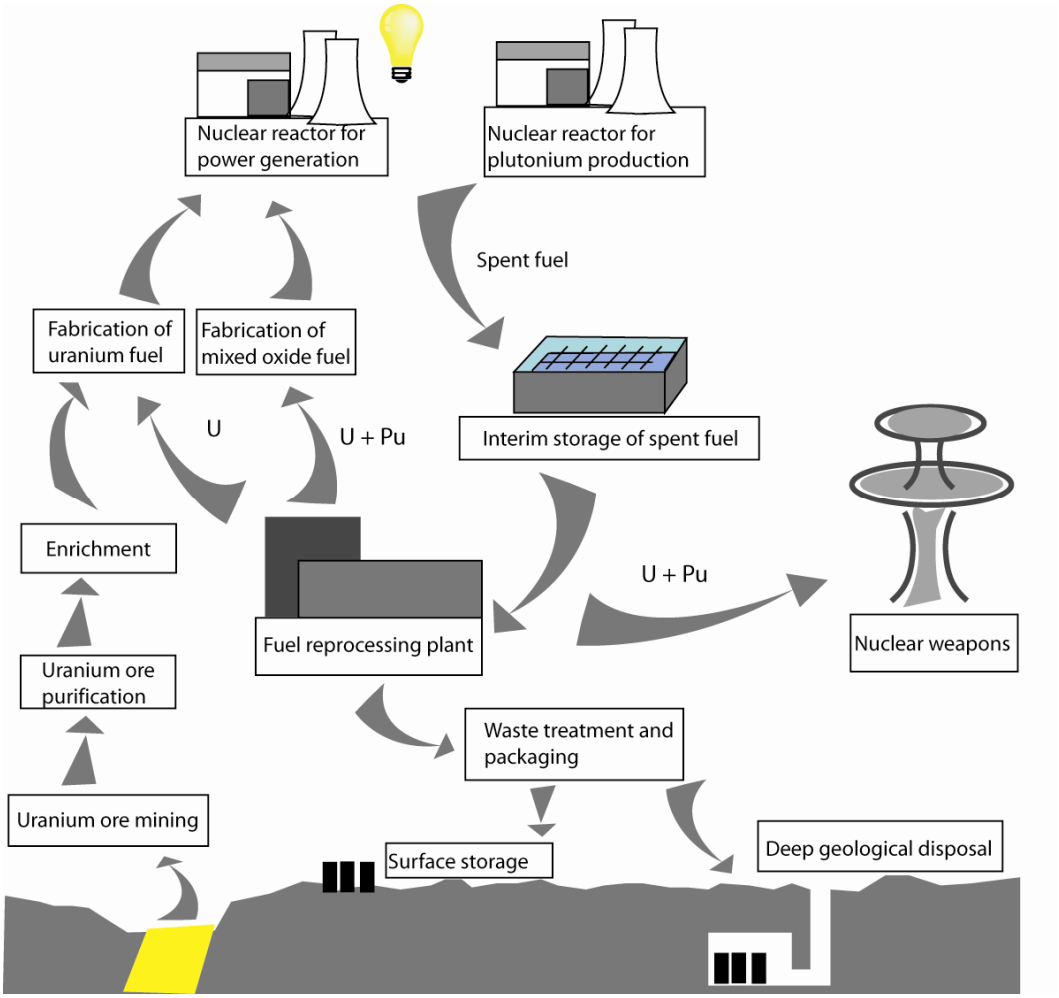

Figure 1. The nuclear fuel cycle from ore to waste (data sourced from Wilson, 1996).

The nuclear fuel cycle from uranium mining through to waste is summarised in Figure 1. Uranium ore is mined in Africa, Asia, North America and Australia, is milled to a sand like consistency and either an acid or alkali leach is used to extract the uranium as the soluble U(VI) (Wilson, 1996; RSC, 2011; WNA, 2011a). The uranium rich solution is then concentrated and dried, usually at site, before being shipped to the fuel manufacturing plant. Here, uranium is separated from impurities such as boron and

cadmium by solvent extraction using nitric acid and tri-n-butyl phosphate (TBP), then, depending on the fuel type, is either reduced directly to uranium metal (MAGNOX type) or enriched in a gas centrifuge prior to conversion to uranium dioxide (oxide type) (RSC, 2011). The fuel is 'burnt' in a reactor until there are too many fission products and insufficient U-235 to maintain an effective reaction at which point it is termed 'spent' and removed for either storage or in some countries, including the UK, for reprocessing (Openshaw et al., 1989; Wilson, 1996). Reprocessing aims to separate uranium and plutonium from the other radionuclides remaining in irradiated fuel from which the uranium can be used to manufacture new fuel and the plutonium can be used in mixed oxide (MOX) fuel or weapons manufacturing (Openshaw et al., 1989; DECC, 2011). During reprocessing, nitric acid is used to dissolve the spent fuel and TBP is used to extract both uranium and plutonium (Wilson, 1996; RSC, 2011). The 'waste' containing fission products is concentrated and contained for storage and ultimately disposal whilst the separated U and Pu can be used to manufacture new fuel (DECC, 2011). On average reprocessing recovers 96 wt % of spent fuel as U, 1 wt % as Pu and 3 wt % as waste carrying the majority (~95%) of the total activity (RSC, 2011; WNA, 2011b). Liquid effluent leaked during fuel reprocessing accounts for much of the contaminated land inventory and key impacted reprocessing sites are described more fully in section 2.4. Typically, reprocessing impacted sites are often contaminated with a mixture of uranium, fission products and can often have elevated levels of nitrate from fugitive industrial reprocessing liquors (Table 1).

2.2 A brief history of nuclear power

The present legacy of nuclear contaminated land is the result of controlled and accidental release of radionuclides over ~ 60 years of nuclear fuel cycle operations beginning with the first example of nuclear fission in 1942 (Figure 2).

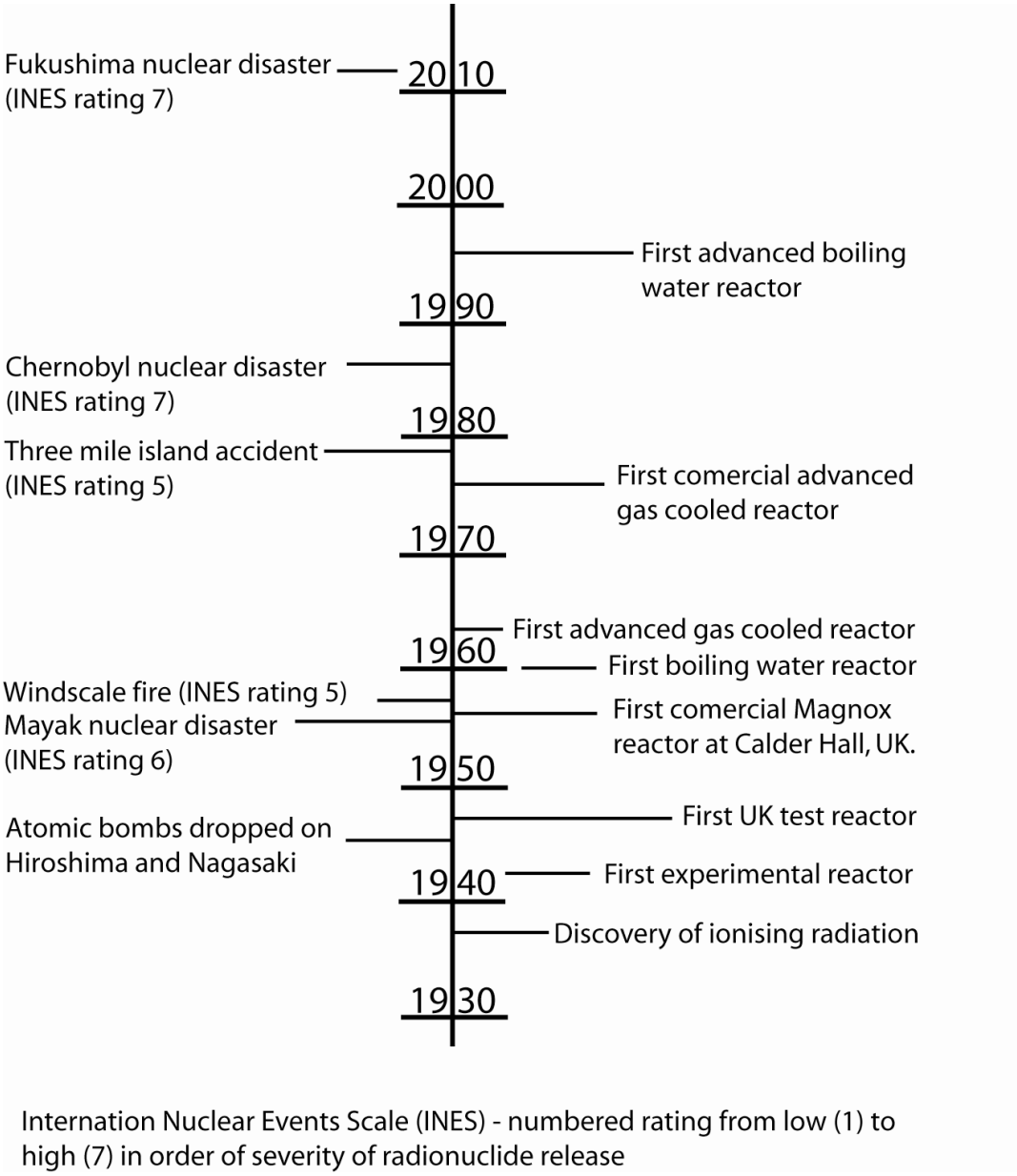

Figure 2. Summary of key events in the history of nuclear power (information sourced from: Szasz, 1984; Glasstone and Sesonske, 1994; Eisenbud and Gesell, 1997).

The first nuclear facilities were built by the UK, Russia, Germany and America during World War II in the race to produce plutonium for the atomic bomb; only after the war ended did nuclear research consider power generation (Szasz, 1984; Eisenbud and Gesell, 1997). The first commercial nuclear power facility in the world was Calder Hall power station that operated between 1956 and 2003 at what is now the Sellafield nuclear facility (UK). Early reactor designs such as the Calder Hall 'MAGNOX' reactors were termed 'first generation' and technologies quickly evolved to make successive 'second generation' rectors that were safer and more economical.

Second generation reactors were developed from the 1970s to the 1990s, featured improved power output using enriched uranium fuel rods with stainless steel cladding, and included pressurised water reactors, light water reactors, advanced gas cooled reactors and boiling water reactors (Figure 2; Glasstone and Sesonske, 1994; Nuttall, 2005). Third generation reactors improved on the second generation to include passive safety features and a more standardised design for easier maintenance and include the advanced boiling water reactor and advanced pressurised boiling water reactor (Figure 2; Nuttall, 2005). Reactor design is now moving towards generation four and focuses on 'thermal' and 'fast' reactors that have not yet been commissioned. Generation four nuclear power has experienced setbacks following a serious nuclear accident at Fukushima Daiichi, Japan, in March 2011 which resulted in many governments reconsidering their nuclear policy and most notably Germany, previously pioneers of generation four development, opting to phase out nuclear power altogether (Evans, 2011; Foulkes, 2011).

Thirty one countries currently operate nuclear power stations, with a total of 422 nuclear power plants in operation and a further 62 under construction (Figure 3; European Nuclear Society, 2011).

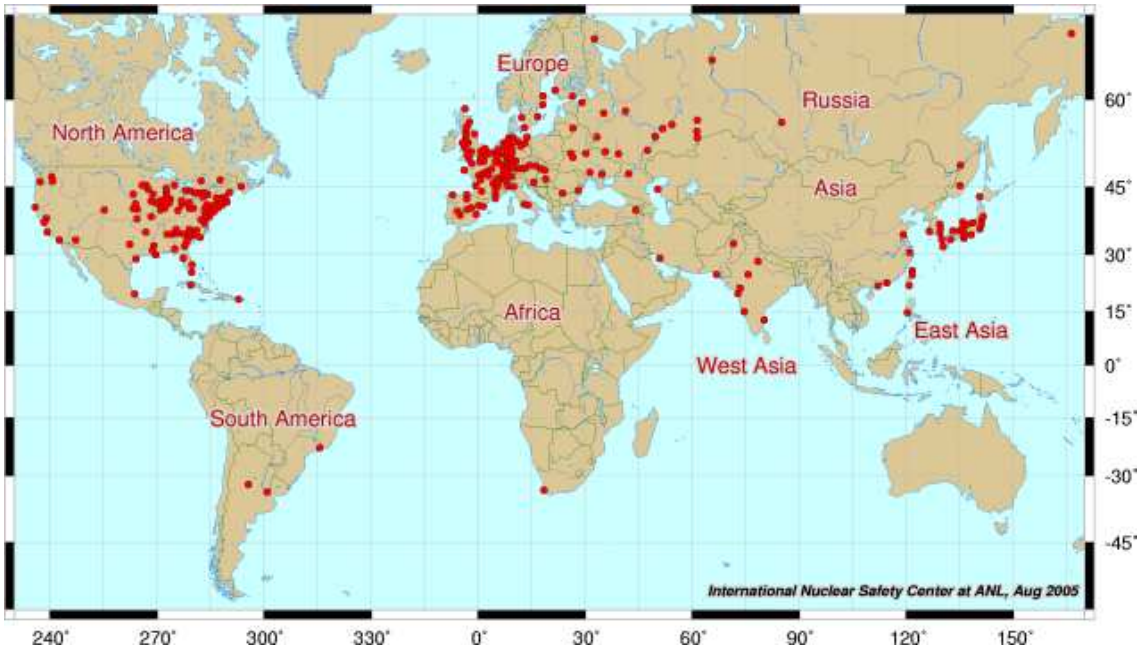

Figure 3. The location of nuclear reactor facilities around the world. Sourced from: http//www.mapcruzin.com/low-level-radiation/world-nuclear-reactor-map/.

2.3 The global nuclear legacy

The global nuclear legacy consists of nuclear reactor sites, associated fuel fabrication and reprocessing facilities, nuclear weapons testing, uranium ore mining and fallout from major nuclear accidents (Eisenbud and Gesell, 1997; Bayliss and Langley, 2003). The largest volumes of contaminated land exist as a result of controlled or accidental release of effluents from spent fuel reprocessing and storage facilities as radionuclide release direct from nuclear reactors in any significant quantity has occurred only during major nuclear accidents, most notably Chernobyl and now Fukushima, both rated 7 on the INES scale for nuclear events (IAEA, 2008). At the Fukushima Daiichi plant, an earthquake and tsunami led to damage and overheating of the reactor core and spent fuel stored in storage ponds. Although this is still an evolving situation, ^{90}Sr and ^{137}Cs have been measured at elevated concentrations in sediments within a 20 km radius of the

Fukushima site (Yoshida, 2011; Yamamoto et al., 2011; ACRO, 2011). The earthquake raised worldwide concern over the safe storage of spent nuclear fuel (Bradsher and Tabuchi, 2011; Fukushima Update, 2011). Following the Fukushima Daiichi accident the New York Times reported that 'Greater danger lies in spent fuel than in reactors' because of the difficulties of safe transport and containment during reprocessing and storage; the radioactively contaminated land legacy supports this statement (Bradsher and Tabuchi, 2011).

Those countries with the most extensive contaminated land legacy are those with the longest history of using nuclear fission and operating early reactor designs: the United States of America, United Kingdom and the former USSR. These countries host four of the world's most contaminated sites, Hanford, USA, Oak Ridge, USA, Mayak, Russia, and Sellafield, UK, which are all spent fuel processing facilities at which accidental and in some cases deliberate release of effluents from fuel storage tanks has lead to plumes of radionuclides in the subsurface (Table 1; McKinley et al., 2007; Sandring et al., 2009b; McKenzie and Armstrong-Pope, 2010).

In the USA an estimated 8000 km^2 of contaminated land exists at ninety one sites managed by the US Department of Energy (DOE) and these include the reprocessing facilities at Hanford, WA and Oak Ridge, TN (Riley and Zachara, 1992; Whicker et al., 2004). At Hanford and Oak Ridge leaks from waste storage tanks or reprocessing liqueurs have resulted in large volumes of contaminated land and plumes of mobile radionuclides in groundwater (Table 1: Riley and Zachara, 1992; Istok et al., 2004; Edwards et al., 2007).

Russia (former USSR) as early pioneers of nuclear fission have an extensive, though less well documented, nuclear legacy including significant radionuclide release from the

spent fuel reprocessing facility, Mayak (Chelyabinsk 65) (Standring et al., 2002; Henry and Douhovikoff, 2008; Priest et al., 2008; Shandala et al., 2008; Standring et al., 2009a). At Mayak nuclear facility (Chelyabinsk 65) where there remains widespread contamination of the Techa River and Lake Karachay due to intentional discharge of liquid waste, the explosion of a high level waste tank, and the windblown resuspension of sediments from Lake Karachay (Table 1: Christensen et al., 1997; Aarkrog et al., 1997; Beasley et al., 1998; Standring et al., 2002, Standring et al., 2009b).

The United Kingdom's nuclear legacy is managed by the Nuclear Decommissioning Authority (NDA) and comprises 39 reactors, 5 reprocessing plants, 3 fuel fabrication plants an enrichment plant and 5 nuclear laboratory complexes (NDA, 2011a). The most contaminated UK site, Sellafield reprocessing facility, is small in size in comparison to US or Russian facilities but ranks as one of the most contaminated sites in the world (Table 1; McKie, 2009). Contamination at the Sellafield site is discussed in more detail in chapter 2.4.

All radionuclides are considered contaminants and the World Health Organisation (WHO) has set guidelines of 0.1 Bq/L total alpha activity and 1 Bq/L total beta activity for drinking water supplies (WHO, 1993). In addition a dose guideline of 0.1 mSv/year allows a guideline activity for individual radionuclides to be calculated, and groundwater around nuclear facilities is evaluated on this basis (WHO, 1993). Radionuclide contaminants pose most risk to human health when they are mobile, bioavailable and relatively long lived such that they will persist for a number of years in the environment and may migrate in the subsurface.

Radionuclides that are most commonly reported in groundwater at contaminated reprocessing facilities are uranium ($t^{½}$ = 4.47 x10^9 years), the intermediate lived fission

products ^{90}Sr ($t^{½}$ = 28 years), ^{137}Cs ($t^{½}$ = 30 years), tritium ($t^{½}$ = 12 years) and the more long lived fission product ^{99}Tc ($t^{½}$ = 2.1 x10^5 years) (Table 1). Other radionuclides such as Pu, Am and Np are often present at contaminated sites but, however, are infrequently reported in groundwaters above WHO guideline concentrations.

	Sellafield, UK [1,2,3]	**Hanford, USA [4, 5, 6, 7, 8, 9]**	**Oak Ridge, USA [10, 11]**	**Mayak, Russia [12, 13]**
Site area in km^2	6	1500	220	200
Volume of waste stored onsite m^2	**HLW:** 1,620 **ILW:** 66,500 **LLW:** 6,310	**HLW(liquid):** 200,000 **HLW(Solid):** 750,000	**LLW:** 73,000	**HLW:** 56,753 **ILW:** 232,000 **LLW:** 429,000,000
Contaminated land m^2	An area 10 km^2 **LLW:** 13,000,000 **ILW:** 1,600	An area 200 km^2 1,100,000,000	An area 200 km^2	An area 20,000 km^2
Site usage	Plutonium production; Power generating reactors; spent fuel and waste storage; fuel reprocessing; research facilities	Plutonium production; power generating reactors; spent fuel and waste storage; fuel reprocessing; research facilities	Plutonium production and uranium purification; low level waste storage; research facilities.	Plutonium production and heavy water reactors; spent fuel and waste storage; MOX fuel production; research facilities.
Groundwater nitrate (mM)	Up to 5	Up to 20	> 150	No data available
Dominant groundwater radionuclides	^{99}Tc, ^{90}Sr, tritium, ^{137}Cs	U, ^{99}Tc, ^{90}Sr, tritium, ^{137}Cs	U, ^{99}Tc, ^{90}Sr,	^{99}Tc, ^{90}Sr, tritium, ^{137}Cs

Table 1. Summary of contaminated fuel reprocessing sites: Sellafield (UK), Oak Ridge, (USA), Hanford (USA) and Mayak (Russia). (Data sourced from [1] McKie, 2009, [2] McKenzie and Armstrong-Pope, 2010, [3] NDA, 2010, [4] Department of Ecology, 2011, [5] Carter et al., 2011, [6] Hoitink et al., 2005; [7] DOE, 2011; [8] Long, 2012; [9] Singleton et al., 2005, [10] ORNL, 2011, [11] Watson et al., 2004, [12] Standring et al., 2002, [13] Smith-Briggs et al., 2000).

Tritium (^3H) is practically inseparable from groundwater making *in situ* dilution and dispersion usually the most effective remediation strategy (Geniesse and Stegen, 2009). However ^{90}Sr, ^{137}Cs, U and ^{99}Tc have become the subject of substantial groundwater remediation research (Lloyd and Renshaw, 2005b). In addition to radionuclides, nitrate is common at reprocessing facilities due to the use of nitric acid and nitrate salts in fuel fabrication, dissolving spent fuel rods and purification processes; nitrate was the most

commonly reported anion at both UK and US reprocessing facilities (Riley and Zachara, 1992; McKenzie and Armstrong-Pope, 2010).

2.4 Introduction to the Sellafield site

This section comprises a detailed description of the history, geological setting and subsurface contamination at the Sellafield site. Sellafield is the case study site for the research conducted in this thesis.

2.4.1 A history of the Sellafield site

Sellafield was established in 1941 as a Royal Ordnance Factory for the production of trinitrotoluene (TNT) for the Second World War effort. Following the decision that the UK was to have a nuclear deterrent, two air cooled uranium reactors 'the Windscale piles' and the Windscale reprocessing facility were constructed in 1947 to produce plutonium for Britain's nuclear bomb (Openshaw et al., 1989; Gray et al., 1995). Extraction and purification of plutonium took place onsite and irradiated uranium fuel and fuel cladding from the Windscale piles were stored in waste silos (Gray et al., 1995).

The first power generating reactor was constructed at Calder Hall in 1956 and was the first in a fleet of MAGNOX reactors. These were bespoke reactors to the UK which used carbon dioxide as a coolant and graphite moderated natural uranium fuel rods clad in a magnesium alloy as the power source (Glasstone and Sesonske, 1994; Ellis and Staples, 2005). The UK nuclear industry has always been in favour of reprocessing its spent fuel and so a MAGNOX reprocessing plant was constructed at Sellafield to meet this requirement (Openshaw et al., 1989). Spent fuel from the four MAGNOX reactors

at Calder Hall was stored prior to reprocessing under water in ponds and fuel cladding 'swarf' remains stored in a wet silo (Gray et al., 1995). The land around the reactors (termed the Separation Area) was acquired to construct a prototype Advanced Gas Reactor, the THORP thermal oxide reprocessing plant for AGR fuel and storage facilities for nuclear wastes prior to vitrification, encapsulation and disposal and retains a significant legacy of contamination from the MAGNOX operations in the 1970s (Hunter, 2004).

Throughout plant operations low level liquid effluents have been discharged to the Irish Sea under authorisation *via* a pipeline that extends 2.5 km from the high water mark (Grey et al., 1995; Hamilton, 1999). This effluent included transuranic elements such as Pu, Np and Am and the fate of this contamination has been studied in sediments and living organisms as far north as Norway and the Arctic (Morris and Livens, 1996; Kershaw et al., 1999; Keith- Roach et al., 2000; Keith-Roach et al., 2003; Burke et al., 2006). Aside from these authorised releases, a number of significant leaks within the site boundary are known to have occurred from the reprocessing plant buildings within the Separation Area and these, in addition to minor spills over the ~ 60 year period of plant operations, have resulted in ~1.2-1.8 x 10^7 m^3 of contaminated land at Sellafield (Gray et al., 1995; Hunter, 2004; Webb et al., 2006).

At Sellafield, plutonium production and power generation technologies advanced faster than fuel reprocessing and waste disposal leading to a backlog of radioactive waste that remains to the present day unprocessed and stored in aging facilities (McKie, 2009). All but one of the UK's reactors are scheduled for demolition and new build planned for ~ 2025 but the nuclear waste legacy will persist for many decades to come (NDA, 2011b). With the likelihood that new reactors will be built in the UK comes the urgent

need to understand and control current contamination to improve public confidence and prepare for possible future leakage, for example a fuel storage tank failure (Bayliss and Langley, 2003; DECC, 2010; NDA, 2011b).

2.4.2 Sellafield regional geology, hydrology and hydrogeology

Sellafield nuclear facility is situated in the Calder Basin, Cumbria, UK. The geology (0-2000 m below the surface) below Sellafield is summarised in Figure 8 depicting the flow regimes that may affect the offsite migration of radionuclides from near surface leaks and spillage. Near surface quaternary geology comprises unconsolidated glacial till, marine and terrestrial sediments of grain size ranging from sandy clays to gravel (Figure 4; Chaplow, 1994; Hunter, 2004; Mckenzie and Armstrong-Pope, 2010).

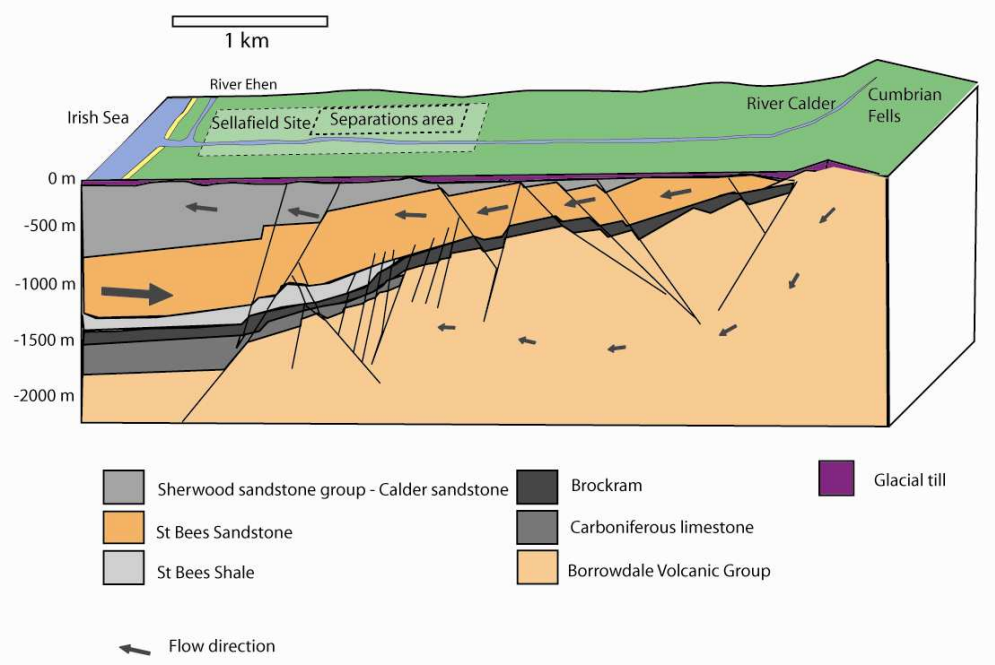

Figure 4. Geological cross section of the Sellafield site and the direction of flow for the sites three major groundwater regimes. Figure adapted from: fig. 4 Chaplow, 1994; McKenzie and Armstrong-pope, 2010.

Below the glacial till the Sherwood Sandstone Group (SSG) extends ~ 500 m comprising the Calder and Ormskirk sandstones. These overlie the St. Bees sandstone

formation that outcrops only to the north of the site (Figure 4; Hunter, 2004). Both sandstone groups are of Aeolian origin, reddish brown and feature mudstone/clay bands that dip South-west at ~ 23 degrees (Hunter, 2004). A series of E-W faults trend across the site and could act either as barriers or conduits to groundwater migration (Figure 4).

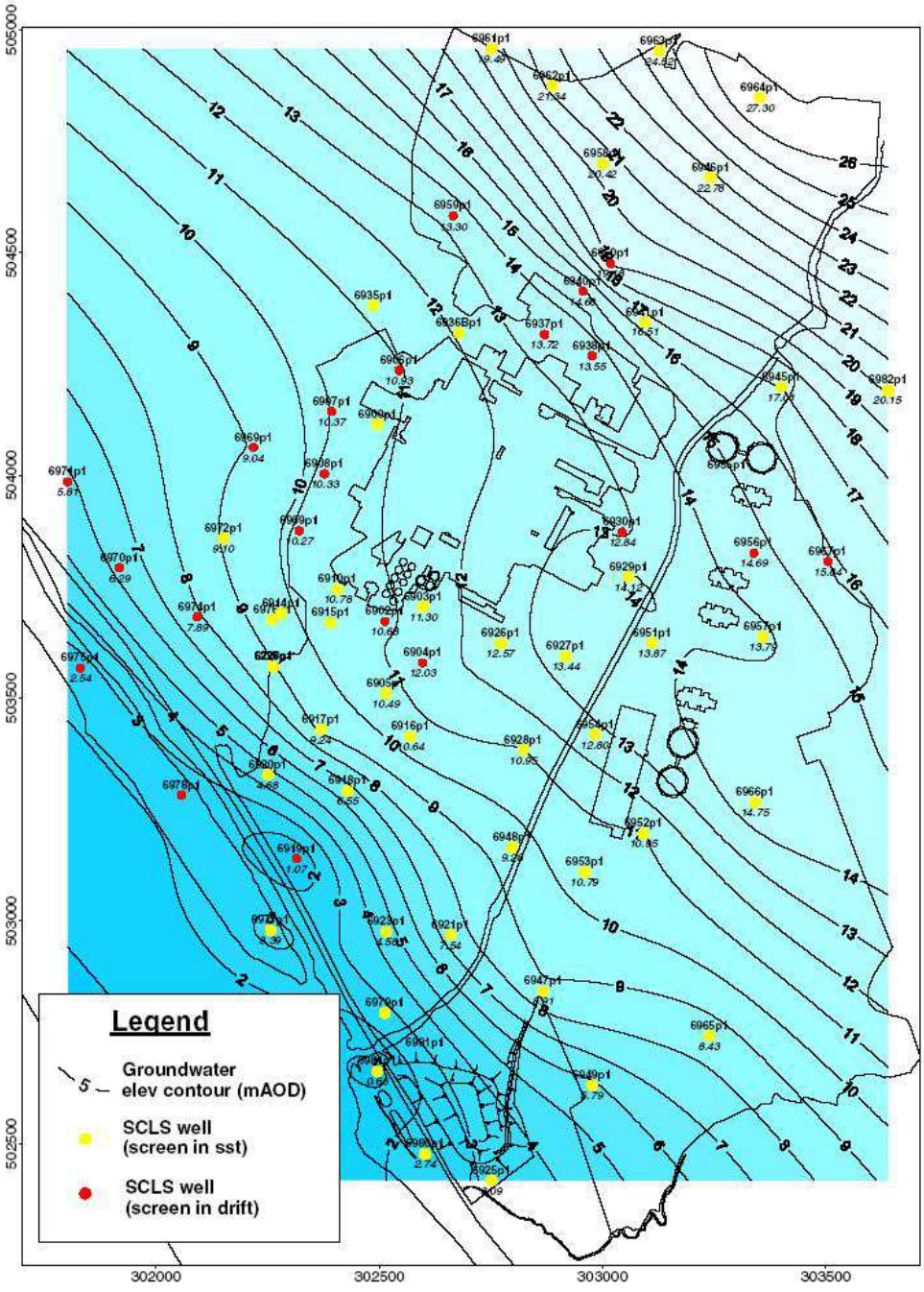

Figure 5. Conceptual model for the groundwater flow in Sellafield surface sediments; contours represent groundwater elevation above ordnance datum. Figure sourced from Figure 8, El-Ghonemy, 2004.

Groundwater flow is recognised at Sellafield as the dominant mechanism of radionuclide transport offsite (El-Ghonemy, 2004; Hunter, 2004). The Environment Agency has classified the underlying Sherwood sandstone as a Major Aquifer and the overlying glacial till deposits a Minor Aquifer (Mckenzie and Armstrong-Pope, 2010).

Migration of contaminants is largely associated with surface groundwater flow in a in a South-westerly direction as depicted in Figure 5 with tritium migration measured at 200 m $year^{-1}$ giving an indication of groundwater flow rates through glacial till (Chaplow, 1994; El-Ghonemy, 2004; Hunter, 2004; Black and Brightman, 1996; McKenzie and Armstrong-Pope, 2010). Below the surface glacial till, groundwater flow through the uppermost units of the Sherwood sandstone group is driven by precipitation and topography at hydraulic conductivities calculated between 10^{-8} and 10^{-5} cm s^{-1} (~ 3 m yr^{-1}) (Michie, 1996; Black and Brightman, 1996). Flow through the volcanic basement units is mostly related to fractures with a median hydraulic conductivity of 1.0 $x10^{-10}$ units (~3 x 10^{-5} m yr^{-1}). Saline groundwater at depth within this unit has a residence time of >10,000 years (Michie, 1996).

2.4.3 Radioactive Contamination in the Sellafield shallow sub-surface

At the Sellafield site an ongoing groundwater monitoring program shows that radioactively contaminated groundwater containing tritium and ^{99}Tc has migrated beyond the licensed site boundary in the vicinity of the main site gate (McKenzie and Armstrong-Pope, 2010). In addition ^{90}Sr, which is migrating more slowly than ^{99}Tc, can be found outside the Separations Area in two distinct zones although still within the licensed site boundary (McKenzie and Armstrong-Pope, 2010). Onsite contamination of groundwater by inorganic solutes (nitrate and ammonia) has been observed in the same area as the tritium, ^{99}Tc and ^{90}Sr plume near to the main gate (Hunter, 2004;

McKenzie and Armstrong- Pope, 2010). The source of elevated nitrate concentrations onsite is thought to result from the spillage of nitric acid used extensively within nuclear fuel cycle operations at the THORP and MAGNOX reprocessing plants. However, offsite there is nitrate run off from agricultural practices on adjacent farmland (Hunter, 2004). Other contamination detected on site includes elevated concentrations of petroleum hydrocarbons, polycyclic hydrocarbons, lead, zinc and chromium (McKenzie and Armstrong-Pope, 2010).

Contaminant migration is in the direction of the hydraulic gradient (Figure 5) and the plume is known to have migrated vertically downwards up to 50 m into the underlying sandstone aquifer and SW towards the coast (Hunter, 2004; McKenzie and Armstrong-Pope, 2010). An ongoing groundwater monitoring program has allowed Sellafield Ltd to record the concentration of contaminants in a series of monitoring wells since 2006. This allows maps to be constructed detailing the spread of contaminant plumes based on borehole data: Figures 6-10 show data for total alpha, total beta, ^{99}Tc, ^{90}Sr and ^{137}Cs. Strontium-90 was found to be the predominant beta-emitting contaminant and as such has a similar spatial distribution to the total beta activity distribution (Figures 9 and 10). Tritium, ^{99}Tc, ^{90}Sr and ^{137}Cs exist in the subsurface as they are major constituents of spent fuel storage tank liquors that have leaked over 60 years of plant operations (Gray et al., 1995; Wilson, 1996).

The highest ^{90}Sr activites (100 - >1000 Bq L^{-1}) are measured in multiple boreholes within and to the south-west of the separation area at relatively shallow depths of < 10 m although 208 Bq L^{-1} was measured in drift and < 10 Bq L^{-1} was measured in sandstone at depths > 10 metres (Figure 9; McKenzie and Armstrong-Pope, 2010). Caesium-137 concentrations in groundwaters on site are very low in relation to ^{90}Sr despite ^{137}Cs forming a significant component of many waste liquors; monitoring

throughout 2009/10 found that ^{137}Cs was migrating in the shallow subsurface at <0.09 m/year compared to the average groundwater flow rate of 10 m/year and that no borehole recorded groundwater ^{137}Cs above the WHO guideline value of 10 Bq L^{-1} (Figure 10; Table 2; McKenzie and Armstrong-Pope, 2010).

The highest concentration of ^{99}Tc in groundwater was found to the south-west of the site close to the main gate (Figure 8) and averaged 154 Bq L^{-1} with a maximum of 277 Bq L^{-1} ; a concentration of 155 Bq L^{-1} of ^{90}Sr was measured in the same area (Figures 8 and 9; Table 2). Tritium is below WHO guideline limits in all wells except three in the South-western corner of the separations area in the vicinity of the highest ^{99}Tc values (Figure 8). The monitoring program shows that although alpha emitters such as ^{238}U, ^{235}U, ^{234}U, ^{237}Np and Pu are all present as contaminants within the Sellafield site they are largely confined to the 'near field' immediately within the separation area (Figure 6) and have not significantly migrated to the 'far field' (away from the site of release).

Radionuclide	WHO drinking water guideline Bq L^{-1}	Max found 2006-7 Bq L^{-1}	Max found 2007-8 Bq L^{-1}	Max found 2008-9 Bq L^{-1}	Max found 2009-10 Bq L^{-1}
Total Alpha	0.5	145	113	133	116
Total Beta	0.30	119000	194000	162000	2470
Americium	1	0.86	1.10	0.089	0.020
Carbon-14	100	2130	5500	4813	53.4
Chlorine	100	0.49	1.30	0.65	1.34
Caesium-137	10	9.10	10.0	6.90	1.34
Tritium	10000	99700	105100	85400	76300
Iodine-129	100	9.30	6.80	3.96	1.58
Potassium-40	N/A	5.90	4.80		4.56
Neptunium-237	1	0.89	0.21	0.20	0.30
Plutonium-238	1	-	0.022	< 0.006	0.003
Plutonium-239/240	1	-	0.13	0.027	0.04
Plutonium-241	10	-	1.100	0.138	0.460
Radium	1	0.051	0.030	0.052	0.050
Strontium-90	10	65700	110600	96100	1770
Technetium-99	100	383	365	218	277
Uranium-234	10	51.0	57.1	74.9	59.0
Uranium-235	1	2.0	2.3	2.4	2.4
Uranium-236	1	2.4	2.7	4.8	4.6
Uranium-238	10	54	61	75	72

Table 2. Maximum concentrations of key radionuclides found onsite by the Sellafield groundwater monitoring program in for the years 2006-2010 (McKenzie and Armstrong-Pope, 2010).

The groundwater monitoring report 2010 reports the pH as variable in the range pH 6 – 8.5 although experiments using sediments from the vicinity of the Calder River report groundwater pH as low as 5.5 (McKenzie and Armstrong-Pope, 2010; Law et al., 2010a). The average composition of the regional Sellafield groundwater is defined in Wilson (1996) (Table 3) and is consistent with the slightly acidic pH in the regional shallow sub-surface groundwaters.

Species	**Na^+**	**K^+**	**Ca^{2+}**	**Fe^{2+}**	**Mg^{2+}**	**Cs^+**	**Sr^{2+}**	**Cl^-**	**NO_3^-**	**CO_3^-**	**PO_4^-**	**C**	**pH**	**Eh mV**
ppm	**26**	**1**	**38**	**0.2**	**9**	**0.1**	**0.1**	**54**	**12**	**30**	**0.1**	**0.8**	**5.7**	**+200**

Table 3. Average composition of Sellafield regional groundwater (Wilson, 1996).

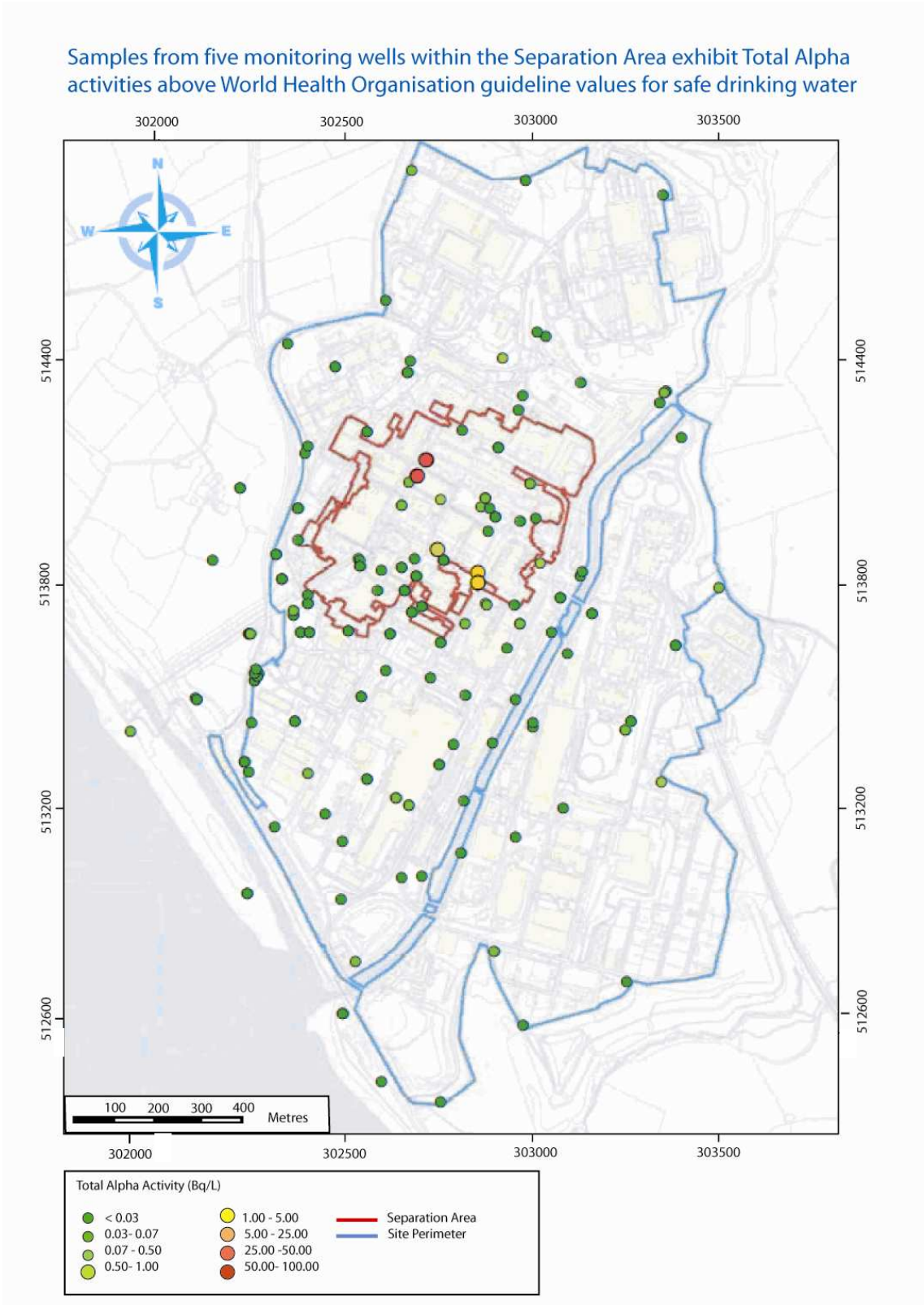

Figure 6. Borehole map showing total alpha concentrations in selected boreholes around the Sellafield site (Sourced from McKenzie and Armstrong-Pope, 2010).

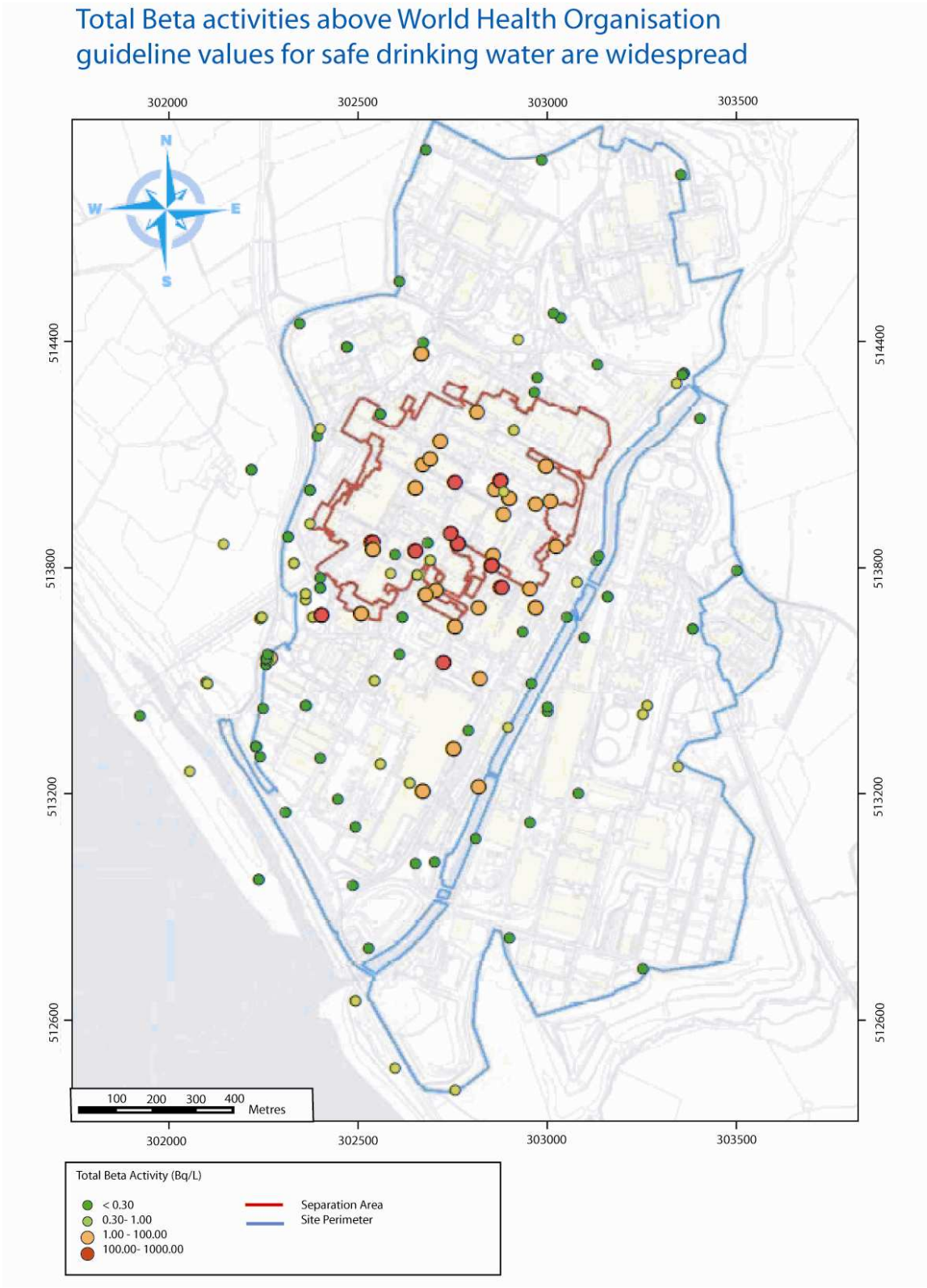

Figure 7. Borehole map showing total beta concentrations in selected boreholes around the Sellafield site (Sourced from McKenzie and Armstrong-Pope, 2010).

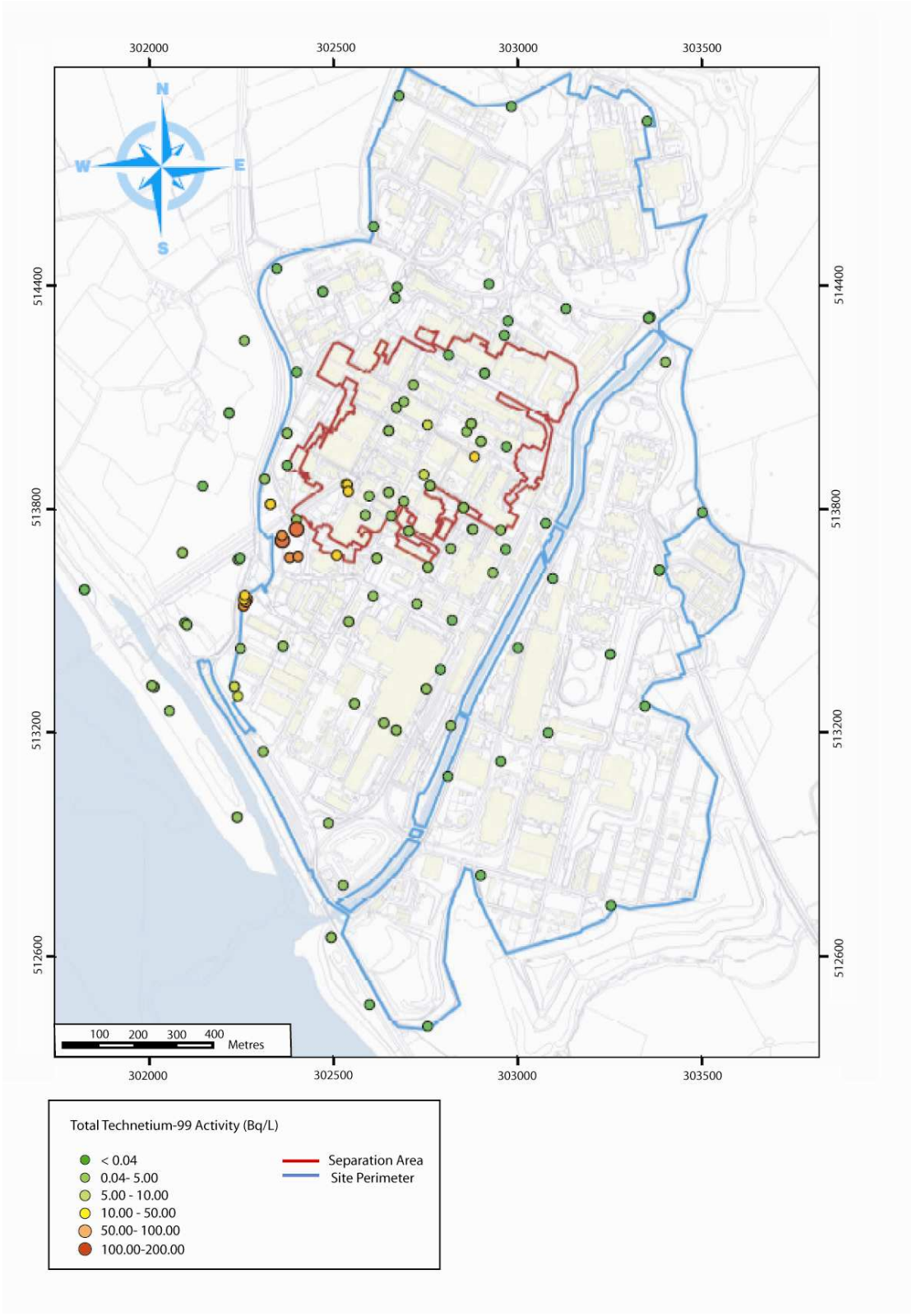

Figure 8. Borehole map showing Strontium-90 concentrations in selected boreholes around the Sellafield site (Sourced from McKenzie and Armstrong-Pope, 2010).

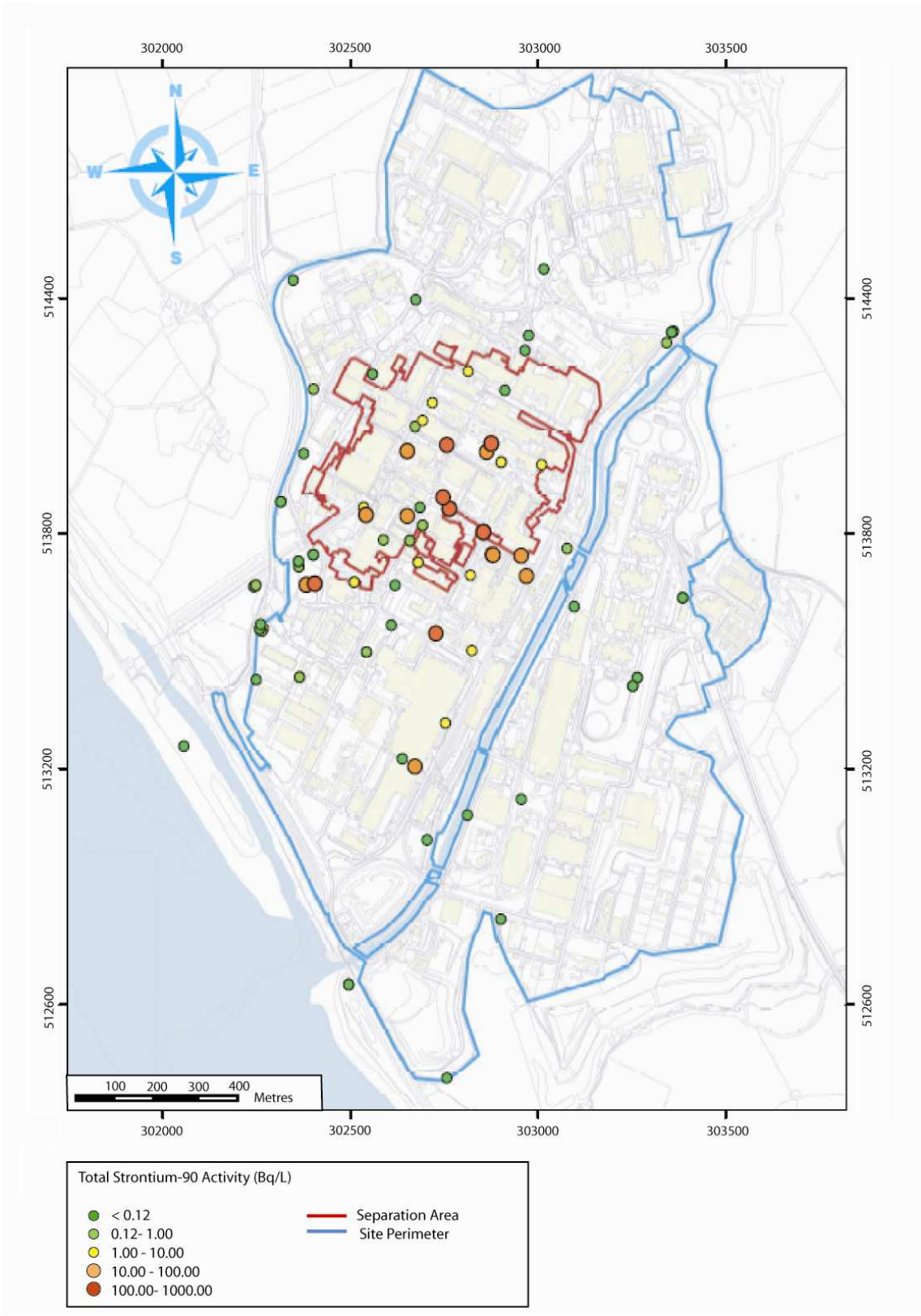

Figure 9. Borehole map showing technetium-99 concentrations in selected boreholes around the Sellafield site (Sourced from McKenzie and Armstrong-Pope, 2010).

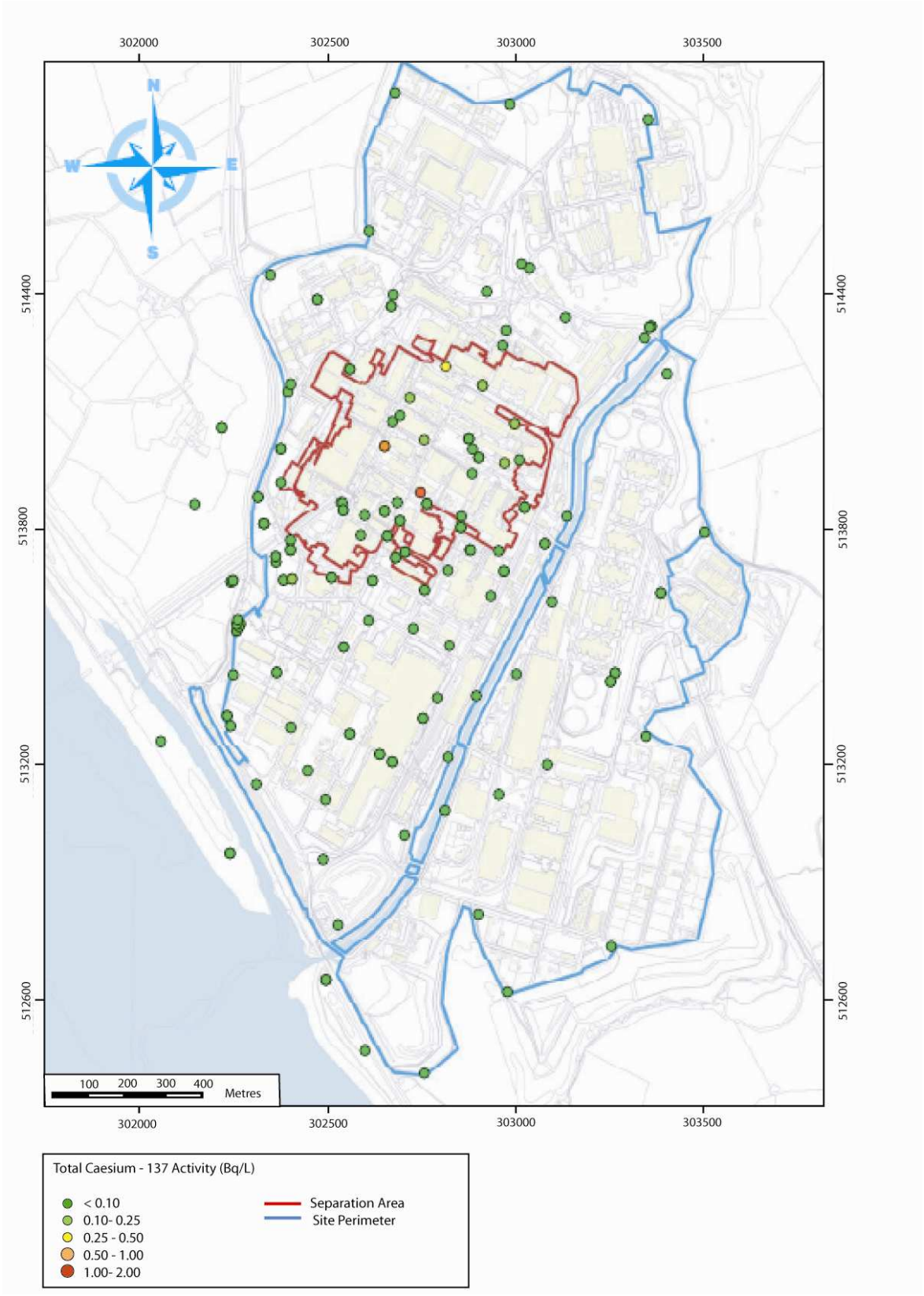

Figure 10. Borehole map showing caesium-137 concentrations in selected boreholes around the Sellafield site (Sourced from McKenzie and Armstrong-Pope, 2010).

2.5 Biogeochemistry of the subsurface

In this section summarises stable element and radionuclide biogeochemistry. The environmental behaviour of the mobile fission products ^{90}Sr and ^{99}Tc is then discussed in more detail.

2.5.1 Introduction to biogeochemistry

Microbes are ubiquitous in soils and sediments. Microbial respiration controls many processes that affect the geochemistry of the subsurface including the breakdown of organic matter, the dissolution and bio-precipitation of mineral phases and microbially mediated redox transformation metals. In some cases microbes can affect the speciation of an element directly, for example *via* sorption or uptake into the cell (biosorption or bioaccumulation), the breakdown of molecules during respiration (biodegradation) or direct enzymatic reduction to gain energy for metabolism (bioreduction) (Barkay and Schaefer, 2001; Lloyd, 2003; Gadd, 2010). In addition, microbial respiration can indirectly affect the speciation of an element, for example through microbially induced changes in pH or redox potential, sequestration into biogenic mineral phases or indirect reduction by the products of microbial respiration (Lloyd, 2003; Lloyd and Renshaw, 2005a; Gadd, 2010). Understanding the biogeochemistry of the subsurface is therefore key to predicting contaminant behaviour and in some cases microbial processes can help in providing solutions for contaminated land scenarios.

2.5.2 Microbial metabolism in the subsurface

In aerobic sediments microorganisms couple the oxidation of an electron donor to the reduction of oxygen as the terminal electron acceptor (TEA) in a redox reaction that releases energy for metabolism and growth (Konhauser, 2007; Madigan and Martinko, 2006). Electrons are transferred from the electron donor (usually an organic

compound), *via* an electron transport chain consisting of carrier enzymes, onto the TEA (Konhauser, 2007; Madigan and Martinko, 2006). The net energy gained is determined from the difference in reduction potential between the electron donor and TEA (Table 4). In the subsurface, where oxygen is depleted, alternative TEAs can be used and those relevant to contaminated land scenarios include nitrate (NO_3^-), nitrite (NO_2^-), bioavailable manganese (Mn(IV)), bioavailable iron (Fe(III)) and sulfate (SO_4^{2-}). The order in which TEAs are utilised depends on their concentration and the free energy yield of the redox couple (Table 4).

Terminal electron accepting process	**ΔG kJ/mol CH_3COO^- (pH 7)**
$CH_3COO^- + 2O_2 \rightarrow H_2O + 2CO_2 + OH^-$	-854
$CH_3COO^- + 1.6NO_3^- \rightarrow 0.8N_2 + 0.2H_2O + 2CO_2 + 2.6OH^-$	-801
$CH_3COO^- + 2MnO_2 + 3H_2O \rightarrow 4Mn^{2+} + 2HCO_3^- + 7OH^-$	-558
$3CH_3COO^- + 8TcO_4^- + 17H_2O \rightarrow 6HCO_3^- + 8TcO_2 + 16H^+ + 21OH^-$	-436
$CH_3COO^- + 8Fe(OH)_3 \rightarrow 8Fe^{2+} + 5H_2O + 2HCO_3^- + 15OH^-$	-337
$CH_3COO^- + 4UO_2^{2+} + 4H_2O \rightarrow 4UO_2 + 2HCO_3- + 9H^+$	-264
$CH_3COO^- + SO_4^{2-} \rightarrow HS^- + 2HCO_3^-$	-48
$CH_3COO^- + 2H_2O \rightarrow CH_4 + HCO_3^-$	-31

Table 4. Energy yield of terminal electron accepting processes at pH 7 (Konhauser, 2007; Konhauser et al., 2002).

At ambient pH, the cascade of terminal electron accepting processes (TEAPs) proceeds *via* $O_2 > NO_3^- > NO_2^- >$ Mn(IV) > Fe(III) > SO_4^{2-} and the resulting reduced products from anaerobic metabolism will be N_2 / N_2O / NH_4^+, Mn(II), Fe(II) and H_2S. Microbial communities in sediment systems will respond to the conditions in the subsurface, for example a high abundance of nitrate or Fe(III) in sediments will usually stimulate denitrifying or metal reducing communities (North et al., 2004; Law et al., 2010a; Thorpe et al., 2012a; Stewart et al., 2010).

Bioreduction in sediments is limited by the availability of electron donors which are commonly organic compounds from the breakdown of organic matter (Madigan and

Martinko, 2006). More rapidly occurring engineered bioreduction is possible *via* 'biostimulation': the addition of a simple electron donor to stimulate and increase the microbial population and rate of TEAP's (Lloyd and Renshaw, 2005b; Gadd, 2010). Biostimulation is the basis for many bioremediation scenarios.

2.5.3 Introduction to radionuclide biogeochemistry

Micro-organisms have been used successfully at contaminated sites to degrade compounds such as nitrate and chlorinated hydrocarbons using the biostimulation of indigenous bacteria to increase the rate of natural metabolic processes (NRC, 1993; Ronneau and Bitchaeva, 1997). Although micro-organisms cannot degrade metals and radionuclides it has been shown that the addition of an electron donor to radioactively contaminated land can stimulate biogeochemical changes that reduce the mobility of certain problematic metals and radionuclides and retard their migration through the subsurface (Barkay and Schaefer, 2001; Lloyd, 2003; Lloyd and Renshaw, 2005a, 2005b; Gadd, 2010).

Many radionuclides including ^{60}Co, the fission products ^{99}Tc and ^{129}I and the actinide elements $^{235/238}$U, $^{238\text{-}241}$Pu, ^{237}Np and ^{241}Am have variable oxidation states (Table 5) that can be affected by the development of reducing conditions during microbial respiration in the subsurface (Lloyd et al., 2002; Lloyd, 2003; Lloyd and Renshaw, 2005a; Gadd, 2010; Icenhower et al., 2010). In the case of U, ^{99}Tc and ^{237}Np, reduction to a lower environmentally relevant oxidation state results in a reduction in solubility and removal from groundwaters (Lloyd et al., 2002; Lloyd, 2003; Wall and Krumholz, 2006; Icenhower et al., 2010; Law et al., 2010b). Actinide element redox chemistry is complicated: in general in their oxic 5+ and 6+ oxidation states actinide ions tend to be soluble and therefore more mobile and in their reduced 3+ and 4+ oxidation states they tend to be less soluble and sorb more strongly to sediments (Lloyd and Renshaw, 2005).

In the case of ^{99}Tc, mobile Tc(VII) is reduced to less mobile Tc(IV) (Icenhower et al., 2010) and this process is discussed in more detail in section 2.6.8.

Key Problematic Radionuclides	Half life (years)	Oxidation state
Tritium -H-3	12.3	+1
Fission products		
Strontium -Sr-90	29	2+
Technetium -Tc-99	$2.1x10^5$	7+, 4+
Cobalt -Co-60	5.27	3+, 2+
Iodine -I-129	$1.57x10^7$	1-, 0, 1+
Caesium -Cs-**137**-134	**30.23;** 2.06	1+
Actinides		
Plutonium -Pu-**238**-239-**241**	**88**; 24,100; **14**	6+, 5+, 4+, 3+
Americium -Am-241	432.2	6+, 5+, 4+, 3+
Uranium -U-**238**-235	**$4.4x10^9$**; $7.0x10^8$	6+, 5+, 4+, 3+
Thorium -Th-230	75380	4+
Neptunium -Np-237	$2.14x10^6$	6+, 5+, 4+, 3+
Atmospheric discharge		
Carbon -C-14	5730	4+, 3+, 2+, 1+, 0, 1-, 2-, 3-, 4-
Europium -Eu-152	13.5	3+, 2+

Table 5. Variable oxidation states of radioactive contaminants found at nuclear facilities. Sourced from Lloyd and Renshaw, (2005a).

Furthermore, the speciation and mobility of non-redox active radionuclides can also be influenced during bioreduction by increased sorption or desorption due to changes in pH and mineralogy or by precipitation or incorporation into biogenic mineral phases (Ferris et al., 2000; Mason, 2000; Roden et al., 2002; Mitchell and Ferris, 2005). Both ^{137}Cs and ^{90}Sr only exist in only one oxidation state and therefore their behaviour is not directly affected by changes in redox chemistry during bioreduction although their speciation can still be affected by microbially induced changes in mineralogy, geochemistry, pH or sorption to microbial biomass (Lloyd and Renshaw, 2005). The environmental behaviour of ^{90}Sr is further described in section 2.6.7 as it is a key subsurface contaminant at Sellafield nuclear facility.

The microbial reduction of key stable elements in environmental systems, NO_3^- /Mn(IV)/Fe(III)/SO_4^{2-}, are discussed below with focus on the effect each process may have on the sediment mineralogy, geochemistry and the mobility of key problematic radionuclides. The reduction of key mobile fission products ^{90}Sr and ^{99}Tc is then discussed in more detail.

2.5.4 Nitrate reduction in radioactively contaminated land

Nitrate (NO_3^-) is a naturally occurring anion typically found at concentrations of less than 10 mg L^{-1} in surface and groundwaters (WHO, 1993). Nitrate, and the nitrate reduction intermediate species nitrite, are both considered harmful and the World Health Organisation gives guideline values of 50 mg L^{-1} (0.8 mM) for nitrate and 3 mg L^{-1} (0.065 mM) for nitrite in drinking water which are exceeded at Sellafield and at other contaminated sites (Riley and Zachara, 1992; WHO, 1993; McKenzie and Armstrong-Pope, 2010). Microbial reduction of nitrate occurs as part of the nitrogen cycle where nitrate (NO_3^-) is reduced to nitrite (NO_2^-) and then to nitrous oxide and nitrogen gas (NO/N_2) in denitrification or in some cases to ammonia (NH_4^+) (Figure 11; Konhauser, 2007). Nitrate is an energetically more favourable electron acceptor than Mn(IV), Fe(III) and SO_4^{2-} and thus can inhibit TEAP progression to metal reducing conditions. If metal reducing conditions do not develop then key redox active radionuclides such as ^{99}Tc and U will remain in their oxic, soluble form and thus nitrate can inhibit bioremediation scenarios (DiChristina 1992; Lloyd et al., 2002, Lloyd, 2003; Lloyd and Renshaw, 2005a). Sediment microcosm studies generally show that both microbially-mediated metal and U(VI), Np(V) and Tc(VII) reduction does not commence until nitrate and the intermediary reduction product nitrite are depleted (Burke et al., 2005; Edwards et al., 2007; McBeth et al., 2007; Li and Krumholz, 2008; Law et al., 2010a) although an *in situ* study reported co-removal of NO_3^- and Tc(VII) from porewaters

(Istok et al., 2004). Stimulating the microbial population to bioreduction has the potential to remove NO_3^- *via* denitrification and the added benefit that once nitrate is removed then metal reducing conditions can follow.

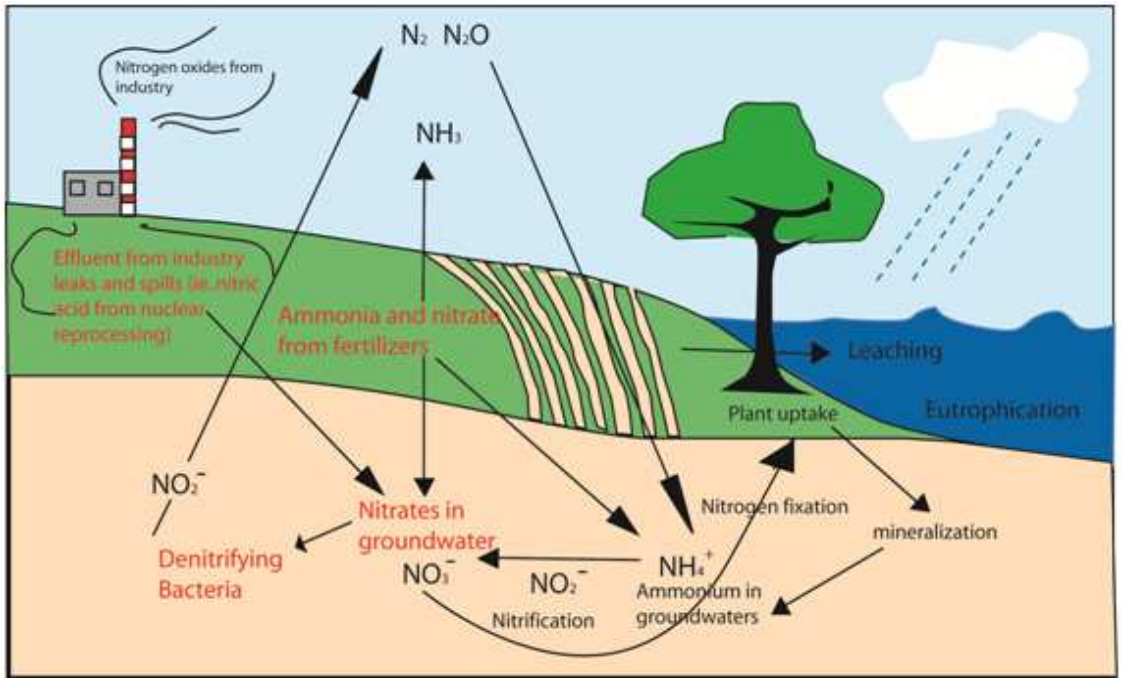

Figure 11. The nitrogen cycle.

Nitrate reduction coupled to the oxidation of a simple carbon source such as acetate results in the release of OH^- and CO_2 affecting the pH and geochemistry of groundwaters (Table 4). Increase in pH increases metal cation sorption to sediments, through increased deprotonation of mineral surfaces (Dyer et al., 2000; Ferris et al., 2000; Hoffman et al., 2005; Alvarez-Silva et al., 2010); this may affect the sorption of radionuclide cations such as ^{137}Cs and ^{90}Sr. Furthermore, an increase in pH and dissolved inorganic carbon may induce oversaturation with regard to carbonate mineral phases (Coleman et al., 1993; Mitchell and Ferris, 2005).

Nitrate is present in elevated concentrations in radionuclide contaminated groundwater at many nuclear legacy sites including Sellafield, UK, Oak Ridge Field Research Centre, USA, Hanford, USA and Shiprock, New Mexico, at several tens of mM as a

result of spent nuclear fuel reprocessing activities and uranium extraction processes (Finneran et al., 2002; Singleton et al., 2005; Edwards et al., 2007; McKenzie and Armstrong-Pope, 2010). Around Sellafield, the majority of nitrate is thought to be present as a result of industrial spillage, although additional nitrate is present in the far field due to run off from fertilizer use on local farms (Hunter, 2004).

At Oak Ridge, TN, very high nitrate > 100 mM is found in combination with low pH (pH 4-6) (Petrie et al., 2003; North et al., 2004; Edwards et al., 2007) presenting challenging conditions for bioremediation. Low pH critically decreases microbial diversity and metabolic function (Madigan and Martinko 2006; Robinson et al. 2009) which can lead to the temporary or prolonged accumulation of intermediary product NO_2^- that is toxic to microorganisms at low pH due to the presence of HNO_2 that can enter the cell and interfere with the pH gradient across the cell membrane (Weon et al., 2002; Zhou et al., 2007, Zhou et al., 2010). The success of biostimulation under low pH conditions is variable and some biostimulation studies with low pH (4 - 5) sediments have demonstrated that pH amendment *via* the addition of $NaHCO_3$ or crushed lime was necessary before the cascade of TEAPs occurred (North et al., 2004; Istok et al., 2004; Edwards et al., 2007; Michalsen et al., 2009). Conversely, microcosm studies with sediments representative of the shallow Sellafield subsurface show that bioreduction did not stall in systems at pH 5.5 in the presence of 10 mM nitrate where nitrate and nitrite reduction was then followed by metal and radionuclide reduction (Law et al., 2010a).

2.5.5 Metal reduction in radioactively contaminated land

Manganese and iron reduction are important biochemical processes in the shallow subsurface as a wide range of archaea and bacteria are able to conserve energy through the reduction of Fe(III) to Fe(II) and of Mn(III, IV) to Mn(II) (Lovley, 1991; Thamdrup, 2000; Lloyd, 2003). Manganese (Mn) reduction is more energetically favourable than

iron reduction but Mn is typically much less abundant in sediments (the Mn concentration is < 10 % that of Fe in Sellafield type sediments) and so the two processes are often observed to occur virtually simultaneously in laboratory experiments (Nealson and Saffarini, 1994; Law et al., 2010a). Many organisms capable of Mn reduction can also reduce Fe(III) (Lloyd, 2003) and so many papers discuss the biological reduction of Fe(III) and Mn(IV) as 'metal reduction' (Lovley, 1991; Lloyd, 2003).

Metal reducing bacteria couple the oxidation of organic matter to the reduction of bioavailable Mn(IV) and Fe(III) which includes aqueous, sorbed and poorly crystalline oxides such as ferrihydrite or δMnO_2 (Nealson and Saffarini, 1994; Kappler and Staub, 2005; Cutting et al., 2009). During dissimilatory metal reduction, species such as *Shewanella oneidensis* and *Geobacter metallireducens* can gain energy for growth by directly coupling organic substrate oxidation with reduction of Fe(III) to Fe(II) or Mn(IV) to Mn(II) whilst other metal reducing species can grow by fermentation but pass electrons to Fe(III)/Mn(IV) adventitiously as minor electron acceptors (Lovley et al., 1989; Lovley et al., 1993; Lloyd, 2003; Konhauser, 2007; Stewart et al., 2010). Both of these mechanisms are important and lead to subsurface metal reduction in a wide range of environments.

As the standard redox potential of ferrihydrite / Fe^{2+} species (~ 0 mV; Lloyd et al., 2002; Thamdrup, 2000) is more electronegative than the reduction potentials for key radionuclides, for example U(VI/U(IV) (~ 100 mV; Lloyd et al., 2002) and Np(V)/Np(IV) (~ 450 mV; Lloyd et al., 2002) then iron reducing bacteria should have the metabolic potential to reduce radionuclides enzymatically. This has been demonstrated: in the case of uranium where pure culture studies suggest enzymatic reduction *via* C-type cytochromes is a significant reduction pathway for uranium (Lloyd et al., 2000; Konhauser, 2007). For ^{99}Tc, enzymatic reduction is thought to be mediated

by nickel-iron hydrogenase enzymes and although is possible that energy is gained from this reaction under constrained conditions it is thought to be largely adventitious (De Luca et al., 2001). Although enzymatic reduction of radionuclides is possible, in many sediments abiotic reduction by biogenic Fe(II) minerals (magnetite, siderite, vivianite and sorbed Fe^{2+}) is thought to be the dominant mechanism of U, ^{237}Np and ^{99}Tc reduction (Lloyd et al., 2000, 2002; Fredrickson et al., 2004; McBeth et al., 2007; Law et al., 2010a; Law et al., 2010b; McBeth et al., 2011).

The rate of metal and radionuclide reduction can be affected by the pH of the sediment (Law et al., 2010; Roden et al., 2010; Thorpe et al., 2012a). For most Fe(III) reducing bacteria the optimum pH for growth is circumneutral and studies indicate that below pH 5.5 and above pH 8 Fe(III) reduction is compromised with few species having been found capable of dissimilatory Fe(III) reduction above pH 9 or below pH 4 (Baker and Banfield, 2003; Adams et al., 2007; Stewart et al., 2010; Thorpe et al., 2012b). In addition, bacterial reduction of crystalline Fe(III) phases such as haematite and goethite is limited (Cutting et al., 2009) and although bioavailability can be aided by the presence of electron shuttling compounds such as humic acids (Luu and Ramsay, 2003), generally, the more crystalline the sediment, the less Fe(III) is bioavailable.

Non redox active species such as ^{137}Cs and ^{90}Sr may be affected indirectly during Fe(III) reduction by changes in geochemistry or mineralogy. The dissolution of metal oxides, and especially bioavailable poorly crystalline phases that are a key sink for metal cations, may increase the mobility of sorbed species through loss of sorption sites (Gadde and Laitinen, 1974; Hoffman et al., 2005; Langley et al., 2009b). Conversely, the release of OH^- during Mn(IV) and Fe(III) reduction has the potential to increase the sediment pH and result in increased cation sorption due to increased mineral surface charge (Konhauser, 2007; Dyer et al., 2000; Ferris et al., 2000; Hoffman et al., 2005;

Alvarez-Silva et al., 2010). The effects of bioreduction on species such as ^{90}Sr are not fully understood and possible controlling factors are discussed further in section 2.6.7.

2.5.6 Sulfate reduction in radioactively contaminated land

In sediment microcosms, including those using sediment representative of the Sellafield region, sulphate reduction is observed to follow Fe(III) reduction (Law et al., 2010a; Wilkins et al., 2007). The standard redox potential for the SO_4^{2-}/HS^- redox couple is -0.22 V (Madigan and Martinko, 2006) and much lower than the redox potentials for most redox active radionuclide species and therefore radionuclide reduction is typically associated with Fe(III) reduction rather than with sulfate reduction (Lloyd et al., 2002). However, if sulphate levels are high then sulfate reduction can lead to changes in the mineralogy of sediments; hydrogen sulfide is released into porewater and Fe(II) is scavenged to form iron sulfide precipitates (Herbert et al., 1998). A field study into bioreduction in a uranium contaminated aquifer at the Rifle site, Colorado, suggested that uranium that had been immobilised by Fe(III) reduction was remobilised during sulfate reduction (Anderson et al., 2003). However, this has not been observed to be the case in other field tests and microcosm studies (Suzuki et al., 2003; Begg et al., 2007; Law et al., 2010a).

2.5.7 Environmental behaviour and biogeochemistry of ^{90}Sr

^{90}Sr is a high yield (~ 6 %) product of uranium fission (and to a lesser extent of plutonium fission) that decays (β^- emission, E_{max} = 0.546 MeV and half life ~ 29 years) to produce the isotope ^{90}Y (β^- emission, E_{max} = 2.28 MeV and half life 64.2 hours) (Equation 1).

(1) $^{90}_{38}Sr \rightarrow {}^{90}_{39}Y + \beta^-$

Strontium-90 is a non-redox active radionuclide present primarily as the Sr^{2+} ion and is a particular risk to human health due to its potential to substitute for Ca^{2+} in bones leading to an increased risk of diseases such as leukaemia (Raabe, 2010). Strontium-90 contaminates all sites where nuclear bombs have been detonated, where reactor fuel has been accidentally exposed and many sites where fuel storage and reprocessing effluents have been leaked (Jackson and Inch, 1989; Riley and Zachara, 1992; Mason et al., 2000; Dewiere et al., 2004; McKinley et al., 2007; Priest et al., 2008; McKenzie and Armstrong-Pope, 2010). At Sellafield nuclear facility, ^{90}Sr is widespread but has migrated further than ^{137}Cs but is retarded in comparison to tritium and ^{99}Tc (McKenzie and Armstrong-Pope, 2010).

In sediments ^{90}Sr associates with the stable Sr^{2+} and XAS studies have shown that at circumneutral pH Sr^{2+} typically forms outer sphere complexes that are electrostatically bound to the surface of clay and metal oxide mineral surfaces (Axe et al., 1995; Axe et al., 1998; Parkman et al, 1998; Chen and Hayes, 1999; Sahai et al., 2000; O'Day et al., 2000; Carroll et al., 2008). Studies show that pH is critical to Sr^{2+} sorption and that increasing sorption occurs with increasing pH due to increased negative charge on mineral surfaces above their point of zero charge (PZC) (Dyer et al., 2000; Ferris et al., 2000; Hoffman et al., 2005; Alvarez-Silva et al., 2010). Ionic strength of groundwater is also important as the presence of competing cations such as Na^{+}, Mg^{2+} and particularly Ca^{2+} can lead to decreased Sr^{2+} adsorption (Hull and Scharfer, 2008).

In the presence of dissolved inorganic carbon and alkaline pH (> 8), groundwater systems can become supersaturated with regard to carbonate phases and Sr^{2+} may precipitate as $SrCO_3$ (strontianite) or be removed from solution *via* substitution into $CaCO_3$ minerals such as calcite or aragonite (Pingatore et al., 1992; Greegor et al.,

1997; Parkman et al., 1998; Finch et al., 2003; Fujita et al., 2004). Some studies show Sr^{2+} incorporation into Ca-phosphate minerals (Handley-Sidhu et al., 2011).

Electron donor breakdrown can change the pH, mineralogy and redox state of the sediment and releasing hydroxide ions and dissolved inorganic carbon (Table 4; Konhauser, 2007). The effects of these changes during sediment bioreduction on Sr^{2+} are as yet poorly constrained although a number of mineral system studies exist. Studies show how microbially mediated precipitation of calcium carbonate minerals can lead to incorporation of Sr^{2+} into calcite (Fujita et al., 2004; Mitchell and Ferris, 2005) or biogenic apatite (Handley-Sidhu et al., 2011) and there is some evidence to suggest that the precipitation of siderite may also remove Sr^{2+} from solution (Roden et al., 2002). However, some mineral studies suggest that microbial dissolution of metal oxide minerals has the potential to cause Sr^{2+} release due to loss of sorption sites (Small et al., 1999; Ferris et al., 2000; Parmar et al., 2000; Roden et al., 2002; Langley et al., 2009b).

Overall, elevating the pH of the contaminated sub-surface environment appears, from laboratory studies, to be the simplest method for immobilising Sr^{2+} in contaminated sediments by encouraging increased sorption and precipitation (Small et al., 1999; Ferris et al., 2000; Roden et al., 2002; Fujita et al., 2004; Mitchell and Ferris, 2005; Langley et al., 2009a). The effects of bioreduction on Sr^{2+} mobility are unclear and are investigated within this thesis in sediments of varying pH and nitrate concentration.

2.5.8 Environmental behaviour and biogeochemistry of ^{99}Tc

^{99}Tc is a high yield fission product and decays by β^- emission (E_{max} = 0.29 MeV) to produce the stable isotope ruthenium-99 (Equation 2).

(2) $^{99}_{43}Tc = ^{99}_{44}Ru + \beta^-$

Natural Tc is essentially non-existent on Earth so anthropogenic Tc sources are the sole contributors of this radionuclide to the environment. Like ^{90}Sr, ^{99}Tc is a fission product and is therefore present at nuclear test sites, spent fuel reprocessing facilities where leaks have occurred, and at the sites of major nuclear accidents. It is predicted that all elements of Tc will be unstable; however ^{99}Tc is of environmental concern due to its long half life (2.1×10^5 years) and its mobility in groundwaters at nuclear sites worldwide (Table 1 and references therein). Technetium is a redox active radionuclide and under typical environmental pH and Eh conditions is stable in two environmentally relevant valence states; Tc(VII) and Tc(IV) (Morris et al., 2008; Icenhower et al., 2010). ^{99}Tc is typically released into the environment in the oxidised Tc(VII) valence state as TcO_4^- (pertechnetate). Pertechnetate is usually mobile in groundwaters as, due to its large size and negative charge, it is not expected to be adsorbed significantly onto clays or metal oxide minerals at environmentally relevant pH (Bird and Schwartz, 1997; Lieser and Bauscher, 1987; Lieser and Bauscher, 1988; Liu and Fan, 2005). TcO_4^- can be readily accumulated by both terrestrial and aquatic plants and organisms as a sulfate analogue and there are concerns that this could lead to contamination of the food chain (Cataldo et al., 1989; Krijger et al., 1999; Harms et al., 1999; Tagami and Uchida, 2004).

In reduced sediments ^{99}Tc exists in the Tc(IV) valence state and is found in laboratory studies primarily as hydrous TcO_2-like phases that have reduced solubility and associate with metal mineral surfaces, organic matter, carbonates and sulphides (Bird and Schwartz, 1997; Lieser and Bauscher, 1987; Wildung et al., 2004; Keith-Roach et al., 2003; Fredrickson et al., 2004; Begg et al., 2007; McBeth et al., 2007; Icenhower et al., 2010). At very low (10^{-12} mol L^{-1}) environmentally relevant concentrations where systems are undersaturated with regard to hydrous TcO_2, ^{99}Tc remained associated with the sediment (Lear et al., 2010). Consequently a useful strategy for the immobilization

of ^{99}Tc in groundwater is to reduce Tc(VII) to Tc(IV). One exception would be in the presence of soluble complexing ligands (humic acids and carbonates) when Tc(IV) may form soluble complexes and remain in solution (Wildung et al., 2000; Keith-Roach et al., 2003).

Laboratory studies have found that some dissimilatory metal reducing bacteria (*Shewanella putrefaciens, Shewanella oneidensis,Geobacter metallireducens, Clostridium sphenoides* and *Desulfovibrio fructosovorans*) are capable of reducing Tc(VII) to Tc(IV) enzymatically and this is commonly thought to occur adventitiously *via* nickel-iron hydrogenase (Lloyd et al., 1997; Wildung et al., 2004; De Luca et al., 2001; Francis et al., 2002; Marshall et al., 2008). However microbially mediated reduction of ^{99}Tc can also take place indirectly *via* reduction of Fe(III) to Fe(II) and the subsequent abiotic reaction of Tc(VII) with Fe^{2+} (Lovely et al., 1993; Lloyd et al., 1997; Lloyd and Macaskie, 1997; Lloyd et al., 1999, 2000; Wildung et al., 2000; Fredrickson et al., 2004). In most subsurface environments ^{99}Tc concentrations are low and ^{99}Tc reduction by Fe(II) species is likely to be the faster and therefore dominant reaction (Lloyd et al., 2002; Fredrickson et al., 2004; Peretyazhko et al., 2008). ^{99}Tc reduction concurrent with Fe(III) reduction has been demonstrated in numerous microcosm studies on both marine and freshwater sediments (e.g. Wildung et al., 2004; Burke et al., 2005; Burke et al., 2006; McBeth et al., 2007; Begg et al., 2007; Morris et al., 2008; Law et al., 2010a) and in field studies at Oak Ridge (Istok et al., 2004).

2.6 Research goals and approach

Due to the cost and complexity of remediating the large volumes of radioactively contaminated land, many site managing bodies are investigating the use of natural attenuation processes in place of large scale invasive treatment methods (NRC, 1993; Bayliss and Langley, 2003; Whicker et al., 2004; NDA, 2011b). The goal of this

research project was to assess the effect of bioreduction on the mobility of co-contaminants ^{90}Sr and ^{99}Tc under a pH range and nitrate concentrations relevant to the Sellafield facility, Cumbria, UK. This research was funded through the DIAMOND (Decommissioning, Immobilisation and Management of Nuclear waste for Disposal) consortium and aims to understand the effect of natural microbial processes and engineered bioreduction on the mobility of groundwater contaminants at the Sellafield site. This will enable Sellafield Ltd to further understand the behaviour of existing contaminant plumes and help predict what effect stimulating the *in-situ* microbial community might have in the event of future accidental release.

The Sellafield groundwater monitoring program has identified a contaminant plume comprised of ^{99}Tc, ^{90}Sr and nitrate that is migrating to the South-west towards the licensed site boundary (Hunter, 2004; McKenzie and Armstrong-Pope, 2010). In this project the *in situ* microbial community was stimulated *via* the addition of a simple electron donor, acetate, and the resultant changes in microbial diversity and sediment geochemistry were studied using a range of techniques. In particular the project focused on a) the effect of nitrate on the development of metal reducing conditions in which ^{99}Tc may be immobilized and b) the behaviour of Sr^{2+} during bioreduction processes. The behaviour of Sr^{2+} during bioreduction has not to our knowledge been studied in sediment systems.

2.7 References

Aarkrog, A., Dahlgaard, H., Nielsen, S.P., Trapeznikov, A.V., Molchanova, I.V., Pozolotina, V.N. Karavaeva E.N. Yushkov P.I., Polikarpov, G.G. (1997). Radioactive inventories from the Kyshtym and Karachay accidents: Estimates based on soil samples collected in the South Urals (1990-1995). *Science of the Total Environment*, 201, 137-154.

ACRO (Association pour le Contrôle de la Radioactivité de l'Ouest). (2011). Results of ACRO monitoring in Japan (15th December 2011 update). Available at: http://www.acro.eu.org/OCJ_en.html#23. Last accessed: January 11th 2012.

Adams, L.K., Boothman, C., Lloyd, J.R. (2007). Identification and characterization of a novel aciotolerant Fe(III)-reducing bacterium from a 3000-year-old acidic rock drainage site. *FEMS Microbiology Letters*, 268, 151-157.

Alvarez-Silva, M., Uribe-Salas, A., Mirnezami, M., Finch, J.A. (2010). The point of zero charge of phyllosilicate minerals using the Mular-Roberts titration technique. *Minerals Engineering*, 23, 383-389.

Anderson, R.T., Vrionis, H.A., Ortiz-Bernad, I., Resch, C.T., Long, P.E., Dayvault, R., Karp, K., Marutzky, S., Metzler, D.R., Peacock, A., White, D.C., Lowe, M. Lovley, D.R. (2003). Stimulating the in situ activity of Geobacter species to remove uranium from the groundwater of a uranium-contaminated aquifer. *Applied and Environmental Microbiology*, 69, 5884-5891.

Axe, L., Bunker, G.B., Anderson, P.R., Tyson, T.A. (1998). An XAFS analysis of strontium at the hydrous ferric oxide surface. *Journal of Colloid and Interface Science*, 199, 44-52.

Axe, L., Anderson, P.R. (1995). Sr Diffusion and Reaction within Fe Oxides - Evaluation of the Rate-Limiting Mechanism for Sorption. *Journal of Colloid and Interface Science*, 175, 157-165.

Baker, B.J., Banfield, J.F. (2003). Microbial communities in acid mine drainage. *Fems Microbiology Ecology*, 44, 139-152.

Barkay, T., Schaefer, J. (2001). Metal and radionuclide bioremediation: issues, considerations and potentials. *Current opinion in microbiology*, 4, 318-323.

Bayliss, C.R., Langley, K.F. (2003). Nuclear decommissioning, waste management, and environmental site remediation. Butterworth-Heinemann.

Beasley, T.M., Kelley, J.M., Orlandini, K.A., Bond, L.A., Aarkrog, A., Trapeznikov, A.P., Pozolotina, V.N. (1998). Isotopic Pu, U, and Np signatures in soils from Semipalatinsk-21, Kazakh Republic and the Southern Urals, Russia. *Journal of Environmental Radioactivity*, 39, 215-230.

Begg, J.D.C., Burke, I.T., Morris, K. (2007). The behaviour of technetium during microbial reduction in amended soils from Dounreay, UK. *Science of the Total Environment*, 373, 297-304.

Bird, G.A., Schwartz, W.J. (1997). Partition coefficients (K-d values) for Tc in shield lake sediments under oxidizing and reducing conditions. *Water Research*, 31, 1673-1678.

Black, J.H., Brightman, M.A. (1996). Conceptual model of the hydrogeology of Sellafield. *Quarterly Journal of Engineering Geology*, 29, S83-S93.

Bradsher, K., Tabuchi, H. (2011). Greater danger lies in spent fuel than in reactors – New York Times. Available at: http://www.nytimes.com/2011/03/18/world/asia/18spent.html?_r=1&pagewanted=2&src=twrhp. Last accessed: January 6th 2012.

Burke, I.T., Boothman, C., Lloyd, J.R., Mortimer, R.J.G., Livens, F.R., Morris, K. (2005). Effects of progressive anoxia on the solubility of technetium in sediments. *Environmental Science & Technology*, 39, 4109-4116.

Burke, I.T., Boothman, C., Lloyd, J.R., Livens, F.R., Charnock, J.M., McBeth, J.M., Mortimer, R.J.G., Morris, K. (2006). Reoxidation behavior of technetium, iron, and sulfur in estuarine sediments. *Environmental Science & Technology*, 40, 3529-3535.

Carroll, S.A., Roberts, S.K., Criscenti, L.J., O'Day, P.A. (2008). Surface complexation model for strontium sorption to amorphous silica and goethite. *Geochemical Transactions*, 2, 9.

Carter, J.T., Jones R.H., Luptak, A.J. (2011). U.S radioactive waste inventory and characteristics related to potential future nuclear energy systems. Department of Energy Report: FCRD-USED-2011-000068, Rev 2.

Cataldo, D.A., Garland, T.R., Wildung, R.E., Fellows, R.J. (1987). Comparative metabolic behaviour and interrelationships of Tc and S in soybean plants. *Health Physics*, 57, 281-287.

Chaplow, R. (1994). The geology and hydrogeology of Sellafield: An overview. *Quarterly Journal of Engineering Geology*, 29, S1- S12.

Chen, C.C., Hayes, K.F. (1999). X-ray absorption spectroscopy investigation of aqueous Co(II) and Sr(II) sorption at clay-water interfaces. *Geochimica Et Cosmochimica Acta*, 63, 3205-3215.

Christensen, G.C., Romanov, G.N., Strand, P., Salbu, B., Malyshev, S.V., Bergan, T.D., Oughton, D., Drozhko, E.G., Glagolenko, Y.V., Amundsen, I., Rudjord, A.L., Bjerk, T.O., Lind, B.(1997). Radioactive contamination in the environment of the nuclear enterprise 'Mayak' PA. Results from the joint Russian-Norwegian field work in 1994. *Science of the Total Environment*, 202, 237-248.

Coleman, M.L., Hedrick, D.B., Lovley, D.R., White, D.C., Pye, K. (1993). Reduction of Fe(III) in sediments by sulphate reducing bacteria. *Nature*, 361, 436-438.

Cutting, R.S., Coker, V.S., Fellowes, J.W., Lloyd, J.R., Vaughan, D.J. (2009). Mineralogical and morphological constraints on the reduction of Fe(III) minerals by Geobacter sulfurreducens. *Geochimica et Cosmochimica Acta*, 73, 4004-4022.

De Luca, G., De Philip, P., Dermoun, Z., Rousset, M., Vermeglio, A. (2001). Reduction of technetium(VII) by *Desulfovibrio fructosovorans* is mediated by the nickel-iron hydrogenase. *Applied and Environmental Microbiology*, 67, 4583-4587.

DECC (Department of Energy and Climate Change). (2010). Planning for new energy infrastructure – consultation on revised draft policy statements for energy infrastructure. London. HMSO. Available at: http://webarchive.nationalarchives.gov.uk/20110302182042/https://www.energynpsconsultation.decc.gov.uk/docs/ConsultationDocument.pdf. Last accessed: February 27th 2012.

DECC (Department of Energy and Climate Change). (2011). Management of the UK's plutonium stocks – a consultation response on the long-term management of UK-owned separated civil plutonium. London. Available at: http://www.decc.gov.uk/assets/decc/Consultations/plutonium-stocks/3694-govt-resp-mgmt-of-uk-plutonium-stocks.pdf. Last accessed: February 27th 2012.

Department of Ecology (state of Washington). (2011). About Hanford. Available at: http://www.ecy.wa.gov/programs/nwp/. Last accessed: January 3rd 2012.

Dewiere, L., Bugai, D., Grenier, C., Kashparov, V., Ahamdach, N. (2004). Sr-90 migration to the geo-sphere from a waste burial in the Chernobyl exclusion zone. *Journal of Environmental Radioactivity*, 74, 139-150.

Dichristina, T.J. (1992). Effects of Nitrate and Nitrite on Dissimilatory Iron Reduction by Shewanella-Putrefaciens Strain-200. *Abstracts of Papers of the American Chemical Society*, 203, 127.

DOE (Department of Energy). (2010). Nevada National Security Site Environmental Report. Available at: http://www.nv.energy.gov/library/Publications/aser.aspx. Last accessed: February 27th 2012.

Dyer, A., Chow, J.K.K., Umar, I.M. (2000). The uptake of caesium and strontium radioisotopes onto clays. *Journal of Material Chemistry*, 10, 2734-2740.

Edwards, L., Kusel, K., Drake, H., Kostka, J.E. (2007). Electron flow in acidic subsurface sediments co-contaminated with nitrate and uranium. *Geochimica Et Cosmochimica Acta*, 71, 643-654.

Eisenbud, M., Gesell, T. (1997) Environmental Radioactivity- from natural, industrial and military sources. Fourth edition. Academic press Ltd, London.

El-Ghonemy, H. (2004). SCLS Groundwater conceptual model. Nuclear Science and Technology Sevices. BNFL technical report: NSTS 4443. Available at: http://www.sellafieldsites.com/land/documents/Hydrogeological%20Conceptual%20Model.pdf. Last accessed: March 21st 2012.

Ellis, A.T., Staples, K.M. (2005). The management of magnox graphite reactor cores to underwrite continued safe operation. In Conference on Ageing Management of Graphite Reactor Cores. Neighbour, G.B. (ed). Royal Society of Chemistry, pp. 3-10, Cardiff.

European Nuclear Society. (2011). Nuclear power plants world-wide. Available at: http://www.euronuclear.org/1-information/npp-ww.htm. Last accessed: October 1st 2011.

Evans, S. (2011). Germany: nuclear power plants to close by 2022, BBC News website, 30th May 2011. Available at: http://www.bbc.co.uk/news/world-europe-13592208. Last accessed: February 20th 2012.

Ferris, F.G., Hallberg, R.O., Lyvén, B., Pedersen, K., (2000). Retention of strontium, cesium, lead and uranium by bacterial iron oxides from a subterranean environment. *Applied Geochemistry*, 15, 1035-1042.

Finch, A.A., Allison, N., Sutton, S.R., Newville, M. (2003). Strontium in coral aragonite: 1. Characterization of Sr coordination by extended absorption X-ray fine structure. *Geochimica et Cosmochimica Acta*, 67, 1189-1194.

Finneran, K.T., Housewright, M.E., Lovley, D.R. (2002). Multiple influences of nitrate on uranium solubility during bioremediation of uranium-contaminated subsurface sediments. *Environmental Microbiology*, 4, 510-516.

Foulkes, I. (2011). Swiss search for strategy on nuclear power. BBC News, Geneva. 23rd March 2011. Available at: http://www.bbc.co.uk/news/world-europe-12822969. Last accessed: Feburary 22nd 2012.

Francis, AJ, Dodge, CJ and Meinken, GE. (2002). Biotransformation of pertechnetate by Clostridia. Radiochimica Acta, 90: 791-797.

Fredrickson, J.K., Zachara, J.M., Balkwill, D.L., Kennedy, D., Li, S.M.W., Kostandarithes, H.M., Daley, M.J., Romine, M.F., Brockman, F.J. (2004). Geomicrobiology of high-level nuclear waste-contaminated vadose sediments at the Hanford Site, Washington State. *Applied Environmental Microbiology*, 70, 4230-4241.

Fujita, Y., Redden, G.D., Ingram, J.C., Cortez, M.M., Ferris, F.G., Smith, R.W. (2004). Strontium incorporation into calcite generated by bacterial ureolysis. *Geochimica Et Cosmochimica Acta*, 68, 3261-3270.

Fukushima update. (2011). Available at: http://fukushimaupdate.com/. Last accessed: January 6th 2012.

Gadd, G.M. (2010). Metals, minerals and microbes: geomicrobiology and bioremediation. SGM prize lecture. *Microbiology*, 156, 609-643.

Gadde, R.R., Laitinen, H.A. (1974). Heavy metal absorption by hydrous iron and manganese oxides. *Analytical Chemistry*, 46, 2022-2026.

Gazea, B, Adam, K., Kontopoulos, A. (1996). A review of passive systems for the treatment of acid mine drainage. *Minerals Engineering*, 9, 23-42.

Geniesse, D.J., Stegen, G.E. (2009). 2009 evaluation of tritium removal and mitigation technologies for wastewater treatment. US Department of Energy report DOE/RL-2009-18.

Glasstone, S., Sesonske, A. (1994). Nuclear reactor engineering - 4th edition. Chapman and Hall, London.

Gray, J., Jones, S.R., Smith, A.D. (1995). Discharges to the environment from the Sellafield site, 1951-1992. *Journal of Radiological Protection*, 15, 99-131.

Greegor, R.B., Pingitore, N.E., Lytle, F.W. (1997). Strontianite in coral skeletal aragonite. *Science*, 275, 1452-1454.

Hamilton, E.I. (1999). The role of near-shore industrial waste releases in the dispersion of radionuclides in the NE Irish Sea. *Journal of Environmental Radioactivity*, 44, 297- 333.

Handley-Sidhu, S., Renshaw, J.C., Moriyama, S., Stolpe, B., Mennan, C., Bagheriasl, S., Yong, P., Stamboulis, A., Paterson-Beedle, M., Sasaki, K., Pattrick, R.A.D., Lead, J.R., MacAskie, L.E. (2011). Uptake of Sr^{2+} and Co^{2+} into biogenic hydroxyapatite: Implications for biomineral ion exchange synthesis. *Environmental Science & Technology*, 45, 6985-6990.

Harms, A.V., Krijger, G.C., van Elteren, J.T., de Goeij, J.J.M. (1999). Characterization of technetium species induced in spinach. *Journal of Environmental Quality*, 28, 1188-1194.

Henry, L.A., Douhovnikoff, V. (2008). Environmental issues in Russia. *In Annual Review of Environment and Resources*, 437-460.

Herbert, R.B., Benner, S.G., Pratt, A.R., Blowes, D.W. (1998). Surface chemistry and morphology of poorly crystalline iron sulfides precipitated in media containing sulphate -reducing bacteria. *Chemical Geology*, 144, 87-97.

Hoffman, D.C., Stone, R., Dudley, W.W. (1977). Radioactivity in the underground environment of the Cambric nuclear explosion at the Nevada test site. Technical Report: LA--6877-MS. U.S. Government printing office.

Hoffman, A., Beinum, W.V., Meeussen, J.C.L., Kretzschmar, R. (2005). Sorption kinetics of strontium in porous hydrous ferric oxide aggregates II. Comparison of experimental results and model predictions. *Journal of Colloid and Interface Science*, 283, 29-40.

Hoitink, D.J., Burk, K.W., Ramsdell, J.V., Shaw, W.J. (2005). Hanford site climatological summary 2004 with historical data. DOE Report. Available at: http://www.pnl.gov/main/publications/external/technical_reports/PNNL-15160.pdf. Last accessed: February 22nd 2012.

Hull, L.C., Schafer, A.L. (2008). Accelerated transport of Sr-90 following a release of high ionic strength solution in vadose zone sediments. *Journal of Contaminant Hydrology*, 97, 135-157.

Hunter, J. (2004). SCLS Phase 1- Conceptual Model of Contamination Below Ground at Sellafield. Nuclear Sciences and Technology Services, BNFL. Report NSTS 4920. Available at: http://www.sellafieldsites.com/land/documents/ContaminationConceptualmodel.pdf. Last accessed: February 27th 2012.

IAEA (International Atomic Energy Agency). (2008). INES – The international nuclear and radiological events scale. Factsheet available at: http://www.iaea.org/Publications/Factsheets/English/ines.pdf. Last accessed: 22nd February 2012.

Icenhower, J.P., Qafoku, N.P., Zachara, J.M., Martin, W.J. (2010). The biogeochemistry of technetium: a review of the behaviour of an artificial element in the natural environment. *American Journal of Science*, 310, 721-752.

Istok, J.D., Senko, J.M., Krumholz, L.R., Watson, D., Bogle, M.A., Peacock, A., Chang, Y.J., White, D.C. (2004). In situ bioreduction of technetium and uranium in a nitrate-contaminated aquifer. *Environmental Science & Technology*, 38, 468-475.

Jackson, R.E., Inch, K.J. (1989). The in-situ adsorption of strontium-90 in a sand aquifer at the chalk river nuclear laboratories Canada. *Journal of Contaminant Hydrology*, 4, 27-50.

Kappler, A., Straub, K.L. (2005). Geomicrobiological cycling of iron. *Reviews in Mineralogy and Geochemistry*, 59, 85-108.

Keith-Roach, M.J., Day, P.J., Fifield, K.L., Bryan, N.D., Livens, F.R. (2000). Seasonal variations in interstitial water transuranium element concentrations. *Environmental Science & Technology*, 34, 4273-4277.

Keith-Roach, M.J., Morris, K., Dahlgaard, H. (2003). An investigation into technetium binding in sediments. *Marine Chemistry*, 81, 149-162.

Kershaw, P.J., McCubbin, D., Leonard, K.S. (1999). Continuing contamination of north Atlantic and Arctic waters by Sellafield radionuclides. *Science of the Total Environment*, 237-238, 119-132.

Konhauser, K.O., Mortimer, R.J.G., Morris, K., Dunn, V. (2002). Chapter 3 The role of microorganisms during sediment diagenesis: Implications for radionuclide mobility. Interactions of Microorganisms with Radionuclides. *Radioactivity in the Environment*, 2, 61-100.

Konhauser, K. (2007). Introduction to geomicrobiology. Blackwell Science Ltd, Oxford,UK.

Krijger, G.C., Harms, A.V., Leen, R., Verburg, T.G., Wolterbeek, B. (1999). Chemical forms of technetium in tomato plants; TcO4-, Tc-cysteine, Tc-glutathione and Tc-proteins. *Environmental and Experimental Botany*, 42, 69-81.

Langley, S., Gault, A.G., Ibrahim, A., Takahashi, Y., Renaud, R., Fortin, D., Clark, I.D. Ferris, F.G. (2009a). Sorption of Strontium onto bacteriogenic iron oxides. *Environmental Science & Technology*, 43, 1008-1014.

Langley, S., Gault, A.G., Ibrahim, A., Takahashi, Y., Renaud, R., Fortin, D., Clark, I.D., Ferris, F.G. (2009b). Strontium desorption from bacteriogenic iron oxides (BIOS) subjected to microbial Fe(III) reduction. *Chemical Geolology*, 262.

Law, G.T.W., Geissler, A., Boothman, C., Burke, I.T., Livens, F.R., Lloyd, J.R., Morris, K. (2010a). Role of nitrate in conditioning aquifer sediments for technetium bioreduction. *Environmental Science & Technology*, 44, 150-155.

Law, G.T.W., Geissler, A., Lloyd, J.R., Livens, F.R., Boothman, C., Begg, J.D., Denecke, M.A., Rothe, J., Dardene, K., Burke, I.T., Charnock, J.M., Morris, K. (2010b).Geomicrobiological redox cycling of the transuranic element neptunium. *Environmental Science & Technology*, 44, 8924-8929.

Lear, G., McBeth, J.M., Boothman, C., Gunning, D.J., Ellis, B.L., Lawson, R.S., Morris, K., Burke, I.T., Bryan, N.D., Brown, A.P., Livens, F.R., Lloyd, J.R. (2010). Probing the biogeochemical behaviour of technetium using a novel nuclear imaging approach. *Environmental Science & Technology*, 44, 156-162.

Li, X.Z., Krumholz, L.R. (2008). Influence of nitrate on microbial reduction of pertechnetate. *Environmental Science & Technology*, 42, 1910-1915.

Li, X.Z., Spain, A.M., Senko, J.M., Istok, J.D., Krumholz, L.R. (2008). Interactions of Nitrate, Iron, Uranium and Technetium during bioremediation. *Geochimica et Cosmochimica Acta*, 72, A546-A546.

Lieser, K.H., Bauscher, C. (1987). Technetium in the Hydrosphere and in the Geosphere .1. Chemistry of Technetium and Iron in Natural-Waters and Influence of the Redox Potential on the Sorption of Technetium. *Radiochimica Acta*, 42, 205-213.

Lieser, K.H., Bauscher, C. (1988). Technetium in the Hydrosphere and in the Geosphere .2. Influence of Ph, of Complexing Agents and of Some Minerals on the Sorption of Technetium. *Radiochimica Acta*, 44, 125-128.

Liu, D.J., Fan, X.H. (2005). Adsorption behaviour of ^{99}Tc on Fe, Fe_2O_3 and Fe_3O_4. *Journal of Radioanalytical and Nuclear Chemistry*, 264, 691-698.

Lloyd, J.R., Cole, J.A., Macaskie, L.E. (1997). Reduction and removal of heptavalent technetium from solution by *Escherichia coli*. *Journal of Bacteriology*, 179, 2014-2021.

Lloyd, J.R., Chesnes, J., Glasauer, S., Bunker, D.J., Livens, F.R., Lovley, D.R. (2002). Reduction of actinides and fission products by Fe(III)-reducing bacteria. *Geomicrobiology Journal*, 19, 103-120.

Lloyd, J.R. (2003). Microbial reduction of metals and radionuclides. *FEMS Microbiology Reviews*, 27, 411-425.

Lloyd, J.R., Renshaw, J.C. (2005a). Microbial transformations of radionuclides: Fundamental mechanisms and biogeochemical implications. *Metal Ions in Biological Systems*, 44, 205-240.

Lloyd, J.R., Renshaw, J.C. (2005b). Bioremediation of radioactive waste: radionuclide-microbe interactions in laboratory and field-scale studies. *Current Opinion in Biotechnology*, 16, 254-260.

Long, M.E. (2012). Half life - The lethal legacy of Americas nuclear waste. National Geographic online. Available at:

http://science.nationalgeographic.com/science/earth/inside-the-earth/nuclear-waste/#page=10. Last accessed: February 26th 2012.

Lovley, D.R. (1991). Dissimilatory Fe(III) and Mn(IV) reduction. *Microbiological Reviews*, 55, 259-287.

Lovley, D.R., Phillips, E.J.P., Lonergan, D.J. (1989). Hydrogen and formate oxidation coupled to dissimilatory reduction of iron or manganese by *alteromonas-putrefaciens*. *Applied and Environmental Microbiology*, 55, 700-706.

Lovley, D.R., Giovannoni, S.J., White, D.C., Champine, J.E., Phillips, E.J.P., Gorby, Y.A., Goodwin, S. (1993). *Geobacter-metallireducens* gen-nov, a microorganism capable of coupling the complete oxidation of organic-compounds to the reduction of iron and other metals. *Archives of Microbiology*, 159, 336-344.

Luu, Y., Ramsay, J.A. (2003). Review: microbial mechanisms of accessing insoluble Fe(III) as an energy source. *World Journal of Microbiology and Biotechnology*, 19, 215-225.

Madigan, M.T., Martinko, J.M. (2006). Brock Biology of Microorganisms: eleventh edition. Pearson Education LTD.

Marshall, M.J., Plymale, A.E., Kennedy, D.W., Shi, L., Wang, Z.M., Reed, S.B. Dohonalkova, S.B., Simonson, C.J. Liu, C.X., Saffarini, D.A., Romine, M.F., Zachara, J.M., Beliaev, A.S., Fredrickson, J.K. (2008). Hydrogenase- and outer membrane c-type cytochrome-facilitated reduction of technetium(VII) by *Shewanella oneidensis* MR-1. *Environmental Microbiology*, 10, 125-136

Mason, C.F.V., Lu, N., Conca, J. (2000). Radioactive strontium- and caesium-contaminated sites: Characterisation, transport, and remedial options. *Nuclear Physical Methods in Radioecological Investigations of Nuclear Test Sites*, 31, 89-97.

McBeth, J.M., Lear, G., Lloyd, J.R., Livens, F.R., Morris, K., Burke, I.T. (2007). Technetium reduction and reoxidation in aquifer sediments. *Geomicrobiology Journal*, 24, 189-197.

McBeth, J.M., Lloyd, J.R., Law, G.T.W., Livens, F.R., Burke, I.T., Morris, K. (2011). Redox interactions of technetium with iron-bearing minerals. *Mineralogical Magazine*, 75, 2419-2430.

McKenzie, H, Armstrong-Pope, N. (2010). Groundwater Annual Report 2010. Sellafield Ltd. Technical report TECH000613. Available at: http://www.sellafieldsites.com/land/documents/Groundwater_Annual_Report_2010.pdf. Last accessed: February 11th 2012.

McKie, R. (2009). Sellafield: the most hazardous place in Europe. The Observer – published Sunday 19th April 2009. Available at: http://www.guardian.co.uk/environment/2009/apr/19/sellafield-nuclear-plant-cumbria-hazards. Last accessed: January 11th 2012.

McKinley, J.P., Zachara, J.M., Smith, S.C., Liu, C. (2007). Cation exchange reactions controlling desorption of Sr-90(2+) from coarse-grained contaminated sediments at the Hanford site, Washington. *Geochimica et Cosmochimica Acta*, 71, 305-325.

Michalsen, M.M., Peacock, A.D., Smithgal, A.N., White, D.C., Spain, A.M., Sanchez-Rosario, Y., Krumholz, M.R., Kelly, S.D., Kemner, K.M., McKinley, J., Heald, S.M., Bogle, M.A., Watson, D.B., Istok J.D. (2009). Treatment of Nitric Acid-, U(VI)-, and Tc(VII)-Contaminated Groundwater in Intermediate-Scale Physical Models of an In Situ Biobarrier. *Environmental Science & Technology*, 43, 1952-1961.

Michie, U. (1996). The geological framework of the Sellafield are and its relationship to hydrogeology. *Quarterly Journal of Engineering Geology*, 29, S13- S27

Mitchell, A.C., Ferris, F.G. (2005). The coprecipitation of Sr into calcite precipitates induced by bacterial ureolysis in artificial groundwater: Temperature and kinetic dependence. *Geochimica et Cosmochimica Acta*, 69, 4199-4210.

Morris, K., Livens, F.R. (1996). The distribution of transuranic elements in sediment profiles from an intertidal area in West Cumbria, UK. *Radiochimica Acta*, 74, 195-198.

Morris, K., Livens, F.R., Charnock, J.M., Burke, I.T., McBeth, J.M., Begg, J.D.C., Boothman, C., Lloyd, J.M. (2008). An X-ray absorption study of the fate of technetium in reduced and reoxidised sediments and mineral phases. *Applied Geochemistry.* 23, 603-617.

NDA (Nuclear Decommissioning Authority). (2010). Radioactive wastes in the UK: The 2010 estimate of radioactive waste for geological disposal, NDA/ST/STY(11)0050. Available at: http://www.nda.gov.uk/documents/loader.cfm?csModule=security/getfile&PageID=48209. Last accessed: February 22nd 2012.

NDA (Nuclear Decommissioning Authority). (2011a). Nuclear Decommissioning Authority Annual Report & Accounts 2010/11. HC1244. Available at: http://www.nda.gov.uk/documents/upload/Annual-Report-and-Accounts-2010-2011.pdf. Last accessed: February 16th 2012.

NDA (Nuclear Decommissioning Authority). (2011b). Nuclear Decommissioning Authority: Strategy - effective from April 2011. Available at: http://www.nda.gov.uk/documents/upload/NDA-Strategy-Effective-from-April-2011-full-colour-version.pdf. Last accessed: February 22nd 2012.

Nealson, K.H., Saffarini, D. (1994). Iron and manganese in anaerobic respiration: Environmental significance, physiology, and regulation. *Annual Review of Microbiology*, 311-343.

North, N.N., Dollhopf, S.L., Petrie, L., Istok, J.D., Balkwill, D.L., Kostka, J.E. (2004). Change in bacterial community structure during in situ biostimulation of subsurface sediment cocontaminated with uranium and nitrate. *Applied and Environmental Microbiology*, 70, 4911-4920.

NRC (National Research Council). (1993). In Situ Bioremediation: When Does It Work? National Academy Press, Washington, DC.

Nuttall, W.J. (2005). Nuclear renaissance - technologies and policies for the future of nuclear power. Taylor and Francis, New York.

O'Day, P.A., Newville, M., Neuhoff, P.S., Sahai, N., Carroll, S.A. (2000). X-ray absorption spectroscopy of strontium(II) coordination - I. Static and thermal disorder in crystalline, hydrated, and precipitated solids and in aqueous solution. *Journal of Colloid Interface Science*, 222, 184-197.

Openshaw, S., Caver, S., Fernie, J. (1989). Britain's nuclear waste: safety and siting. Belhaven Press, London.

ORNL (Oak Ridge National Laboratory). (2011). Subsurface biogeochemical research website. Available at: http://www.esd.ornl.gov/orifrc/. Last accessed March 22nd 2012.

Parkman, R.H., Charnock, J.M., Livens, F.R., Vaughan, D.J. (1998). A study of the interaction of strontium ions in aqueous solution with the surfaces of calcite and kaolinite. *Geochimica Et Cosmochimica Acta*, 62, 1481-1492.

Parmar, N., Warren, L.A., Roden, E.E., Ferris, F.G. (2000). Solid phase capture of strontium by the iron reducing bacteria *Shewanella alga* strain BrY. *Chemical Geology*, 169, 281-288.

Petrie, L., North, N.N., Dollhopf, S.L., Balkwill, D.L., Kostka, J.E. (2003). Enumeration and characterisation of Fe(III) reducing microbial communities from acidic subsurface sediments contaminated with uranium (VI). *Applied Environmental Microbiology*, 69, 7467-7479.

Pingitore, N.E., Lytle, F.W., Davies, B.M., Eastman, M.P., Eller, P.G., Larson, E.M. (1992). Mode of incorporation of Sr^{2+} in calcite – determination by X-ray absorption-spectroscopy. *Geochimica et Cosmochimica Acta*, 56, 1531-1538.

Priest, N.D., Kuyanova, Y., Pohl, P., Burkitbayev, M., Mitchell, P.I., Vintro, L.L., Strilchuk, Y.G., Lukashenko, S.N. (2008). Strontium-90 contamination within the Semipalatinsk nuclear test site: Results of SEMIRAD1 and SEMIRAD2 projects - Contamination levels and projected doses to local populations. *Nuclear Risks in Central Asia*, 87-105.

Raabe, O.G. (2010). Concerning the health effects of internally deposited radionuclides. *Health Physics*, 98, 515-536.

Riley, R.G., Zachara, J.M. (1992). Chemical Contaminants on DOE Lands and Selection of Contaminant Mixtures for Subsurface Science Research. DOE/ER-0547T. US Department of Energy, 77.

Robinson, C., Barry, D.A., McCarty, P.L., Gerhard, J.I., Kouznetsova, I. (2009). pH control for enhanced reductive bioremediation of chlorinated solvent source zones. *Science of the Total Environment*, 407, 4560-4573.

Roden, E.E., Leonardo, M.R., Ferris, F.G. (2002). Immobilization of strontium during iron biomineralization coupled to dissimilatory hydrous ferric oxide reduction. *Geochimica Et Cosmochimica Acta*, 66, 2823-2839.

Roden, E.E., Kappler, A., Bauer, I., Jiang, J., Paul, A., Stoesser, R., Konishi, H., Xu, H. (2010). Extracellular electron transfer through microbial reduction of solid-phase humic substances. *Nature Geoscience*, 3, 417-421.

Ronneau, C., Bitchaeva, O. (1997). Biotechnology for Waste Management and Site Restoration: technological, Educational, Business, Political Aspects. NATO ASI Series, Volume 34 – Chapter 6. Kluwer academic publishers, Dordrecht, Netherlands.

RSC (Royal Society of Chemistry). (2011). Royal Society of Chemistry-Radiochemistry group essays on radiochemistry. Essay 7: The Nuclear Fuel Cycle. Available on: http://www.rsc.org/Membership/Networking/InterestGroups/Radiochemistry/Essays.asp. Last accessed: February 26th 2012.

Sahai, N., Carroll, S.A., Roberts, S., O'Day, P.A. (2000). X-ray absorption spectroscopy of strontium(II) coordination - II. Sorption and precipitation at kaolinite, amorphous silica, and goethite surfaces. *Journal of Colloid & Interface Science*, 222, 198-212.

Sellafield Ltd. (2011). Sellafield Ltd website. Available at: http://www.sellafieldsites.com/. Last accessed: March 21st 2012.

Shandala, N.K., Sneve, M.K., Smith, G.M., Kiselev, M.F., Kochetkov, O.A., Savkin, M.N., Simakov, A.V., Novikova, N.Y., Titov, A.V., Romanov, V.V., Seragin, V.A., Filonova, A.V., Semenova, M.P. (2008). Regulatory supervision of sites for spent fuel and radioactive waste storage in the Russian Northwest. *Journal of Radiological Protection*, 28, 453-465.

Singleton, M.J., Woods, K.N., Conrad, M.E., Depaolo, D.J., Dresel, P.E. (2005). Tracking sources of unsaturated zone and groundwater nitrate contamination using nitrogen and oxygen stable isotopes at the Hanford Site, Washington. *Environmental Science & Technology*, 39, 3563-3570.

Small, T.D., Warren, L.A., Roden, E.E., Ferris, F.G. (1999). Sorption of strontium by bacteria, Fe(III) oxide, and bacteria-Fe(III) oxide composites. *Environmental Science & Technology*, 33, 4465-4470.

Smith-Briggs, J.L., Craig, D.R., Wells, D.A., Crookshanks, C.E., Poole, M., Hooker, P.J., Shaw, R.P., Chertkov, L.G., Glinsky, M.L., Glagolev, A.V., Samsonova, L., Drozhko, E.G., Glagolenko, Y., Mokrov, Y.G., Ivanov, I.A., Stukalov, P., Yegorov, V., Glagoleva, M. (2000). Assessment of situation and disposal concepts for radioactive waste arising from reprocessing operations at Chelyabinsk-65 (Mayak), European Commission- nuclear safety and the environment. Overview Report, EUR 19262. Available at: http://ec.europa.eu/energy/nuclear/studies/doc/other/eur19262.pdf. Last accessed: March 21st 2012.

Solecki, J. (2005). Investigation of Sr-85 adsorption on selected soils of different horizons. *Journal of Environmental Radioactivity*, 82, 303-320.

Standring, W.J.F., Oughton, D.H., Salbu, B. (2002). Potential remobilization of Cs-137, Co-60, Tc-99 and Sr-90 from contaminated Mayak sediments river and estuary environments. *Environmental Science & Technology*, 36, 2330-2337.

Standring, W.J.F., Dowdall, M., Reistad, O., Amundsen, I.B. (2009a). Radioactive contamination of groundwater at the Andreeva Bay Shore Technical Base, Northwest Russia. *Journal of Radioanalytical and Nuclear Chemistry*, 279, 227-235.

Standring, W.J.F., Dowdall, M., Strand, P. (2009b). Overview of dose assessment developments and the health of riverside residents close to the "Mayak" PA facilities, Russia. *International Journal of Environmental Research and Public Health*, 6, 174-199.

Stewart, D.I., Burke, I.T., Hughes-Berry, D.V., Whittleston, R.A. (2010). Microbially mediated chromate reduction in soil contaminated by highly alkaline leachate from chromium containing waste. *Ecological Engineering*, 36, 211-221.

Suzuki, J., Kelly, S.D., Kemner, K.M., Banfield, J.F. (2003). Microbial populations stimulated for hexavalent uranium reduction in uranium mine sediment. *Applied and Environmental Microbiology*, 69, 1337-1346.

Szasz, F,M. (1984). The Day the Sun Rose Twice: University of New Mexico Press.

Tagami, K., Uchida, S. (2004). Comparison of transfer and distribution of technetium and rhenium in radish plants from nutrient solution. *Applied Radiation and Isotopes*, 61, 1203-1210.

Thamdrup, B. (2000). Bacterial manganese and iron reduction in aquatic sediments. *Advances in Microbial Ecology*,16, 41-84.

Thorpe, C.L., Law, G.T.W., Boothman, C., Lloyd, J.R., Burke, I.T., Morris, K. (2012a). The synergistic effects of high nitrate concentrations on sediment bioreduction. *Geomicrobiology Journal*, 29, 484-493.

Thorpe, C.L., Morris, K., Boothman, C., Lloyd, J.R., (2012b). Alkaline Fe(III) reduction by a novel alkali-tolerant *Serratia* sp. isolated from surface sediments close to Sellafield nuclear facility, UK. *FEMS Microbiology Letters*, 327, 87-92.

Wall, J.D., Krumholz, L.R. (2006). Uranium Reduction. *Annual Review of Microbiology*, 60, 149-166.

Watson, D.B., Kostka, J.E., Fields, M.W., Jadine, P.M. (2004). The Oak Ridge Field Research Centre conceptual model. NABIR. Available at: http://public.ornl.gov/orifc/FRC-conceptual-model.pdf. Last accessed: February 28th 2012.

Webb, G.A.M., Anderson, R.W., Gaffney, M.J.S. (2006). Classification of events with an off-site radiological impact at the Sellafield site between 1950 and 2000, using the International Nuclear Event Scale. *Journal of Radiological Protection* 26, 33-49.

Weon, S.Y., Lee, C.W., Lee, S.I., Koopman, B. (2002). Nitrite inhibition of aerobic growth of *Acinetobacter sp*. *Water Research*, 36, 4471-4476.

Whicker, F.W., Hinton, T.G., MacDonell, M.M., Pinder, J.E., Habegger L.J. (2004). Avoiding destructive remediation at DOE sites. *Science*, 303, 1615-1616.

Wildung, R.E., Li, S.W., Murray, C.J., Krupka, K.M., Xie, Y., Hess, N.J., Roden, E.E. (2004). Technetium reduction in sediments of a shallow aquifer exhibiting dissimilatory iron reduction potential. *FEMS Microbiology Ecology*, 49, 151-162.

Wilkins, M.J., Livens, F.R., Vaughan, D.J., Beadle, I., Lloyd, J.R. (2007). The influence of microbial redox cycling on radionuclide mobility in the subsurface at a low-level radioactive waste storage site. *Geobiology*, 5, 293-301.

Wilson, PD. (1996). Nuclear fuel cycle: from ore to wastes. Oxford University Press.

WNA (World Nuclear Association). (2011a). World uranium mining. Available on: http://www.world-nuclear.org/info/inf23.html. Last accessed: October 1st 2011.

WNA (World Nuclear Association). (2011b). Processing of used nuclear fuel. Available on: http://www.world-nuclear.org/info/inf69.html. Last accessed: March 22nd 2012.

WHO (World Health Organisation). (1993). Guidelines for drinking-water quality – 2nd Edition. Volume 1: Recommendations, World Health Organisation Press, Geneva.

Yamamoto, M., Takada, T., Nagao, N., Hoshi, M., Zumadiov, K., Shima, T., Fukuoka, M., Kimura, S. (2011). Present situation of radioactive contamination in soil by the Fukushima Dai-Ichi accident. Session 23A Goldschmidt conference, Prague

Yoshida, N. (2011). A preliminary overview of studies on dispersals of radionuclides from Fukushima nuclear power plants. Session 23A Goldschmidt conference, Prague.

Zhou, Y., Pijuan, M., Yuan, Z.G. (2007). Free nitrous acid inhibition on anoxic phosphorus uptake and denitrification by poly-phosphate accumulating organisms. *Biotechnology and Bioengineering*, 98, 903-912.

Zhou, Y., Ganda, L., Lim, M., Yuan, Z.G., Kjelleberg, S., Ng, W.J. (2010). Free nitrous acid (FNA) inhibition on denitrifying poly-phosphate accumulating organisms (DPAOs). *Applied Microbiology and Biotechnology*, 88, 359-369.

Chapter 3: The synergistic effects of high nitrate concentrations on sediment bioreduction

This chapter contains the following published paper:

Thorpe, C.L., Law, G.T.W., Boothman, C., Lloyd, J.R., Burke, I.T., Morris, K. (2012). The Synergistic Effects of High Nitrate Concentrations on Sediment Bioreduction. *Geomicrobiology Journal*, 29:5, 484-493. http://dx.doi.org/10.1080/01490451.2011.581332

Geomicrobiology Journal, 29:484–493, 2012

ISSN: 0149-0451 print / 1521-0529 online
DOI: 10.1080/01490451.2011.581332

Taylor & Francis
Taylor & Francis Group

The Synergistic Effects of High Nitrate Concentrations on Sediment Bioreduction

Clare L. Thorpe,[1] Gareth T. W. Law,[1] Christopher Boothman,[1] Jonathan R. Lloyd,[1] Ian T. Burke,[2] and Katherine Morris[1]

[1]*Research Centre for Radwaste and Decommissioning and Williamson Research Centre for Molecular Environmental Science, School of Earth, Atmospheric and Environmental Sciences, The University of Manchester, Manchester, United Kingdom*

[2]*Earth System Science Institute, School of Earth and Environment, The University of Leeds, Leeds, United Kingdom*

Groundwaters at nuclear sites can be characterized by low pH and high nitrate concentrations (10–100 mM). These conditions are challenging for bioremediation, often inhibiting microbial Fe(III)-reduction which can limit radionuclide migration. Here, sediment microcosms representative of the UK Sellafield site were used to study the influence of variable pH and nitrate concentrations on microbially-mediated TEAP (terminal electron accepting processes) progression. The rate of reduction through the terminal electron accepting cascade NO_3^- > NO_2^- > Mn(IV)/Fe(III) > SO_4^{2-} at low pH (∼5.5) was slower than that in bicarbonate buffered systems (pH ∼ 7.0), but in the low pH systems, denitrification and associated pH buffering resulted in conditioning of the sediments for subsequent Fe(III) and sulfate-reduction. Under very high nitrate conditions (100 mM), bicarbonate buffering (pH ∼ 7.0) was necessary for TEAP progression beyond denitrification and the reduction of 100 mM nitrate created alkaline conditions (pH 9.5). 16S rRNA gene analysis showed that close relatives of known nitrate reducers *Bacillus niacini* and *Ochrobactrum grignonense* dominated the microbial communities in this reduced sediment. In Fe(III)-reducing enrichment cultures from the 100 mM nitrate system, close relatives of the Fe(III)-reducing species *Alkaliphilus crotonatoxidans* and *Serratia liquifaciens* were observed. These results highlight that under certain conditions and contrary to expectations, denitrification may support bioreduction *via* pH conditioning for optimal metal reduction and radionuclide immobilization.

Keywords nitrate, bioreduction, iron reduction, radionuclides, microcosms

INTRODUCTION

The remediation of radioactively contaminated land in the UK is of immediate concern due to the ongoing decommissioning of British nuclear sites. Further, there is a need for solutions to existing contaminant problems prior to the possible onset of new nuclear power. At the Sellafield nuclear reprocessing site in Cumbria, mobile groundwater contaminant radionuclides include ^{99}Tc and ^{90}Sr, and groundwater co-contaminants include nitrate (from nitric acid), organic acids, and pH variance (BNFL 2003; McKenzie and Armstrong-Pope 2010).

Similar contamination issues have been documented at a range of US nuclear sites (e.g., Oak Ridge, TN (Edwards et al. 2007; Istok et al. 2004; Li and Krumholz 2008; McBeth et al. 2007), San Juan River, Shiprock, NM (Finneran et al. 2002), and Hanford, WA (Singleton et al. 2005)). A proposed *in situ* strategy to remediate contaminants at such sites is "biostimulation." Here, an electron donor is added to the subsurface to stimulate the indigenous microbial community, promoting a cascade of terminal electron accepting processes (TEAPs) that favour radionuclide removal from groundwaters (Lloyd and Renshaw 2005; Lovley and Coates 1997).

This approach has been shown to reduce the mobility of redox-active radionuclides such as ^{99}Tc and U, *via* the reduction of soluble oxidized species (Tc(VII), U(VI)) to poorly-soluble reduced species (Tc(IV), U(IV)) (Edwards et al. 2007; Istok et al. 2004; Law et al. 2010; McBeth et al. 2007; Morris et al. 2008). It may also be possible for bioreduction to occur in sediments via natural attenuation without electron donor addition (Alvarez

Received 9 February 2011; accepted 7 April 2011.

We thank David Ashley (University of Leeds) and John Waters (University of Manchester) for help in data acquisition and Chris Hubbard and Sarah Wallace for help with sample collection. This work was funded by the Engineering and Physical Science Research Council (EPSRC) as part of the Decommissioning, Immobilization and Management of Nuclear Waste for Disposal (DIAMOND) consortium grant EP/F055412/1. We also acknowledge support of NERC grant NE/H007768/1.

Address correspondence to Katherine Morris, Research Centre for Radwaste and Decommissioning and Williamson Research Centre for Molecular Environmental Science, School of Earth, Atmospheric and Environmental Sciences, The University of Manchester, Manchester M13 9PL, United Kingdom. E-mail: katherine.morris@manchester.ac.uk

et al. 2006; Burke et al. 2010; Manaka et al. 2007). Regardless, in most cases, radionuclide reduction is associated with microbially mediated Fe(III) reduction (Lloyd 2003; Lloyd and Renshaw 2005).

As a consequence, the actions of Fe(III)-reducing bacteria and subsequent changes in Fe redox chemistry and Fe mineralogy are likely to play a key role in governing the mobility of redox-active radionuclides. Furthermore, changes in Fe mineralogy have the potential to affect the sorption and mobility of other (non-redox-active) radionuclides e.g., ^{137}Cs or ^{90}Sr (Chiang et al. 2010; Langley et al. 2009; Roden et al. 2002).

However, the comparatively low groundwater pH conditions and/or high nitrate concentrations that can characterize nuclear sites represent challenging bioremediation scenarios. Low pH decreases microbial diversity and metabolic function (Baker and Banfield 2003; Robinson et al. 2009) whilst nitrate is an energetically more favourable electron acceptor than Fe(III) (and redox active radionuclides) and thus can inhibit TEAP progression and reductive immobilization of radionuclides (DiChristina 1992).

Indeed, whilst some studies demonstrate microbially-mediated metal reduction in the presence of high nitrate (Madden et al. 2007), numerous sediment microcosm studies indicate that microbially mediated metal and radionuclide reduction does not commence until nitrate and nitrite are reduced (e.g. Burke et al. 2005; Edwards et al. 2007; Law et al. 2010; Li and Krumholz 2008; McBeth et al. 2007; Wilkins et al. 2010). Further, some biostimulation studies with low pH sediments have demonstrated that the extent of nitrate removal is strongly pH dependant, with $NaHCO_3$ or crushed lime amendment necessary to stimulate bioreduction and TEAP progression (Edwards et al. 2007; Michalsen et al. 2009; North et al. 2004).

Conversely, in field studies, dual denitrification and metal reduction was observed at low-pH (Istok et al. 2004) and in microcosm studies, denitrification and associated pH buffering (*via* OH^- and HCO_3^- production) has been shown to stimulate TEAP progression to metal reduction (Law et al. 2010). Clearly, the variable effects of low-pH and nitrate on electron flow warrant further study and here, electron flow in representative Sellafield sediments was studied under a range of environmentally relevant nitrate (0.4–100 mM), pH, and carbonate conditions.

EXPERIMENTAL

Sample Collection

Sediments representative of the Quaternary unconsolidated alluvial flood-plain deposits that underlie the UK Sellafield reprocessing site (Law et al. 2010) were collected from the Calder Valley, Cumbria, during December 2008 (herein called Sellafield sediment). The sampling area was located ~ 2 km from the Sellafield site (Lat 54°26′30 N, Long 03°28′09 W). Sediments were transferred directly into sterile containers, sealed, and stored at 4°C. Experiments began within 6 months of field sampling.

Bioreduction Microcosms

Sediment microcosms (10 ± 0.1 g Sellafield sediment, 100 ± 1 ml groundwater) were prepared using a synthetic groundwater representative of the Sellafield region, with background nitrate present at ~0.4 mM (Law et al. 2010; Wilkins et al. 2007). The groundwater was manipulated to produce a range of treatments (Table 1). Bicarbonate-free systems with an initial pH of ~5.5 were prepared with 0.4, 2, 10, and 100 mM nitrate. Bicarbonate buffered systems with an initial pH of 6.8 were prepared with 0.4, 10, and 100 mM nitrate.

Sodium acetate was added as an electron donor in excess of extant available electron acceptors (14 mM for 0.4–10 mM nitrate treatments, and 70 mM for 100 mM nitrate treatments) and anoxic $NaNO_3$ was used as a NO_3^- source. The groundwater was sterilized by autoclaving (1 hour at 120°C), and then bubbled with filtered 80/20 N_2/CO_2, and the pH set *via* dropwise addition of 0.5 M HCl or 1M NaOH. Sediment and sterile groundwaters were added to sterile 120 ml glass serum bottles (Wheaton Scientific, USA) using aseptic technique and sealed with butyl rubber stoppers.

All microcosms were then incubated anaerobically at 21°C in the dark for 80–230 days and each treatment was run in triplicate. Throughout the incubation, sediment slurry was periodically extracted under an O_2-free Ar atmosphere using aseptic technique. The extracted sediment slurry was centrifuged (15,000 *g*; 10 minutes) to provide separate sediment and porewater samples and ~0.5 g of sediment was stored at −80°C

TABLE 1
Initial composition of microcosm systems

System name	Amendment	Nitrate	pH
0.4 mM nitrate	None	0.4 mM $NaNO_3$	~5.5
2 mM nitrate	None	2 mM $NaNO_3$	~5.5
10 mM nitrate	None	10 mM $NaNO_3$	~5.5
100 mM nitrate	None	100 mM $NaNO_3$	~5.5
Bicarbonate buffered 0.4 mM nitrate	3 mM $NaHCO_3$ and OH^-	0.4 mM $NaNO_3$	6.8–7.0
Bicarbonate buffered 10 mM nitrate	3 mM $NaHCO_3$ and OH	10 mM $NaNO_3$	6.8–7.0
Bicarbonate buffered 100 mM nitrate	3 mM $NaHCO_3$ and OH	100 mM $NaNO_3$	6.8–7.0

TABLE 2
Details of Fe extraction series (Poulton and Canfield 2005)

Fraction	Extraction	pH	Time
Carbonate associated	1 M sodium acetate	4.5	24 hours
Easily reducible oxides	1 M hydroxylamine HCl in 25 % v/v acetic acid		48 hours
Reducible oxides	50 gL^{-1} sodium dithionite	4.8	2 hours
Magnetite	0.2 M ammonium oxalate	3.2	6 hours
Residual Fe	XRF	N/A	N/A

for microbiological characterization. Sediments from the initial and final time points of each treatment underwent a sequential extraction procedure to assess changes in Fe mineralogy during biostimulation (Poulton and Canfield 2005; Tessier et al. 1979). Sequential extractions procedures targeted: i) carbonate associated Fe; ii) easily reducible oxides; iii) reducible oxides; iv) magnetite; and, v) residual Fe (Table 2). These extractions comprised i) 1 M sodium acetate (pH 4.5); ii) 1 M hydroxylamine HCl; iii) sodium dithionite—sodium citrate (pH 4.8); iv) 0.2 M ammonium oxalate (pH 3.2); and, v) residual Fe was determined by XRF minus the extracted phases (Poulton and Canfield 2005). The sediment to solution ratio was 0.1 g in 10 ml (1:100) at each stage.

Geochemical Analyses

During microcosm sampling, total dissolved Fe, Mn(II), and NO_2^- concentrations were measured with standard UV-Vis spectroscopy methods on a Cecil CE 3021 spectrophotometer (Goto et al. 1997; Harris and Mortimer 2002; Viollier et al. 2000). Aqueous NO_3^-, SO_4^{2-}, and acetate were measured by ion chromatography (Dionex ICS-90) (Burke et al. 2005). Ammonium was measured by flow injection analysis (Dionex ICS-90) (Hall and Aller 1992). Total bioavailable Fe(III) and the proportion of extractable Fe(II) in the sediment was estimated by digestion of 0.1 g of sediment in 5 ml of 0.5 N HCl for 60 minutes followed by the ferrozine assay, with and without hydroxylammonium HCl (1.4M $H_2NOH.HCl$ in 2M HCl) (Lovley and Phillips 1987; Stookey 1970; Viollier et al. 2000).

The pH and Eh were measured with an Orion 420A digital meter and calibrated electrodes. Standards were routinely used to check the reliability of all methods and calibration regressions had $R^2 \geq 0.99$. The elemental composition and bulk mineralogy of the sediment were determined by XRF (Thermo ARL 9400 XRF) and XRD (Philips PW 1050 XRD).

Microbial Community Analysis

Selected samples from bicarbonate-free microcosms containing 0.4 and 10 mM nitrate and bicarbonate buffered microcosms containing 100 mM nitrate underwent PCR-based 16S rRNA gene analysis. Additionally, sub-aliquots of sediment slurry from the 100 mM nitrate treatment were added (1:10 sediment/solution ratio) to an Fe(III)-citrate containing medium (Lovley and Phillips 1986) with 20 mM acetate or 0.2% (w/v) yeast extract as an electron donor, to make an enrichment culture to identify the microorganisms responsible for Fe(III) reduction at pH > 9. Enrichment cultures were incubated at 20° C for 4–5 weeks before further sub-aliquots were transferred (1:10 sediment/solution ratio) to fresh Fe(III)-citrate medium. This procedure was repeated 7 times and then finally 16S rRNA gene analysis was used to identify the species present in the final enrichment. XRD was used to analyse the mineralogical products of Fe(III) reduction in the enrichment systems.

Amplification of 16S rRNA Gene Sequences

DNA was extracted from samples using a PowerSoil DNA Isolation Kit (MO BIO, USA). Copies of the 16S rRNA gene (approximately 1490 b.p. fragment) was amplified from samples using the broad-specificity primers 8F (Eden et al. 1991) and 1492R (Lane et al. 1985). PCR reactions were performed in thin-walled tubes using a BioRad iCycler (BioRad, UK). The PCR amplification protocol used with the 8F and 1492R primers was: initial denaturation at 94°C for 4 minutes, melting at 94°C for 30 seconds, annealing at 57°C for 30 seconds, elongation at 72°C for 1 minute; 35 cycles, followed by a final extension step at 72°C for 10 minutes. The purity of the amplified products was determined by electrophoresis in a tris-acetate-EDTA (TAE) gel. DNA was stained with ethidium bromide and viewed under short-wave UV light using a BioRad Geldoc 2000 system (BioRad, UK).

Cloning

PCR products were purified using a QIAquick PCR purification kit (Qiagen, UK) and ligated directly into a cloning vector containing topoisomerase I-charged vector arms (Agilent Technologies, UK) prior to transformation into *E. coli* competent cells expressing Cre recombinase (Agilent Technologies, UK). White transformants that grew on LB agar containing ampicillin and X-Gal were screened for an insert using PCR. Primers were complementary to the flanking regions of the PCR insertion site of the cloning vector. The PCR method used was: an initial denaturation at 94°C for 4 minutes, melting at 94°C for 30 seconds, annealing at 55°C for 30 seconds, extension at 72°C for 1 minute; 35 cycles, followed by a final extension step at 72°C for 5 minutes. The resulting PCR products were purified using an ExoSap protocol, and 2 μl of ExoSap mix (0.058 μl Exonuclease I, 0.5 μl Shrimp Alkaline Phosphatase, and 1.442 μl QH_2O) was added to 5 μl of PCR product and incubated at 37°C for 30 minutes followed by 80°C for 15 minutes.

DNA Sequencing and Phylogenetic Analysis

Nucleotide sequences were determined by the dideoxynucleotide method. An ABI Prism BigDye Terminator Cycle Sequencing Kit was used in combination with an ABI Prism 877

Integrated Thermal Cycler and ABI Prism 377 DNA Sequencer (Perkin Elmer Applied Biosystems, UK). Sequences (typically 900 base pairs in length) were analysed against the NCBI (USA) database using the BLAST program packages and matched to known 16S rRNA gene sequences.

RESULTS AND DISCUSSION

Sediment Characteristics

The mineral content of the sediment as sampled was dominated by quartz, feldspars (albite and microcline), and sheet silicates (muscovite and chlorite). The sediment had a high Si content (33.2 wt %) and contained Al (5.9%), Fe (4.2%), K (2.6%), Na (1.1%), Mg (<0.1 %), Ti (0.4%), Ca (0.14%), and Mn (<0.1%). The concentration of 0.5 N HCl extractable Fe in the sediment was 5.6 ± 0.5 mmol kg^{-1} prior to incubation and the sediment pH was ~5.5.

Progressive Bioreduction in Bicarbonate-Free Systems

In bicarbonate-free systems with initially low pH (5.5) and with varying initial nitrate concentrations (Table 1), microbially mediated TEAP progression was monitored as bioreduction developed. Microbial activity was observed in all electron donor amended microcosms (Figure 1), whereas no biogeochemical changes were observed in sterile-controls (data not shown). Electron acceptor utilization was observed in the order NO_3^-, NO_2, Mn(IV), Fe(III) and SO_4^{2-} as indicated by changes in the relevant biogeochemical indicators (Figure 1).

Furthermore, Eh decreased during TEAP progression and acetate was removed from porewaters (Table 3). As expected, the onset of microbially-mediated Mn(IV) and Fe(III) reduction was largely inhibited until nitrate and nitrite were removed *via* denitrification. The inhibition time was dependent on the initial nitrate concentration with 0.4, 2, and 10 mM nitrate removed by 14, 18 and 25 days, respectively, and with the onset of metal reduction indicated by increased Fe(II) in sediments, occurring immediately afterwards (Figure 1).

Interestingly, the rates of Mn(IV) and Fe(III) reduction were increased, compared to the low nitrate systems after nitrate had been removed from microcosms in the systems with higher nitrate additions. For example, in the 0.4, 2, and 10 mM nitrate systems, essentially complete Fe(III) reduction was seen at ~50 days despite the delay in onset of Fe(III) reduction in the 10 mM system compared to the lower nitrate concentration experiments. By contrast, the 100 mM nitrate, bicarbonate-free system appeared to be overwhelmed by the competing electron acceptor and although substantial nitrate reduction had occurred, 60 mM nitrate remained in solution after 230 days incubation and no evidence for Fe(III) reduction was observed (Figure 1).

Previous work has reported an increase in Fe(III) reduction rates in low pH sediments following nitrate reduction and attributed this to a rise in pH due to OH^- and HCO_3^- production during denitrification (Law et al. 2010). In this study the pH in bicarbonate-free systems with an initial pH of 5.5 and nitrate concentrations of 0.4 2 and 10 mM, increased to pH 6.8, 7.0, and 7.5 respectively (Figure 1). Thus, the pH adjustment from pH ~5.5 to circumneutral caused by nitrate reduction apparently stimulated metal reduction in these sediments. This is consistent with the fact that the diversity and metabolic function of neutrophilic metal reducers is decreased at low pH (Lloyd 2003; Reardon et al. 2004; Fields et al. 2005; Edwards et al. 2007).

In these microcosms, reduction of even relatively low concentrations of nitrate (0.4 mM) were sufficient to increase pH to a region where Fe(III) reduction became viable. By contrast, in the bicarbonate-free system with 100 mM nitrate, nitrite accumulation in the microcosm was almost stoichiometric with respect to observed nitrate reduction. This implied that nitrite remained unreduced in this system which "stalled" at ~40% nitrate removal (Figure 1).

Several studies have demonstrated the increased toxicity of nitrite with decreasing pH and this is likely due to the presence of nitrous acid (HNO_2) at low pH entering the cell and interfering with the pH gradient across the cell membrane (Weon et al. 2002; Zhou et al. 2007; Zhou et al. 2010). Thus, stoichiometric accumulation of nitrite combined with the low initial pH (5.5) of sediments suggests that nitrite toxicity may be an issue for this system although, interestingly after extended (230 days) incubation, nitrate and nitrite levels did appear to fall and pH did rise (Figure 1).

Bioreduction Pathways

Calculations based on acetate consumption compared to nitrate reduction, combined with only a minor amount of ammonia being detected in the bioreduced microcosms suggest that denitrification to N_2 or N_2O is the dominant pathway for nitrate reduction in these systems (Table 3). Equations for the 5 electron transfer from NO_3^- to N_2 coupled to acetate oxidation show the production of OH^- during NO_2^- reduction to N_2O with HCO_3^- produced at all stages (Equations 1–3) and in agreement with the observed rise in pH in our systems.

$$CH_3COO^- + 4NO_3^- \rightarrow 4NO_2^- + HCO_3^- + CO_2 + H_2O \quad [1]$$

$$CH_3COO^- + 2NO_2^- + 2H^+ \rightarrow 2N_2O + HCO_3^- + CO_2 + H_2O + 2OH^- \quad [2]$$

$$CH_3COO^- + 4N_2O \rightarrow 4N_2 + HCO_3^- + CO_2 + H_2O \quad [3]$$

Metal reduction then followed nitrate reduction with 0.5 N HCl extractable Fe(II) ingrowth to sediments observed followed by accumulation of Mn in porewaters (Figure 1). Although the pH rose most steeply during nitrate reduction, the pH in all microcosms continued to trend upwards during Fe(III) reduction consistent with continued consumption of H^+ and release of HCO_3^- during Fe(III) oxide reduction coupled to acetate oxidation (Equation 4).

$$CH_3COO^- + 8FeOOH + 15H^+ \rightarrow 8Fe^{2+} + 2HCO_3^- + 12H_2O \quad [4]$$

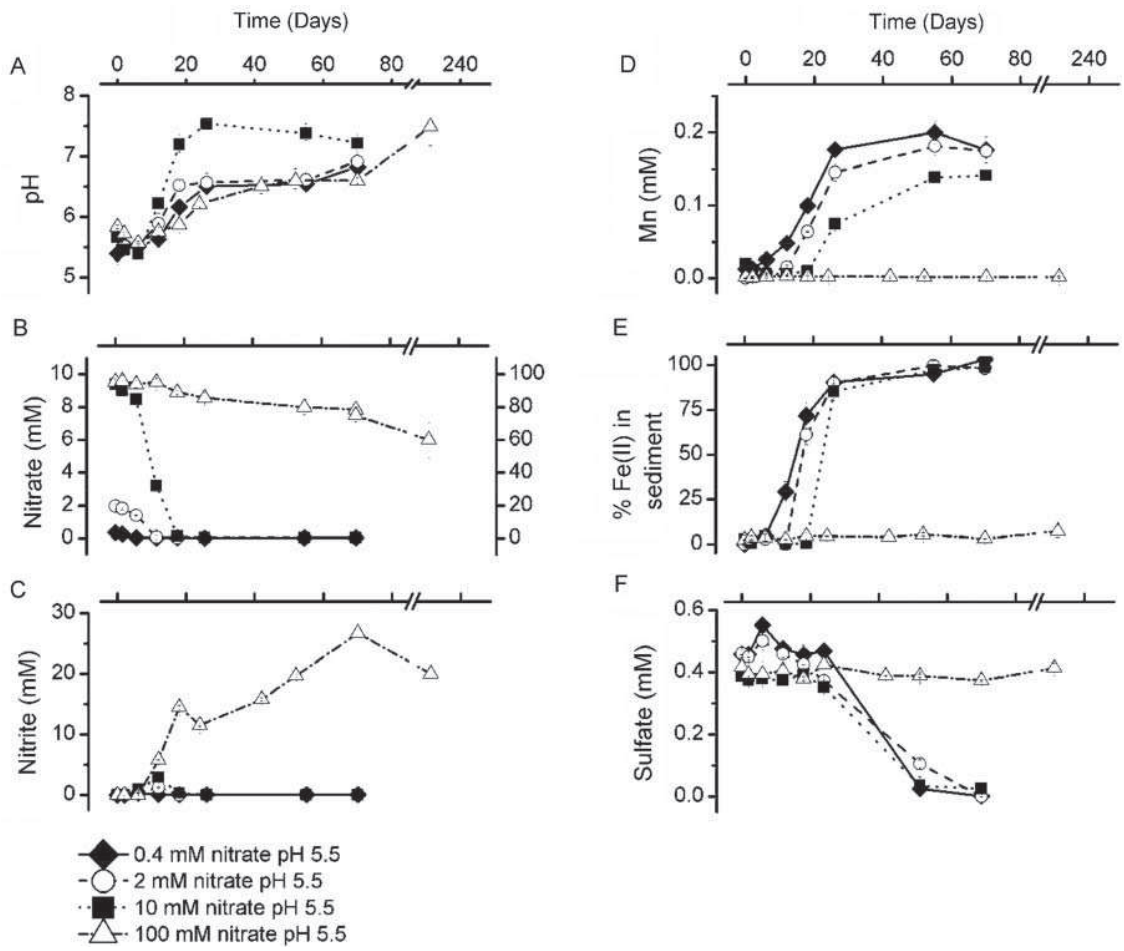

FIG. 1. Microcosm incubation time-series data (days 0-230). (A) pH, (B) NO_3^-, (C) NO_2^-, (D) porewater Mn, (E) 0.5 N HCl% extractable sedimentary Fe as Fe(II), (F) porewater SO_4^{2-}. Black diamonds = 0.4 mM nitrate system; unfilled circles = 2mM nitrate system; black squares = 10 mM nitrate system; unfilled triangles = 100 mM nitrate system. Initial pH in all microcosms was ~5.5. Error bars represent 1σ experimental uncertainty from triplicate microcosm experiments (where not visible error bars are within symbol size).

Interestingly, sequential extractions conducted on sediment from the bicarbonate buffered system with 10 mM nitrate before and after bioreduction suggest an increase in the "carbonate fraction" coupled to a reduction in the "easily reducible" fraction in the sediments after bioreduction (Figure 2). The final pH in these systems was between pH 7.5 and 8. This is consistent with observations that Fe^{2+}, alkalinity, and HCO_3^- all favour the formation of carbonate minerals such as siderite (Equation 5) (Coleman et al. 1993; Roden et al. 2002).

$$Fe^{2+} + HCO_3^- + OH^- \rightarrow FeCO_3 + H_2O \quad [5]$$

Microbial Community Analysis in Bicarbonate-Free Systems

The microbial ecology of the pH ~5.5 microcosms was assessed by 16S rRNA gene analysis at key points as bioreduction progressed. Analysis of the oxic sediment revealed a diverse population with 11 different phyla and 59 distinct organisms detected in 73 clones. The clone library was dominated by species from the phylum *Aciodobacteria* (~50%) with close relatives of *Bacillus* species present (~7%) (Figure 3). This is similar to past work with Sellafield-type sediments where *Acidobacteria* also dominated the clone libraries (Law et al. 2010).

When the 0.4 mM nitrate system had undergone nitrate and Fe(III) reduction (at day 50) the microbial community had changed and comprised 11 different phyla and 71 distinct sequences from the 83 clones analysed. Members of *Clostridiales* now made up ~17% of the clone library and *Acidobacteria* only ~21% (Figure 3). Organisms affiliated with the *Clostridiales* order included close relatives of known Gram-positive metal-reducing species *Desulfosporosinus sp.* S8 and *Desulfitobacterium metallireducens* (Robertson et al. 2000; Spring and Rozenzweig 2006), which have been isolated as key

TABLE 3
pH, Eh and acetate utilization data

System	pH		Eh		Acetate (mM)		NH_4^+ (mM)
	Initial	Final	Initial	Final	Utilized during nitrate reduction	Required for denitrification to N_2	Max. in porewaters
0.4 mM nitrate	5.5	6.8	+187	-86	0.22 ± 0.01	0.25	—
2 mM nitrate	5.5	6.95	+240	-67	2.58 ± 0.06	1.25	—
10 mM nitrate	5.5	7.25	+273	-62	7.25 ± 0.32	6.25	<0.5
100 mM nitrate	5.5	6.5-8	+184	+166	17.3 ± 0.45*	62.2	—
Bicarbonate buffered 0.4 mM nitrate	7	7.2	+274	-57	1.63 ± 0.15	0.25	—
Bicarbonate buffered 10 mM nitrate	7	7.5	+274	-20	8.23 ± 0.32	6.25	<0.7
Bicarbonate buffered 100 mM nitrate	7	9.3	+286	50	86.4 ± 4.56	62.2	—

Errors are 1σ of triplicate measurements. *reduced only ~40% of nitrate.

metal-reducing bacteria in high nitrate sediments at Oak Ridge, TN (Li and Krumholz 2008; Shelobolina et al. 2003).

Also present in the clone library were species of the known Fe(III)-reducing genus *Geobacter* and the known nitrate-reducing genus *Bacillus*. In contrast, when the bicarbonate-free 10 mM nitrate system had undergone nitrate and Fe(III) reduction (50 days), the diversity was very much reduced even compared to the 0.4 mM system at 50 days, and 87% of the clone library (76 of 87 clones sequenced) comprised of close relatives (>99%) of *Bacillus niacini* (Figure 3).

Bacillus niacini has been shown to reduce nitrate to nitrite under anaerobic conditions (Nagel and Andreeson 1991) and close relatives have been identified in nitrate amended sediments at a uranium waste tailing site and in Sellafield-type sediments (Law et al. 2010; Selenska-Pobell and Geissler 2008). These results suggest a trend toward much lower microbial diversity

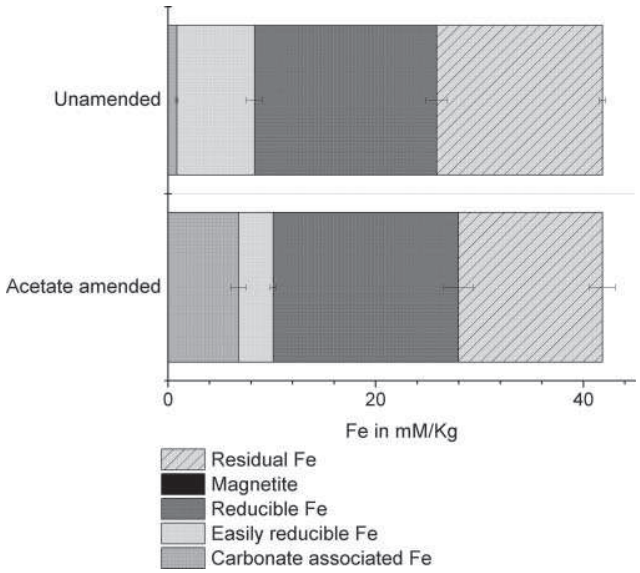

FIG. 2. Sequential extraction data comparing the Fe mineralogy of bicarbonate buffered 10 mM nitrate reduced sediments with that of oxic sediment. Dark grey = carbonate associated Fe; light gray = easily reducible Fe oxides; very dark grey = reducible oxides; black = magnetite; striped = residual Fe as determined by XRF.

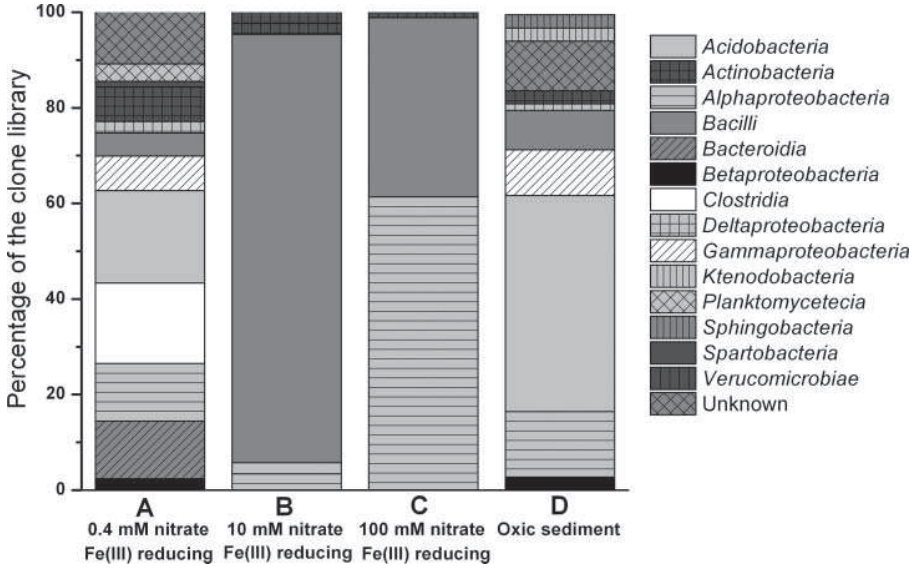

FIG. 3. Microbial community analysis of (A) Fe(III)-reducing bicarbonate-free sediment with 0.4 mM initial nitrate (T = 50), (B) Fe(III)-reducing bicarbonate-free sediment with 10 mM initial nitrate (T = 50), (C) Fe(III)-reducing bicarbonate-free sediment with 100 mM initial nitrate (T = 70) and (D) oxic sediment.

as initial nitrate concentrations increase, with a close relative (>99%) of *Bacillus niacini* suggested as a key, acid tolerant nitrate-reducing organism in systems with elevated nitrate, and with *Gram-positive* species potentially significant in mediating Fe(III) reduction.

Progressive Bioreduction in Bicarbonate Buffered Systems

When systems were buffered with bicarbonate to pH 7 to stimulate bioreduction, there was a general increase in the rate of bioreduction compared to the unbuffered pH 5.5 microcosms. For example, in the bicarbonate buffered 0.4 and 10 mM nitrate systems, extensive Fe(III)-reduction, indicated by ~100% 0.5 M HCl extractable Fe converted to Fe(II), was observed by 21 days compared to 50 days in the parallel unbuffered system (Figures 1 and 4). Interestingly, although the microbial community was unable to reduce 100 mM nitrate at pH 5.5 (Figure 1), when the pH was buffered to circumneutral prior to incubation, the system was able to facilitate complete reduction of 100 mM nitrate by 70 days and metal reduction commenced thereafter (Figure 4).

Nitrite in this system was transient and it is probable that the higher initial pH reduced the toxicity of nitrite in this system and thereby allowed nitrite metabolism to proceed (Zhou et al. 2010). Development of metal-reducing conditions in microcosms with very high nitrate is variable with some studies reporting development of Fe(III)-reduction in 100 mM nitrate, carbonate buffered experiments (Edwards et al. 2007), whilst other workers observed only partial reduction of 100 mM nitrate and no development of Fe(III)-reducing conditions (McBeth et al. 2007). Interestingly, in dynamic push-pull tests at the Field Research Centre in Oak Ridge Tennessee, electron donor amendment and pH neutralization was needed to reduce > 100 mM nitrate (Istok et al. 2004; North et al. 2004). In the bicarbonate buffered experiments, pH increased from pH 7.0 to 7.2, 8.1 and 9.5 for systems with 0.4, 10 and 100 mM nitrate respectively, and as expected the onset of metal-reducing conditions was delayed as the initial nitrate concentration increased. For example, complete reduction of 0.5 N HCl extractable Fe(III) took 18, 25 and 230 days in the 0.4, 10 and 100 mM nitrate systems respectively (Figure 4). Indeed, the observation of Fe(III)-reduction in microcosms where pH was greater than 9 is interesting in terms of the microbial tolerance of the system across pH 5.5–9. Indeed, there are few published studies on metal reduction in alkaline sediments and the majority of available studies focus on halophillic species from alkaline soda lakes (Gorlenko et al. 2004; Pollock et al. 2007).

Only a few species including *Alkaliphilus metalireducens* and *Anaerobranca californiensis* have been isolated and shown to reduce Fe(III) above pH 9 (Gorlenko et al. 2004; Ye et al. 2004). More recently, Fe(III) reduction has been demonstrated in a highly contaminated, high pH chromium waste site in the UK (Stewart et al. 2010). In our study, sequence analyses of amplified 16S rRNA genes showed that during Fe(III) reduction after incubation for 70 days the bicarbonate buffered 100 mM nitrate system had a restricted clone library with only 5 different species detected in 88 clones.

The system was dominated by a close relative (>99% sequence homology) of *Ochrobactrum grignonense* strain c259 (59% of the clones) with a close relative (>99% sequence homology) of *Bacillus niacini* also significant at ~37% of the clone library (Figure 3). *Ochrobactrum grignonense* is

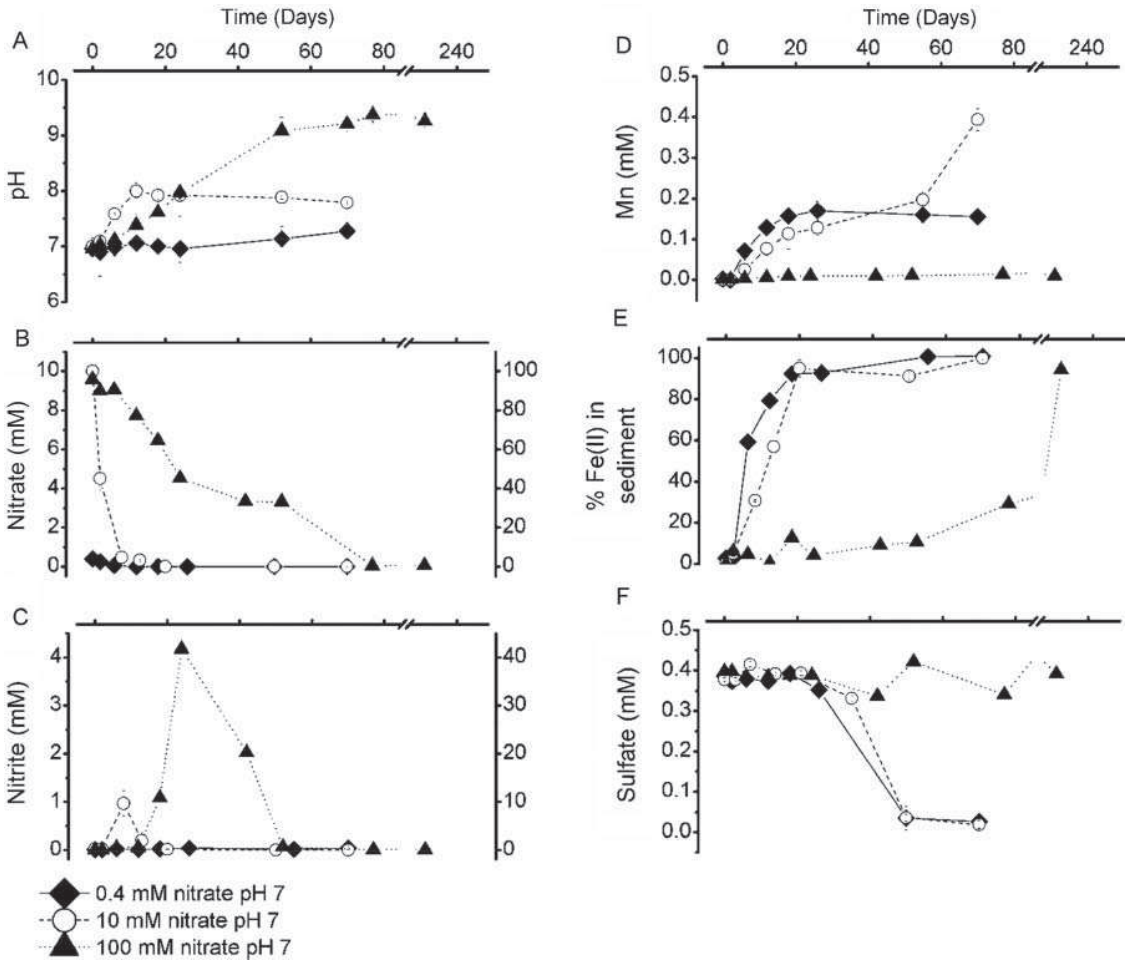

FIG. 4. Microcosm incubation time-series data (days 0–230). (A) pH, (B) NO_3^-, (C) NO_2^-, (D) porewater Mn, (E) 0.5 N HCl% extractable sedimentary Fe as Fe(II), (F) porewater Fe, (G) porewater SO_4^{2-} and (H) Eh. Black diamonds = bicarbonate buffered 0.4 mM nitrate system; unfilled circles = bicarbonate buffered 10 mM nitrate system; black triangles = bicarbonate buffered 100 mM nitrate system. The initial pH in all microcosms was ~7.0. Error bars represent 1σ experimental uncertainty from triplicate microcosm experiments (where not visible error bars are within symbol size).

capable of denitrification and growth between pH 3–9 (Lebuhn et al. 2000) and some species of *Bacillus* are presumably alkali tolerant as they have been isolated from soda lakes at pH > 9 (Carrasco et al. 2007; Pollock et al. 2007).

Enrichment Cultures

In the 100 mM bicarbonate buffered system that had undergone bioreduction and was poised at pH 9.5, the sediment molecular ecology studies were dominated by close relatives of known nitrate-reducing microorganisms and thus the Fe(III)-reducing bacteria, which were obviously active, could not be identified unequivocally in the clone library. Therefore, in order to gain further insight into the alkali tolerant Fe(III)-reducing species that were active in these systems, enrichment cultures were established with medium containing Fe(III)-citrate as the sole electron acceptor at pH 9.5 and inoculated initially with 10% of the bioreduced 100 mM carbonated buffered sediment (see methods).

After seven enrichment subcultures (using 10% v/v inocula throughout), a sample was taken for molecular characterization. Here, 16S rRNA gene analysis revealed that a bacterium closely related (>99%) to *Alkaliphilus crotonatoxidans* made up 41% of the enrichment culture (37 of 91 clones) and a bacterium closely related (>99%) to *Serratia liquifaciens* made up a further 56% (51 of 91 clones) (Table 4).

Alkaliphilus crotonatoxidans is a strict anaerobe with a reported growth range of pH 5.5–9 (Cao et al. 2003), whereas *Serraitia liquifaciens* is a facultative anaerobe and has not previously reported as alkali tolerant. Repeated subcultures of the enrichment consortium over several months show that the consortium is stable and capable of growth at pH >9, while facilitating Fe(III)-reduction in this high pH system.

TABLE 4
Phylogenetic affiliation of 16S rRNA gene sequences detected in the clone library from the Fe(III) reducing enrichment culture at pH 9.5

No. in Clone Library	Closest Matching Micro-organism [accession Number]	% Match	% Present	Phylogenetic Class
37	Alkaliphilus crotonatoxidans [AF467248]	99%	40.7%	Clostridia
51	Serratia liquefaciens[AJ306725]	99%	56%	Gammaproteobacteria
2	Clostridium celerecrescens clone IrT-JG1-12[AJ295659]	98%	2.2%	Clostridia
1	uncultured bacterium; 3BH-2FF [EU937958]	97%	1.1%	Betaproteobacteria

Implications for Bioremediation

This study highlights the sensitivity of nitrate and Fe(III)-reducing communities in Sellafield-type sediments to initial pH conditions. It was found that in these batch experiments, while low pH may inhibit the progression of TEAPs in nitrate amended systems, moderate nitrate concentrations up to 10 mM actually stimulated the development of metal-reducing conditions *via* production of OH^- and HCO_3^- during nitrate reduction and resultant pH amendment (Figure 1).

These observations are in contrast to similar studies with nitrate contaminated sediments from the Oak Ridge nuclear site where pH buffering with $NaHCO_3$ or crushed lime was necessary to stimulate bioreduction (Edwards et al. 2007; Michalsen et al. 2009; North et al. 2004). In our systems, we observed faster TEAP progression when microcosms were buffered to an initial pH of 7.0 with bicarbonate buffer compared to the naturally mildly acidic Sellafield material. Indeed, in our experiments very high (100 mM) nitrate was only fully reduced in bicarbonate buffered systems.

This information is useful in understanding pH amendment *via* bioreduction that may be occurring in high nitrate groundwaters, and may be beneficial in planning engineered bioreduction treatments in low pH environments although clearly there is a need for further lab and field scale studies on dynamic flow systems to constrain this potential further. Interestingly, although reduction of a pH 7 microcosm containing 100 mM nitrate lead to the development of a pH of 9.5 prior to metal reduction starting, the system appeared robust and progression to Fe(III) reduction occurred at these alkaline conditions.

Overall, the representative Sellafield sediments appear to support a diverse range of microorganisms which in batch experiments are capable of metal reduction between pH 6 and 9.5 provided there is sufficient electron donor to first deplete nitrate. Interestingly, a rise in pH during bioreduction may also benefit the removal of non redox active radionuclides such as ^{90}Sr which is less mobile at alkaline pH and is predicted to associate with carbonate phases above pH $\sim$ 9 (Ferris and Roden 2000; Langley et al. 2009; Roden et al. 2002). This work highlights that biostimulation coupled to pH modification by denitrification is possible under constrained, batch experiment conditions and, contrary to initial expectations, may provide some potential for enhanced removal of problematic radionuclides and contaminants at industrial sites.

REFERENCES

Alvarez PJJ, Illman WA. 2006. Bioremediation and Natural Attenuation: Processes Fundamentals and Mathematical Models. Hoboken, NJ: Wiley.

BNFL (British Nuclear Fuels Ltd). 2003. SCLS Phase 1 – conceptual model of contamination below ground at Sellafield. Nuclear Sciences and Technology Services: Report NSTS 4866.

Baker BJ, Banfield JF. 2003. Microbial communities in acid mine drainage. FEMS Microbiol Ecol 44:139–152.

Burke IT, Boothman C, Lloyd JR, Mortimer RJG, Livens FR, Morris K. 2005. Effects of progressive anoxia on the solubility of technetium in sediments. Environ Sci Technol 39:4109–4116.

Burke IT, Livens FR, Lloyd JR, Brown AP, Law GTW, McBeth JM, Ellis BL, Lawson RS, Morris K. 2010. The fate of technetium in reduced estuarine sediments: combining direct and indirect analysis. Appl Geochem 25:233–241.

Cao X, Liu X, Dong X. 2003. *Alkaliphilus crotonatoxidans* sp. nov., a strictly anaerobic, crotonate-dismutating bacterium isolated from a methanogenic environment. Inter J Syst Evol Microbiol 53:971–975.

Carrasco IJ, Marquez MC, Xue Y, Ma Y, Cowan DA, Jones BE, Grant WD, Ventosa A. 2007. *Bacillus chagannorensis* sp. nov., a moderate halophile from a soda lake in Inner Mongolia, China. Int J Syst Evol Microbiol 57:2084–2088.

Chiang PN, Wang MK, Huang PM, Wang JJ, Chiu CY. 2010. Caesium and strontium sorption by selected tropical and subtropical soils around nuclear facilities. J Environ Radioact 101:472–481.

Coleman MC, Hedrick DB, Lovely DR, White DC, Pye K. 1993. Reduction of Fe(III) in sediments by sulphate-reducing bacteria. Nature 361:436–438.

DiChristina TJ. 1992. Effects of nitrate and nitrite on dissimilatory iron reduction by *Shewanella putrefaciens 200*. J Bacteriol 174:1891–1896.

Eden PE, Schmidt TM, Blakemore RP, Pace NR. 1991. Phylogenetic analysis of *Aquaspirillum magnetotacticum* using polymerase chain reaction-amplified 16S rRNA-specific DNA. Inter J System Bacteriol 41:324–325.

Edwards L, Kusel K, Drake H, Kostka JE. 2007. Electron flow in acidic subsurface sediments co-contaminated with nitrate and uranium. Geochim Cosmochim Acta 71:643–654.

Ferris FG, Roden EE. 2000. Microbial mineral transformations at the Fe(II)/Fe(III) redox boundary for solid phase capture of strontium and other metal/radionuclide contaminants. US Department of Energy. Report: DE-FG07-96ER62317.

Fields MW, Yan T, Rhee SK, Carroll SL, Jardine PM, Watson DB. 2005. Impacts on microbial communities and cultivable isolates from groundwater contaminated with high levels of nitric acid-uranium waste. FEMS Microbiol Ecol 53:417–428.

Finneran KT, Housewright ME, Lovley DR. 2002. Multiple influences of nitrate on uranium solubility during bioremediation of uranium-contaminated subsurface sediments. Environ Microbiol 4:510–516.

Gorlenko V, Tsapin A, Namsaraev Z, Teal T, Tourova T, Engler D, Mielke R, Nealson K. 2004. *Anaerobranca californiensis* sp nov., an anaerobic,

alkalithermophilic, fermentative bacterium isolated from a hot spring on Mono Lake. Int J Syst Evol Microbiol 54:739–743.

Goto K, Taguchi S, Fukue Y, Ohta K, Watanabe H. 1997. Spectrophotometric determination of manganese with 1-(2-pyridylazo)-2-naphthol and a non-ionic surfactant. Talanta 24:752–753.

Hall PO, Aller RC. 1992. Rapid small-volume flow-injection analysis for sigma-CO_2 and NH_4^+ in marine and freshwaters. Limnol Oceanog 37:1113–1119.

Harris SJ, Mortimer RJG. 2002. Determination of nitrate in small water samples by the cadmium-copper reduction method: a manual technique with application to the interstitial waters of marine sediments. Inter J Environ Anal Chem 82:369–376.

Istok JD, Senko JM, Krumholz LR, Watson D, Bogle MA, Peacock A, Chang YJ, White DC. 2004. In situ bioreduction of technetium and uranium in a nitrate-contaminated aquifer. Environ Sci Technol 38:468–475.

Lane DJ, Pace B, Olsen GJ, Stahl DA, Sogin ML, Pace NR. Rapid determination of 16S ribosomal-RNA sequences for phylogenetic analysis. Proc Natl Acad Sci USA 82:6955–6959.

Langley S, Gault AG, Ibrahim A, Takahashi Y, Renaud R, Fortin D, Clark ID, Ferris FG. 2009. Sorption of strontium onto bacteriogenic iron oxides. Environ Sci Technol 43:1008–1014.

Law GTW, Geissler A, Boothman C, Burke IT, Livens FR, Lloyd JR, Morris K. 2010. Role of nitrate in conditioning aquifer sediments for technetium bioreduction. Environ Sci Technol 44:150–155.

Lebuhn M, Achouak W, Schloter M, Berge O, Meier H, Barakat M, Hartman A, Heulin T. 2000. Taxonomic characterization of *Ochrobactrum sp.* isolates from soil samples and wheat roots, and description of *Ochrobactrum tritici* sp. Nov. and *Ochrobactrum grignonense*. Inter J Syst Evolut Microbiol 50:2207–2223.

Li XZ, Krumholz LR. 2008. Influence of nitrate on microbial reduction of pertechnatate. Environ Sci Technol 42:1910–1915.

Lloyd JR, Renshaw JC. 2005. Bioremediation of radioactive waste: radionuclide-microbe interactions in laboratory and field-scale studies. Curr Opin Biotechnol 16:254–260.

Lloyd JR. 2003. Microbial reduction of metals and radionuclides. FEMS Microbiol Rev 27: 411–425.

Lovley DR, Coates JD. 1997. Bioremediation of metal contamination. Curr Opin Biotechnol 8:285–289.

Lovley DR, Phillips EJP. 1986. Organic-matter mineralization with reduction of ferric iron in anaerobic sediments. Appl Environ Microbiol 51:683–689.

Lovley DR, Phillips EJP. 1987. Rapid assay for microbially reducible ferric iron in aquatic sediments. Appl Environ Microbial 53:1536–1540.

Madden AS, Smith AC, Balkwill DL, Fagan LA, Phelps TJ. 2007. Microbial uranium immobilization independent of nitrate reduction. Environ Microbiol 9:2321–2330.

McKenzie H, Armstrong-Pope N. 2010. Groundwater Annual Report 2010. Sellafield Ltd. Technical report TECH000613. Available from: http://www.sellafieldsites.com/land/documents/Groundwater_Annual_Report_2010.pdf

Manaka M, Seki Y, Okuzawa K, Kamioka H, Watanabe Y. 2007. Natural attenuation of dissolved uranium within a small stream of central Japan. Limnology 8:143–153.

McBeth JM, Lear G, Lloyd JR, Livens FR, Morris K Burke IT. 2007. Technetium reduction and reoxidation in aquifer sediments. Geomicrobiol J 24:189–197.

Michalsen MM, Peacock AD, Smithgal AN, White DC, Spain AM, Sanchez-Rosario Y, Krumholz LR, Kelly SD, Kemner KM, McKinley J, Heald SM, Bogle MA, Watson DB, Istok JD. 2009. Treatment of nitric acid-, U(VI)-, and Tc(VII)-contaminated groundwater in intermediate-scale physical models of an in situ biobarrier. Environ Sci Technol 43:1952–1961.

Morris K, Livens FR, Charnock JM, Burke IT, McBeth JM, Begg JDC, Boothman C, Lloyd JR. 2008. An X-ray absorption study of the fate of technetium in reduced and reoxidised sediments and mineral phases. Appl Geochem 23: 603–617.

Nagel M, Andreesen JR. 1991. *Bacillus-niacini* sp. Nov, a nicotinate-metabolizing mesophile isolated from soil. Int J Syst Bacteriol 41:134–139.

North NN, Dollhopf SL, Petrie L, Istok JD, Balkwill DL, Kostka JE. 2004. Change in bacterial community structure during in situ biostimulation of subsurface sediment co-contaminated with uranium and nitrate. Appl Environ Microbiol 70:4911–4920.

Pollock J, Weber KA, Lack J, Achenbach LA, Mormile MR, Coates JD. 2007. Alkaline iron(III) reduction by a novel alkaliphilic, halotolerant, *Bacillus sp.* isolated from salt flat sediments of Soap Lake. Appl Microbiol Biotechnol 77:927–934.

Poulton SW, Canfield DE. 2005. Development of a sequential extraction procedure for iron: implications for iron partitioning in continentally derived particulates. Chem Geol 214:209–221.

Reardon CL, Cummings DE, Petzke LM, Kinsall BL, Watson DB, Peyton BM, Geesey GG. 2004. Composition and diversity of microbial communities recovered from surrogate minerals incubated in an acidic uranium-contaminated aquifer. Appl Environ Microbiol 70:6037–6046.

Robertson WJ, Franzmann PD, Mee BJ. 2000. Spore-forming, *Desulfosporosinus*-like sulphate-reducing bacteria from a shallow aquifer contaminated with gasoline. J Appl Microbiol 88: 248–259.

Robinson C, Barry DA, McCarty PL, Gerhard JI, Kouznetsova I. 2009. pH control for enhanced reductive bioremediation of chlorinated solvent source zones. Sci Tot Environ 407:4560–4573.

Roden EE, Leonardo MR, Ferris FG. 2002. Immobilization of strontium during iron biomineralization coupled to dissimilatory hydrous ferric oxide reduction. Geochim Cosmochim Acta 66:2823–2839.

Selenska-Pobell S, Geissler A, Merroun M, Flemming K, Geipel G, Reuther H. 2008. Biogeochemical changes induced by uranyl nitrate in a uranium waste pile. In: Merkel BJ, Hasche-Berger A, editors. Uranium Mining and Hydrology. Freiberg: Springer. p. 743–752.

Shelobolina ES, O'Niell K, Finneran KT, Hayes LA, Lovley DR. 2003. Potential for in situ bioremediation of low pH, high nitrate uranium-contaminated groundwater. Soil Sed Contam 12:865–884.

Singleton MJ, Woods KN, Conrad ME, Depaolo DJ, Dresel PE. 2005. Tracking sources of unsaturated zone and groundwater nitrate contamination using nitrogen and oxygen stable isotopes at the Hanford Site, Washington. Environ Sci Technol 39:3563–3570.

Spring S, Rosenzweig F. 2006. The Genera *Desulfitobacterium* and *Desulfosporosinus*: Taxonomy. In: Prokaryotes: A Handbook on the Biology of Bacteria, Volume 4, Bacteria: Firmicutes, Cyanobacteria, 3rd ed. New York: Springer. p. 771–786.

Stewart DI, Burke IT, Hughes-Berry DV, Whittleston RA. 2010. Microbially mediated chromate reduction in soil contaminated by highly alkaline leachate from chromium containing waste. Ecol Eng 36:211–221.

Stookey LL. 1970. Ferrozine—a new spectrophotometric reagent for iron. Anal Chem 42:779–781.

Tessier A, Campbell PGC, Bisson M. 1979. Sequential extraction procedure for the speciation of particulate trace-metals. Anal Chem 51:844–851.

Viollier E, Inglett PW, Hunter K, Roychoudhury AN, Van Cappellen P. 2000. The ferrozine method revisited: Fe(II)/Fe(III) determination in natural waters. Appl Geochem 15:785–790.

Weon SY, Lee CW, Lee SI, Koopman B. 2002. Nitrite inhibition of aerobic growth of *Acinetobacter* sp. Water Res 36:4471–4476.

Wilkins MJ, Livens FR, Vaughan DJ, Beadle I, Lloyd JR. 2007. The influence of microbial redox cycling on radionuclide mobility in the subsurface at a low-level radioactive waste storage site. Geobiology 5:293–301.

Wilkins MJ, Livens FR, Vaughan DJ, Lloyd JR, Beadle I, Small JS. 2010. Fe(III) Reduction in the subsurface at a low-level radioactive waste disposal site. Geomicrobiol J 27:231–239.

Ye O, Roh Y, Carroll SL, Blair B, Zhou J, Zhang CL, Fields MW. 2004. Alkaline anaerobic respiration: isolation and characterization of a novel alkaliphilic and metal reducing bacterium. Appl Environ Microbiol 70:5595–5602.

Zhou Y, Ganda L, Lim M, Yuan ZG, Kielleberg S, Ng WJ. 2010. Free nitrous acid (FNA) inhibition on denitrifying poly-phosphate accumulating organisms (DPAOs). Appl Microbiol Biotech 88:359–369.

Zhou Y, Pijuan M, Yuan ZG. 2007. Free nitrous acid inhibition on anoxic phosphorus uptake and denitrification by poly-phosphate accumulating organisms. Biotech Bioeng 98:903–912.

Chapter 4: Alkaline Fe(III) reduction by a novel alkali-tolerant *Serratia* sp. isolated from surface sediments close to Sellafield nuclear facility, UK

This chapter contains the following published paper:

Thorpe, C.L., Morris, K., Boothman, C., Lloyd, J.R., (2012). Alkaline Fe(III) reduction by a novel alkali-tolerant *Serratia* sp. isolated from surface sediments close to Sellafield nuclear facility, UK. *FEMS Microbiology Letters*, 327, 87-92.

RESEARCH LETTER

Alkaline Fe(III) reduction by a novel alkali-tolerant *Serratia* sp. isolated from surface sediments close to Sellafield nuclear facility, UK

Clare L. Thorpe, Katherine Morris, Christopher Boothman & Jonathan R. Lloyd

Research Centre for Radwaste and Decommissioning and Williamson Research Centre for Molecular Environmental Science, School of Earth, Atmospheric and Environmental Sciences, The University of Manchester, Manchester, UK

Correspondence: Jonathan R. Lloyd, Research Centre for Radwaste and Decommissioning and Williamson Research Centre for Molecular Environmental Science, School of Earth, Atmospheric and Environmental Sciences, The University of Manchester, Manchester M13 9PL, UK. Tel.: +44 161 275 7155; fax: +44 161 275 0310; e-mail: jon.lloyd@manchester.ac.uk

Received 3 October 2011; accepted 10 November 2011.
Final version published online 15 December 2011.

DOI: 10.1111/j.1574-6968.2011.02455.x

Editor: J. Colin Murrell

Keywords
bioreduction; nitrate; bioremediation; iron reduction.

Abstract

Extensive denitrification resulted in a dramatic increase in pH (from 6.8 to 9.5) in nitrate-impacted, acetate-amended sediment microcosms containing sediment representative of the Sellafield nuclear facility, UK. Denitrification was followed by Fe(III) reduction, indicating the presence of alkali-tolerant, metal-reducing bacteria. A close relative (99% 16S rRNA gene sequence homology) to *Serratia liquefaciens* dominated progressive enrichment cultures containing Fe(III)-citrate as the sole electron acceptor at pH 9 and was isolated aerobically using solid media. The optimum growth conditions for this facultatively anaerobic *Serratia* species were investigated, and it was capable of metabolizing a wide range of electron acceptors including oxygen, nitrate, FeGel, Fe-NTA and Fe-citrate and electron donors including acetate, lactate, formate, ethanol, glucose, glycerol and yeast extract at an optimum pH of *c.* 6.5 at 20 °C. The alkali tolerance of this strain extends the pH range of highly adaptable Fe (III)-reducing *Serratia* species from mildly acidic pH values associated with acid mine drainage conditions to alkali conditions representative of subsurface sediments stimulated for extensive denitrification and metal reduction.

Introduction

Dissimilatory Fe(III)-reducing bacteria are widely distributed in freshwater and marine environments and have the ability to utilize a wide range of compounds as electron donors (Lovley *et al.*, 2004; Weber *et al.*, 2006). Dissimilatory Fe(III) reduction has been shown to occur over a wide pH range from acid mine drainage sites to alkaline soda lakes (Johnson, 1995; Straub *et al.*, 2001; Pollock *et al.*, 2007). Although Fe(III) reduction at low (< pH 3) and circumneutral pH is well documented, few studies exist showing Fe(III) reduction above pH 9 (Gorlenko *et al.*, 2004; Pollock *et al.*, 2007), despite the potential significance of these reactions in a range of natural and engineered environments. Alkaline pH is challenging for microbial metabolism as microorganisms must maintain their optimum intracellular pH and possess a mechanism for creating an electron motive force capable of driving solutes across the cell membrane against a proton counter gradient (Krulwich *et al.*, 2001; Detkova & Pusheva, 2006; Stewart *et al.*, 2010). It is suggested that in extreme alkaline environments, Na^+ may replace H^+ to create an electron motive force in some alkaliphilic microorganisms (Kevbrin *et al.*, 1998; Krulwich *et al.*, 2001; Detkova & Pusheva, 2006). Fe(III) reduction at a pH > 9 has been observed by several species isolated from natural alkaline soda lakes, including *Anaerobranca californiensis* (Gorlenko *et al.*, 2004), *Alkaliphilus metaliredigens* (Ye *et al.*, 2004), *Tindallia magadii* (Kevbrin *et al.*, 1998) and species most similar to (96%) *Bacillus agaradhaerens* (Pollock *et al.*, 2007). In addition to natural high pH environments, such as soda lakes, there is interest in the biogeochemistry of engineered high pH sediments, for example those resulting from industrial contamination and the use of alkaline cements as a building material. Alkaline sediment geomicrobiology is of particular current interest to the nuclear industry owing to the proposed use of cement containment for deep geological disposal of radioactive

FEMS MICROBIOLOGY LETTERS

wastes and for remediation scenarios for existing contaminated land (NDA, 2011). It is important to understand how changes in pH may affect the microbial community and therefore the biogeochemical processes occurring in the subsurface. Microbial processes are a key to predicting the mobility of problematic radionuclides in the subsurface (Lloyd, 2003). In addition, understanding the extent and impact of alkali-generating biogeochemical processes such as nitrate, iron or sulphate reduction is also of wider interest in both natural and engineered environments.

In this study, the pH of sediments representative of the Sellafield nuclear facility was increased via extensive reduction of nitrate, a common contaminant at nuclear sites, from *c.* pH 6.8 to 9.3, and Fe(III) reduction was observed to occur thereafter (Thorpe *et al.*, in press). Here, a gradual increase in pH resulted in adaptation of the moderately acidotolerant microbial community to a moderately alkaline environment where the dominance of alkali-tolerant bacteria would be expected. PCR-based 16S rRNA gene analyses of an enrichment culture taken from a pH *c.* 9.3 Fe(III)-reducing sediment stimulated with acetate as the electron donor identified a close relative (99% sequence homology) of the known alkaliphilic bacterium *Alkaliphilus crotonatoxidans* (41% of 16S rRNA genes in a clone library prepared from the enriched community) and a close relative (99% sequence homology) of *Serratia liquefaciens* (56% of the clone library). Surprisingly, over successive enrichment cultures at pH *c.* 9, the known alkaliphilic species *A. crotonatoxidans* was outcompeted by the *Serratia* species not previously reported as alkali-tolerant. Interestingly, previous work suggests that members of the genus *Serratia* favour low pH with strains reported as acidotolerant with an optimum growth pH of *c.* 6.5 and a growth range pH as low as 3 (Adams *et al.*, 2007). Enrichment for, isolation of and characterization of this new *Serratia* species are described.

Materials and methods

Study site

Sediments representative of the quaternary unconsolidated alluvial flood-plain deposits that underlie the Sellafield site were collected from the Calder Valley, Cumbria (Law *et al.*, 2010). Sampling was conducted *c.* 2 km from the site at Lat 54°26′30N, Long 03°28′09W.

Cultivation of Fe(III)-reducing bacteria

Sediment samples from bioreduced pH *c.* 9.5 sediment were used to inoculate enrichment cultures (10 % inoculum) with acetate as the electron donor (10 mM) and Fe (III)-citrate as the electron acceptor (20 mM). The enrichment medium was based on the recipe of Lovley *et al.* (1991) and comprised (in grams per litre of deionized water) $NaHCO_3$, 2.5; NH_4Cl, 0.25; $NaH_2PO_4{\cdot}H_2O$, 0.6; and KCl, 0.1. In addition, stock solutions of vitamins and minerals were added (Lovley & Phillips, 1988). The medium was adjusted to *c.* 9.3 with the addition of NaOH, sparged with N_2/CO_2 (80 : 20) gas mix and filter-sterilized (0.2 μm) before dispensing into autoclaved 30-mL serum bottles and sealing with sterile butyl rubber stoppers and aluminium crimp caps. Inoculated bottles were kept in the dark at 20 °C. Standard anaerobic sampling techniques were used throughout for monitoring the cultures.

Isolation of an axenic Fe(III)-reducing culture

The sediment enrichment culture grown in Fe(III)-citrate medium was transferred seven times at pH *c.* 9.3, and 16S rRNA gene analysis was then performed. A culture of the *Serratia* species that dominated final 16S rRNA clone libraries was isolated by streaking onto 4% Luria–Bertani (LB) agar plates at pH 7 (Fisher Scientific, UK) and incubating aerobically at 20 °C. A single colony of this species was transferred to fresh medium and used for all subsequent experiments. The culture was confirmed as axenic by microscopy, colony morphology and 16S rRNA cloning and analyses.

Characterization

To explore the ability of the isolate to metabolize a range of electron acceptors, nitrate, Fe(III)-NTA, Fe(III)-oxyhydroxide or Fe(III)-citrate was added (20 mM) to minimal medium with either acetate or glycerol (10 mM) as an electron donor. Electron donor utilization was tested using Fe(III)-citrate (20 mM) as the electron acceptor and lactate, formate, ethanol, glucose, yeast extract, benzoate, acetate or glycerol (10 mM) as potential electron donors. The pH tolerance was assessed using Fe(III)-citrate medium (20 mM) with glycerol (10 mM) as the electron donor at pH ranging from 3.5 to 10. The pH of the medium was adjusted with NaOH or HCl prior to inoculation.

Amplification of 16S rRNA gene sequences

The 16S–23S rRNA intergenic spacer region from the bacterial RNA operon was amplified as described previously using primers ITSF and ITSReub (Cardinale *et al.*, 2004). The amplified products were separated by electrophoresis in Tris-acetate–EDTA gel. DNA was stained with ethidium bromide and viewed under short-wave UV light. Positive microbial community changes identified by the Ribosomal Intergenic Spacer Analysis (RISA) justified further investigation by DNA sequencing of 16S rRNA gene clone libraries.

Cloning

PCR products were purified using a QIAquick PCR purification kit (Qiagen, UK) and ligated directly into a cloning vector containing topoisomerase I-charged vector arms (Agilent Technologies, UK) prior to transformation into *Escherichia coli*-competent cells expressing Cre recombinase (Agilent Technologies). White transformants that grew on LB agar containing ampicillin and X-Gal were screened for an insert using PCR. Primers were complementary to the flanking regions of the PCR insertion site of the cloning vector. The conditions for PCR method were as follows: an initial denaturation at 94 °C for 4 min, melting at 94 °C for 30 s, annealing at 55 °C for 30 s, extension at 72 °C for 1 min, 35 cycles, followed by a final extension step at 72 °C for 5 min. The resulting PCR products were purified using an ExoSap protocol, and 2 μL of ExoSap mix (0.058 μL exonuclease I, 0.5 μL Shrimp alkaline phosphatase and 1.442 μL QH_2O) was added to 5 μL of PCR product and incubated at 37 °C for 30 min followed by 80 °C for 15 min.

DNA sequencing and phylogenetic analysis

Nucleotide sequences were determined by the dideoxynucleotide method (Sanger *et al.*, 1977). An ABI Prism Big-Dye Terminator Cycle Sequencing kit was used in combination with an ABI Prism 877 Integrated Thermal Cycler and ABI Prism 377 DNA Sequencer (Perkin Elmer Applied Biosystems, UK). Sequences (typically 900 base pairs in length) were analysed against the NCBI (USA) database using the BLAST program packages and matched to known 16S rRNA gene sequences.

Analytical methods

Nitrate reduction was monitored by UV–vis spectroscopy: increasing cell density OD 600 nm and appearance of nitrite in solution via a UV–vis spectroscopic method (Harris & Mortimer, 2002). Fe(III) reduction was monitored by measuring the increase in 0.5 N HCl-extractable Fe(II) over time using a ferrozine assay (Stookey, 1970). Mineral products of Fe(III) reduction were analysed using X-ray powder diffraction (XRD) obtained with a Bruker D8Advance instrument using Cu $K_{\alpha 1}$ radiation.

Results and discussion

Enrichment and isolation

In incubation experiments exploring the biogeochemistry of sediments representative of the Sellafield site, the pH rose from 6.8 to *c.* 9.3 during reduction of 100 mM

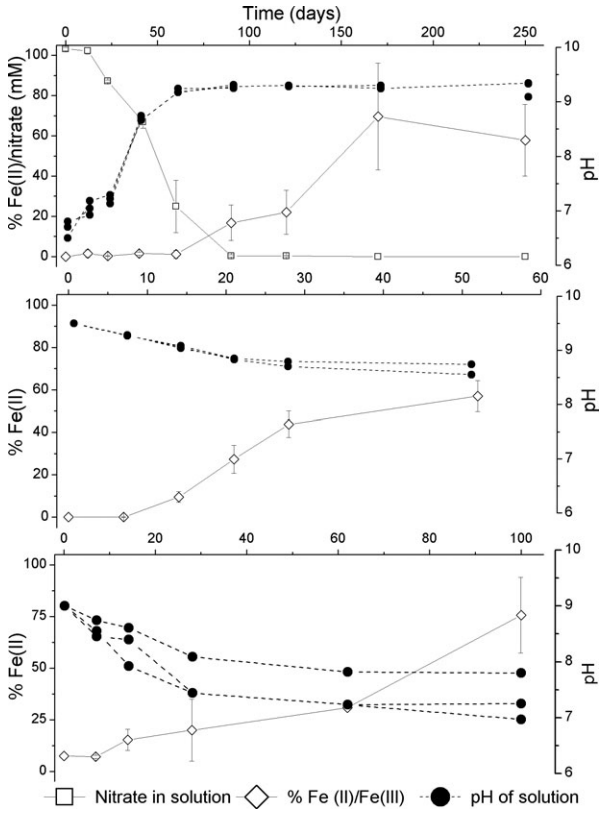

Fig. 1. Percentage of 0.5 N HCl extractable Fe(II), pH and nitrate in solution (where relevant) for (a) acetate amended 100 mM nitrate impacted sediment, (b) acetate amended Fe(III)-citrate medium inoculated with Fe(III) reducing pH 9 sediment, 4th in the series of inoculums and (c) acetate amended Fe(III)-citrate medium inoculated with the *Serratia* sp. isolate. Error bars represent 1σ of triplicate analysis.

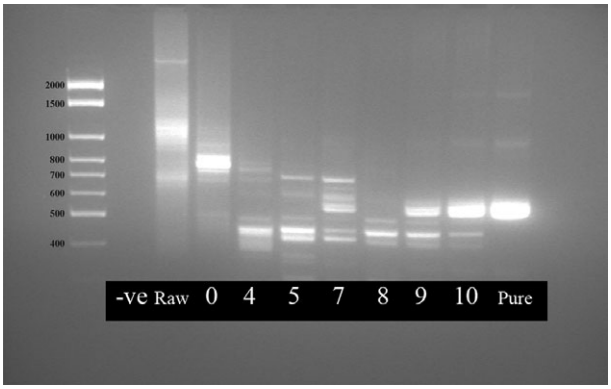

Fig. 2. RISA analysis of progressive subcultures showing the diversity of the microbial community over time. Raw = raw bioreduced sediment, 0 = first Fe(III)-citrate enrichment culture inoculated from the raw sediment, 4–10 = number of successive transfers to fresh media (10% inoculation) and Pure = the *Serratia* sp. isolate.

Table 1. Phylogenetic affiliation of 16S rRNA gene sequences detected in the clone library from an Fe(III)-reducing enrichment culture at pH 9.5

Clone representative	No in clone library	Closest matching microorganism (accession number)	Identities (% match)	% Present	Phylogenetic class
CT-Fecit-87	37	*Alkaliphilus crotonatoxidans* (AF467248)	890/896 (99%)	40.7	*Clostridia*
CT-Fecit-66	51	*Serratia liquefaciens* (AJ306725)	871/872 (99%)	56.0	*Gammaproteobacteria*
CT-Fecit-80	2	*Clostridium celerecrescens* clone IrT-JG1-12 (AJ295659)	863/876 (98%)	2.2	*Clostridia*
CT-Fecit-35	1	Uncultured bacterium; 3BH-2FF (EU937958)	839/858 (97%)	1.1	*Betaproteobacteria*

nitrate (in the presence of added acetate) and Fe(III) reduction was observed to follow (Fig. 1a). Subaliquots from these sediment incubations added to acetate-amended, Fe(III)-citrate medium were enriched further for the Fe(III)-reducing microbial community and continued to support stable Fe(III) reduction at pH > 9 (Fig. 1b). RISA results illustrate that the microbial community became less diverse as the subculture was transferred to fresh medium every *c.* 6 weeks (10 % inoculum) (Fig. 2). After seven transfers, 16S rRNA gene analysis identified a mixed culture, with 41 % of the clone library comprising genes most closely related (99 % identical) to the known alkaliphilic bacterium *Alkaliphilus cronotoxidens* and 56 % most closely related (99 % identical) to *S. liquefaciens CIP 103238T*, with other species making up < 3 % of the clone library (Table 1). However, after 10 transfers, the community was much less diverse, and by plating out onto LB agar plates, an axenic culture that was shown to reduce Fe(III) at pH *c.* 9.0 was obtained (Fig. 1c). RISA analysis confirmed that this isolated species was the organism that dominated the mixed culture at subculture 10, and 16S rRNA gene sequence confirmed that this was the *Serratia* species identified previously (Fig. 2). The phylogenetic placement of this organism compared with other Fe(III)-reducing bacteria is shown in Fig. 3. It is interesting that despite the consis-

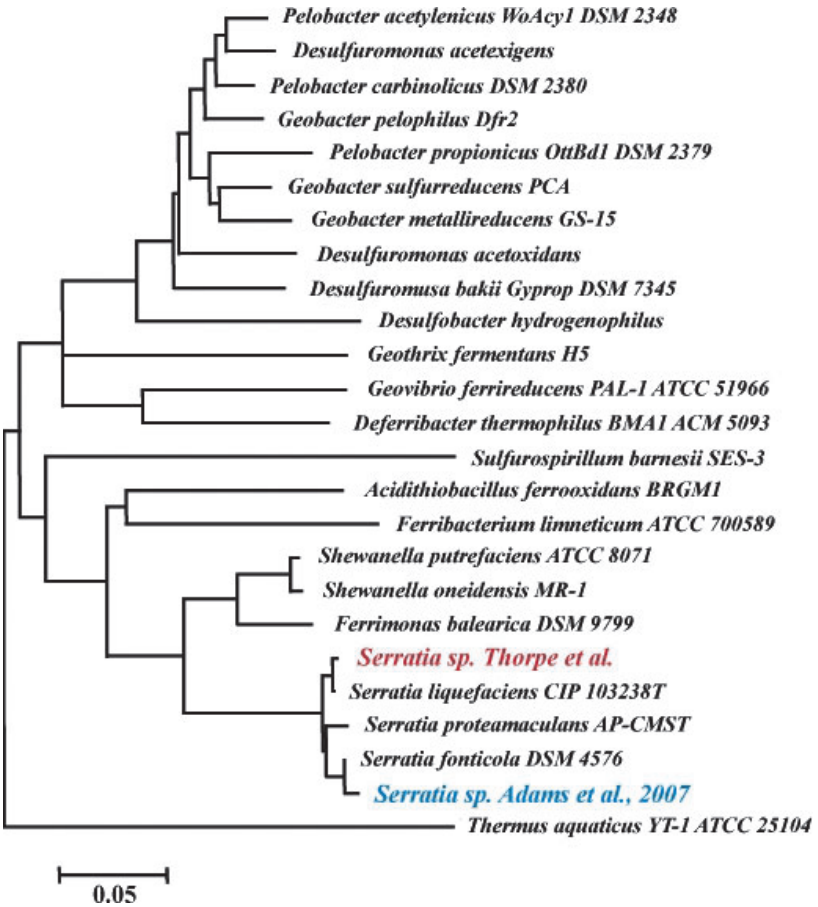

Fig. 3. Phylogenetic placement of the Sellafield sediment isolate (Thorpe *et al.* this study) compared to relevant microorganisms. Scale bar = 5% sequence difference.

tently high pH in these subcultures, and the presence of a close relative to a known alkaliphile, the *Serratia* species was shown to predominate in these systems. In a previous study at an acidic rock drainage site, a *Serratia* species was isolated and shown to respire using Fe(III) ('*Serratia* Adams *et al.*, 2007' on Fig. 3) and was characterized as acidotolerant with an optimum growth pH of 6.5 (Adams *et al.*, 2007).

Anaerobic growth of the *Serratia* isolate

In addition to aerobic growth on LB medium, the *Serratia* species was found to be capable of utilizing a variety of electron acceptors under anaerobic conditions: NO_3^-, Fe(III)-NTA, Fe(III)-citrate and Fe(III)-oxyhydroxide (ferrihydrite), although only minimal reduction of ferrihydrite (< 10%) was observed (data not shown). Electron donors (10 mM) were utilized with Fe(III)-citrate (20 mM) as the electron acceptor included, in order of the rate of Fe(III) reduction supported: glycerol > formate > ethanol > yeast extract > lactate > acetate > benzoic acid (Fig. 4). These findings are similar to previous work on *Serratia* sp. (Adams *et al.*, 2007) where glycerol was found to be the most favourable electron donor tested and acetate and benzoate resulted in slow rates of Fe(III) reduction.

Effects of pH on Fe(III) reduction

The *Serratia* species isolated from Sellafield sediment was found to reduce Fe(III) optimally at the pH of 4.5–6.5 with a range of activity between pH 3.5 to 9.5 (Fig. 5). No Fe(III) reduction was observed above pH 9.5, and rates of Fe(III) reduction were observed to slow above pH *c.* 6.5 and below pH *c.* 4.5 (Fig. 5a). In cultures where the pH was initially < 6.5, the microbial Fe(III) reduction was observed to shift the pH towards alkalinity presumably because of the release of OH^- during Fe(III) reduction (Fig. 5b) (Mortimer *et al.*, 1997; Adams *et al.*, 2007). However, the pH in Fe(III)-citrate cultures with an initial pH > 6.5 decreased during Fe(III) reduction presumably because of an increase in aqueous CO_2 resulting from microbial respiration and subsequent formation and dissociation of carbonic acid (Figs 1b,c and 5b). In addition, after Fe(III) reduction had developed, a white precipitate was observed above pH 7 and this was identified via XRD analysis as containing both siderite and vivianite (data not shown). Siderite and vivianite production consumes HCO_3^- and OH^- acting to decrease the pH. It is interesting that the biogeochemical processes occurring in these microcosms act to buffer the pH towards the optimum growth pH for *Serratia* sp.

Implications

The bacterium isolated in this study appears to be a robust and highly adaptable species that is capable of surviving dramatic changes in sediment geochemistry. *Serratia* species are reported to reduce Fe(III) over a wide spectrum of pH values and utilize a diverse range of alternative

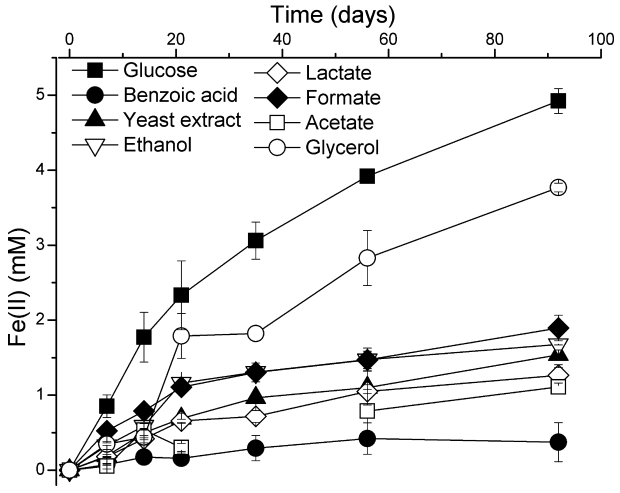

Fig. 4. Fe(II) production in a pure culture of *Serratia* grown with a range of electron donors (10 mM) and 10 mM Fe(III)-citrate in systems with starting pH *c.* 7. Error bars represent 1σ of triplicate analysis.

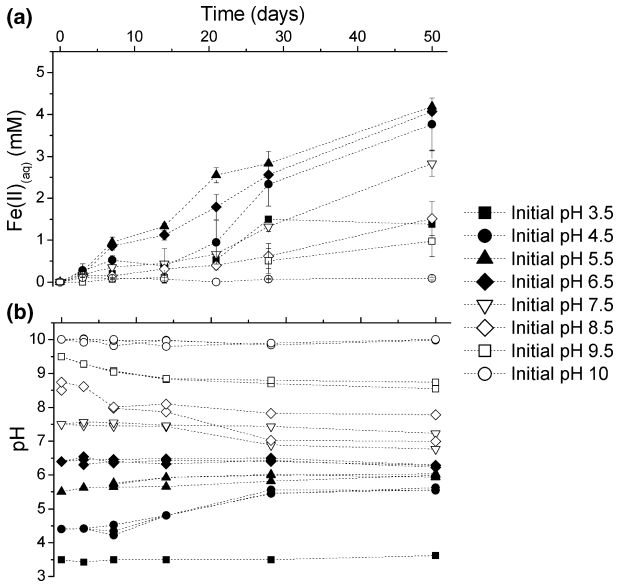

Fig. 5. Graphs showing (a) Fe(II) production in pure culture of *Serratia* grown with 10 mM glycerol and 20 mM Fe(III)-citrate over the range of pH values from pH 3.5 to 10 in initial experiments; and (b) the pH over time in these systems. Error bars represent 1σ of triplicate analysis.

electron acceptors and electron donors (This study and Adams *et al.*, 2007). It appears that during microbial stimulation scenarios, changes in pH and available electron donors/acceptors can result in unusually resilient rather than more commonly identified Fe(III)-reducing organisms becoming dominant. Here, an organism rarely reported as an Fe(III)-reducing bacterium with an optimum growth pH of < 7 was observed to dominate in a pH 9 system which had undergone extensive denitrification prior to metal reduction. Thus, it is possible that during remediation scenarios where sediment geochemistry is altered during bioremediation, the microbial community may shift to favour less typical, but more adaptable species.

Acknowledgements

This work was funded by the Engineering and Physical Science Research Council (EPSRC) as part of the Decommissioning, Immobilisation and Management of Nuclear Waste for Disposal (DIAMOND) consortium grant EP/F055412/1. We also acknowledge the support of NERC grants NE/H007768/1 for the molecular ecology work.

References

Adams LK, Boothman C & Lloyd JR (2007) Identification and characterization of a novel aciotolerant Fe(III)-reducing bacterium from a 3000-year-old acidic rock drainage site. *FEMS Microbiol Lett* **268**: 151–157.

Cardinale M, Brusetti L, Quatrini P, Borin S, Puglia AM, Rizzi A, Zanardini E, Sorlini C, Corselli C & Daffonchio D (2004) Comparison of different primer sets for use in automated ribosomal intergenic spacer analysis of complex bacterial communities. *Appl Environ Microbiol* **70**: 6147–6156.

Detkova EN & Pusheva MA (2006) Energy metabolism in halophilic and alkaliphilic acetogenic bacteria. *Microbiol* **75**: 1–11.

Gorlenko V, Tsapin A, Namsaraev Z, Teal T, Tourova T, Engler D, Mielke R & Nealson K (2004) *Anaerobranca californiensis* sp nov., an anaerobic, alkalithermophilic, fermentative bacterium isolated from a hot spring on Mono Lake. *Int J Syst Evol Microbiol* **54**: 739–743.

Harris SJ & Mortimer RJG (2002) Determination of nitrate in small water samples (100 μL) by the cadmium-copper reduction method: A manual technique with application to the interstitial waters of marine sediments. *Int J Environ Anal Chem* **82**: 369–376.

Johnson DB (1995) Selective solid media for isolating and enumerating acidophilic bacteria. *J Microbiol Methods* **23**: 205–218.

Kevbrin VV, Zhilina TN, Rainey FA & Zavarzin GA (1998) *Tindallia magadii* gen. nov., sp. nov.: An alkaliphilic anaerobic ammonifier from soda lake deposits. *Current Microbiology* **37**: 94–100.

Krulwich TA, Ito M & Guffanti AA (2001) The Na^+-dependence of alkaliphily in *Bacillus*. *Biochim Biophy Acta – Bioenergetics* **1505**: 158–168.

Law GTW, Geissler A, Boothman C, Burke IT, Livens FR, Lloyd JR & Morris K (2010) Role of nitrate in conditioning aquifer sediments for technetium bioreduction. *Environ Sci Technol* **44**: 150–155.

Lloyd JR (2003) Microbial reduction of metals and radionuclides. *FEMS Microbiol Rev* **27**: 411–425.

Lovley DR & Phillips EJP (1988) Novel mode of microbial energy metabolism: organic carbon oxidation coupled to dissimilatory reduction of iron or manganese. *Appl Environ Microbiol* **54**: 1472–1480.

Lovley DR, Phillips EJP & Lonergan DJ (1991) Enzymatic versus monenzymatic mechanisms for Fe(III) reduction in aquatic sediments. *Environ Sci Technol* **25**: 1062–1067.

Lovley DR, Holmes DE & Nevin KP (2004) Dissimilatory Fe (III) and Mn(IV) reduction. *Adv Microb Physiol* **49**: 219–286.

Mortimer RJG, Coleman ML & Rae JE (1997) Effect of bacteria on the elemental composition of early diagenetic siderite: implications for palaeoenvironmental interpretations. *Sedimentology* **44**: 759–765.

NDA (2011) *Strategy – effective from April 2011*. Nuclear Decommissioning Authority report. Available on: http://www.nda.gov.uk/loader.cfm?csModule=security/getfile&pageid=44503.

Pollock J, Weber KA, Lack J, Achenbach LA, Mormile MR & Coates JD (2007) Alkaline iron(III) reduction by a novel alkaliphilic, halotolerant, *Bacillus sp.* isolated from salt flat sediments of Soap Lake. *Appl Microbiol Biotechnol* **77**: 927–934.

Sanger F, Nicklen S & Coulsen AR (1977) DNA sequencing chain terminating inhibitors. *P Natl Acad Sci USA* **74**: 5463–5467.

Stewart DI, Burke IT, Hughes-Berry DV & Whittleston RA (2010) Microbially mediated chromate reduction in soil contaminated by highly alkaline leachate from chromium containing waste. *Ecol Eng* **36**: 211–221.

Stookey LL (1970) Ferrozine – a new spectrophotometric reagent for iron. *Anal Chem* **42**: 779–781.

Straub KL, Benz M & Schink B (2001) Iron metabolism in anoxic environments at near neutral pH. *FEMS Microbiol Ecol* **34**: 181–186.

Thorpe CL, Law GTW, Boothman C, Lloyd JR, Burke IT & Morris K (in press) Synergistic effect of high nitrate concentrations on sediment bioreduction. *Geomicrobiol J*, in press.

Weber KA, Achenbach LA & Coates JD (2006) Microorganisms pumping iron: anaerobic microbial iron oxidation and reduction. *Nat Rev Microbiol* **4**: 752–764.

Ye Q, Roh Y, Carroll SL, Blair B, Zhou JZ, Zhang CL & Fields MW (2004) Alkaline anaerobic respiration: Isolation and characterization of a novel alkaliphilic and metal-reducing bacterium. *Appl Environ Microbiol* **70**: 5595–5602.

Chapter 5: Strontium sorption and precipitation behaviour during bioreduction in nitrate impacted sediments

This chapter contains the following paper accepted for publication in Chemical Geology:

Thorpe, C.L., Lloyd, J.R., Law, G.T.W., Burke, I.T., Shaw, S., Bryan, N.D., Morris, K. (2012). Strontium sorption and precipitation behaviour during bioreduction in nitrate impacted sediments. *Chemical Geology*, (in press).

Chemical Geology 306–307 (2012) 114–122

Contents lists available at SciVerse ScienceDirect

Chemical Geology

journal homepage: www.elsevier.com/locate/chemgeo

Strontium sorption and precipitation behaviour during bioreduction in nitrate impacted sediments

Clare L. Thorpe [a], Jonathan R. Lloyd [a], Gareth T.W. Law [a], Ian T. Burke [b], Samuel Shaw [b], Nicholas D. Bryan [a], Katherine Morris [a,*]

[a] Research Centre for Radwaste and Decommissioning and Williamson Research Centre for Molecular Environmental Science, School of Earth, Atmospheric and Environmental Sciences, The University of Manchester, Manchester M13 9PL, UK
[b] Earth Surface Science Institute, School of Earth and Environment, The University of Leeds, Leeds LS2 9JT, UK

ARTICLE INFO

Article history:
Received 20 December 2011
Received in revised form 1 March 2012
Accepted 2 March 2012
Available online 9 March 2012

Editor: J. Fein

Keywords:
Strontium
Bioreduction
Incorporation
Sorption
Nitrate
Nuclear

ABSTRACT

The behaviour of strontium (Sr^{2+}) during microbial reduction in nitrate impacted sediments was investigated in sediment microcosm experiments relevant to nuclear sites. Although Sr^{2+} is not expected to be influenced directly by redox state, bioreduction of nitrate caused reduced Sr^{2+} solubility due to an increase in pH during bioreduction and denitrification. Sr^{2+} removal was greatest in systems with the highest initial nitrate loading and consequently more alkaline conditions at the end of denitrification. After denitrification, a limited re-release of Sr^{2+} back into solution occurred coincident with the onset of metal (Mn(IV) and Fe(III)) reduction which caused minor pH changes in all microcosms with the exception of the bicarbonate buffered system with initial nitrate of 100 mM and final pH > 9. In this system ~95% of Sr^{2+} remained associated with the sediment throughout the progression of bioreduction. Analysis of this pH 9 system using X-ray absorption spectroscopy (XAS) and electron microscopy coupled to thermodynamic modelling showed that Sr^{2+} became partially incorporated within carbonate phases which were formed at higher pH. This is in contrast to all other systems where final pH was <9, here XAS analysis showed that outer sphere Sr^{2+} sorption predominated. These results provide novel insight into the likely environmental fate of the significant radioactive contaminant, ^{90}Sr, during changes in sediment biogeochemistry induced by bioreduction in nitrate impacted nuclear contaminated environments.

1. Introduction

Strontium-90, a high yield fission product resulting from nuclear fuel cycle operations, is a significant radioactive contaminant at nuclear facilities worldwide (Jackson and Inch, 1989; Riley and Zachara, 1992; Mason et al., 2000; Dewiere et al., 2004; McKinley et al., 2007; Priest et al., 2008; McKenzie and Armstrong-Pope, 2010). The behaviour of ^{90}Sr is of particular environmental concern in contaminated land due to both its ~29 year half-life (meaning that it will persist over several hundred years), and it is relative mobility in the shallow sub-surface at some nuclear facilities (McKinley et al., 2007; McKenzie and Armstrong-Pope, 2010). The remediation of ^{90}Sr and other radionuclides (e.g. U and Tc) from groundwaters at these sites is a key challenge for nuclear decommissioning. It is therefore important to explore remediation strategies which show promise of removing or immobilising a wide variety of problematic radionuclides with differing biogeochemical behaviour (e.g. ^{90}Sr, U and Tc) using a single methodology. Furthermore, the geochemical conditions at many nuclear facilities are mildly acidic to neutral, have high nitrate and also have significant naturally occurring iron(III) oxyhydroxide phases that must be taken into account when investigating remediation scenarios (Fredrickson et al., 2004; Istok et al., 2004; Begg et al., 2007; Edwards et al., 2007; McBeth et al., 2007; Law et al., 2010; McKenzie and Armstrong-Pope, 2010).

Strontium-90 exists in the natural environment solely as the Sr^{2+} ion, has very similar geochemical behaviour to Ca^{2+} and is therefore not directly affected by changes in redox conditions. Strontium speciation is controlled primarily by adsorption to mineral surfaces and incorporation or at high concentrations precipitation into Ca^{2+} bearing mineral phases (e.g. $CaCO_3$). Strontium mobility in the subsurface is influenced by the adsorption capacity of the minerals within the sediment as well as the pH and ionic strength of the groundwaters, temperature, organic matter concentration and the exchangeable Ca^{2+}/Mg^{2+} content (Cowan et al., 1991; Chen and Hayes, 1999; Solecki, 2005; Hull and Schafer, 2008; Chiang et al., 2010). The Sr^{2+} ion typically forms outer sphere adsorption complexes which are electrostatically bound to negatively charged mineral surfaces. As expected, increasing adsorption is observed as pH increases above the point of zero charge (PZC) of the relevant mineral phases (Cowan et al., 1991; Ferris et al., 2000; Sahai et al., 2000; Hofmann et al., 2005; Bascetin and Atun, 2006;

* Corresponding author. Tel.: +44 161 275 7541.
E-mail address: katherine.morris@manchester.ac.uk (K. Morris).

0009-2541/$ – see front matter © 2012 Elsevier B.V. All rights reserved.
doi:10.1016/j.chemgeo.2012.03.001

Bellenger and Staunton, 2008; Chorover et al., 2008). In iron rich sediments, adsorption to both aluminosilicate clays and Fe(III)-oxyhydroxide minerals will have a significant control over Sr^{2+} mobility with pH important in controlling the mineral surface charge and therefore the extent of cation adsorption (Chiang et al., 2010). Clay minerals (eg illite, chlorite, kaolinite and montmorillonite) provide important adsorption surfaces for cations even at low pH due to their relatively low PZC (pH 4–6) and permanent structural charge, (Hussain et al., 1996; Dyer et al., 2000; Coppin et al., 2002; Zhuang and Yu, 2002; Alvarez-Silva et al., 2010) whilst Fe(III)-hydroxides tend to contribute significant adsoption sites at higher pH (PZC pH 7–8) (Small et al., 1999; Hofmann et al., 2005). With increasing pH and alkalinity, groundwater will become oversaturated with regard to carbonate phases and at high Sr^{2+} concentrations, this may allow the precipitation of Sr^{2+} as strontianite ($SrCO_3$) or at lower Sr^{2+} concentrations, the incorporation of Sr^{2+} into $CaCO_3$ phases such as calcite or aragonite (Zachara et al., 1991; Tesoriero and Pankow, 1996; Greegor et al., 1997; Parkman et al., 1998; Finch et al., 2003; Fujita et al., 2004; Mitchell and Ferris, 2005). Additionally, where phosphate is present in the contaminated environment at significant concentrations, the sequestration of Sr^{2+} by phosphate minerals such as apatite is also likely to be a significant control on its behaviour (Handley-Sidhu et al., 2011).

Microbial metabolism has the ability to affect the geochemistry and mineralogy of subsurface sediments, as a result "bioreduction" systems have been considered for the remediation of groundwaters containing the redox active radionuclides Tc and U (Lloyd and Renshaw, 2005). Tc and U have been shown to be immobilised by reduction from the more soluble Tc(VII) and U(VI) to poorly soluble Tc(IV) and U(IV) during Fe(III) reducing conditions (Lloyd, 2003; Law et al., 2010, 2011). As radioactive ^{90}Sr is often found as a co-contaminant in Tc/U contaminated land (Riley and Zachara, 1992; Hartman et al., 2007; McKenzie and Armstrong-Pope, 2010), understanding the behaviour of Sr^{2+} during bioreduction is essential in predicting and managing the mobility of this problematic contaminant in both natural and engineered bioreduction scenarios. During bioreduction the solution pH will be affected by the reaction products which include OH^- and HCO_3^-, and metal reduction will affect sediment mineralogy (Law et al., 2010; Thorpe et al., 2012). Reductive dissolution of bioavailable Fe(III)/Mn oxides and formation of new Fe(II) mineral phases may result in Sr^{2+} that was sorbed to Fe(III) oxide surfaces being released due to mineral dissolution (Langley et al., 2009a, b). However, it has been shown that during Fe(III) oxide crystallisation adsorbed contaminant metals (e.g. Pb^{2+}) can become incorporated into the newly formed phase, therefore, the effect of Fe(III) oxide recrystallisation has the potential to increase or decrease Sr^{2+} environmental mobility. At the same time, the increase in pH caused by bioreduction processes may lead to enhanced removal of Sr^{2+} through increased sorption to mineral surfaces and carbonate precipitation/substitution (Roden et al., 2002; Mitchell and Ferris, 2005; Chorover et al., 2008). Microbial metabolism can result in the production of CO_3^{2-}/HCO_3^- which promotes alkaline pH conditions and supersaturation with regard to carbonate mineral phases ($SrCO_3$ or $CaCO_3$) in which Sr^{2+} can be precipitated (Coleman et al., 1993; Fujita et al., 2004; Mitchell and Ferris, 2005). These processes can also lead to siderite ($Fe(II)CO_3$) formation during microbial reduction of Fe(III), which may result in minor Sr^{2+} becoming incorporated into the newly formed mineral phase (Parmar et al., 2000; Roden et al., 2002).

Here, we consider the effects of microbial metabolism on the biogeochemistry and speciation of Sr^{2+} in conditions relevant to radioactively contaminated sites using stable Sr^{2+} as an analogue for ^{90}Sr. Specifically, sub-surface nitrate concentrations are often elevated and have been reported in excess of 100 mM some nuclear facilities (Riley and Zachara, 1992; Finneran et al., 2002; Fredrickson et al., 2004; Istok et al., 2004; Senko et al., 2005; McKenzie and Armstrong-Pope, 2010). In this study, we have examined the behaviour of Sr^{2+} during the development of bioreducing conditions in sediments representative of the Sellafield nuclear facility that have been amended with between 0.3 and 100 mM nitrate. We tested the hypothesis that an increase in OH^- and CO_3^{2-}/HCO_3^- during nitrate reduction may lead to increased adsorption of Sr^{2+} to mineral surfaces and, once over-saturation was reached, the precipitation and or incorporation of Sr^{2+} into carbonate phases at the high Sr/Ca ratio used in this study (1:1.5). Overall, our aim is to assess whether bioreduction approaches may be relevant to a range of problematic radionuclides including redox active U and Tc as well as ^{90}Sr and thus provide a holistic remediation strategy where co-contamination of these radionuclides occurs.

2. Methods

2.1. Experimental section

2.1.1. Sample collection

Sediments representative of the Quaternary unconsolidated alluvial flood-plain deposits that underlie the UK Sellafield reprocessing site were collected from the Calder Valley, Cumbria, during December 2008 (Law et al., 2010). The sampling area was located ~2 km from the Sellafield site and sediments were extracted from the shallow sub-surface (Lat 54°26′30 N, Long 03°28′09 W). Sediments were transferred directly into sterile containers, sealed, and stored at 4 °C prior to use.

2.1.2. Bioreduction microcosms

Sediment microcosms (10 ± 0.1 g Sellafield sediment, 100 ± 1 ml groundwater) were prepared using a synthetic groundwater representative of the Sellafield region (Wilkins et al., 2007) that was manipulated to produce a range of treatments (Table 1). Aerated systems were first established at variable pH (4.5, 5.5 and 7) to assess Sr^{2+} sorption in oxic systems. Following this a range of sealed microcosm systems were prepared. Unbuffered systems with an initial pH of ~5.5, and representative of the mildly acidic in situ pH at the sample site, were prepared with 0.3, 10, and 25 mM nitrate amendments. Bicarbonate buffered systems with an initial pH of ~7 were prepared with 0.3, 10, 25, and 100 mM nitrate amendments. Sodium acetate was added as an electron donor in excess of available electron acceptors (10 mM for 0.3–10 mM nitrate treatments, 20 mM for 25 mM nitrate treatments and 70 mM for 100 mM nitrate treatments) and a deoxygenated $NaNO_3$ solution was used for NO_3^- amendment. Finally, Sr^{2+} (as stable $SrCl_2$) was added to each microcosm to achieve 1.15 mM (100 ppm). Both the Sr concentration and the solid-solution ratio were chosen to allow full geochemical and spectroscopic characterisation and therefore are very much higher than values of ^{90}Sr encountered at even the most contaminated sites (Riley and Zachara, 1992; McKenzie and Armstrong-Pope, 2010). It should be noted that ^{90}Sr has a relatively

Table 1
Initial geochemical composition of microcosm systems.

System	Initial pH	Nitrate (mM)	Acetate (mM)	Ionic strength
Bicarbonate unamended 0.3 mM nitrate	5.5	0.3	10	0.024
Bicarbonate unamended 10 mM nitrate	5.5	10	10	0.034
Bicarbonate unamended 25 mM nitrate	5.5	25	20	0.059
Bicarbonate amended 0.3 mM nitrate	7	0.3	10	0.027
Bicarbonate amended 10 mM nitrate	7	10	10	0.037
Bicarbonate amended 25 mM nitrate	7	25	20	0.062
Bicarbonate amended 100 mM nitrate	7	100	70	0.190

short half-life and thus high specific activity and even for the most impacted sites where groundwater concentrations of >1000 Bq l^{-1} have been reported the molar concentration of ^{90}Sr will be very low (<10^{-11} mol l^{-1}) compared to our experimental concentrations (Riley and Zachara, 1992; McKinley et al., 2007; Mckenzie and Armstrong-Pope, 2010). Triplicate microcosms were then sealed with buytl rubber stoppers and incubated anaerobically at 20 °C in the dark for 110–250 days. At appropriate time points, sediment slurry was extracted under an O_2 free Ar atmosphere using aseptic technique and centrifuged (15,000 *g*; 10 min) to provide wet sediment pellets and porewater samples for analysis of bioreduction products and strontium.

2.1.3. Geochemical analyses and imaging

During microcosm sampling, total dissolved Fe, Mn(II), and NO_2^- concentrations were measured with standard UV–vis spectroscopy methods on a Jenway 6715 UV–vis spectrophotometer (Goto et al., 1977; Viollier et al., 2000; Harris and Mortimer, 2002). Aqueous NO_3^-, SO_4^{2-}, HCO_3^-/CO_3^{2-} and acetate were measured by ion chromatography (Dionex 4000i liquid chromatography). Aqueous Sr^{2+} and Ca^{2+} were measured by ICP-AES (Perkin-Elmer Optima 5300). Total bioavailable Fe(III) and the proportion of extractable Fe(II) in the sediment was estimated by digestion of ~0.1 g of sediment in 5 ml of 0.5 N HCl for 60 min followed by the ferrozine assay (Stookey, 1970; Lovley and Phillips, 1986). The pH and Eh were measured with a pH/Eh metre (Denver Instruments, UB10) and probes calibrated to pH 4, 7 and 10. Standards were routinely used to check the reliability of all methods and calibration regressions typically had $R^2 \geq 0.99$. The elemental composition and bulk mineralogy of the sediment were determined by X-ray fluorescence (Thermo ARL 9400 XRF) and X-ray diffraction (Philips PW 1050 XRD). Selected end point samples were imaged using Environmental Scanning Electron Microscope (ESEM) in combination with Backscattering Electron Detection (BSE) and Energy Dispersive X-ray Analysis (EDAX) (Philips XL30 ESEM-FG).

2.1.4. X-ray absorption spectroscopy

Selected samples from the bicarbonate buffered pH 7 systems with 10, 25 and 100 mM nitrate amendments were chosen to examine Sr^{2+} speciation in: (1) oxic sterile control pH 7 sediment; (2) Fe(III)/SO_4^{2-} reducing end point pH 7.2 sediments, (3) Fe(III)/SO_4^{2-} reducing end point pH 8.1 sediments; and (4) Fe(III) reducing end point pH 9.3 sediments. Typical concentrations of Sr^{2+} in these samples were in the range 600–1000 ppm. Standards: (1) $SrCl_2$ (aq), 3000 ppm (Fisher Scientific), (2) $SrCO_3$ (s) (Fisher Scientific) and (3) natural Sr^{2+} substituted aragonite from crushed aragonite mineral sample (Sr^{2+} concentration ~1000 ppm), were prepared and diluted with boron nitride where necessary. Samples were transferred to XAS cells under anaerobic conditions, cooled to − 80 K with a liquid nitrogen cryostat (see Nikitenko et al., 2008), and Sr K-edge XAS spectra were collected on beamline BM26A at the European Synchrotron Radiation Facility (ESRF). For sediment samples, Sr K-edge spectra (16115.26 keV) were collected in fluorescence mode using a 9 element solid state Ge detector. Multiple scans were averaged in Athena version 0.8.061 (Ravel and Newville, 2005) and normalised XANES data plotted. Background subtraction for EXAFS analysis was performed using PySpline v1.1 (Tenderholt et al., 2007). EXAFS data were fitted using DLexcurv v1.0 (Tomic et al., 2005) using full curve wave theory (Gurman et al., 1984) by defining a theoretical model which was informed by the relevant literature (e.g. O'Day et al., 2000; Finch et al., 2003) and comparing the model to the experimental data. Shells of backscatterers were added around the Sr^{2+} and by refining an energy correction Ef (the Fermi Energy; which for final fits typically varied between −3.8 and −2.6), the absorber–scatterer distance, and the Debye–Waller factor for each shell. Model iterations were performed until a least squares residual was minimised. Shells were only included in the model fit if the overall least square residual (the R-factor; Binsted et al., 1992) was improved by >5%.

3. Results and discussion

3.1. Sediment characteristics

Sediment composition was measured by X-ray fluorescence and was found to comprise Si (31.57%), Al (7.63%), Fe (3.64%), K (2.79%), Na (0.99%), C (0.96%), Mn (0.87%), Ti (0.45%), Ca (0.23%) and P, S and Cl (<0.1%). We note that XRF analyses show that phosphate is present in our systems at very low concentrations (<0.008%) and is not likely to be a significant control on Sr^{2+} behaviour in this system.

Trace metal analysis showed natural Sr^{2+} to be present in sediments at 62.8 ± 0.2 ppm and natural aqueous Sr^{2+} was <1 ppm. Strontium was added to groundwater media in significant excess to the natural background at 100 ppm (1.15 mM Sr^{2+}) and Ca^{2+} was present at 67 ppm (1.67 mM) thus a Sr/Ca ratio of ~1:1.5 was present in the synthetic groundwater media. The concentration of 0.5 N HCl extractable Fe(III) in the sediment was 5.6 ± 0.5 mmol kg^{-1} prior to incubation and the sediment pH was ~5.5.

3.2. Sorption to oxic sediment

In sterile control microcosms, increased Sr^{2+} sorption was observed in microcosms with a high pH and a low ionic strength. For example, for a constant ionic strength system (I = 0.027 mol dm^{-3}) run at pH 4.5, 5.5 and 7, the Sr^{2+} removal from solution was 35.6 ± 1.9%, 47.4 ± 5.3% and 63.2 ± 2.1% respectively (equating to K_d values of 5.5, 9.0 and 17.1 ml g^{-1}). Differences in strontium behaviour in the sterile microcosms were attributed to pH dependent differences in sorption to mineral surfaces present in the sediment. Sorption to both clays and Fe(III)-oxyhydroxide surfaces is possible although clay minerals is likely to predominate in unbuffered microcosms in which the pH of 4.5–5.5 is above the PZC for many clay minerals (Coppin et al., 2002; Zhuang and Yu, 2002; Alvarez-Silva et al., 2010) whilst Fe-oxyhydroxides become more significant as pH approaches their PZC at pH ~7 (Dyer et al., 2000; Hofmann et al., 2005). Additionally, in control experiments at pH 7 and with increasing ionic strength (0.027, 0.037, 0.062 and 0.190 mol dm^{-3}) resulting from sodium nitrate and sodium acetate additions, Sr^{2+} sorption was 68, 65, 55 and 28% respectively (equating to K_d values of 21.2, 18.5, 12.2 and 3.8 ml/g), presumably reflecting increased competition for Sr^{2+} sorption sites at higher ionic strengths due to cation exchange processes (Hull and Schafer, 2008).

3.3. Biogeochemistry in sediment microcosms

The unbuffered (initial pH 5.5; nitrate range 0.3–25 mM) and bicarbonate buffered (initial pH 7.0; nitrate range 0.3–100 mM) experiments all underwent progressive anoxia and electron acceptors were utilised in the order $NO_3^- > NO_2^- > Mn/Fe(III) > SO_4^{2-}$ (Figs. 1 and 2). Microbially mediated nitrate reduction caused a decrease in porewater nitrate and transient accumulation of nitrite in all systems. The onset of Fe(III) reduction was indicated by an increase in sediment extractable Fe(II) and this was then followed by a decrease in porewater SO_4^{2-} indicating sulfate reduction. No geochemical changes were observed in sterile control microcosms. In unbuffered systems (initial pH 5.5), as expected, microbial activity was inhibited at low pH and terminal electron accepting processes proceeded more slowly than in the parallel bicarbonate buffered microcosms (initial pH 7.0) (Figs. 1 and 2) (e.g. Law et al., 2010; Thorpe et al., 2012). However, in the unbuffered systems, nitrate reduction led to the release of OH^- and HCO_3^-, amending the pH such that a pH increase from 5.5 to 6.8, 7.5 and 8.3 occurred during the reduction of 0.3, 10 and 25 mM nitrate respectively (Fig. 1; Table 2; Thorpe et al., 2012). Metal reduction commenced once nitrate reduction had occurred and mid-point 0.5 N HCl extractable Fe(III) reduction was observed at approximately 25, 35 and 45 days for systems with 0.3, 10 and 25 mM nitrate (Fig. 1). Nitrate reduction and the associated pH increase in all microcosms coincided with removal of Sr^{2+}

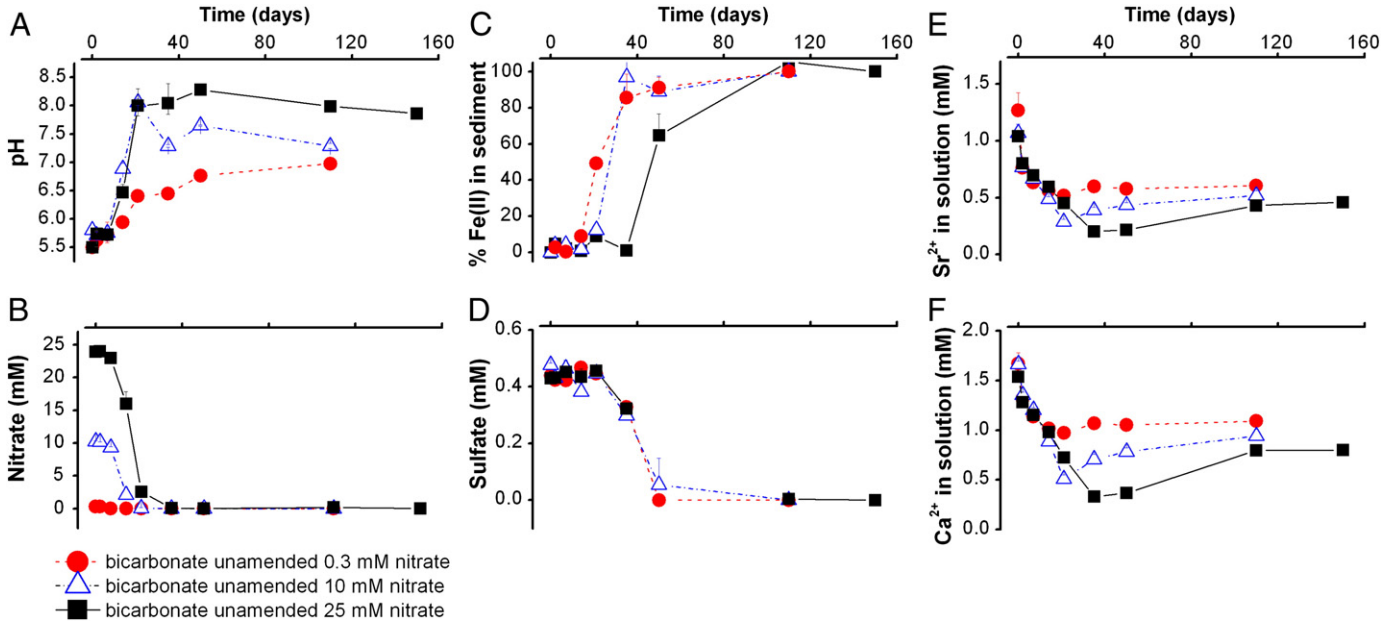

Fig. 1. Unbuffered, microcosm incubation time-series data (days 0−160). (A) pH (B) NO_3^-, (C) 0.5 N HCl % extractable sedimentary Fe as Fe(II), (D) SO_4^{2-}, (E) porewater Sr and (F) porewater Ca. ● = 0.3 mM nitrate system; Δ = 10 mM nitrate system; ■ = 25 mM nitrate system. Initial pH in all microcosms was ~5.5. Error bars represent 1σ experimental uncertainty from triplicate microcosm experiments (where not visible error bars are within symbol size).

and Ca^{2+} from solution (Fig. 1). Interestingly, as bioreduction progressed through Fe(III) and SO_4^{2-} reduction in these dynamic systems, a small amount of both Sr^{2+} and Ca^{2+} (<10% of that sorbed after nitrate reduction) was remobilised to solution. This re-release coincided with a slight decrease in pH (<0.5 pH units) presumably due to re-equilibration of the microcosm system following nitrate reduction. The re-release of sorbed Sr^{2+} and Ca^{2+} may be due solely to pH dependent sorption/desorption to mineral surfaces or in some systems (for example above pH 7) there may be release of Sr^{2+} and Ca^{2+} sorbed to Fe(III)-oxyhydroxides as reductive dissolution of the Fe(III) phases occurred (Small et al., 1999; Roden et al., 2002; Langley et al., 2009a, b).

In bicarbonate buffered systems with an initial pH of 7, the final pH following the reduction of 0.3, 10, 25 and 100 mM nitrate was 7.5, 8.0, 8.5 and 9.4 (Fig. 2: Table 2). Terminal electron accepting processes proceeded faster than in unbuffered microcosms with mid-point 0.5 N HCl extractable Fe(III) reduction occurring at <20 days for 0.3 and 10 mM nitrate systems and around 40 and 160 days for systems with 25 and 100 mM nitrate (Fig. 2). As with the unbuffered systems, Sr^{2+} and Ca^{2+} were removed from solution during nitrate reduction with increasing pH and a small amount (<10% of that sorbed after nitrate reduction) of Sr^{2+} and Ca^{2+} was re-released into solution in all systems apart from the bicarbonate buffered,

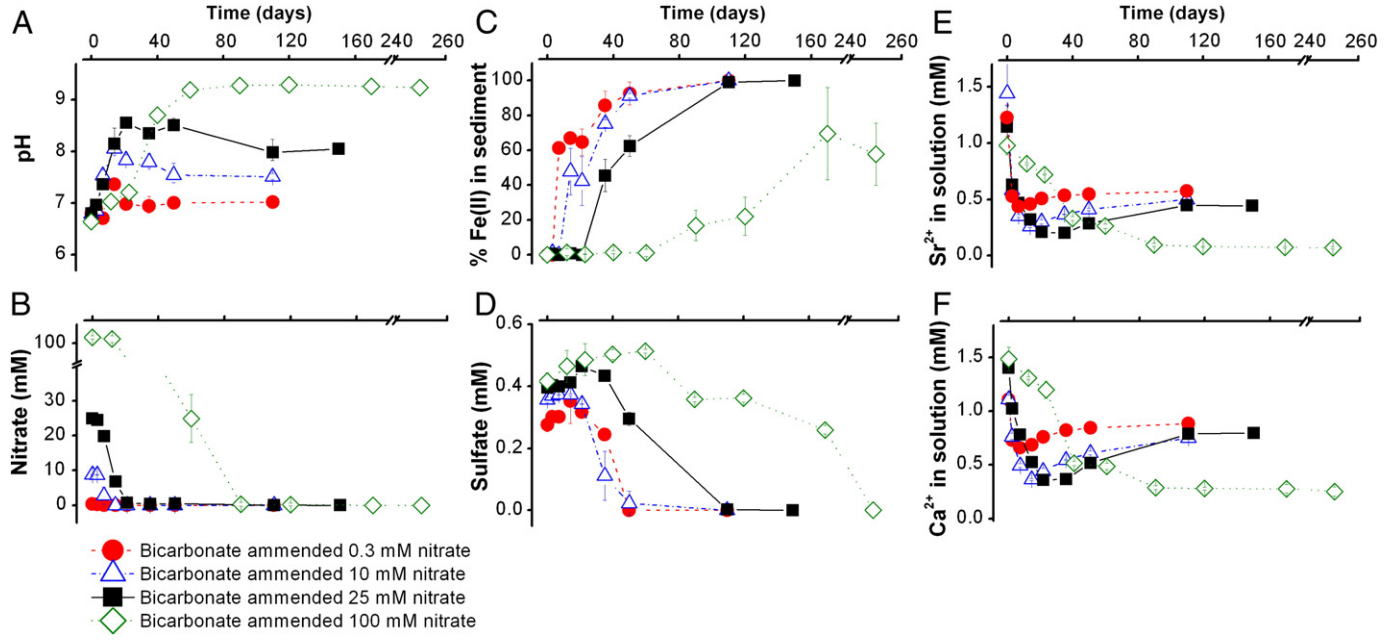

Fig. 2. Buffered, microcosm incubation time-series data (days 0–160/260). (A) pH, (B) NO_3^-, (C) 0.5 N HCl % extractable sedimentary Fe as Fe(II), (D) SO_4^{2-}, (E) porewater Sr and (F) porewater Ca. ● = bicarbonate buffered 0.3 mM nitrate system; Δ = bicarbonate buffered 10 mM nitrate system; ■ = bicarbonate buffered 25 mM nitrate system; ◊ = bicarbonate buffered100 mM nitrate system. Initial pH in all microcosms was ~7. Error bars represent 1σ experimental uncertainty from triplicate microcosm experiments (where not visible error bars are within symbol size).

Table 2
Percentage strontium sorbed to sediments during nitrate and metal reduction compared to an oxic control.

System	Sterile oxic		90% nitrate reduction		90% Fe(III)/SO_4 reduction		End point
	% Sr^{2+} on sediment[a]	pH	% Sr^{2+} on sediment	pH	% Sr on sediment	pH	Net decrease (−) or increase (+) of Sr^{2+} on sediments
Bicarbonate unamended 0.3 mM nitrate	47.0	5.5	54 ± 2.2	6.6	50 ± 2.3	6.7	+~2%
Bicarbonate unamended 10 mM nitrate	47.3	5.5	75 ± 1.8	8.0	55 ± 3.6	7.5	+~9%
Bicarbonate unamended 25 mM nitrate	45.5	5.5	82 ± 2.1	8.2	60 ± 0.5	7.8	+~18%
Bicarbonate amended 0.3 mM nitrate	67.9	7.0	63 ± 1.4	7.0	50 ± 1.8	7.0	−~16%
Bicarbonate amended 10 mM nitrate	64.2	7.0	78 ± 0.7	8.0	57 ± 0.3	7.5	−~6%
Bicarbonate unamended 25 mM nitrate	54.8	7.0	84 ± 0.4	8.5	62 ± 0.7	8.1	+~7%
Bicarbonate unamended 100 mM nitrate	32.6	7.0	93 ± 1.4	9.3	94 ± 0.8	9.3	+~61%

[a] Differences in Sr^{2+} sorption to sterile controls occur due to varying pH and ionic strength due to the addition of $NaHCO_3$, Na-acetate and $NaNO_3$.

100 mM nitrate system (Fig. 2). Here, the final pH was 9.3 and interestingly, Sr^{2+} remained associated with the sediment throughout Fe(III) and sulfate reduction. In this high nitrate loaded system, the utilisation of 70 mM acetate resulted in the accumulation of 207 ± 4.9 mM of dissolved inorganic carbon and amended the pH to alkaline conditions.

For comparison with other studies it is useful to examine distribution coefficients for Sr^{2+} (K_d = (solid in g g^{-1}/aqueous in g ml^{-1})). Distribution coefficients are only relevant to the specific geochemical conditions of each system of study and give an indication of the extent of Sr^{2+} partitioning onto the solid phase in different systems. Here K_d values ranged from <10 ml g^{-1} in systems with a high ionic strength (0.190 mol dm^{-3}) or a low pH (5.5) and increased to >50 ml g^{-1} with increasing pH. The distribution coefficient in systems with a final pH>9 was calculated to be 133 ml g^{-1}. These K_d values compare well with literature values where surface sediment K_d values are typically between 10 and 200 ml g^{-1} (Deldebbio, 1991; Liszewski et al., 1998; Fernandez et al., 2006) and deeper more quartz rich sediments have K_d values of <10 ml g^{-1} (Stephens et al., 1998; Dewiere et al., 2004).

Modelling of the solution chemistry in bioreduced systems (PHREEQC-2: LLNL database) suggested that for all unbuffered bioreduced system end-points, Fe(II)CO_3 and $SrCO_3$ were oversaturated in all the different nitrate amendments whilst the $CaCO_3$ phases were undersaturated in the bioreduced 0.3 mM nitrate amended systems and oversaturated in all other treatments (Table 3). As expected for these carbonate phases, the degree of oversaturation increased as alkalinity increased. In the bicarbonate amended bioreduced system end points, all nitrate amendments showed oversaturation of Fe(II)CO_3, $CaCO_3$, and $SrCO_3$ and with increasing oversaturation with increasing alkalinity (Table 3). Clearly, although unable to resolve the detail of the dynamic bioreduction experiments, these modelling data suggest an increased tendency to oversaturation of carbonate mineral phases with increased nitrate reduction and microbially produced alkalinity.

ESEM (Environmental Scanning Electron Microcoscopy) was used to assess the distribution of Sr^{2+} in end point pH 7 (bicarbonate buffered 10 mM nitrate) and pH 9.3 (bicarbonate buffered 100 mM nitrate) sediments (Fig. 3). In backscattering mode image brightness is related to the average atomic mass present (Z contrast). In the pH 9.3 system, secondary electron and backscatter images in combination with EDAX analysis show a number localised bright spots of ~20 μm diameter enriched in Sr^{2+} (Fig. 3) whilst there were no observed localised bright spots in the pH 7 system. Semi-quantitive analysis of EDAX spectra of the localised bright spots showed a significant concentration of Ca^{2+} and Sr^{2+} in agreement with predicted $SrCO_3$ and $CaCO_3$ oversaturation.

In order to further understand Sr^{2+} speciation during bioreduction in these complex systems, samples from an oxic pH 7 control with Sr^{2+} sorption, and selected bicarbonate buffered, nitrate amended (0.3, 25 and 100 mM) bioreduced end points with a final pH of 7.2, 8.1 and 9.3 were analysed using X-ray absorption spectroscopy. XANES spectra for all samples show a single peak indicative of 9 fold coordination and there was no evidence for 6 fold coordination (as in the calcite standard which has a clear doublet). Thus our experiments show no evidence for Sr^{2+} substituted calcite formation (Fig. 4; Parkman et al., 1998). XANES spectra for the oxic, bioreduced pH 7.2, and bioreduced pH 8.1 samples all comprised a single peak and compared well with a $SrCl_2$ aqueous standard, implying that in these sediments, after bioreduction, Sr^{2+} was present primarily as adsorbed Sr^{2+} (Fig. 4). By contrast, the XANES spectra for the pH 9.3 bioreduced sample showed some evidence for peak flattening and thus some similarity to the model Sr-carbonate phases (e.g. strontianite and Sr-substituted aragonite) (Fig. 4). Modelling of the EXAFS spectra for the oxic, bioreduced pH 7.2 and bioreduced pH 8.1 samples showed an approximate 9-fold coordination environment at 2.60 Å, indicative of outer sphere Sr^{2+} adsorption to mineral surfaces (Parkman et al., 1998; Chen and Hayes, 1999; Carroll et al., 2008; Fig. 5; Table 4). EXAFS for the pH 9.3 bioreduced sample could also be modelled with 9 fold "outer sphere" co-ordination. However, EXAFS model fits for this system were significantly improved by addition of shells of carbon and strontium backscatters at 3.03, 4.18 and 4.87 Å (Table 4; Fig. 5) respectively. This clearly indicates a contribution from an additional Sr^{2+} species in this spectrum with bond distances indicative of $SrCO_3$ (Parkman et al., 1998;

Table 3
Saturation index for key carbonate minerals in microcosm systems. Modelled using PHREEQC-2 (Lawrence Livermore National Laboratory database— llnl.dat).

	Saturation index (PHREEQC-2)[a]					
	Sr^{2+} (ppm)	Final pH	Siderite	Calcite	Aragonite	Strontianite
Oxic sediment	100	5.5	−1.16	−3.52	−3.67	−2.87
Bioreduced sediments	100					
Unbuffered 0.3 mM nitrate	100	6.7	1.97	−0.17	−0.32	0.47
Unbuffered 10 mM nitrate	100	7.5	2.76	0.70	0.55	1.35
Unbuffered 25 mM nitrate	100	7.8	3.07	1.18	1.03	1.83
Bicarbonate buffered 0.3 mM nitrate	100	7.0	2.31	0.22	0.08	0.86
Bicarbonate buffered 10 mM nitrate	100	7.2	2.49	0.42	0.28	1.07
Bicarbonate buffered 25 mM nitrate	100	8.1	3.28	1.48	1.33	2.14
Bicarbonate buffered 100 mM nitrate	100	9.3	3.25	2.36	2.21	3.65
Bicarbonate buffered 100 mM nitrate	10	9.3	3.25	2.36	2.21	2.25
Bicarbonate buffered 100 mM nitrate	1	9.3	3.25	2.36	2.21	1.15
Bicarbonate buffered 100 mM nitrate	0.1	9.3	3.25	2.36	2.21	0.25
Bicarbonate buffered 100 mM nitrate	0.01	9.3	3.25	2.36	2.21	-0.75

[a] Temperature 21 °C, concentration of ions in solution from Table 1, pH as measured.

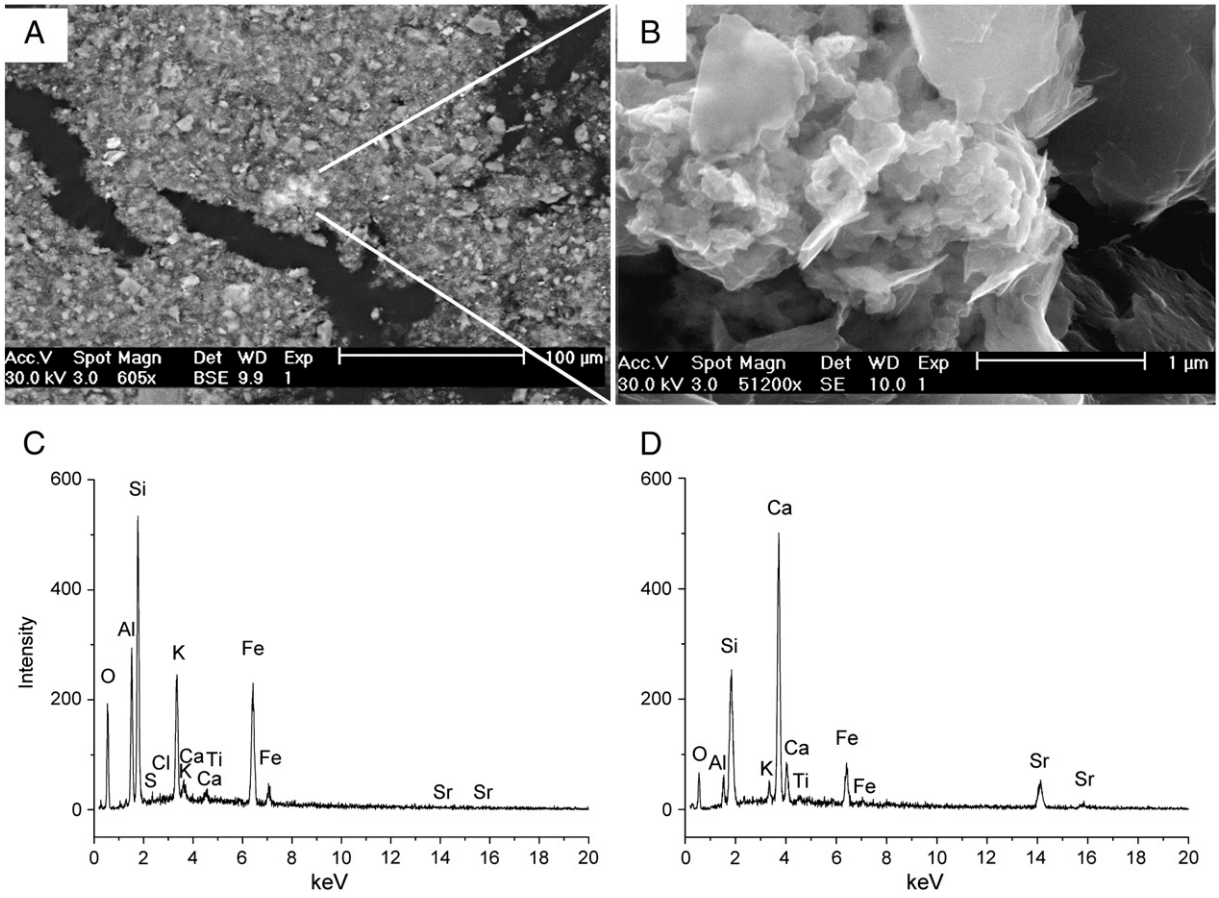

Fig. 3. ESEM images of the Fe(III) reducing bicarbonate buffered 100 mM nitrate sample at final pH 9 containing Sr- and Ca-rich crystalline structures and corresponding EDAX spectra. Images show: (A) ESEM backscatted detection mode image of sediment indicating heavier elements (Sr) as bright patches in the field of view 300 µm; (B) Secondary electron image showing the structure of Sr/Ca rich area at a field of view 3 µm; (C) the energy dispersive electron analysis (EDAX) spectra for the entire sample; and (D) a spot EDAX analysis on the Sr/Ca rich structure.

O'Day et al., 2000). Further analysis showed that a model EXAFS fit was possible with additional shells of 2.6 carbon atoms at 3.03 Å, 2.8 strontium atoms at 4.18 Å and 2.5 strontium atoms at 4.87 Å; these values are approximately 50% of what is expected for pure $SrCO_3$, which is consistent with a model where approximately half of Sr^{2+} is present in a $SrCO_3$ like environment (Table 4; Fig. 5). Indeed, this model, which is geochemically sensible, resulted in a better fit to the spectrum and a 27% reduction in the least square residual when compared to the data modelled as 100% adsorbed Sr^{2+} suggesting that both adsorption and incorporation occurred in this system (Table 4).

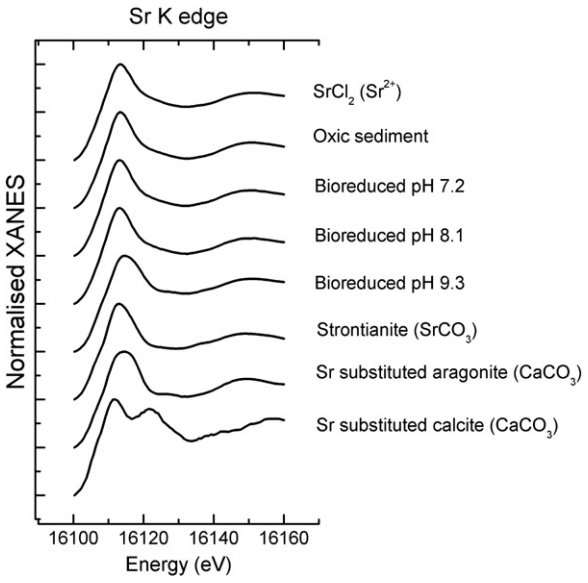

Fig. 4. Normalised Sr K-edge XANES spectra for selected standards and microcosm systems. From top to bottom: $SrCl_2$ aqueous standard, oxic sediment sample, bioreduced pH 7.2 sample, bioreduced pH 8.1 sample, bioreduced pH 9.3 sample, Sr substituted aragonite standard and strontianite standard.

In natural and engineered environments concentrations of Sr^{2+} and ^{90}Sr are generally much lower than in these experiments (eg 0.1 ppm natural Sellafield groundwater) (Wilson, 1996). Under Sellafield conditions, model simulations predicted that bioreduced system even at pH 9 would be undersaturated with regard to $SrCO_3$ below ~0.1 ppm strontium (Table 3); nonetheless, at a pH > 7, systems would remain supersaturated with respect to $CaCO_3$. It is therefore feasible that substitution of Sr^{2+} into $CaCO_3$ rather than precipitation as $SrCO_3$ will be important in controlling the mobility of both natural Sr^{2+} and artificial ^{90}Sr in such systems. Indeed, it is well documented that Sr^{2+} can substitute for Ca^{2+} within the calcium carbonate lattice (Pingitore et al., 1992; Tesoriero and Pankow, 1996; Greegor et al., 1997; Warren et al., 2001; Finch et al., 2003). Recent studies, focused on bacterial urolysis, have found that Sr^{2+} incorporation into the $CaCO_3$ lattice was enhanced by the rapid precipitation rates resulting from HCO_3^- production and the pH rise associated with microbial respiration (Fujita et al., 2004; Mitchell and Ferris, 2005). Both a pH rise and dissolved organic carbon production were observed during bioreduction by indigenous microorganisms in this study suggesting that nitrate reduction might also result in enhanced Sr^{2+} uptake into calcite compared to those observed under slower precipitation rates.

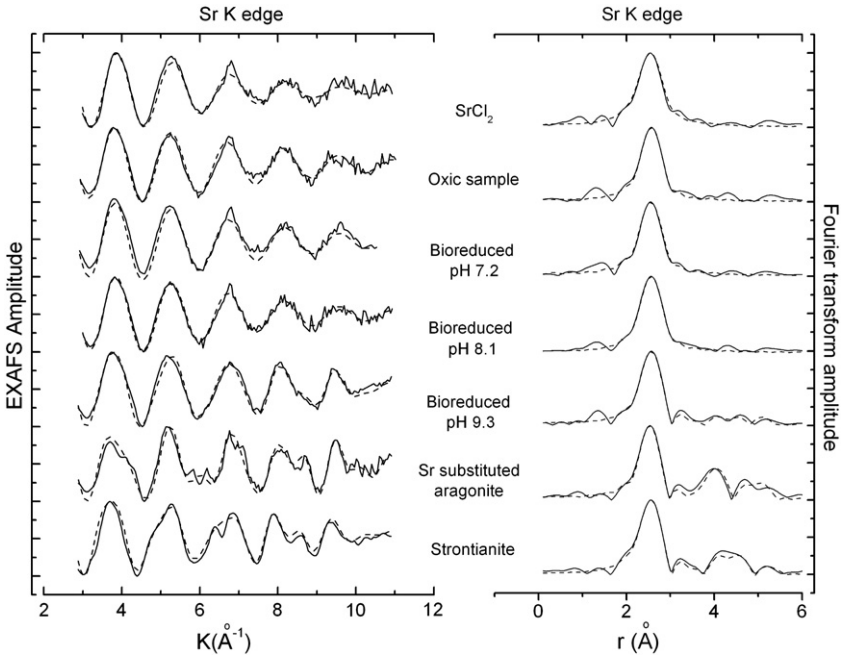

Fig. 5. Experimental (solid) and theoretical best fit (dashed) EXAFS spectra and corresponding Fourier transforms obtained for (from top to bottom): $SrCl_2$ aqueous standard, oxic sediment sample, bioreduced pH 7.2 sample, bioreduced pH 8.1 sample, bioreduced pH 9.3 sample, Sr substituted aragonite standard and strontianite standard. Solid lines are the data and dashed lines are the fits to the data.

3.4. Summary and environmental relevance

Overall, our experiments showed that there is increased Sr^{2+} removal from solution during bioreduction in nitrate impacted sediments compared to sterile control systems. In systems with an initially low pH (5.5), removal of Sr^{2+} from solution after bioreduction was particularly enhanced, presumably due to the increased sorption onto deprotonated mineral surfaces as the pH increased above 6. After nitrate reduction, system re-equilibration and an associated decrease (<0.5 pH units) in pH resulted in modest (<10%) re-release of Sr^{2+} into solution highlighting the vulnerability of adsorbed Sr^{2+} to re-release due to changing geochemical conditions.

Table 4
Parameters obtained from EXAFS data fitting of Sr K-edge spectra from Sr^{2+} associated with sediment at various sediment conditions.

Sample	Shell no	Bond	C.N.	R(Å)	$2\sigma^2$ (Å^2)	R-factor
$SrCl_2$	1	Sr–O	8.75	2.60	0.029	23.0
Oxic sample pH 7	1	Sr–O	8.83	2.61	0.019	22.1
Bioreduced pH 7.2	1	Sr–O	8.68	2.60	0.020	18.0
Bioreduced pH 8.1	1	Sr–O	8.89	2.61	0.021	19.6
Bioreduced pH 9.3 (1)	1	Sr–O	8.03	2.60	0.024	27.9
Bioreduced pH 9.3 (2)	1	Sr–O	8.19	2.61	0.021	20.2
	2	Sr–C	2.68	3.03	0.015	
	3	Sr–Sr	2.78	4.18	0.029	
	4	Sr–Sr	2.47	4.88	0.024	
Strontianite	1	Sr–O	9[a]	2.64	0.027	20.3
	2	Sr–C	6[a]	3.04	0.032	
	3	Sr–Sr	6[a]	4.22	0.029	
	4	Sr–Sr	4[a]	4.97	0.033	
Sr substituted aragonite	1	Sr–O	9[a]	2.59	0.015	29.1
	2	Sr–C	6[a]	2.98	0.031	
	3	Sr–Ca	6[a]	4.02	0.020	
	4	Sr–Ca	4[a]	4.87	0.013	

N is the occupancy (±~25%), R(Å) (is the interatomic distance (±~0.02 Å), $2\sigma^2$ is the Debye–Waller factor (Å^2) and *R* (least squares residual) is a measure of the overall goodness of fit.
[a] Fixed.

In extreme environments with very high (100 mM) nitrate concentrations, bioreduction led to a final pH of >9 and enhanced removal of Sr^{2+} from solution occurred throughout the bioreduction cascade. This study has shown that in very high nitrate systems an increase in pH and dissolved inorganic carbon associated with microbial reduction and particularly denitrification can promote the precipitation and incorporation of Sr^{2+} into carbonate phases although the engineering aspects of this process are as yet unexplored. Clearly, radio-strontium incorporation into carbonate phases is desirable in remediation scenarios as they are redox insensitive phases and are potentially more resistant to remobilization than sorbed Sr^{2+}. It is also clear that bioreduction scenarios have the potential to impact Sr^{2+} mobility in the subsurface and that understanding the bioreduction behaviour of redox inactive radioactive contaminants can be of significance in assessing the efficacy of bioreduction schemes at nuclear facilities. We further suggest that under constrained conditions, bioreduction may have the potential to co-treat redox active radionuclides and ^{90}Sr increasing the range of applications for this clean-up technology across the global nuclear waste legacy.

Acknowledgments

We thank Jon Fellowes, Alastair Bewsher and Paul Lythgoe for help in data acquisition. We also thank the ESRF beamline (B-26) scientists and Sarah Wallace (University of Leeds) for their help in XAS analysis. This work was supported by a studentship to CLT from the Engineering and Physical Science Research Council (EPSRC) as part of the Decommissioning, Immobilisation and Management of Nuclear Waste for Disposal (DIAMOND) consortium: grant EP/F055412/1. We also acknowledge the support of the Natural Environment Research Council grant NE/H007768/1.

References

Alvarez-Silva, M., Uribe-Salas, A., Mirnezami, M., Finch, J.A., 2010. The point of zero charge of phyllosilicate minerals using the Mular–Roberts titration technique. Mining and Engineering 23, 383–389.

Bascetin, E., Atun, G., 2006. Adsorption behavior of strontium on binary mineral mixtures of montmorillonite and kaolinite. Applied Radiation and Isotopes 64, 957–964.
Begg, J.D.C., Burke, I.T., Morris, K., 2007. The behaviour of technetium during microbial reduction in amended soils from Dounreay, UK. Science of the Total Environment 373, 297–304.
Bellenger, J.P., Staunton, S., 2008. Adsorption and desorption of Sr-85 and Cs-137 on reference minerals, with and without inorganic and organic surface coatings. Journal of Environmental Radioactivity 99, 831–840.
Binsted, N., Strange, R.W., Hasnain, S.S., 1992. Constrained and restrained refinement in EXAFS data analysis with curved wave theory. Biochemistry 31, 12117–12125.
Carroll, S.A., Roberts, S.K., Criscenti, L.J., O'Day, P.A., 2008. Surface complexation model for strontium sorption to amorphous silica and goethite. Geochemical Transactions 9, 2.
Chen, C.C., Hayes, K.F., 1999. X-ray absorption spectroscopy investigation of aqueous Co(II) and Sr(II) sorption at clay–water interfaces. Geochimica et Cosmochimica Acta 63, 3205–3215.
Chiang, P.N., Wang, M.K., Huang, P.M., Wang, J.J., Chiu, C.Y., 2010. Cesium and strontium sorption by selected tropical and subtropical soils around nuclear facilities. Journal of Environmental Radioactivity 101, 472–481.
Chorover, J., Choi, S., Rotenberg, P., Serne, R.J., Rivera, N., Strepka, C., Thompson, A., Mueller, K.T., O'Day, P.A., 2008. Silicon control of strontium and cesium partitioning in hydroxide-weathered sediments. Geochimica et Cosmochimica Acta 72, 2024–2047.
Coleman, M.L., Hedrick, D.B., Lovley, D.R., White, D.C., Pye, K., 1993. Reduction of Fe(III) in sediments by sulfate-reducing bacteria. Nature 361, 436–438.
Coppin, F., Berger, G., Bauer, A., Castet, S., Loubet, M., 2002. Sorption of lanthanides on smectite and kaolinite. Chemical Geology 182, 57–68.
Cowan, C.E., Zachara, J.M., Resch, C.T., 1991. Cadmium adsorption on iron-oxides in the presence of alkaline-earth elements. Environmental Science and Technology 25, 437–446.
Deldebbio, J.A., 1991. Sorption of strontium, selenium, cadmium and mercury in soil. Radiochimica Acta 52–3, 181–186.
Dewiere, L., Bugai, D., Grenier, C., Kashparov, V., Ahamdach, N., 2004. Sr-90 migration to the geo-sphere from a waste burial in the Chernobyl exclusion zone. Journal of Environmental Radioactivity 74, 139–150.
Dyer, A., Chow, J.K.K., Umar, I.M., 2000. The uptake of caesium and strontium radioisotopes onto clays. Journal of Materials Chemistry 10, 2734–2740.
Edwards, L., Kusel, K., Drake, H., Kostka, J.E., 2007. Electron flow in acidic subsurface sediments co-contaminated with nitrate and uranium. Geochimica et Cosmochimica Acta 71, 643–654.
Fernandez, J.M., Piault, E., Macouillard, D., Juncos, C., 2006. Forty years of Sr-90 in situ migration: importance of soil characterization in modeling transport phenomena. Journal of Environmental Radioactivity 87, 209–226.
Ferris, F.G., Hallberg, R.O., Lyvén, B., Pedersen, K., 2000. Retention of strontium, cesium, lead and uranium by bacterial iron oxides from a subterranean environment. Applied Geochemistry 15, 1035–1042.
Finch, A.A., Allison, N., Sutton, S.R., Newville, M., 2003. Strontium in coral aragonite: 1. Characterization of Sr coordination by extended absorption X-ray fine structure. Geochimica et Cosmochimica Acta 67, 1189–1194.
Finneran, K.T., Housewright, M.E., Lovley, D.R., 2002. Multiple influences of nitrate on uranium solubility during bioremediation of uranium-contaminated subsurface sediments. Environmental Microbiology 4, 510–516.
Fredrickson, J.K., Zachara, J.M., Balkwill, D.L., Kennedy, D., Li, S.M.W., Kostandarithes, H.M., Daley, M.J., Romine, M.F., Brockman, F.J., 2004. Geomicrobiology of high-level nuclear waste-contaminated vadose sediments at the Hanford Site, Washington State. Applied and Environmental Microbiology 70, 4230–4241.
Fujita, Y., Redden, G.D., Ingram, J.C., Cortez, M.M., Ferris, F.G., Smith, R.W., 2004. Strontium incorporation into calcite generated by bacterial ureolysis. Geochimica et Cosmochimica Acta 68, 3261–3270.
Goto, K., Taguchi, S., Fukue, Y., Ohta, K., Watanabe, H., 1977. Spectrophotometric determination of manganese with 1-(2-pyridylazo)-2-naphthol and a nonionic surfactant. Talanta 24, 752–753.
Greegor, R.B., Pingitore, N.E., Lytle, F.W., 1997. Strontianite in coral skeletal aragonite. Science 275, 1452–1454.
Gurman, S.J., Binsted, N., Ross, I., 1984. A rapid, exact curved-wave theory for EXAFS calculations. Journal of Physics C: Solid State Physics 17, 143–151.
Handley-Sidhu, S., Renshaw, J.C., Moriyama, S., Stolpe, B., Mennan, C., Bagheriasl, S., Yong, P., Stamboulis, A., Paterson-Beedle, M., Sasaki, K., Pattrick, R.A.D., Lead, J.R., Macaskie, L.E., 2011. Uptake of Sr^{2+} and Co^{2+} into biogenic hydroxyapatite: implications for biomineral ion exchange synthesis. Environmental Science and Technology 45, 6985–6990.
Harris, S.J., Mortimer, R.J.G., 2002. Determination of nitrate in small water samples (100 mu L) by the cadmium–copper reduction method: a manual technique with application to the interstitial waters of marine sediments. International Journal of Environmental and Analytical Chemistry 82, 369–376.
Hartman, M.J., Morasch, L.F., Webber, W.D., 2007. Summary of Hanford Site Groundwater Monitoring for Fiscal Year 2006. PNNL-16346-SUM, Pacific Northwest National Laboratory. Richland, W.A. March 2007Available on: http://ifchanford.pnnl.gov/pdfs/16346_sum.pdf.
Hofmann, A., van Beinum, W., Meeussen, J.C.L., Kretzschmar, R., 2005. Sorption kinetics of strontium in porous hydrous ferric oxide aggregates II. Comparison of experimental results and model predictions. Journal of Colloid and Interface Science 283, 29–40.
Hull, L.C., Schafer, A.L., 2008. Accelerated transport of Sr-90 following a release of high ionic strength solution in vadose zone sediments. Journal of Contaminant Hydrology 97, 135–157.
Hussain, S.A., Demirci, S., Özbayoglu, G., 1996. Zeta potential measurements on three clays from Turkey and effects of clays on coal flotation. Journal of Colloid and Interface Science 184, 535–541.
Istok, J.D., Senko, J.M., Krumholz, L.R., Watson, D., Bogle, M.A., Peacock, A., Chang, Y.J., White, D.C., 2004. In situ bioreduction of technetium and uranium in a nitrate-contaminated aquifer. Environmental Science and Technology 38, 468–475.
Jackson, R.E., Inch, K.J., 1989. The in-situ adsorption of strontium-90 in a sand aquifer at the chalk river nuclear laboratories Canada. Journal of Contaminant Hydrology 4, 27–50.
Langley, S., Gault, A.G., Ibrahim, A., Takahashi, Y., Renaud, R., Fortin, D., Clark, I.D., Ferris, F.G., 2009a. Sorption of strontium onto bacteriogenic iron oxides. Environmental Science and Technology 43, 1008–1014.
Langley, S., Gault, A.G., Ibrahim, A., Takahashi, Y., Renaud, R., Fortin, D., Clark, I.D., Ferris, F.G., 2009b. Strontium desorption from bacteriogenic iron oxides (BIOS) subjected to microbial Fe(III) reduction. Chemical Geology 262, 217–228.
Law, G.T.W., Geissler, A., Boothman, C., Burke, I.T., Livens, F.R., Lloyd, J.R., Morris, K., 2010. Role of nitrate in conditioning aquifer sediments for technetium bioreduction. Environmental Science and Technology 44, 150–155.
Law, G.T.W., Geissler, A., Lloyd, J.R., Burke, I.T., Livens, F.R., Boothman, C., McBeth, J.M., Morris, K., 2011. Uranium cycling in sediment and biomineral systems. Geomicrobiology Journal 28, 497–506.
Liszewski, M.J., Rosentrater, J.J., Miller, K.E., Batholomay, R.C., 1998. Strontium distribution coefficients of surficial and sedimentary interbed samples from the Idaho National Engineering and Environmental Laboratory, Idaho. US Geological Survey — Water Resources Investigations Report 98-4073. .
Lloyd, J.R., 2003. Microbial reduction of metals and radionuclides. FEMS Microbiology Reviews 27, 411–425.
Lloyd, J.R., Renshaw, J.C., 2005. Bioremediation of radioactive waste: radionuclide-microbe interactions in laboratory and field-scale studies. Current Opinion in Biotechnology 16, 254–260.
Lovley, D.R., Phillips, E.J.P., 1986. Availability of ferric iron for microbial reduction in bottom sediments of the fresh-water tidal Potomac River. Applied and Environmental Microbiology 52, 751–757.
Mason, C.F.V., Lu, N., Conca, J., 2000. Radioactive strontium- and caesium-contaminated sites: characterisation, transport, and remedial options. Nuclear Physical Methods in Radioecological Investigations of Nuclear Test Sites, 31, pp. 89–97.
McBeth, J.M., Lear, G., Lloyd, J.R., Livens, F.R., Morris, K., Burke, I.T., 2007. Technetium reduction and reoxidation in aquifer sediments. Geomicrobiology Journal 24, 189–197.
McKenzie, H., Armstrong-Pope, N., 2010. Groundwater Annual Report 2010. Sellafield Ltd. Technical Report TECH000613Available on: http://www.sellafieldsites.com/land/documents/Groundwater_Annual_Report_2010.pdf.
McKinley, J.P., Zachara, J.M., Smith, S.C., Liu, C., 2007. Cation exchange reactions controlling desorption of Sr-90 from coarse-grained contaminated sediments at the Hanford site, Washington. Geochimica et Cosmochimica Acta 71, 305–325.
Mitchell, A.C., Ferris, F.G., 2005. The coprecipitation of Sr into calcite precipitates induced by bacterial ureolysis in artificial groundwater: temperature and kinetic dependence. Geochimica et Cosmochimica Acta 69, 4199–4210.
Nikitenko, S., Beale, A.M., Van der Eerden, A.M.J., Jacques, S.D.M., Leynaud, O., O'Brien, M.G., Detollenaere, D., Kaptein, R., Weckhysen, B.M., 2008. Implementation of a combined SAXS/WAXS/QEXAFS set-up for time-resolved in situ experiments. Journal of Synchrotron Radiation 15, 632–640.
O'Day, P.A., Newville, M., Neuhoff, P.S., Sahai, N., Carroll, S.A., 2000. X-ray absorption spectroscopy of strontium(II) coordination — I. Static and thermal disorder in crystalline, hydrated, and precipitated solids and in aqueous solution. Journal of Colloid and Interface Science 222, 184–197.
Parkman, R.H., Charnock, J.M., Livens, F.R., Vaughan, D.J., 1998. A study of the interaction of strontium ions in aqueous solution with the surfaces of calcite and kaolinite. Geochimica et Cosmochimica Acta 62, 1481–1492.
Parmar, N., Warren, L.A., Roden, E.E., Ferris, F.G., 2000. Solid phase capture of strontium by the iron reducing bacteria *Shewanella alga* strain BrY. Chemical Geology 169, 281–288.
Pingitore, N.E., Lytle, F.W., Davies, B.M., Eastman, M.P., Eller, P.G., Larson, E.M., 1992. Mode of incorporation of Sr^{2+} in calcite — determination by X-ray absorption-spectroscopy. Geochimica et Cosmochimica Acta 56, 1531–1538.
Priest, N.D., Kuyanova, Y., Pohl, P., Burkitbayev, M., Mitchell, P.I., Vintro, L.L., Strilchuk, Y.G., Lukashenko, S.N., 2008. Strontium-90 contamination within the Semipalatinsk nuclear test site: results of SEMIRAD1 and SEMIRAD2 projects — contamination levels and projected doses to local populations. Nuclear Risks in Central Asia, pp. 87–105.
Ravel, B., Newville, M., 2005. Athena, Artemis, Hephaestus: data analysis for X-ray absorption spectroscopy using IFEFFIT. Journal of Synchrotron Radiation 12, 537–541.
Riley, R.G., Zachara, J.M., 1992. Chemical Contaminants on DOE Lands and Selection of Contaminant Mixtures for Subsurface Science Research, DOE/ER-0547T. US Department of Energy, p. 77.
Roden, E.E., Leonardo, M.R., Ferris, F.G., 2002. Immobilization of strontium during iron biomineralization coupled to dissimilatory hydrous ferric oxide reduction. Geochimica et Cosmochimica Acta 66, 2823–2839.
Sahai, N., Carroll, S.A., Roberts, S., O'Day, P.A., 2000. X-ray absorption spectroscopy of strontium(II) coordination — II. Sorption and precipitation at kaolinite, amorphous silica, and goethite surfaces. Journal of Colloid and Interface Science 222, 198–212.
Senko, J.M., Mohamed, Y., Dewers, T.A., Krumholz, L.R., 2005. Role for Fe(III) minerals in nitrate-dependent microbial U(VI) oxidation. Environmental Science and Technology 39, 2529–2536.
Small, T.D., Warren, L.A., Roden, E.E., Ferris, F.G., 1999. Sorption of strontium by bacteria, Fe(III) oxide, and bacteria-Fe(III) oxide composites. Environmental Science and Technology 33, 4465–4470.
Solecki, J., 2005. Investigation of Sr-85 adsorption on selected soils of different horizons. Journal of Environmental Radioactivity 82, 303–320.

Stephens, J.A., Whicker, F.W., Ibrahim, S.A., 1998. Sorption of Cs and Sr to profundal sediments of a Savannah River Site reservoir. Journal of Environmental Radioactivity 38, 293–315.

Stookey, L.L., 1970. Ferrozine— a new spectrophotometric reagent for iron. Analytical Chemistry 42, 779–781.

Tenderholt, A., Hedman, B., Hodgson, K.O., 2007. PySpline: a modern, cross-platform program for the processing of raw averaged XAS edge and EXAFS data. In X-Ray Absorption Fine Structure-XAFS13, pp. 105–107.

Tesoriero, A.J., Pankow, J.F., 1996. Solid solution partitioning of Sr^{2+}, Ba^{2+}, and Cd^{2+} to calcite. Geochimica et Cosmochimica Acta 60 1063-1063.

Thorpe, C.L., Law, G.T.W., Boothman, C., Lloyd, J.R., Burke, I.T., Morris, K., 2012. The synergistic effect of high nitrate concentrations on sediment bioreduction. Geomicrobiology Journal 29, 484–493.

Tomic, S., Searle, B.G., Wander, A., Harrison, N.M., Dent, A.J., Mosselmans, J.F., Inglesfield, J.E., 2005. New tools for the analysis of EXAFS: the DL_EXCURV package. CCLRC Technical Report DL-TR-2005-00. . ISSN 1362-0207, Daresbury SRS 2005.

Viollier, E., Inglett, P.W., Hunter, K., Roychoudhury, A.N., Van Cappellen, P., 2000. The ferrozine method revisited: Fe(II)/Fe(III) determination in natural waters. Applied Geochemistry 15, 785–790.

Warren, L.A., Maurice, P.A., Parmar, N., Ferris, F.G., 2001. Microbially mediated calcium carbonate precipitation: implications for interpreting calcite precipitation and for solid-phase capture of inorganic contaminants. Geomicrobiology Journal 18, 93–115.

Wilkins, M.J., Livens, F.R., Vaughan, D.J., Beadle, I., Lloyd, J.R., 2007. The influence of microbial redox cycling on radionuclide mobility in the subsurface at a low-level radioactive waste storage site. Geobiology 5, 293–301.

Wilson, P.D., 1996. Nuclear Fuel Cycle: From Ore to Wastes. Oxford University Press.

Zachara, J.M., Cowan, C.E., Resch, C.T., 1991. Sorption of divalent metals on calcite. Geochimica et Cosmochimica Acta 55, 1549–1562.

Zhuang, J., Yu, G.R., 2002. Effects of surface coatings on electrochemical properties and contaminant sorption of clay minerals. Chemosphere 49, 619–628.

Chapter 6: Interactions of an Fe(III)-reducing microbial consortium with Sr^{2+} and ^{99}Tc under neutral and alkaline conditions

This chapter contains the following paper prepared for submission to Applied Geochemistry in 2012:

Thorpe, C.L., Law, G.T.W., Lloyd, J.R., Morris, K. Interactions of an Fe(III)-reducing microbial consortium with Sr^{2+} and ^{99}Tc under neutral and alkaline conditions, In Draft.

Interactions of an Fe(III)-reducing microbial consortium with Sr^{2+} and ^{99}Tc under neutral and alkaline conditions

Clare L. Thorpe, Gareth T. W. Law, Jonathan R. Lloyd, Katherine Morris

[1]Research Centre for Radwaste and Decommissioning and Williamson Research Centre for Molecular Environmental Science, School of Earth, Atmospheric and Environmental Sciences, The University of Manchester, Manchester, M13 9PL, U.K.

*Corresponding author: Email: katherine.morris@manchester.ac.uk; Tel: +44 (0)161 275 7541.

Abstract

Microbial Fe(III) reduction has the potential to affect the mobility of radionuclides through redox transformations and interactions with biogenic Fe(II) bearing mineral phases. Here, Fe(III) reduction, and subsequent precipitation of Fe(II) bearing mineral phases, was investigated in model systems using a microbial consortium enriched from sediment representative of Sellafield nuclear facility. In these systems, reduction of Fe(III) citrate resulted in the precipitation of siderite and vivianite at pH 7 and 9. The mobility of key problematic radionuclides in these systems was investigated using ^{99}Tc and stable Sr^{2+} as an analogue for ^{90}Sr. Technetium-99 was > 85 % removed from solution in Fe(III) reducing model systems at pH 7 and 9. X-ray absorption studies confirmed reduction from Tc(VII) to Tc(IV) at neutral and alkaline pH. In contrast, Sr^{2+} remained in solution at pH 7 but precipitated as $SrCO_3$ during Fe(III) reduction at pH > 8.5. Interestingly, $SrCO_3$ precipitation was not observed in pH 9 oxic systems implying that Sr^{2+} precipitation was stimulated by Fe(III) reduction. Findings highlight the pH dependent effects of microbial Fe(III) reduction on the mobility of ^{99}Tc and Sr^{2+} and improve understanding of the behaviour of the problematic radionuclides ^{99}Tc and ^{90}Sr.

Introduction

Microbial Fe(III) reduction has the potential to affect the speciation, and therefore the mobility, of radionuclides (Lloyd et al., 2002). Understanding the mechanisms that control radionuclide mobility is important for the management of the global contaminated land legacy. Strontium-90 and technetium-99 are radionuclide co-contaminants in groundwaters at many sites including Sellafield nuclear facility, Cumbria, UK (McKenzie and Armstrong-Pope, 2010). Their differing chemical behaviour presents a challenge for remediation.

Microbial Fe(III) reduction has been identified as an important mechanism for the *in-situ* immobilisation of ^{99}Tc, that can be reduced from mobile Tc(VII) to the less mobile Tc(IV) either enzymatically or by an abiotic reaction with biogenic Fe(II) phases (Fredrickson et al., 1998; Lloyd, 2003; Istok et al., 2004; Lloyd and Renshaw, 2005; Begg et al., 2007; McBeth et al., 2007; Law et al., 2010; Icenhower, 2010; McBeth et al., 2010). Recent work suggests that raising the pH during Fe(III) reduction may allow co-removal of ^{90}Sr and ^{99}Tc: Tc(VII) *via* reduction to Tc(IV) and Sr *via* increased sorption and incorporation during a microbially induced rise in pH (Ferris and Roden, 2000; Roden et al., 2002; Mitchell and Ferris, 2005; Thorpe et al., in press). In a recent study, biostimulation by acetate addition in high nitrate sediments removed Sr^{2+} from solution following the development of alkaline conditions during nitrate reduction and alkaline Fe(III) reduction occurred thereafter (Thorpe et al., in press). Alkaline Fe(III) reduction is rare as microbial metabolism is challenged at high pH (Krulwich et al. 2001; Detkova & Pusheva, 2006; Stewart et al. 2010). However, in sediments representative of Sellafield nuclear facility, Fe(III) reduction has been shown to occur over a pH range of pH 5.5 – 9.5 (Law et al., 2010; Thorpe et al., 2012a).

The reduction of bioavailable, poorly crystalline Fe(III) oxyhydroxide phases results in their dissolution and the release of Fe(II) that will either remain in solution, sorb, or precipitate as Fe(II) bearing mineral phases such as magnetite (Fe_3O_4), siderite ($FeCO_3$) and vivianite ($Fe_3(PO_4)_2$. $8H_2O$) (Colman et al., 1993; Roden et al., 2002; Islam et al., 2005; de Pablo et al., 2008; Cutting et al., 2009; Langley et al., 2009; McBeth et al., 2011). Poorly crystalline Fe(III) oxyhydroxides are an important sink for adsorbed metal cations including Sr^{2+} (Kinniburgh et al., 1975; Ferris et al., 2000; Langley et al., 2009) and reductive dissolution of Fe(III) phases may result in their release (Roden et al., 2002; Langley et al., 2009). Released Sr^{2+} may remain mobile, associate with other sediment minerals or with newly formed biogenic Fe(II) minerals (Ferris and Roden, 2000; Roden et al., 2002; de Pablo et al., 2008; Langley et al., 2009). In the presence of dissolved inorganic carbon and mildly alkaline pH, Sr^{2+} may become incorporated into carbonate mineral phases or precipitate as $SrCO_3$ (Greegor et al., 1997; Mitchell and Ferris, 2005).

In model systems, biogenic siderite, vivianite and magnetite have all been observed to form as a result of microbial Fe(III) reduction (Roden et al., 2002; Islam et al., 2005; Coker et al., 2008; McBeth et al., 2011). The utilisation of simple organic electron donors such as acetate during coupled to Fe(III) reduction results in the release of dissolved inorganic carbon Fe(II) and generates alkalinity which promotes the formation of siderite (Coleman et al., 1993; Ferris and Roden, 2000; Roden et al., 2002; Thorpe et al., 2012b). Where phosphate is present Fe(III)- phosphate phases such as vivianite form (Islam et al., 2005; McBeth et al., 2011; Thorpe et al., 2012b). Magnetite is observed under some experimental conditions and typically where insoluble Fe(III) is the electron acceptor and under constrained rates of reduction (Islam et al., 2005; Coker et al., 2008). Siderite, vivianite and magnetite have all been shown capable of reducing Tc(VII) to Tc(IV) (McBeth et al., 2011). However, Sr^{2+} behaviour in the presence of

Fe(II) bearing mineral phases is less well documented. Model systems have reported both release of Sr^{2+} (Langley et al., 2009) and removal of Sr^{2+} from solution concurrent with Fe(III) reduction (Ferris and Roden, 2000; Parmar et al., 2000; Roden et al., 2002).

Here we use a model enrichment culture from Fe(III) reducing Sellafield type sediments to investigate the behaviour of ^{99}Tc and Sr^{2+} during Fe(III) reduction and precipitation of Fe(II) mineral phases. A microcosm approach was used to investigate the effect of the formation of an Fe(II) mineral consortium at pH 6.8 - 7 and 8.5 - 9.0.

Materials and Methods

Isolation of Fe(III) reducing enrichment culture

Cultures of Fe(III) reducing bacteria were isolated from Sellafield sediment microcosms that had developed Fe(III) reducing conditions (Thorpe et al., 2012b). Sediment slurry was transferred from Sellafield sediment microcosms to 10 % inoculate serum bottles containing Fe(III) citrate growth media buffered to pH 7 (Lovley et al. 1991) and in systems with the pH buffered to pH 9 with addition of 10M NaOH. Media was prepared with yeast extract (2 g L^{-1}) as the electron donor (Whittleston et al., 2011). Sub aliquots of the enrichment cultures were transferred to fresh media every 4 - 6 weeks and with a total of 6 consecutive subcultures to enrich the Fe(III) reducing microbial population prior to use in the experiments described here. All fresh media was sparged with N_2/CO_2 (80:20) gas mix prior to inoculation and sealed with butyl rubber stoppers. Cultures were incubated under anaerobic conditions in the dark at 20^{o}C. All sampling and inoculations were performed under an Ar atmosphere and using aseptic technique.

Microbial community analysis

The microbial community from samples derived from an Fe(III) reducing enrichment culture at pH 7.5 was analysed to identify the Fe(III) reducing bacteria present *via* 16S gene analysis as described in (Thorpe et al., 2012a). This culture was then used to inoculate further systems at pH 7 and pH 9 to explore the effects of neutral and alkaline Fe(III) reduction on the precipitation of Fe(II) mineral phases and the mobility of ^{99}Tc and Sr^{2+}.

Microcosm preparation

To investigate the effects of microbial Fe(III) reduction and precipitation of biogenic Fe(II) phases on the mobility of key radionuclides Sr^{2+} was added to microcosms as stable Sr^{2+} and Tc as radioactive ^{99}Tc. Stable Sr^{2+} was added to serum bottles as $SrCl_2.6H_2O$ at concentrations of 100 ppm (1.15 mM) as used in Thorpe et al. (in press) and comparable mineralogical studies (Ferris and Roden, 2000; Parmar et al. 2000; Roden et al., 2002; Langley et al., 2009). This is in excess of the 0.1 ppm (0.00115 mM) of natural groundwater Sr^{2+} reported in the Sellafield region by Wilson, 1996. ^{99}Tc was spiked from a standard solution of 0.8 MBq ml^{-1} ammonium pertechnetate stock solution (CERCA LEA, Lyon, France) to a final concentration of 100 Bq ml^{-1} in each 10 ml microcosm. Mineral microcosms were established with a 30 mM solution of Fe(III) citrate. These systems were Ca^{2+} free as precipitation of Ca-carbonate can result in the sequestration of Sr^{2+} and the model systems aimed to investigate only the effects of biogenic Fe(II) minerals on Sr^{2+} (Fujita et al., 2004; Mitchell and Ferris, 2005). Microcosms were established in triplicate at both pH 9 and 7 with oxic, abiotic controls for each system.

Geochemical analysis

During microcosm sampling, Fe(II) concentrations were measured with standard UV-Vis spectroscopy approaches a Jenway 6715 UV-Vis spectrophotometer (Viollier et al., 2000). Aqueous HCO_3^-/CO_3^{2-} and were measured by ion chromatography (Dionex ICS-90). Total bioavailable Fe(III) and in bioreduced systems the proportion of Fe(II) was estimated by digestion of 0.1 ml of slurry in 5 ml of 0.5 N HCl for 60 minutes followed by the ferrozine assay (Lovely and Philips, 1986). The pH was measured with a pH meter and calibrated electrodes (Denver Instruments, UB10) and probes calibrated to pH 4, 7 and 10. Aqueous ^{99}Tc was analysed using liquid scintillation counting Packard Tri-carb 2100 TR liquid scintillation counter. Aqueous Sr^{2+} was measured by ICP-AES. Sequential extractions were performed on the mineral products of Fe-citrate reduction using extractions adapted from Poulton and Canfield (2005) and Tessier et al., (1979). Extractions comprised a) 1M $MgCl_2$, pH 7 for two hours to assess 'exchangeable metal cations', b) 1 M Na-acetate, pH 4.5 for twenty four hours to assess 'carbonate associated' phases, c) sodium dithionate extraction pH 4.8 for 2 hours to assess 'reducible' phases.

Mineral characterisation

Throughout, X-ray diffraction was used to identify any minerals in the experiments. Environmental scanning electron microscopy (ESEM) with Secondary Electron detection (SE) was used to image mineral products and Energy Dispersive X-ray spectroscopy (EDX) was used to assess the elemental composition of samples.

X-ray absorption spectroscopy

X-ray absorption spectroscopy was used to determine the speciation of ^{99}Tc in reduced samples containing biogenic siderite amended with 250 kBq ^{99}Tc to achieve ~ 100 ppm on solids. XANES data was collected on B18 at the DIAMOND synchrotron, UK, at

ambient temperature, in fluorescence mode and using a 9 element germanium solid state detector. Background subtraction was conducted in Athena.

Results and discussion

Fe(III) reduction and mineralogy in model systems

An Fe(III)-citrate reducing culture derived from sediment with circumneutral pH, representative of Sellafield nuclear facility and amended with yeast extract comprised greater than 98 % abundance of close relatives (>95% match) of *Clostridia* (Table 1). Members of the order *Clostridiales* have been shown to reduce Fe(III) in freshwater and marine environments at over a wide range of pH either by dissimilatory Fe(III) reduction (Dobbin et al., 1999) or by using Fe(III) as a minor electron acceptor during fermentation (Lovley and Philips, 1988; Stewart et al., 2010; Lehours et al., 2010).

Closest Match	Accession No.	% Match	Class	% Clone Library
Uncultured bacterium; E50	FJ205825	95.1	Clostridia	22.6
Uncultured bacterium; HAW-R60-B-745d-U	FN436078	98.1	Clostridia	12.9
Clostridium metallolevans; ASI1	DQ133569	99.4	Clostridia	32.3
Sporomusa sphaeroides (T); DSM 2875	AJ279801	99.7	Clostridia	4.8
Tissierella sp. S2	EF202592	98.1	Clostridia	9.7
Uncultured bacterium; clone-30	AB375707	95.1	Unclassified	1.6
Clostridium aerotolerans; DSM 5434	X76163	99.6	Clostridia	3.2
Sporomusa sphaeroides (T); DSM 2875	AJ279801	100	Clostridia	8.1
Clostridium sp. PPf35E8	AY548784	98.8	Clostridia	1.6
Clostridium sp. ArC6	AF443595	96.8	Clostridia	1.6
Clostridium sp. F122	AB277212	99.1	Clostridia	1.6

Table 1. Full 16S Clone Library: Fe(III) reducing enrichment culture.

In this system, the Fe(III)-reducing enrichment culture reduced essentially all of the Fe(III) in the Fe(III)-citrate medium to Fe(II) within 60 days at both pH 7 and pH 9 and analysis of the end point precipitates by XRD revealed the formation of siderite and vivianite at pH 7 and pH 9 (Figure 1).

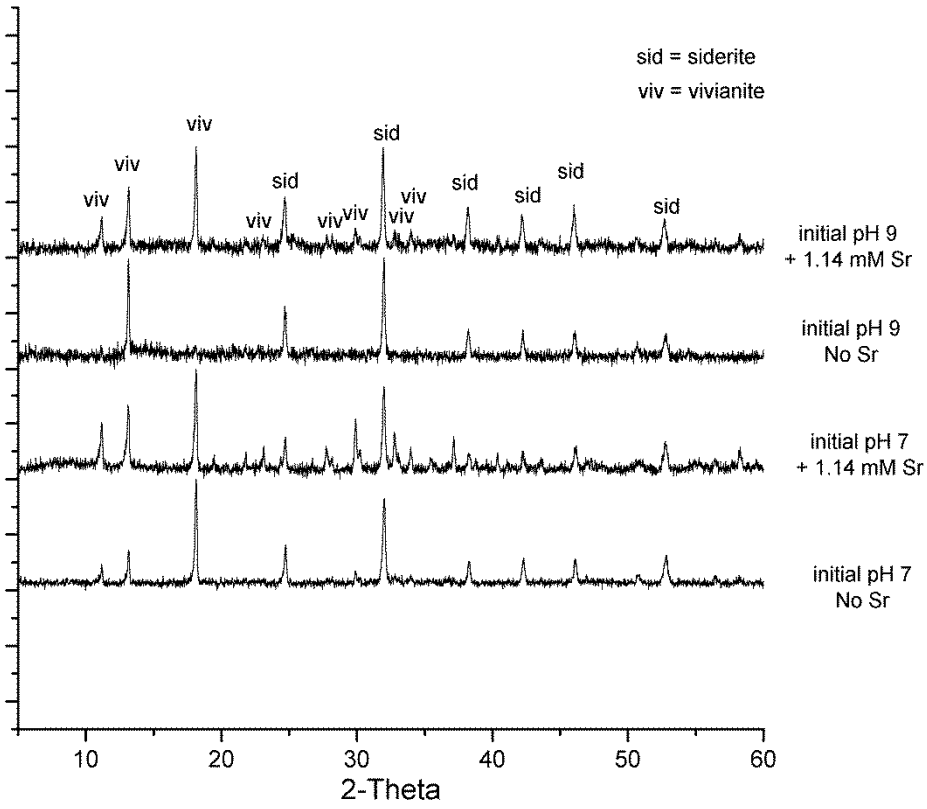

Figure 1. XRD of reduced mineral phases with and without Sr^{2+} addition showing siderite and vivianite to be the only phases detectable above the background.

Further examination of the morphology and chemical composition of the mineral phases using ESEM coupled to EDX analysis was performed for the pH 7 system and pH 9 (Figures 2 - 5). Vivianite, part of the monoclinic crystal system, formed as large prismatic, or in some cases diamond shaped, crystals often radiating from a central point (Figures 2, 3 and 4). Siderite, part of the cubic crystal system, formed smaller crystal aggregates with a spherical morphology made up of smaller cubic crystals (Figure 2, 3 and 5). An image of early Fe(III) reduction in a pH 9 system shows X-ray structure less Fe(III) with 2-3 µm rod shaped areas that could represent microbial cells (Figure 6).

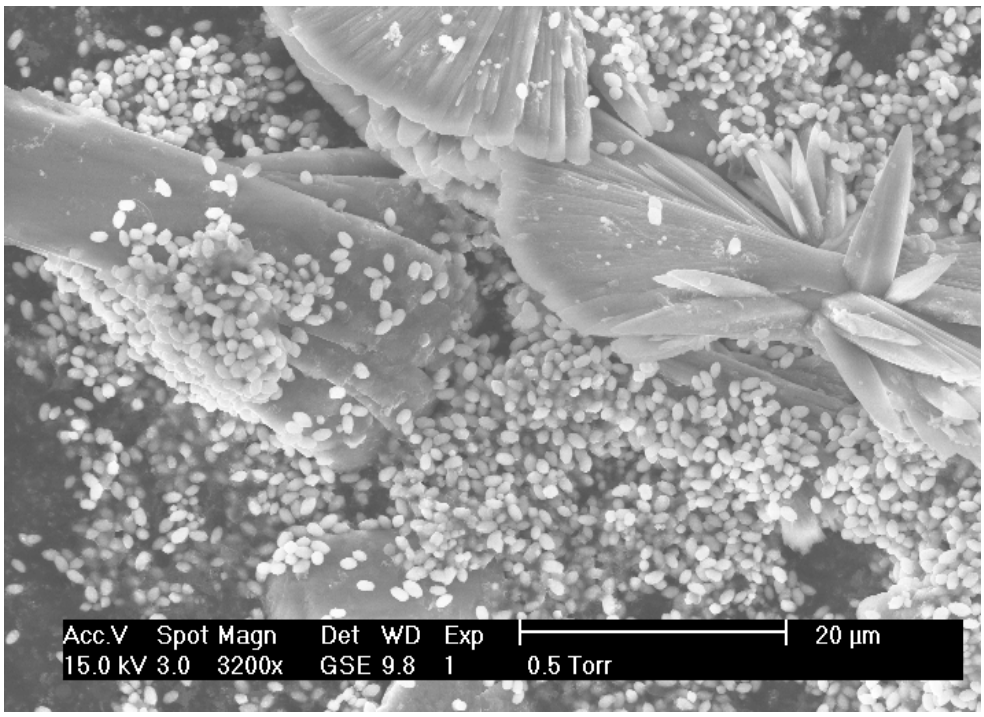

Figure 2. Siderite (spherical crystal aggregates) and vivianite (large prisms radiating from a central point) in the bioreduced system at pH 7.

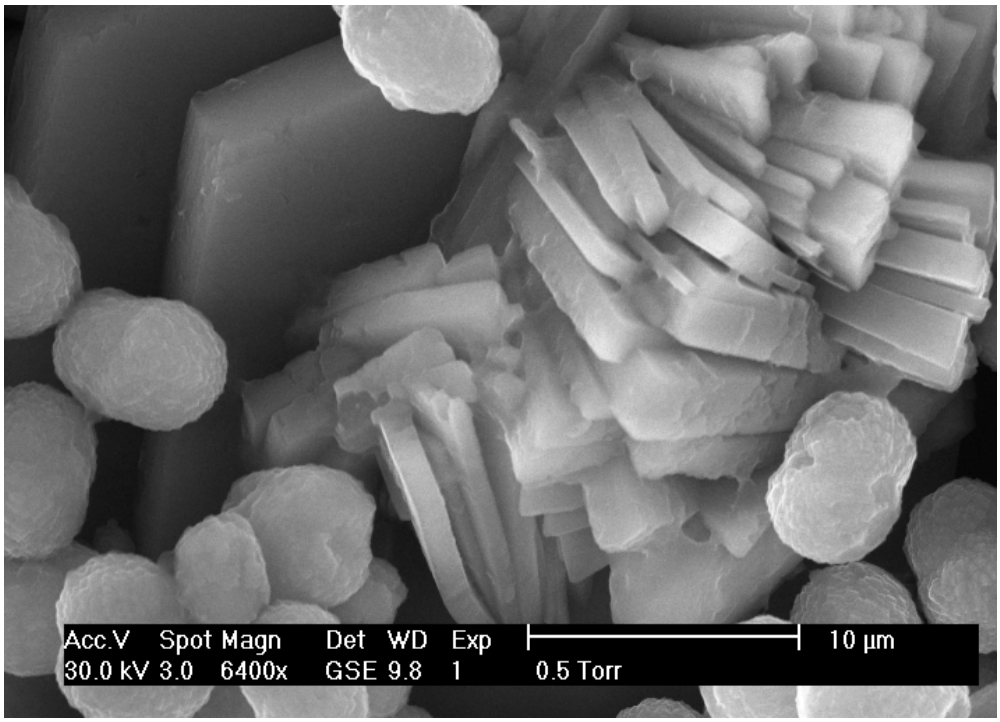

Figure 3. Siderite (spherical crystal aggregates) and vivianite (diamond shaped and prismatic) in the bioreduced system at pH 9.

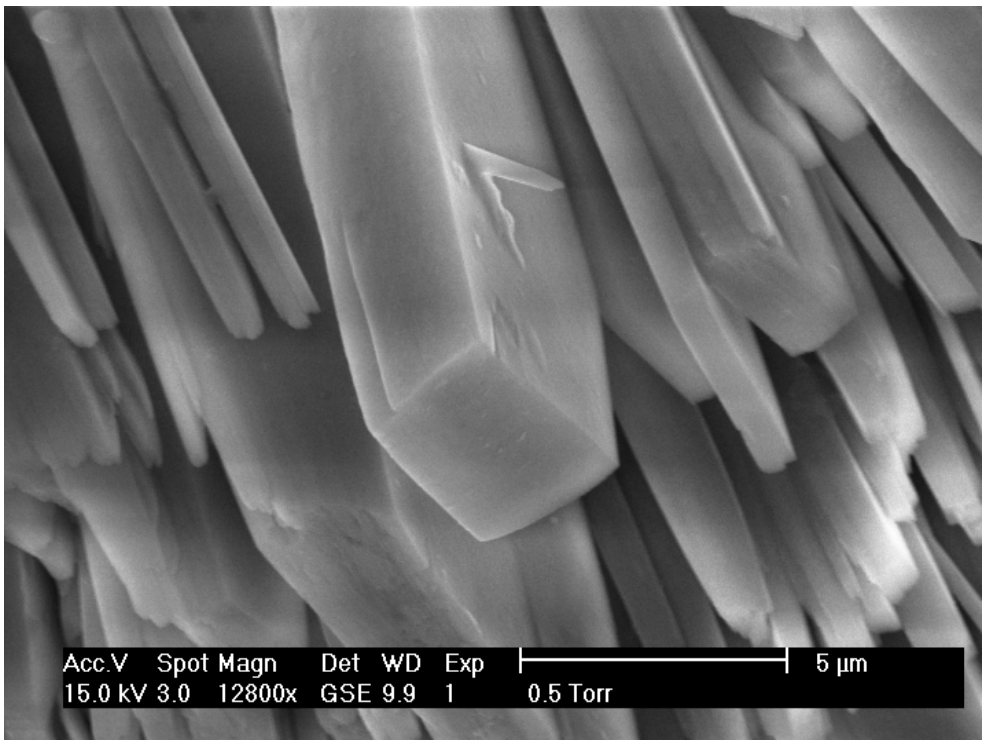

Figure 4. Prismatic vivianite crystals (image taken from a pH 9 system).

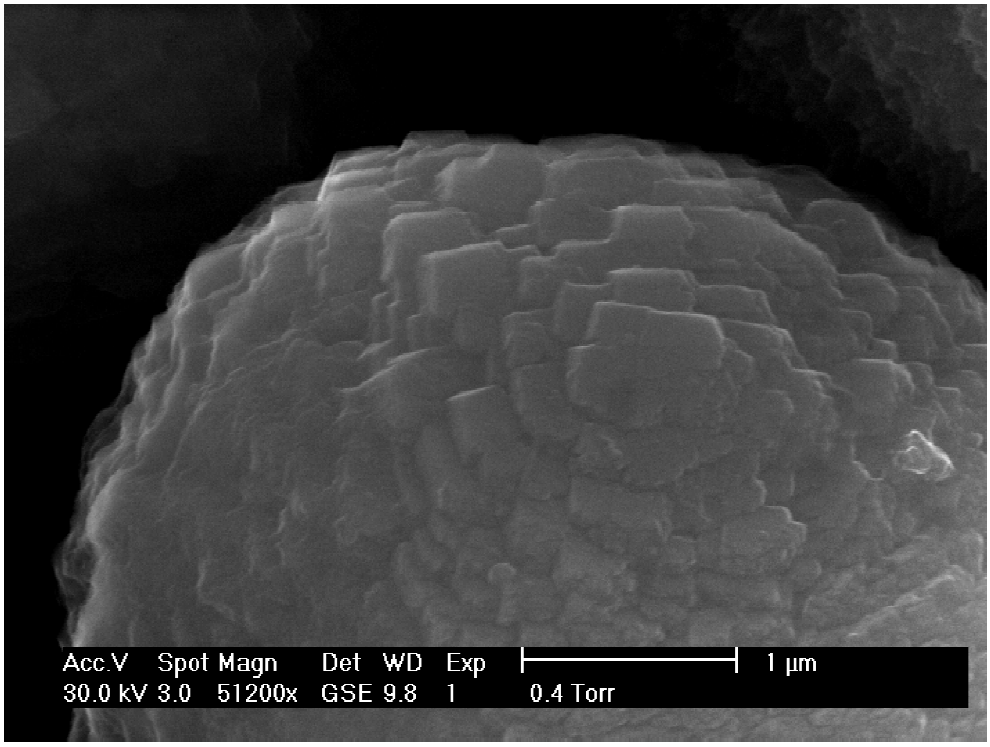

Figure 5. An aggregate of cubic siderite crystals (image taken from a pH 9 system).

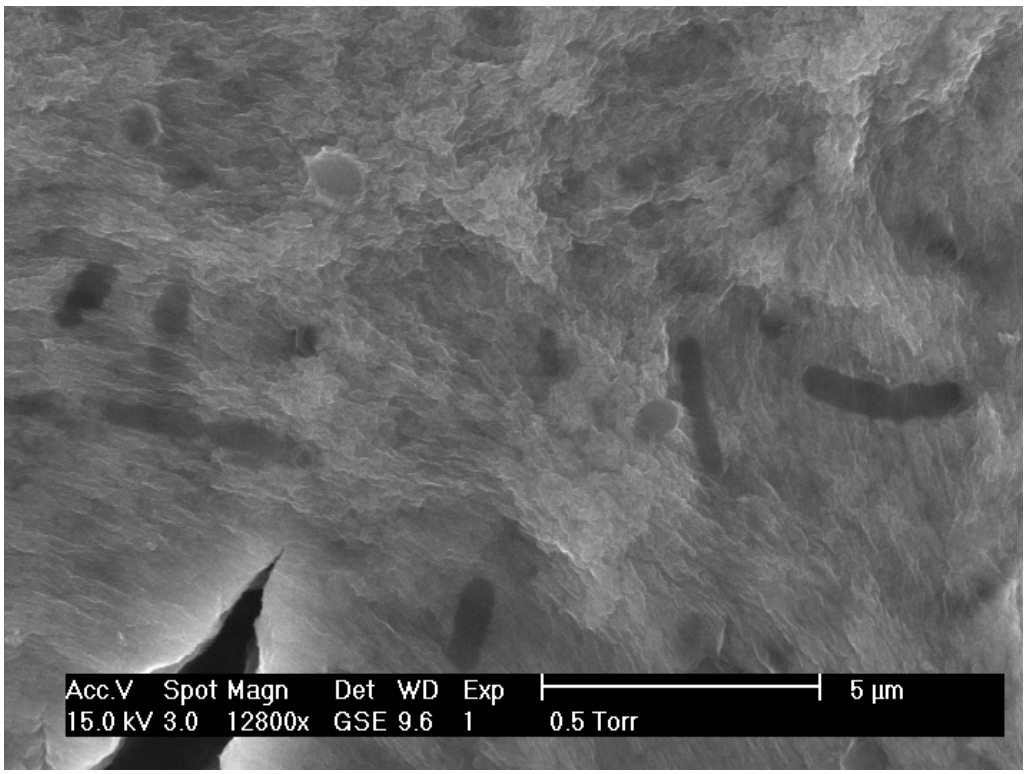

Figure 6. Amorphous Fe(III) during early Fe(III) reduction showing putative microbial cells.

As expected, in sterile microcosms Fe(III) citrate remained in solution at pH 7. However, when sterile media was adjusted to pH 9, an X-ray amorphous Fe(III) phase precipitated out. In microbially active pH 7 systems, during the bioreduction process Fe(III) transiently precipitated as an X-ray amorphous phase (t = 2) prior to its complete reduction to siderite and vivianite. This presumably occurred due to the microbial breakdown of the Fe(III) citrate complex (Francis et al., 1993). At pH 7, bioreduction was essentially complete (> 90 %) within 25 days incubation at 20^{o} C however in the pH 9 systems, Fe(III) reduction was slower with > 90 % reduction occurring after 50 days as a result of the extreme pH challenging microbial respiration (Stewart et al., 2010; Thorpe et al., 2012b). The pH in microbially active systems with an initial pH of 9 reduced by ~ 0.5 pH units during Fe(III) reduction to pH ~ 8.5 and this was attributed to the increase in CO_2 expected from respiration and in solution and the precipitation of

carbonate mineral phases removing OH^- and HCO_3^- from solution (Equation 1; Coleman et al., 1993).

Equation 1: $Fe^{2+} + HCO_3^- + OH^- \rightarrow FeCO_3 + H_2O$

Dissolved inorganic carbon increased in microbially active microcosms presumably due to microbial breakdown of yeast extract and release of CO_2 (data not shown). The exact ratio of siderite to vivianite in these systems is uncertain however the ratio of Fe to PO_4 ratio in the starting media does not allow for more than 20 % of Fe to be present as vivianite. The remaining 80 % must therefore be present as siderite, sorbed Fe(II) or Fe(II)aq. Sequential extractions performed on end-point reduced mineral systems at pH 7 indicated that 30 - 40 % of Fe(II) was aqueous Fe(II), < 5 % of Fe was 'sorbed', 50-60 % was 'carbonate associated' and < 10 % was 'reducible' (Figure 7). By contrast, at pH 9 end point reduction, sequential extraction indicated that less than 1 % of Fe was aqueous Fe or 'sorbed', ~ 80 % was 'carbonate associated' and ~ 20 % was 'reducible' (Figure 7).

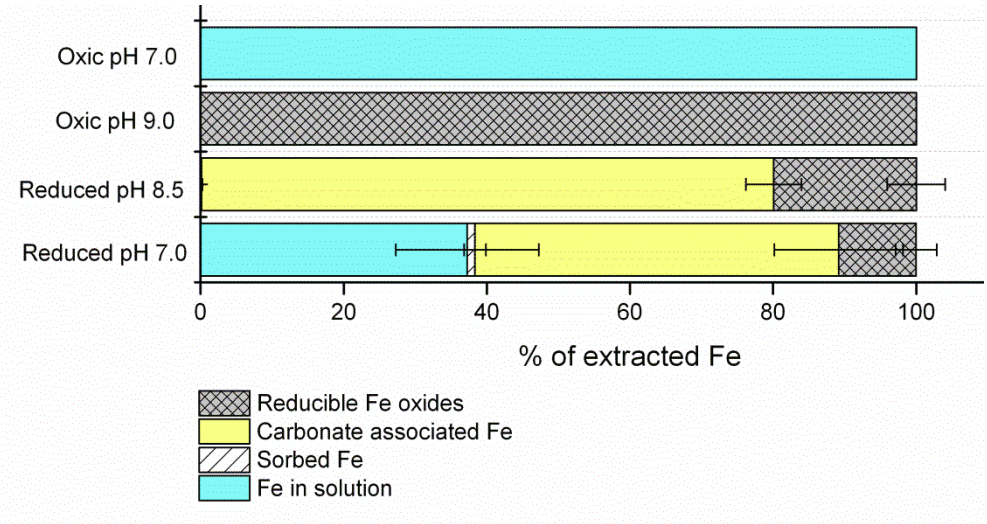

Figure 7. Sequential extraction of oxic and reduced Fe(III) citrate systems at pH 7 and 9 showing blue = % Fe in solution, white striped = % Fe associated with the 'sorbed Fe' extraction, yellow = % Fe associated with the 'carbonate associated' extraction and grey cross hatched = % Fe associated with the 'reducible Fe oxides' extraction. Error bars are the result of triplicate analysis.

Sequential extractions are operationally defined and the reagents are not selective for siderite and vivianite (Keith-Roach et al., 2003; Dodd et al., 2000) and so results must be interpreted carefully. Studies of sequential extraction procedures have shown that vivianite is removed partially during the pH 4.5 1 M Na-acetate 'carbonate associate' extraction and partially during the ammonium oxalate 'reducible' extraction (Dodd et al., 2000). In these systems ferrozine assays imply nearly all Fe(III) was reduced to Fe(II) in both systems and therefore it is likely that the majority of the 'reducible' fraction represents vivianite.

Sr^{2+} behaviour during Fe(III) reduction

Microbially active microcosms were established to investigate Sr^{2+} behaviour during progressive Fe(III) reduction at an initial pH of 7 and 9. Prior to inoculation 1.15 mM Sr^{2+} was added to each microcosm. After 50 days incubation > 85 % of Fe was reduced to Fe(II) at pH 7 and pH 9. However, < 20 % of Sr^{2+} was removed from solution at pH 7 compared to > 95 % at pH 9 (final pH ~ 8.5) (Figure 9a and b). At pH 7, up to 50 % of Sr^{2+} was temporarily removed from solution between days (0 - 30) presumably due to sorption to the transient Fe(III) X-ray amorphous precipitate that formed but this was re-released following complete reduction and recrystallisation to siderite and vivianite (Figure 8a). In oxic controls Sr^{2+} remained in solution at pH 7 where Fe(III)citrate was soluble and > 50 % sorbed to the X-ray amorphous Fe(III) precipitate at pH 9.

To investigate the effects of Fe(II) bearing minerals on Sr^{2+} solubility in the absence of microbial metabolism, 1.15 mM Sr^{2+} was added to Fe(III) reducing, sterilised, end point microcosms (T=60) at a final pH of 7 and ~ 8.5. The results were comparable to progressive Fe(III) reducing systems with < 20 % of Sr^{2+} removed from solution at pH 7 and > 95 % at pH 8.5 (Figures 8c and 8d). In sterile controls, negligible Sr^{2+} was

removed from solution in the pH 7 control and 55 % of Sr^{2+} removed at pH 9 where amorphous Fe(III) mineral precipitate had formed (Figures 8b and 8d).

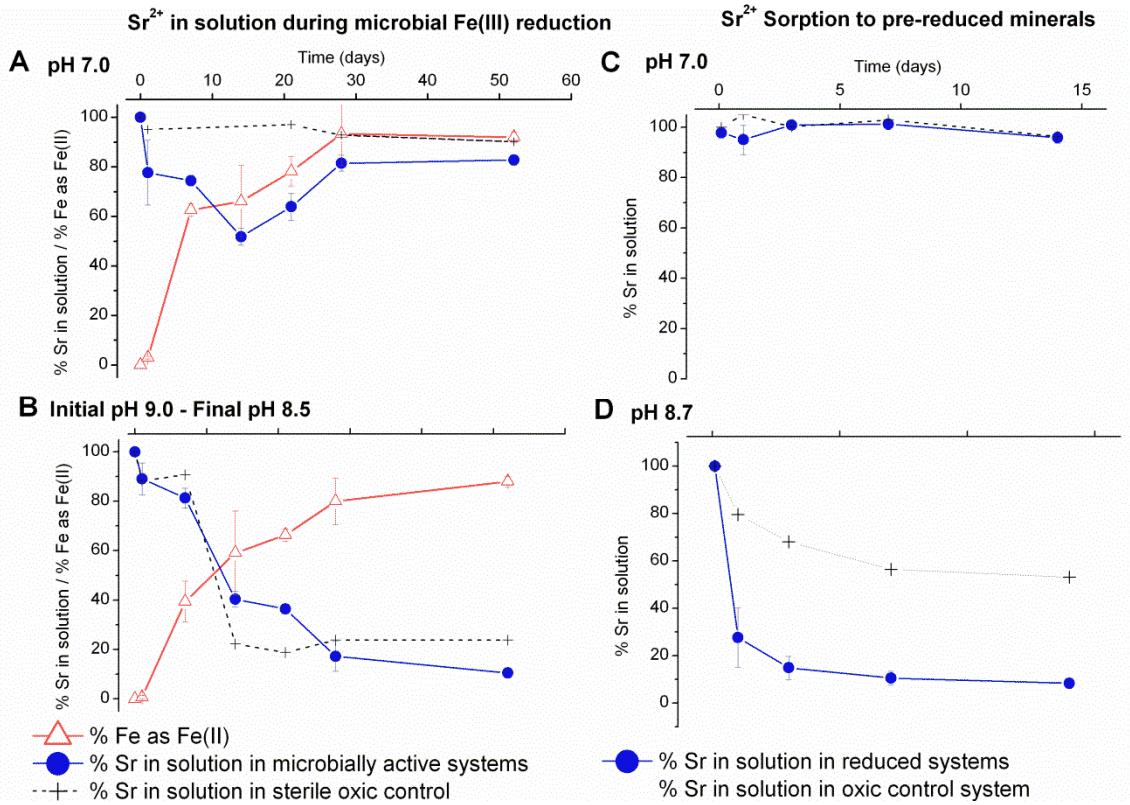

Figure 8. Sr^{2+} removal from solution A) active microbial Fe(III) reducing systems at pH 7.0 B) active microbial Fe(III) reducing systems at an initial pH 9.5 (final pH 8.5) C) pre-reduced mineral systems at pH 7.0 and D) pre-reduced mineral systems at pH 8.7. Error bars represent 1σ experimental uncertainty from triplicate microcosm experiments (where not visible error bars are within symbol size). Experiments were incubated at 20°C.

Sequential extractions revealed that at pH 7 systems, although siderite and vivianite were both present, 95 % of Sr^{2+} was aqueous and < 5 % associated with other fractions (Figure 9). In contrast at pH > 8.5, < 10 % of Sr^{2+} was present as aqueous Sr^{2+}, < 20 % associated with the 'sorbed exchangeable' fraction, > 60 % associated with the carbonate associated Fe fraction and < 10 % with the easily reducible fraction. These results suggest Sr^{2+} may be associated with carbonate mineral phases in alkaline systems where the pH was > 8.5.

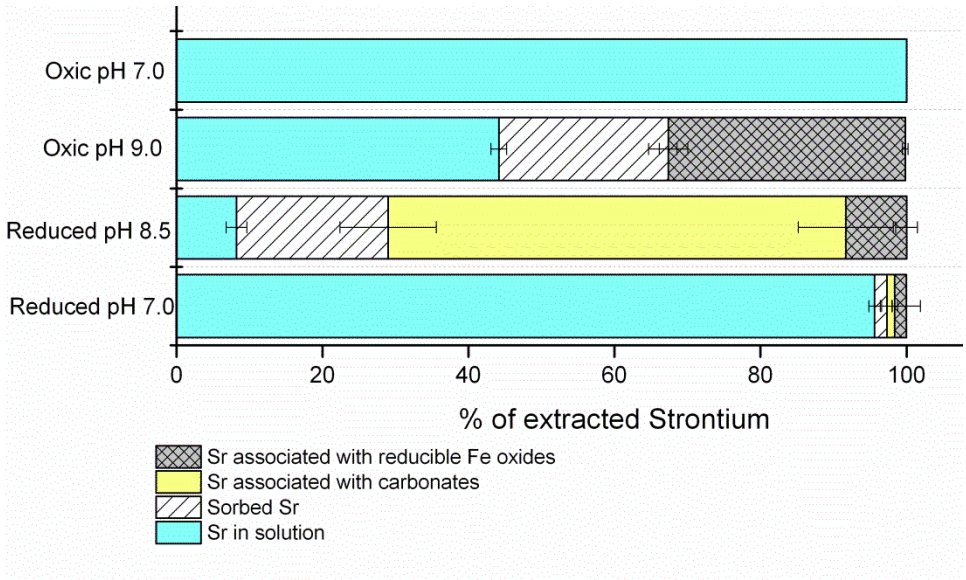

Figure 9. Sequential extraction on oxic and reduced Fe(III) citrate systems pH 7 and 9 showing Sr^{2+} associated with blue = % Fe in solution, white striped = % Fe associated with the 'sorbed Fe' extraction, yellow = % Fe associated with the 'carbonate associated' extraction and grey cross hatched = % Fe associated with the 'reducible Fe oxides' extraction. Error bars are the result of triplicate analysis.

ESEM was used to image the end point mineralogy in selected systems in order to investigate the fate of Sr^{2+} removed from solution in these systems; EDAX spot analysis was used to identify the elemental composition of mineral surfaces. At pH 7 only siderite and vivianite crystals were identified as in Figure 2 and EDAX spot analysis did not detect Sr^{2+} associated with either phase. This was expected as geochemical analysis showed that > 90 % of Sr^{2+} remained in solution. In contrast, at pH > 8.5 siderite, vivianite and strontianite minerals were detectable by XRD and ESEM/EDAX analysis. The XRD trace for strontianite was unclear (Figure 1) due to the low concentrations of Sr^{2+} compared to Fe^{2+} (~ 1 mM Sr^{2+} compared to ~20 mM Fe) but its presence was supported by ESEM images combined with EDAX analysis (Figures 10 – 14 and 15). Strontianite formed in aggregates of acicular crystals and appeared to associate with the aggregates of siderite cubes (Figure 10-14).

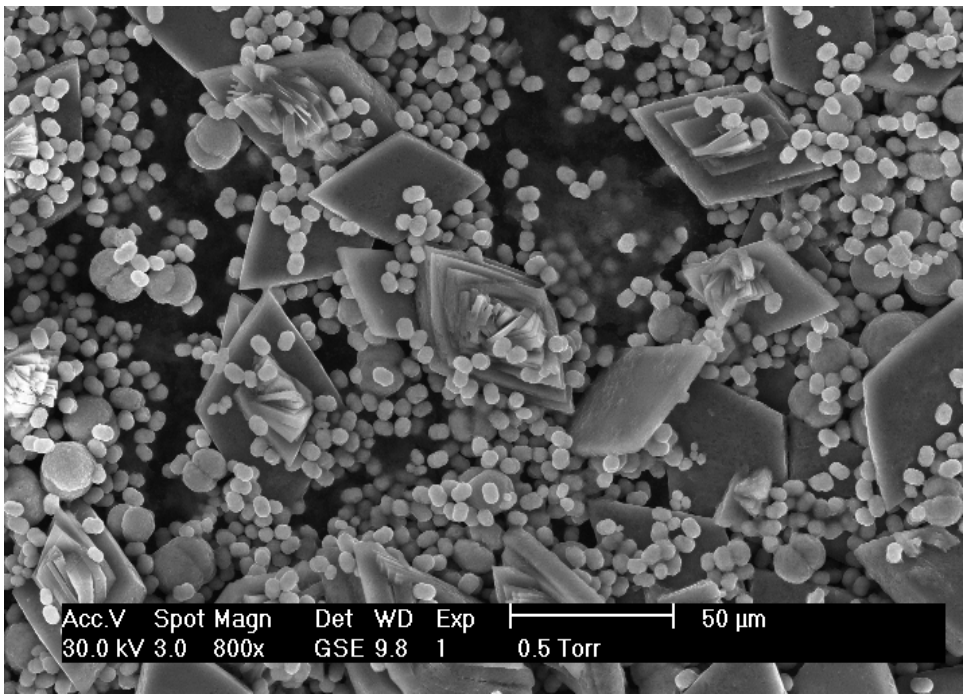

Figure 10. Image showing siderite aggregates (small spheres), vivianite crystals (diamonds) and strontianite aggregates (larger spheres) in the pH 9 system.

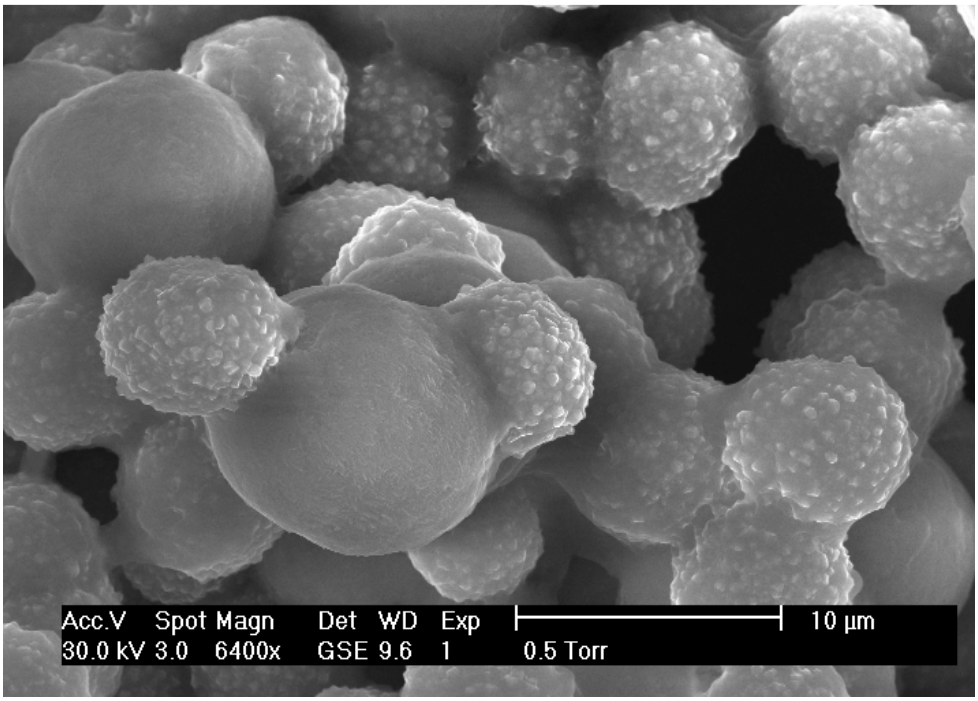

Figure 11. Image showing aggregates of siderite crystals associated with aggregates of strontianite crystals.

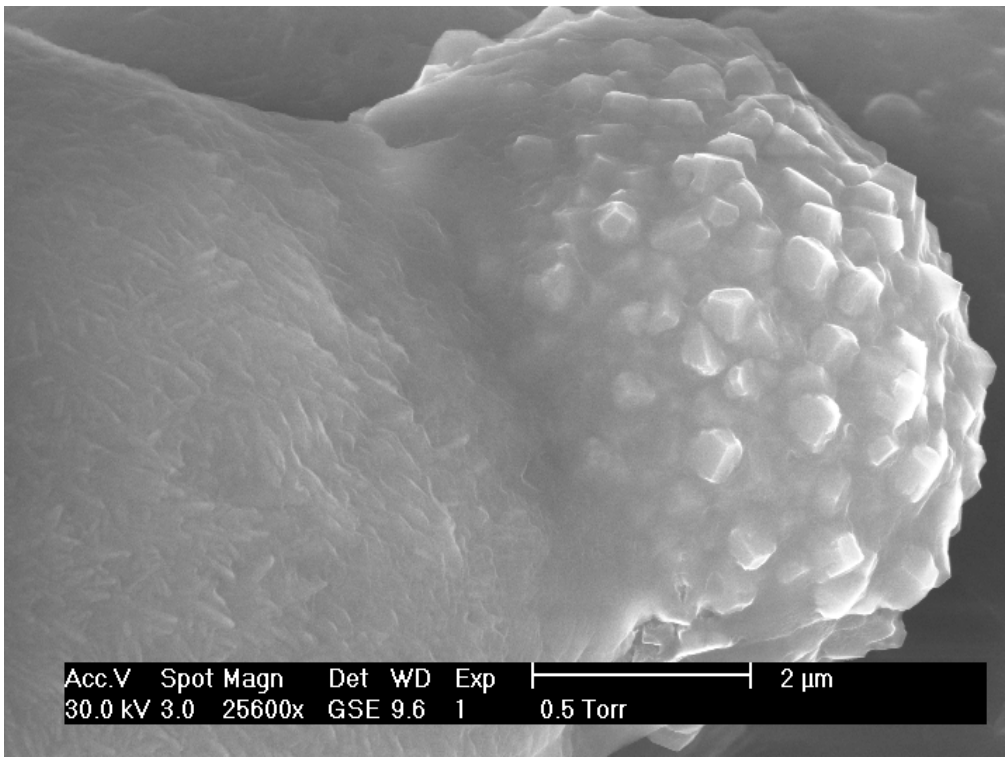

Figure 12. Image showing close up of strontianite and siderite aggregates

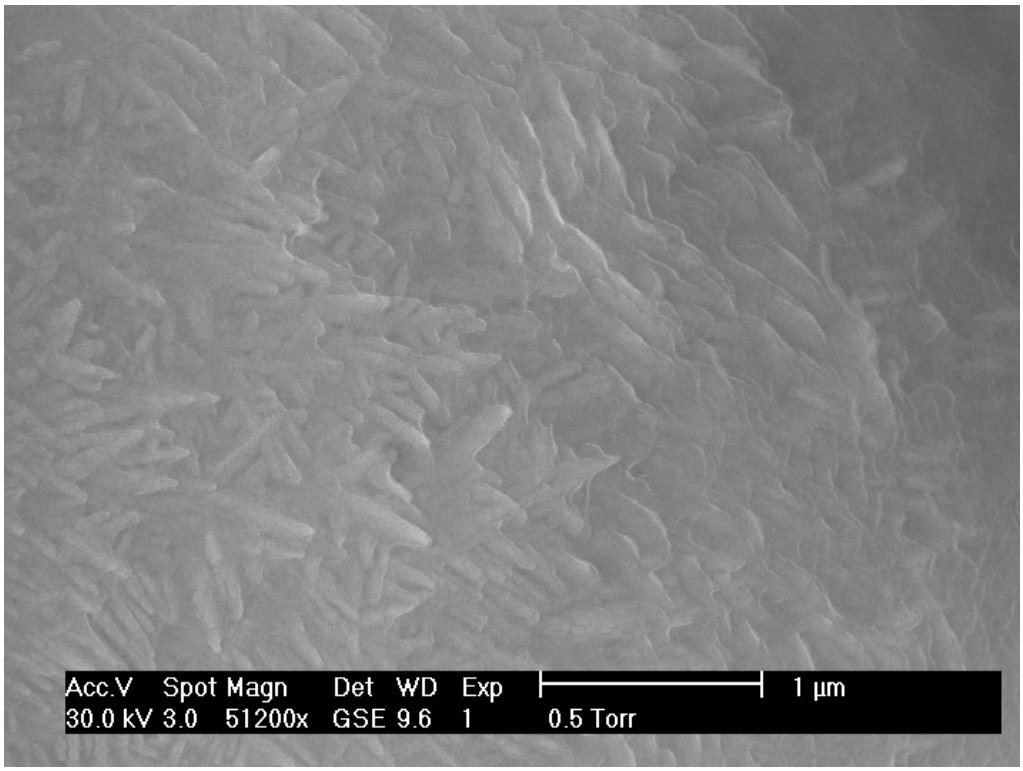

Figure 13. Strontianite acicular crystals of the orthorhombic crystal system.

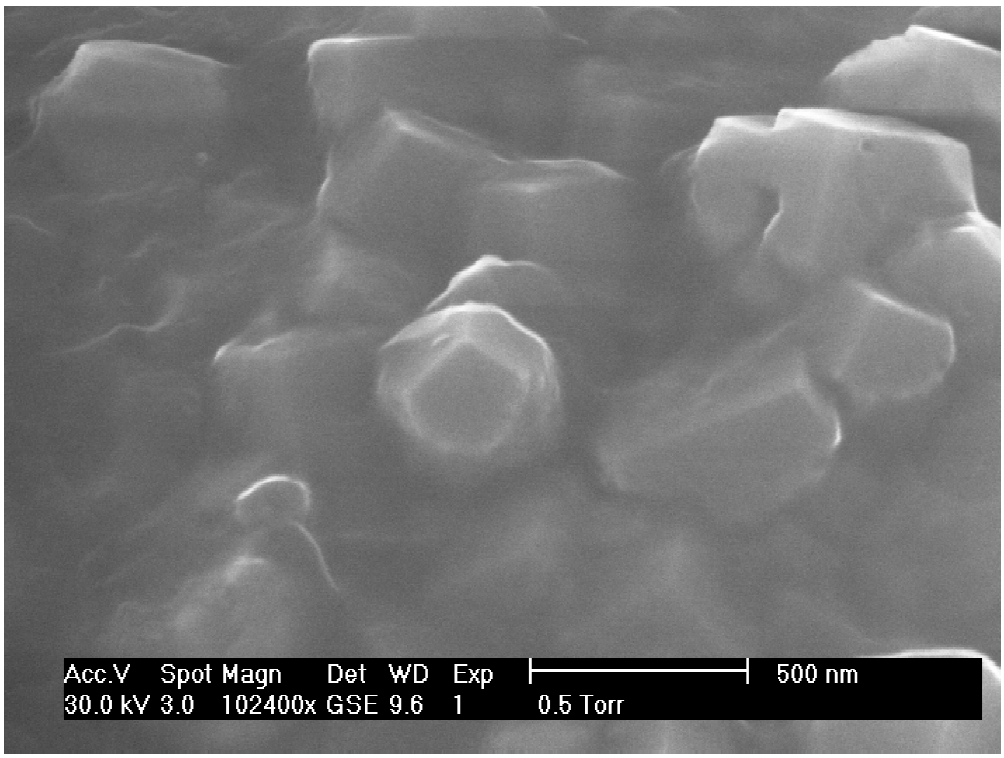

Figure 14. Siderite cubic crystals of the cubic crystal system.

Modelling of systems in PHREEQC-2 (LLNL database) using relevant pH and dissolved inorganic carbon (DIC) measurements predicts increased super-saturation with respect to strontianite at pH 9 compared to pH 7 and also in reduced systems compared to oxic systems due to increased DIC (Table 2). Strontianite precipitation was not observed in pH 9 sterile control systems under XRD or ESEM indicating that strontianite precipitation was stimulated by microbial Fe(III) reduction. It is possible that the increase in super-saturation due to increased DIC was enough to stimulated strontianite precipitation (Table 2). Another explanation is that the presence of microbial cells and biogenic siderite crystals may have provided nucleation sites for strontianite formation (Schultze-Lam and Beveridge, 1994; Parmar et al., 2000; Douglas, 2004).

System	Siderite	Strontianite	Vivianite	Haematite	Goethite	$Fe(OH)_3$
Reduced pH 7	3.17	0.62	10.15	-	-	-
Reduced pH 8.5	4.66	2.67	13.94	-	-	-
Reduced pH 9	4.80	3.05	14.69	-	-	-
Oxic pH 9	-	1.72	-	26.22	12.11	6.37
Oxic pH 7	-	0.80	-	25.79	11.04	6.15

Table 2. Table of modelled saturation indices for key minerals in experimental systems modelled in PHREEQC-2 (LLNL database).

Previous studies at comparable Sr^{2+} concentrations have shown enhanced removal of Sr^{2+} concurrent with siderite production and attributed it to incorporation of Sr^{2+} into the siderite lattice rather than precipitation of strontianite (Ferris and Roden, 2000; Palmer et al., 2000; Roden et al., 2002). In this study, minor Sr^{2+} inclusion into the siderite lattice is suggested, at pH 9, by a slight shift of the C lattice parameter for siderite towards a lower angle possibly implying the incorporation of a larger atom into the structure (Figure 15).

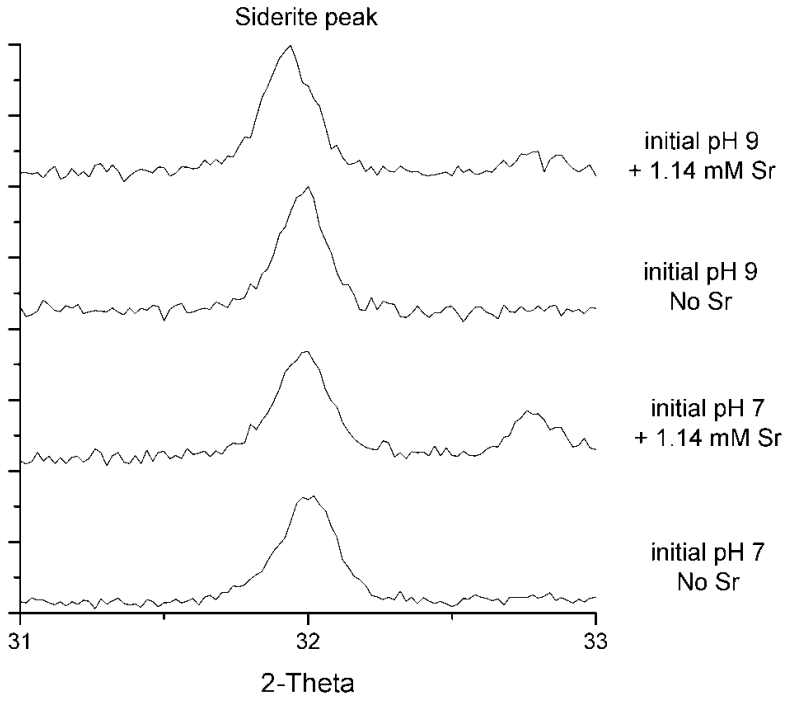

Figure 15. Close up of XRD spectrum showing C lattice peak of siderite in various systems.

However, EDAX analysis of the siderite crystals shows no Sr^{2+} on siderite surfaces except at the join where siderite cubes and strontianite balls are co-located (Figure 16).

These findings are consistent with the expectation that the much larger ionic radius of Sr^{2+} (1.18 for Sr^{2+} compared to 0.78 for Fe^{2+}) would prevent major isomorphic substitution (Reeder, 1990). Thus in our systems it seems Sr^{2+} is incorporated into strontianite as morphological and chemical analysis suggest the predominance of pure $SrCO_3$ and $FeCO_3$ in these systems.

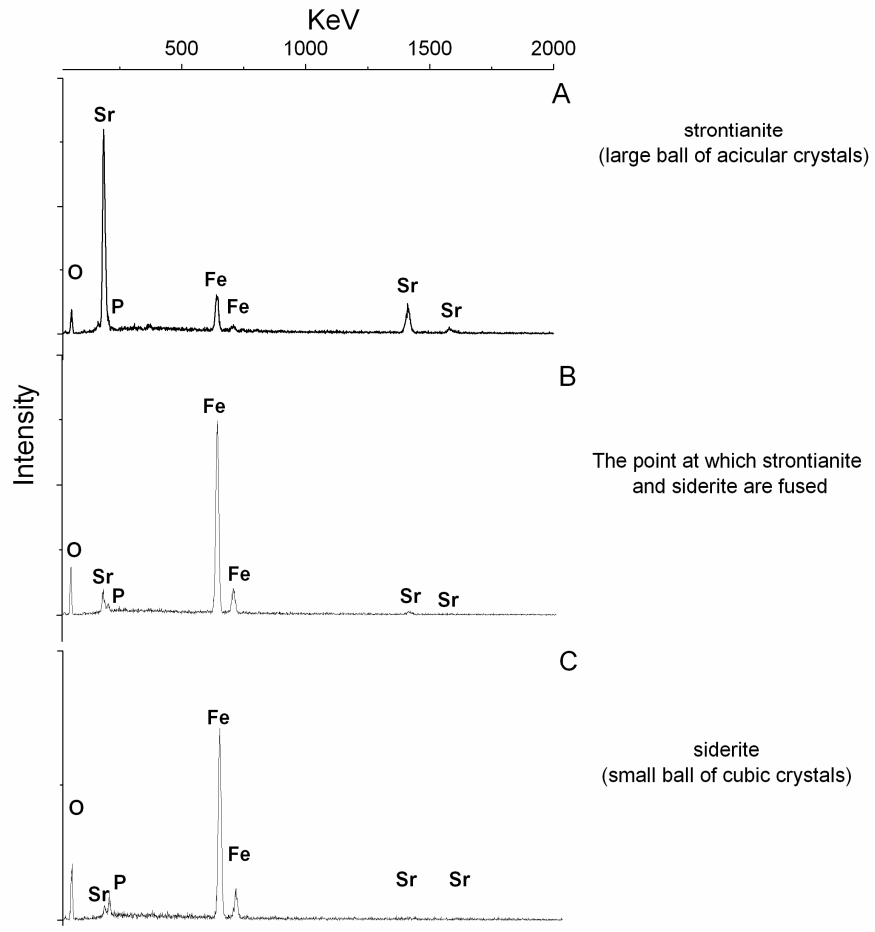

Figure 16. EDX spectrum for A) the centre of a strontianite aggregate, B) the join between a strontianite aggregate and a siderite aggregate and C) the centre of a siderite aggregate.

Tc-99 behaviour during Fe(III) reduction

Experiments were established to investigate the effect of Fe(II) bearing mineral formation on ^{99}Tc at pH 7 and pH 9. Microbially active microcosms were established to investigate ^{99}Tc behaviour during progressive Fe(III) reduction at an initial pH of 7 and

9. Prior to inoculation 100 Bq ml^{-1} (1.58 x 10^{-9} M) ^{99}Tc was added to each microcosm. Removal of ^{99}Tc from solution occurred concurrent with Fe(III) reduction in all progressive reducing microcosm systems (Figure 17a and 17b). At pH 7, 98 ± 0.77 % of ^{99}Tc was removed from solution over 50 days compared to 40 ± 9.9 % removal at pH 9 over 50 days (Figure 8a and 8b). In sterile oxic controls ^{99}Tc remained > 90 % in solution at both pH 7 and 9. Reduction was slower in ^{99}Tc experiments although this was attributed to the ambient temperature (15°C) at which the culture was incubated rather than the presence of ^{99}Tc.

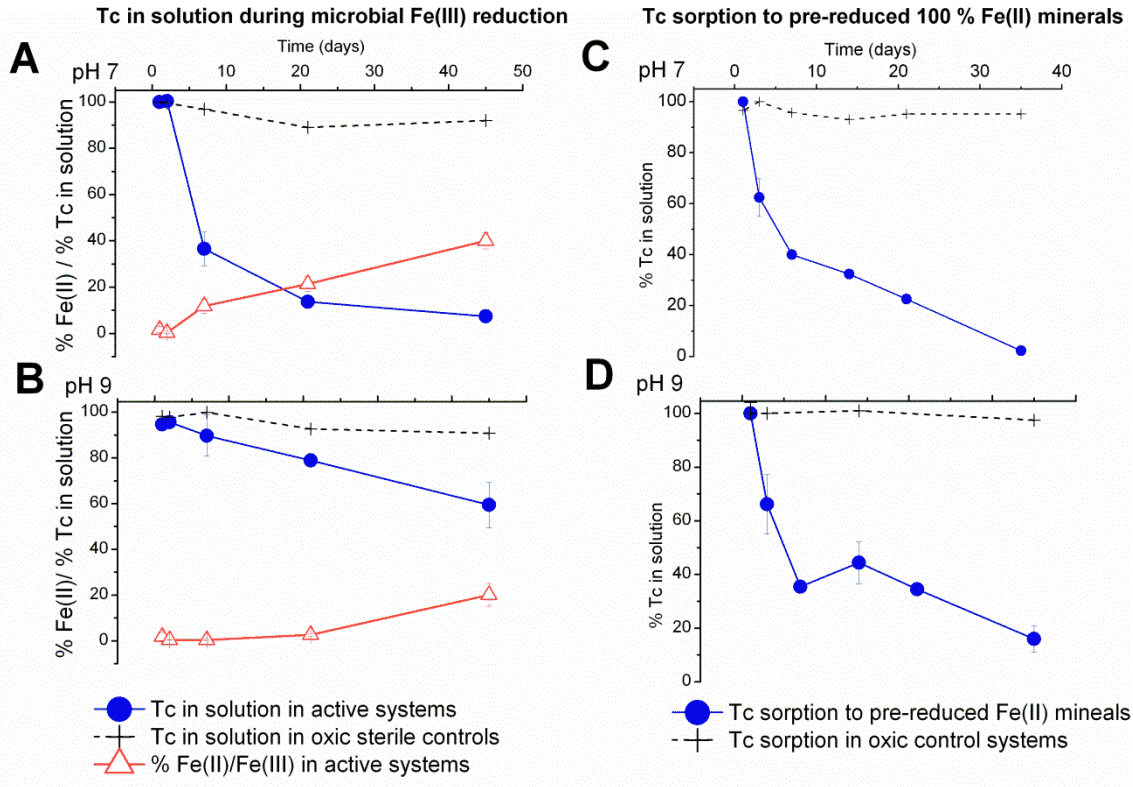

Figure 17: ^{99}Tc removal from solution in A) active microbial Fe(III) reducing systems at pH 7.0 B) active microbial Fe(III) reducing systems at an initial pH 9.0 (final pH 8.5) C) pre-reduced mineral systems at pH 7.0 and D) pre-reduced mineral systems at pH ~ 8.5. Error bars represent 1σ experimental uncertainty from triplicate microcosm experiments (where not visible error bars are within symbol size). Experiments were incubated at 15°C.

In addition, ^{99}Tc was added to sterilised, Fe(II) mineral bearing end point microcosms (T=80) at a final pH of 7 and ~ 8.5 and removal of ^{99}Tc occurred over a period of 35

days (Figure 17c and 17d). Removal of ^{99}Tc in sterilised Fe(II) mineral bearing microcosms indicates that Tc(VII) reduction is primarily abiotic as observed in previous studies (McBeth et al., 2011). In end point microcosms ^{99}Tc was removed from solution 97 ± 1.6 % in pH 7 systems and 85 ± 4.9 % in pH 9 systems. XANES data collected for end point microcosms of final pH 7.0 and 8.7 compared poorly to the Tc(VII) (TcO_4^-) XANES with no sign of the characteristic pre edge feature observed in this and previous studies (Fredrickson et al., 2004; Morris et al., 2008; McBeth et al., 2011). Sample XANES compared well to Tc(IV) spectra found in previous studies (Figure 18; Poineau et al., 2006; Fredrickson et al., 2004; Morris et al., 2008; McBeth et al., 2011). This confirmed Tc(VII) reduction to Tc(IV) as the mechanism for ^{99}Tc removal in these model systems.

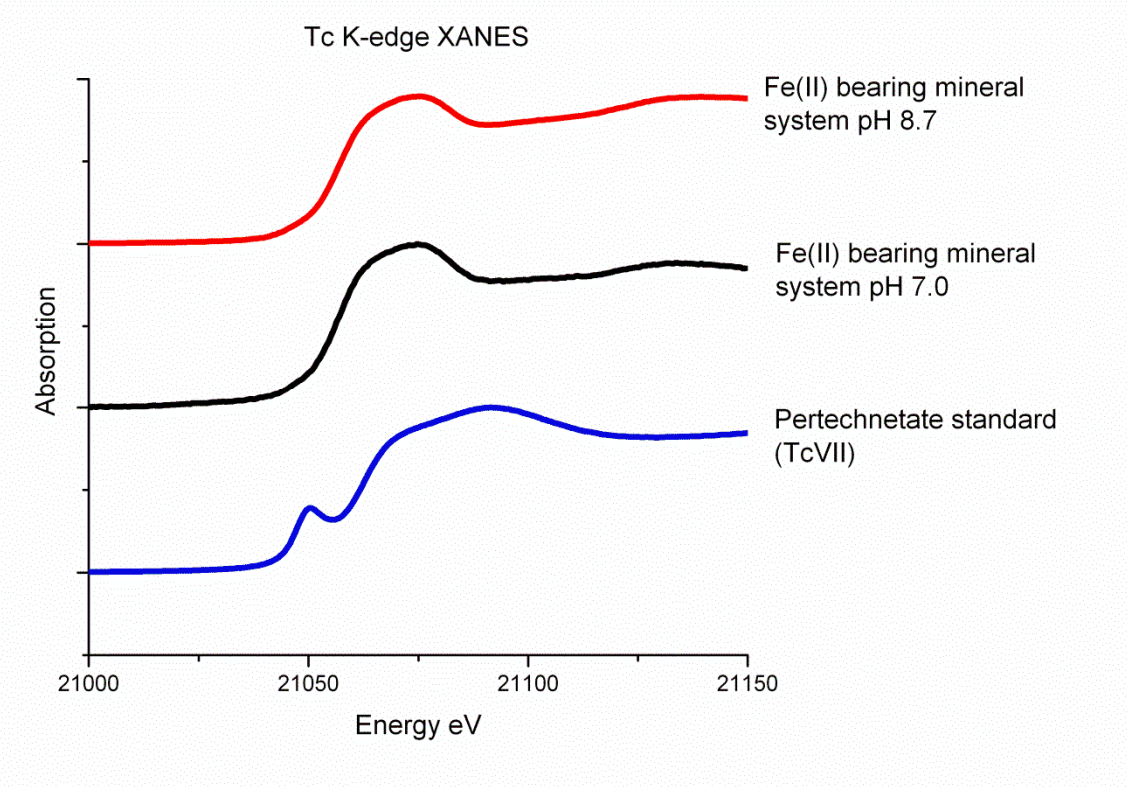

Figure 18. Normalised Tc K-edge XANES for a) Fe(II) bearing mineral system a pH 8.7, b) Fe(II) bearing mineral systems at pH 7.0 and c) Pertechnetate -TcO_4^- standard (Tc(VII)).

Interestingly, ^{99}Tc removal was greater in pH 7 systems compared to pH 9 systems. In progressive microcosms this is most likely due to the slower rate of Fe(III) reduction observed at pH 9 meaning that TcO_4^- might remain in solution for longer. However, this does not explain the difference sorption in end point, Fe(II) bearing mineral systems where 97 ± 1.6 % ^{99}Tc was removed from solution at pH 7 systems compared to 85 ± 4.9 % at pH 9. Nevertheless, overall this study shows that substantial ^{99}Tc (> 80 %) is removed from solution by biogenic Fe(II) bearing mineral phases at both neutral and alkaline pH.

Implications

In these model systems, at neutral pH the precipitation of biogenic Fe(II) bearing mineral phases, siderite and vivianite, resulted in the immobilization of ^{99}Tc *via* reduction from Tc(VII) to Tc(IV) whilst Sr^{2+} remained in solution. In contrast, at mildly alkaline pH > 8.5, reductive removal of ^{99}Tc was accompanied by the precipitation of Sr^{2+} as strontianite apparently stimulated by Fe(III) reduction. Whilst these results highlight the potential for co-treatment of ^{99}Tc and ^{90}Sr at alkaline pH, results also show that Fe(III) reduction at neutral pH, or in systems that are undersaturated with regard to $SrCO_3$, may mobilise sorbed Sr^{2+} and therefore the problematic fission product ^{90}Sr. In heterogeneous sediment systems the fate of mobilised Sr^{2+} would be dependent on its association with other sediment mineral phases, for example clays or Ca carbonates. These results help predict the effects of bioreduction on relevant groundwater soluble radionuclides.

Acknowledgments

We thank Jon Fellowes, Alastair Bewsher and Paul Lythgoe for help in data acquisition. This work was supported by a studentship to CLT from the Engineering and Physical Science Research Council (EPSRC) as part of the Decommissioning, Immobilisation and Management of Nuclear Waste for Disposal (DIAMOND) consortium: grant EP/F055412/1. We also acknowledge the support of the Natural Environment Research Council grant NE/H007768/1.

References

Begg, J.D.C., Burke, I.T., Morris, K. (2007). The behaviour of technetium during microbial reduction in amended soils from Dounreay, UK. *Science of the Total Environment*, 373, 297-304.

Coleman, M.L., Hedrick, D.B., Lovley, D.R., White, D.C., Pye, K. (1993). Reduction of Fe(III) in sediments by sulphate-reducing bacteria. *Nature*, 361, 436-438.

Coker, V.S., Bell, A.M.T., Pearce, C.L., Pattrick, R.A.D., van der Laan, G., Lloyd, J.R. (2008). Time-resolved synchrotron powder X-ray diffraction study of magnetite formation by the Fe(III)-reducing bacterium *Geobacter sulfurreducens*. *American Mineralogist*, 93, 540-547.

Cutting, R.S., Coker, V.S., Fellowes, J.W., Lloyd, J.R., Vaughan, D.J. (2009). Mineralogical and morphological constraints on the reduction of Fe(III) minerals by Geobacter sulfurreducens. *Geochimica Et Cosmochimica Acta*, 73, 4004-4022.

de Pablo, J., Rovira, M., Gimenez, J., Casas, I., and Clarens, F. (2008). Magnetite sorption capacity for strontium as a function of pH. *Scientific Basis for Nuclear Waste Management Xxxi*, 1107, 593-598.

Detkova, E.N., Pusheva, M.A. (2006). Energy metabolism in halophilic and alkaliphilic acetogenic bacteria. *Microbiology*, 75, 1-11.

Dobbin, P.S., Carter, J.P., San Juan, C.G.S., von Hobe, M., Powell, A.K., Richardson, D.J. (1999). Dissimilatory Fe(III) reduction by *Clostridium beijenrickii* isolated from freshwater sediment using Fe(III) maltol enrichment. *FEMS Microbiology Letters*, 176,131–138.

Dodd, J., Large, D.J., Fortey, N.J., Milodowski, A.E., Kemp, S. (2000). A petrographic investigation of two sequential extraction techniques applied to anaerobic canal bed mud. *Environmental Geochemical Health*, 22, 281-296.

Douglas, S. (2004). Microbial biosignatures in evaporite deposits: evidence from Death Valley, California. *Planetary and Space Science*, 52, 223-227.

Icenhower, J.P., Qafoku, N.P., Zachara, J.M., Martin, W.J., (2010). The biogeochemistry of technetium: a review of the behaviour of an artificial element in the natural environment. *American Journal of Science*, 310, 721-752.

Islam, F.S., Pederick, R.L., Gault, A.G., Adams, L.K., Polya, D.A., Charnock, J.M., Lloyd, J.R. (2005). Interactions between the Fe(III)-reducing bacterium Geobacter sulfurreducens and arsenate, and capture of the metalloid by biogenic Fe(II). *Applied and Environmental Microbiology*, 71, 8642-8648.

Istok, J.D., Senko, J.M., Krumholz, L.R., Watson, D., Bogle, M.A., Peacock, A., Chang, Y.J., White, D.C. (2004). In situ bioreduction of technetium and uranium in a nitrate-contaminated aquifer. *Environmental Science & Technology*, 38, 468-475.

Keith-Roach, M.J., Morris, K., Dahlgaard, H. (2003). An investigation into technetium binding in sediments. *Marine Chemistry*, 81, 149-162.

Kinniburgh, D.G., Jackson, M.L., Syers, J.K. (1975). Adsorptionn of alkali earth, transition, and heavy metal cations by hydrous oxide gels of iron and aluminium. *Soil Science Society of America Journal*, 40, 796-799.

Krulwich, T.A., Ito, M. Guffanti, A.A. (2001). The Na+-dependence of alkaliphily in Bacillus. *Biochimica Et Biophysica Acta-Bioenergetics*, 1505, 158-168.

Lane, D. J., Pace, B., Olsen, G. J., Stahl, D. A., Sogin, M. L., Pace, N. R. (1985). Rapid determination of 16S ribosomal-RNA sequences for phylogenetic analyses. *Proceedings of the National Academy of Science of the U.S.A.*, 82, 6955-6959.

Langley, S., Gault, A.G., Ibrahim, A., Takahashi, Y., Renaud, R., Fortin, D., Clark, I.D., Ferris, F.G., 2009. Sorption of Strontium onto Bacteriogenic Iron Oxides. *Environmental Science & Technology*, 43, 1008-1014.

Law, G.T.W., Geissler, A., Boothman, C., Burke, I.T., Livens, F.R., Lloyd, J.R., Morris, K. (2010). Role of Nitrate in Conditioning Aquifer Sediments for Technetium Bioreduction. *Environmental Science & Technology*, 44, 150-155.

Lehours, A., Rabiet, M., Morel-Desrosiers, N., Morel, J., Jouve, L., Arbeile, B, Mailhot, G., Fonty, G. (2010). Ferric iron reduction by fermentative strain BS2 isolated from an iron-rich anoxic environment (Lake Pavin, France). *Geomicrobiology Journal*, 27, 714-722.

Lloyd, J.R., Chesnes, J., Glasauer, S., Bunker, D.J., Livens, F.R., Lovley, D.R. (2002). Reduction of actinides and fission products by Fe(III)-reducing bacteria. *Geomicrobiology Journal*, 19, 103-120.

Lloyd, J.R. (2003). Microbial reduction of metals and radionuclides. *Fems Microbiology Reviews*, 27, 411-425.

Lloyd, J.R., Renshaw, J.C. (2005). Bioremediation of radioactive waste: radionuclide-microbe interactions in laboratory and field-scale studies. *Current Opinion in Biotechnology*, 16, 254-260.

Lovley, D.R., Phillips, E.J.P., Lonergan, D.J. (1991). Enzymatic versus monenzymatic mechanisms for Fe(III) reduction in aquatic sediments. *Environmental Science and Technology*, 25, 1062-1067.

Lovley, D.R., Phillips, E.J.P. (1986). Availability of Ferric Iron for Microbial Reduction in Bottom Sediments of the Fresh-Water Tidal Potomac River. *Applied and Environmental Microbiology*, 52, 751-757.

Lovley, D.R., Phillips, E.J.P. (1988). Novel mode of microbial energy metabolism: organic carbon oxidation coupled to dissimilatory reduction of iron or manganese. *Applied and Environmental Microbiology*, 54, 1472-1480.

McKinley, J.P., Zachara, J.M., Smith, S.C., and Liu, C. (2007) Cation exchange reactions controlling desorption of Sr-90(2+) from coarse-grained contaminated sediments at the Hanford site, Washington. *Geochimica Et Cosmochimica Acta***,** 71, 305-325.

McBeth, J.M., Lear, G., Lloyd, J.R., Livens, F.R., Morris, K., Burke, I.T. (2007). Technetium reduction and reoxidation in aquifer sediments. *Geomicrobiology Journal*, 24, 189-197.

McBeth, J.M., Lloyd, J.R., Law, G.T.W., Livens, F.R., Burke, I.T., Morris, K. (2011). Redox interactions of technetium with iron-bearing minerals. *Mineralogical Magazine*, 75, 2419-2430.

McKenzie, H., Armstrong-Pope, N. (2010). Groundwater Annual Report 2010. Sellafield Ltd. Technical report TECH000613. Available at: http://www.sellafieldsites.com/land/documents/Groundwater_Annual_Report_2010.pdf. Last accessed: 22/3/12.

Mitchell, A.C., Ferris, F.G. (2005). The coprecipitation of Sr into calcite precipitates induced by bacterial ureolysis in artificial groundwater: Temperature and kinetic dependence. *Geochimica Et Cosmochimica Acta* **69**: 4199-4210.

Morris, K., Livens, F.R., Charnock, J.M., Burke, I.T., McBeth, J.M., Begg, J.D.C., Boothman, C., Lloyd, J.M. (2008). An X-ray absorption study of the fate of

technetium in reduced and reoxidised sediments and mineral phases. *Applied Geochemistry.* 23, 603-617.

Ferris, F.G., Roden, E.E., (2000). Microbial mineral transformations at the Fe(II)/Fe(III) redox boundary for solid phase capture of strontium and other metal/radionuclide contaminants. DOE Report DOE/ER/62317.

Ferris, F.G., Hallberg, R.O., Lyvén, B., Pedersen, K. (2000). Retention of strontium, cesium, lead and uranium by bacterial iron oxides from a subterranean environment. *Applied Geochemistry*, 15, 1035-1042.

Francis, A.J., Dodge, C.J. (1993). Influence of complex structure on the biodegradation of iron-citrate complexes. *Applied Environmental Microbialogy*, 59, 109-113.

Fredrickson, J.K., Zachara, J.M., Kennedy, D.W., Dong, H.L., Onstott, T.C., Hinman, N.W., Li, S.M. (1998). Biogenic iron mineralization accompanying the dissimilatory reduction of hydrous ferric oxide by a groundwater bacterium. *Geochimica Et Cosmochimica Acta*, 62, 3239-3257.

Fredrickson, J.K., Zachara, J.M., Balkwill, D.L., Kennedy, D., Li, S.M.W., Kostandarithes, H.M., Daley, M.J., Romine, M.F., Brockman, F.J. (2004). Geomicrobiology of high-level nuclear waste-contaminated vadose sediments at the Hanford Site, Washington State. *Applied Environmental Microbiology*, 70, 4230-4241.

Fujita, Y., Redden, G.D., Ingram, J.C., Cortez, M.M., Ferris, F.G., Smith, R.W. (2004). Strontium incorporation into calcite generated by bacterial ureolysis. *Geochimica Et Cosmochimica Acta*, 68, 3261-3270.

Greegor, R.B., Pingitore, N.E., Lytle, F.W. (1997). Strontianite in coral skeletal aragonite. *Science*, 275, 1452-1454.

Parmar, N., Warren, L.A., Roden, E.E., Ferris, F.G. (2000). Solid phase capture of strontium by the iron reducing bacteria Shewanella alga strain BrY. *Chemical Geology*, 169, 281-288.

Poineau, F., Fattahi, M., Den Auwer, C., Hennig, C., Grambow, B. (2006). Speciation of technetium and rhenium complexes by *in situ* XAS-electrochemistry. *Radiochimica Acta*, 94, 283-289.

Poulton, S.W., and Canfield, D.E. (2005). Development of a sequential extraction procedure for iron: implications for iron partitioning in continentally derived particulates. *Chemical Geology*, 214, 209-221.

Reeder R. J. (1990) Crystal chemistry of the rhombohedral carbonates. *Carbonates: Mineralogy and Chemistry*,11, 1–48. Mineralogical Society of America.

Roden, E.E., Lovley, D.R. (1993). Dissimilatory Fe(III) reduction by the marine microorganism desulfuromonas-acetoxidans. *Applied Envionmental Microcbiology*, 59, 734-742.

Roden, E.E., Leonardo, M.R., Ferris, F.G. (2002). Immobilization of strontium during iron biomineralization coupled to dissimilatory hydrous ferric oxide reduction. *Geochimica Et Cosmochimica Acta*, 66, 2823-2839.

Shultze-lam, S., Beveridge, T.J. (1994). Nucleation of celestite and strontianite on a cyanobacterial S-layer, *Applied Environmental Microbiology*, 60, 447-453.

Stewart, D.I., Burke, I.T., Hughes-Berry, D.V., Whittleston, R.A. (2010). Microbially mediated chromate reduction in soil contaminated by highly alkaline lechate from chromium containing waste. *Ecological Engineering*, 36, 211-221.

Tessier, A., Campbell, P.G.C., Bisson, M. (1979) Sequential extraction procedures for the speciation of particulate trace-metals. *Analytical Chemistry*, 51, 844-851.

Thorpe, C.L., Lloyd, J.R., Law, G.T.W., Burke, I.T., Shaw, S., Bryan, N.D., Morris, K. Strontium sorption and precipitation behaviour during bioreduction in nitrate impacted sediments. *Chemical Geology*, (in press).

Thorpe, C.L., Law, G.T.W., Boothman, C., Lloyd, J.R., Burke, I.T., Morris, K. (2012a). Synergistic effect of high nitrate concentrations on sediment bioreduction. Geomicrobiology Journal, 29, 484-493.

Thorpe, C.L., Morris, K., Boothman, C., Lloyd, J.R., (2012b). Alkaline Fe(III) reduction by a novel alkali-tolerant *Serratia* sp. isolated from surface sediments close to Sellafield nuclear facility, UK. *FEMS Microbiology Letters*, 327, 87-92.

Viollier, E., Inglett, P.W., Hunter, K., Roychoudhury, A.N., Van Cappellen, P., 2000. The ferrozine method revisited: Fe(II)/Fe(III) determination in natural waters. *Applied Geochemistry*, 15, 785-790.

Whittleston, R.A., Stewart, D.I., Mortimer, R.J.G., Tilt, Z.C., Brown, A.P., Geraki, K., and Burke, I.T. (2011) Chromate reduction in Fe(II)-containing soil affected by hyperalkaline leachate from chromite ore processing residue. *Journal of Hazardous Materials*, 194, 15-23.

Chapter 7: Conclusions and future directions

7.1 Conclusions

This project concerns the global legacy of radioactively contaminated land in particular the remediation of mobile radionuclides associated with migrating subsurface contaminant plumes. Using the Sellafield nuclear facility, Cumbria, UK, as the study site, experiments were focused on the biogeochemical mechanisms controlling the environmental behaviour of key groundwater co-contaminants: strontium-90, technetium-99 and nitrate. Bioremediation has the potential for *in-situ* co-treatment of nitrate, *via* denitrification, ^{99}Tc, *via* reductive precipitation, and ^{90}Sr, *via* increased sorption/precipitation resulting from changes in sediment geochemistry during bioreduction. This project used a microbial community representative of the Sellafield site in sediment microcosms and model systems to assess the effects of 'bioremediation' on ^{99}Tc and Sr^{2+} under variable pH and nitrate concentrations.

Firstly this project investigated the effects of high nitrate (0.3-100 mM) on the development of metal reducing conditions at variable pH. At many nuclear legacy sites, including Sellafield, bioremediation strategies are complicated by the presence of elevated nitrate in combination with low pH conditions (pH 5.5) at which microbial metabolism is challenged. In sediment microcosms the onset of metal reduction was delayed until nitrate was depleted and this delay was greatest with high nitrate and low pH. Denitrification resulted in a rise in pH that increased with increasing nitrate. In low pH systems the reduction of 0.3 – 25 mM nitrate conditioned sediments for Fe(III) reduction by buffering pH towards circumneutral: the optimum pH for most metal reducing bacteria. Very high nitrate, 100 mM, in low pH systems caused bioreduction to stall. However, at neutral pH 100 mM nitrate was tolerated and denitrification resulted in a pH of > 9 followed by alkaline Fe(III) reduction. Fe(III) reduction above pH 9 is rare. Microbial community analysis provided insights into the novel

microbiology of high nitrate systems and identified alkali tolerant nitrate reducers as close relatives (99 %) of *Bacillus Niacini* and *Ochrobatrum grignonense.* Following Fe(III) reducing enrichment cultures alkaline Fe(III) reducing bacteria were identified: close relatives (99 %) of *Alkaliphilus crotonatoxidans* and *Serratia Liquifaciens*. The observation of alkaline Fe(III) reduction in these systems implies that extensive denitrification (up to 100 mM) in bioreducing sediments should not inhibit Fe(III) reduction following the depletion of nitrate providing enough electron donor is present.

The isolation of a novel alkaline Fe(III) reducing *Serratia* species provides an example of an organism that may dominate bioreducing environments in which the pH has been increased rapidly *via* denitrification. The isolated strain was found to be alkali tolerant and has a pH range for growth from pH 4 to 9 with an optimum of pH ~ 6.5.

Alkaline Fe(III) reduction suggested the possibility for co-treatment of ^{90}Sr and ^{99}Tc in these systems as Sr^{2+} becomes less mobile with increasing pH. In these systems denitrification provides a novel means to pH amendment. Stable Sr^{2+}, as an analogue for ^{90}Sr, was added to systems under variable nitrate concentrations at an initial pH of 5.5 and 7 to assess what effect the geochemical changes during sediment bioreduction have on the mobility of Sr^{2+}. Concentrations of Sr^{2+} were elevated compared to natural Sr^{2+} to allow X-ray absorption spectroscopy. Strontium mobility in sediments was found to be controlled primarily by pH dependent sorption to mineral surfaces and by groundwater supersaturation with regard to carbonate mineral phases. Where denitrification resulted in a rise in pH, enhanced Sr^{2+} sorption to sediments was observed. Above pH ~ 8.5, X-ray absorption spectroscopy confirmed that a significant proportion of Sr^{2+} was present in 9 fold coordinated carbonate mineral phase. Certainly, Sr^{2+} incorporation into more stable mineral phases is a desirable outcome for bioremediation scenarios. However, it is important to note that under low nitrate conditions the pH rise was negligible, no increased Sr^{2+} sorption occurred and a slight

increase in aqueous Sr^{2+} was observed in some microcosms following metal reduction. Nevertheless, results show that under constrained conditions denitrification can provide a mechanism for Sr^{2+} removal from solution.

In sediment systems it was difficult to isolate the effects of individual processes. Therefore, model systems were established to investigate the effects of neutral and alkaline Fe(III) reduction, and subsequent precipitation of biogenic Fe(II) bearing mineral phases on Sr^{2+} and ^{99}Tc mobility. Model Fe(III) reducing systems used a microbial consortium enriched from Sellafield sediment microcosms and amended with yeast extract as an electron donor. Fe(III) reduction resulted in the precipitation of Fe(II) bearing mineral phases, siderite and vivianite, at pH 7 and 9. Fe(II) bearing mineral phases removed ^{99}Tc from solution at both pH 7 and 9 and X-ray absorption spectroscopy confirmed reduction to Tc(IV). In contrast, Sr^{2+} remained in solution at pH 7 and precipitated as Sr-carbonate at pH > 8.5. Under these constrained conditions results imply that neutral Fe(III) reduction could result in the release of Sr^{2+} associated with bioavailable Fe(III) phases but demonstrate that alkaline Fe(III) reduction, at pH > 8.5, can stimulate Sr^{2+} precipitation.

These studies demonstrate that alkaline Fe(III) reduction has the potential for co-treatment of ^{90}Sr and ^{99}Tc in contaminated sediments and that denitrification can provide a mechanism for pH amendment. Nitrate has typically been considered a negative co-contaminant at nuclear sites, but here it has been shown as a potential stimulant for ^{90}Sr treatment. These findings improve the mechanistic understanding of radionuclide behaviour at contaminated sites and inform possible engineered bioremediation scenarios.

7.2 Future directions

Although significant mechanistic progress has been made in this study, one limitation of this work is the use of static microcosm systems. It would be interesting to determine if the rate of biogeochemical processes observed in microcosms are indeed representative of the natural environment. One improvement would be to use larger, column type experiments, to investigate the magnitude of geochemical changes such as the rise in pH during denitrification and the accumulation of nitrite in dynamic flow through systems at subsurface temperatures, ~ 10 degrees.

In these studies, groundwater Sr^{2+} was artificially elevated to allow mechanistic studies, including XAS analysis, to be conducted. To extend this work, environmentally relevant Sr^{2+} concentrations should be used to test the hypothesis that low concentration of Sr^{2+} will incorporate into Ca-carbonate and Fe-carbonate mineral phases where natural systems are undersaturated with regard to Sr-carbonate. This work may be achieved using radioactive ^{90}Sr or ^{85}Sr at trace levels in sediment and/or model systems.

To date work has focused largely on surface sediments which are rich in microbes. Although contamination is largely within the shallow subsurface, deeper sediments are contaminated where the plume has migrated vertically and these comprise clays and sandstones where porosity and biodiversity are reduced. In addition microbial processes are also relevant to a deep geology disposal scenario where microbes are expected to be present and anaerobic processes expected to dominate. Fe biogeochemistry will be important due to the presence of steel waste canisters and alkaline pH is expected due to the use of concrete in encapsulation and backfill.

Appendix 1: Methods

This section comprises a description of the analytical techniques used during this research project. In addition, Chapters 3, 4, 5 and 6 each contain a methods section detailing the techniques that are relevant to that particular paper.

A1. Geochemical analysis

Serum bottles used in microcosm experiments in chapters 3 and 5 and in model systems in chapters 2 and 6 were sampled anearobically *via* syringe flushed with argon gas. Before sampling each bottle was shaken to suspend the solids and an aliquot (1- 3 ml) of slurry was withdrawn. The slurry was then centrifuged (15,000 g: 5 minutes) to separate porewater from solids. The porewater was then removed by pipette for geochemical analysis (ie. to measure NO_2^-/NO_3^-/Fe(II)/Mn/Sr^{2+}/Ca^{2+}/^{99}Tc in solution). The remaining sediment pellet was then used to measure 0.5 N HCl extractable Fe(II) in sediments. Further sediment pellets were used for microbial community analysis and/or sediment characterisation by XRD and ESEM.

A1.1 UV-vis spectroscopic methods

During this project spectroscopic techniques were used to determine the concentration of NO_2^-, Fe^{2+} and Mn^{2+} in solution and the optical density (OD) of cells in solution. Using a spectrophotometer, monochromatic light of a selected wavelength (Table A1) was directed through a 'blank' cuvette, containing the relevant solution (buffers and chelating compound) but no sample. The absorption was calculated in order to correct for absorption by the background solution. Absorption was then measured for cuvettes containing relevant samples and solution. Chelating compounds were used to bind to the analyte ion of interest to create a coloured compound with a higher molar absorptivity that could be more easily detected by the spectrophotometer (Harris, 1948; Stookey, 1970; Goto et al., 1977; Harris and Mortimer, 2002). Table A1 lists the coloured compound created in each technique and the wavelength at which the absorbance of each compound was measured.

Compound	Chelating compound	Wavelength (nm)	Reference
Fe^{2+}	Ferrozine-Fe^{2+}	562	*Stookey, 1970*
Mn^{2+}	1-(2 Pyridylazo)- 2 Napthol (PAN) - Mn^{2+}	562	*Goto et al., 1977*
NO_2^-	Sulphanilamide - NO_2^-	536.5	*Harris and Mortimer, 2002*
Cell density	N/A	600	*Madigan and Martinko, 2006*

Table A1. Chelating compounds and wavelength of absorbance for UV- vis spectroscopic methods.

For each method a set of standards was created to calibrate the analysis, establish the linear response range (typically between an absorbance of 0.02 and 2.50) and determine what dilution (if any) must be applied to sample prior to analysis *via* spectrophotometry. Two spectrophotometers were used during this project, a Cecil CE 3021 spectrophotometer (Chapter 3) and a Jenway 6715 (Chapters 4, 5 and 6).

Determination of total Fe in solution

The ferrozine assay is a widely used and reliable method to detect and quantify Fe(II) in solution (Lovley and Phillips, 1987; Stookey, 1970). Throughout this project the detection of Fe(II) in porewater was used to track the progress of microbial Fe(III) reduction *via* the method described in Viollier et al. (2000). The ferrozine method relies on the ferrozine molecule, 3-(2-pyridyl)-5,6-bis(4-phenylsufonic acid)-1,2,4-triazine, forming a strong purple coloured complex with Fe(II) (Stookey, 1970). Interferences from Co(II) and Cu(I) which also form coloured compounds with ferrozine are possible but were not a problem in this project as Cu and Co concentrations in systems were several orders of magnitude below concentrations of Fe(II). Other metals can form non-coloured complexes with the ferrozine molecule however as ferrozine was added in excess these did not compete with Fe(II) (Stookey, 1970). Stookey (1970) did report that nitrite could react with ferrozine solution and therefore compete and interfere with results. In these experiments however, nitrite in these systems appeared only as a

transient species and was depleted prior to Fe(III) reduction such that it could not complete with Fe(II).

The method as set out by Viollier et al. (2000) assumes that all aqueous Fe will be present as Fe(II) at circumneutral pH and so hydroxylamine hydrochloride was added to reduce any Fe(III) to Fe(II) that had been oxidised during sample preparation (Table A2). The pH of the analytical solution must be between 4 and 9 in order for ferrozine to complex fully and therefore an ammonium acetate buffer was included to ensure that the pH was circumneutral (Table A2).

Method

Reagents were prepared as described in Table A2. In a 1 cm cuvette the following were added in order:

- 900 µl of deionised water
- 100 µl of porewater
-100 µl of ferrozine solution
- 100 µl hydroxlammonium hydrochloride in 2 mol l^{-1} hydrochloric acid
- 100 µl ammonium acetate buffer

Samples of porewater were left for 10 minutes to allow the reaction to take place before the absorbance was measured at 562 nm on a spectrophotometer. Where Fe(II) concentrations were high, further serial dilution with deionised water was needed prior to addition of 100 µl of sample to the cuvette.

Standards were created from quantitatively dissolving $FeSO_4.7H_2O$ in 0.001 N HCl and analysed periodically to ensure that the calibration values had not changed and that linear R^2 values of > 0.98 were plotted for calibration lines. Samples were analysed in triplicate and error was estimated by calculating the standard deviation (1σ).

Reagent	Preparation
Ferrozine solution	1.23g ferrozine and 1.975g ammonium acetate diluted in 250 ml of deionised water. Stored in the dark.
Hydroxylamonium hydrochloride	9.7g of $H_2NOH.HCl$ made up to 100 ml with 2 N HCl
Ammonium acetate pH 9 buffer	190g of ammonium acetate in 250 ml of deionised water adjusted to pH 9.5 with concentrated sodium hydroxide solution.

Table A2. Preparation of reagents for the ferrozine assay.

Determination of 0.5 N HCl extractable Fe(II) in sediments (as a percentage Fe(II)/Fe(III))

In previous experiments an ingrowth of Fe(II) minerals into sediments was evident before Fe(II) was detected in porewaters (Burke et al., 2006; Begg et al., 2007; Law et al., 2010). Furthermore, when pH values were > 8 very little Fe(II) was present in solution and Fe(III) reduction could not be inferred from studying Fe(II) in solution alone. For these reasons an acid digestion of sediment was used to estimate the proportion of bioavailable Fe present as Fe(II) in addition to taking porewater Fe(II) measurements. Digesting sediment samples in 0.5 N HCl for 1 hour using the method described by Lovley and Phillips (1986) is thought to give a good estimate of the Fe(III) available to microorganisms and has been used to track Fe(III) reduction in column and microcosm experiments (Weber et al., 2001; Fredrickson et al., 2004; Wildung et al., 2004; Burke et al., 2006; Wilkins et al., 2007; Begg et al., 2007; Law et al., 2010). Following a 1 hour 0.5 N HCL extraction, ferrozine assay was used to give the concentration of Fe(II) extracted and this was compared to the total extracted Fe, determined by ferrozine with hydroxylamonium hydrochloride, from which the percentage of 0.5 N HCl extractable Fe(II) was calculated. The measurement is reported as a percentage due to the difficulty in extracting a consistent amount of

sediment from each microcosm and the natural heterogeneity of minerals in sediment samples (Weber et al., 2001; Wilkins et al., 2007; Law et al., 2010).

Method

A sediment pellet (~ 0.3 g) was added to 5 ml 0.5 N HCl and agitated continuously for 1 hour. The solution was then filtered through a 0.22 µm syringe driven filter (Millipore, Millex - GP) and two sub-aliquots were pipetted into separate 4 ml cuvettes.

- The first cuvette was used to determine the Fe(II) concentration and contained 2900 µl deionised water and 300 µl ferrozine solution (Table A1).

- The second curvette was used to determine the total Fe in solution and contained 2000 µl deionised water, 300 µl ferrozine solution, 600µl hydroxylammonium hydrochloride solution and 300 µl ammonium acetate buffer (Table A2).

Both solutions were left for 10 minutes to allow reaction and then analysed at 562 nm on a Spectrophotometer. The percentage of Fe(II) in the 0.5 N HCL extracted sediment pellet was estimated by dividing the absorbance of the Fe(II) by the absorbance of the total Fe and multiplying by 100. Samples were analysed in triplicate and error was estimated by calculating the standard deviation (1σ).

Determination of Mn(II) in solution

Accurate analysis of Mn(II) in solution could only be performed while the pH of the sediment microcosm remained below 8 as Mn was no longer present in solution at alkaline pH. Where possible Mn^{2+} was detected and quantified using a colorimetric method adapted from Goto et al. (1977) with the reagents described in Table A3.

Reagent	Preparation
~0.6 M ascorbic acid	26.5g ascorbic acid dissolved in 250 ml of deionised water
Alkaline cyanide reagent	Manufactured by HACH
PAN indicator solution (1 %)	Manufactured by HACH (1-(2 Pyridylazo)- 2 Napthol)

Table A3. Preparations of reagents for Mn(II) assay.

Method

In a 1 ml cuvette the following were added in order:

- 750 µl of deionised water

- 250 µl of sample

- 50 µl of ascorbic acid

- 70 µl PAN indicator solution (1 %) (HACH, Camlab, UK)

- two drops of alkaline cyanide reagent (HACH, Camlab, UK)

The addition of alkaline cyanide and PAN indicator took place in a fume hood and then cuvettes were then sealed with parafilm. The solution was left for 10 minutes to allow colour to develop before analysing at 562 nm on a spectrophotometer. Standards were created *via* dilution from a certified stock solution (VWR International, UK) and analysed periodically throughout the experimental period. The R^2 value for each linear calibration was typically > 0.98. Samples were analysed in triplicate and error was estimated by calculating the standard deviation (1σ).

Determination of nitrite in solution

Nitrite in solution was determined *via* a colorimetric method adapted by Harris and Mortimer (2002) and used as an indication of nitrate reduction in sediments and water samples (Bendschneider and Robinson, 1952). NO_2^- forms a purple coloured complex

in the presence of napthylethylenediamine dihydrochloride (NED) and sulphanilamide (SAN). The reagents were prepared as described in Table A4.

Reagent	Preparation
Ammonium chloride buffer	Dissolve 1g of ammonium chloride in 90 ml of deionised water. Adjust to pH 8.5 with 30 % NH_3 before making up to 100 ml
SAN reagent	Dissolve 0.25g of sulphanilamide dissolved in 80 ml of deionised water with 2.5 ml concentrated HCl. Add 100 µl $C_{12}E_{23}$, Polyoxyethylene (23) lauryl ether (Brij solution) and make up to 100 ml.
NED reagent	Dilute 0.25g of napthylethylenediamine dihydrochloride in 100 ml of deionised water

Table A4. Preparation of reagents for nitrite assay.

Method

To a 1 ml cuvette, the following were added in order:

- 750 µl of deionised water and 100 µl ammonium chloride buffer

- 100 µl of sample

- 25 µl sulphanilamide (SAN) reagent and 25 µl napthylethylenediamine dihydrochloride solution (NED).

Colour was left to develop for 10 minutes before analysis at 536.5 nm on a spectrophotometer. Standards were created by dilution from a fresh sodium nitrite stock solution and analysed periodically throughout the experiment. The R^2 value for each linear calibration was typically 0.98 or better. Samples were analysed in triplicate and error was estimated by calculation of the standard deviation (1σ).

Quantative analysis by UV-vis spectroscopic methods is only as accurate as the calibration used to convert absorbance to concentration; care was taken preparing standards. Detection limits for the methods described above the lower and upper detection limits were ~ 5- 250 µM (0.02 - 12 ppm) for nitrite, ~ 10 - 700 µM for manganese (0.5 - 38 ppm) and ~ 10 - 1000 µM for Fe(II) (0.56 - 56 ppm). Typically, linear calibration was achieved with an absorbance between 0.01 to ~2.50 and where necessary, the upper limit of detection was extended by dilution.

A1.2 Ion Chromatography

Ion chromatography was used to determine dissolved inorganic carbon (DIC) ($CO_2/CO_3^{2-}/HCO_3^-$), acetate, SO_4^{2-} and NO_3^- in solution throughout microcosm experiments in chapters 3 and 5 (Jackson et al., 1990). Analysis was carried out by David Ashley on a Dionex ICS-90 (Chapter 3) and Alastair Bewsher on a Dionex DX120 and Metrohm 761 Compact IC (Chapters 4, 5 and 6). Follow sampling (as described in section A1) 100µl of each porewater sample was added to 9.9 ml of 2% nitric acid, filtered using 0.45 µm filters and stored in the fridge at (4 ^oC) prior to analysis. Detection limits for species analysed were ~0.001 mM (~ 0.1 ppm) with an accuracy of approximately 3 %. The specifics of these two columns used are described below in Table A5. Further details at:

www.seaes.manchester.ac.uk/research/facilities/agu/equipment/ionchromatography/

Specifications for analysis of sulphate and nitrate analysis	
Metrohm 761 Compact IC	**Ion exchange chromatography**
Guard Column	Dionex AG9-HC (High Capacity)
Analytical Column	Dionex AS9-HC
Injection Loop	100 µl
Mobile phase	9 mM Na_2CO_3
Flow rate	1.4 ml/min
Detector	Conductivity
Specifications for analysis of carbonate and acetate analysis	
Dionex DX120	**Ion exclusion chromatography**
Guard Column	Dionex ICE AS1 4x50 mm
Analytical Column	Dionex ICE AS1 4x50 mm
Injection Loop	50 µl
Mobile phase	1 mM Octane Sulphonic Acid
Flow rate	0.12 ml/min
Detector	Conductivity

Table A5. Specifics of ion chromatography equipment set up for relevant ions.

A1.3 Inductively coupled plasma- atomic emission spectroscopy (ICP-AES)

Inductively coupled plasma atomic emission spectroscopy (ICP-AES) was used to determine the concentration of Sr^{2+} and Ca^{2+} in solution in Chapters 5 and 6 (Boss and Fredeen, 1997). Samples of slurry were taken from microcosm systems and porewaters were separated from solids *via* centrifugation (15,000 g: 10 minutes). 100 µl of sample was then added to 10 ml 2% nitric acid, filtered through 0.45 µm filters and analysed by Paul Lythgoe at the University of Manchester on a Perkin-Elmer Optima 5300 dual view ICP- AES (details available on: http://www.seaes.manchester.ac.uk/research/facilities/agu/equipment/icp_aes/ICP_AES instrumentdetails/index.html). The lower limit of detection was 10-100 ppb using ICP-AES. High concentration of ions with similar wavelength emissions can produce interference but this was not a problem during Sr^{2+} and Ca^{2+} analysis.

A1.4 Flow injection analysis

NH_4^+ in porewaters in chapter 3 was determined with the help of David Ashley using rapid, small volume, flow injection analysis at the University of Leeds. Here a sample of porewater (50 µl) was collected *via* syringe and filtered through 0.45 µm filters prior to injection into a DIONEX flow injection analyser. The sample then passes into alkaline flowing reagent stream (10 mM NaOH) and through a gas exchange cell (with teflon gas exchange membrane) where the gas phase (ie NH_4^+) passed into a second but acidic reagent stream (30 mM HCl) and on to a conductivity detector (Hall and Aller, 1992).

A1.5 Liquid scintillation counting

Liquid scintillation counting (LSC) was used in this project to detect the activity of β-particle emitting radionuclide ^{99}Tc in solution on a Packard Tri-carb 2100 TR liquid scintillation counter. A 500 µl volume of sample was added to 10 ml liquid scintillation cocktail before counting for 100 minutes per sample and recording the results as counts per minute in the energy range 0 – 2000 eV. Counts per minute were then divided by 60 to give 'activity' in Becquerel's (counts per second) and scaled up/down depending on the volume of sample added to achieve a value in Bq ml^{-1}. The measurements were calibrated by comparison with a standard vile of known activity. The background radiation in the laboratory is 27.60 counts per minute (average of 20 blanks) and so accurate detection of sample counts was not possible below these levels. Interference from other radioactive species is possible although natural radiation in samples is expected to be orders of magnitude lower than the 100 Bq ml^{-1} ^{99}Tc added to samples.

A1.6 Sequential extractions

Sequential extractions were used in chapters 3 and 6 on sediments and mineral precipitates to estimate the proportion of Fe associated with different extraction lixivants and Sr^{2+} associated with those Fe fractions. Whilst this operationally defined technique can not identify associations with specific mineral phases it can provide generic (and typically reproducible) information about the proportions of metal ions (e.g. Fe or Sr) bound in various broad 'fractions' i.e. sorbed, associated with carbonates, associated reducible oxides, associated with poorly reducible oxides (Tessier et al., 1979; Poulton and Canfield, 2005). Various published Fe mineral extraction methods exist and each focus on separating out a range of fractions *via* the addition of

progressively stronger lixivants and the methods that were applied in this study were adapted from Tessier et al., (1979), Keith-Roach et al., (2003) and Poulton and Canfield, (2005) (Tables A6 and A7). Here 0.2 g of wet sediment or mineral precipitate was added to 10 ml of the first extraction solution, sparged with N_2, and agitated for the required amount of time (Table A6 and A7). The concentration of Fe in solution was then measured using the ferrozine method (section A1.1) and from this the molarity of Fe in 10 ml was calculated and therefore the mass of Fe removed determined. The remaining solids were then washed three times in degassed, deionised water before addition of 10 ml of the next extraction solution.

Fraction	Extraction	pH	Time
Carbonate associated	1 M sodium acetate	4.5	24 hours
Easily reducible oxides	1 M hydroxylamine HCl in 25 % v/v acetic acid		48 hours
Reducible oxides	50 gL^{-1} sodium dithionite	4.8	2 hours
Magnetite	0.2 M ammonium oxalate	3.2	6 hours
Residual Fe	XRF	N/A	N/A

Table A6. Details of Fe extraction series 1 (Poulton and Canfield, 2005; Chapter 3).

Fraction	Extraction	pH	Time
Sorbed	$MgCl_2$	7	
Carbonate associated	1 M sodium acetate	4.5	24 hours
All reducible oxides	50 gL^{-1} sodium dithionite	4.8	2 hours

Table A7. Details of Fe extraction series 2 (Tessier et al., 1979; Keith-Roach et al., 2003;Chapter 6)

Sequential extraction techniques must be used with caution as the reagents used are not mineral specific and there is often reported an overlap (> 5%) between fractions (Tessier et al., 1979). In addition some minerals (for example vivianite) are removed across several fraction: for example vivianite will start to dissolve in an 1M Na-acetate extraction designed to remove ‘carbonate associated Fe’ but will not be completely removed until the hydroxylamine HCl extraction designed to remove ‘easily reducible’ oxic Fe (Dodd et al., 2000).

A1.7. Soil and porewater Eh and pH

Porewater pH was measured in chapter 3 with an Orion 420A pH meter and in chapters 4, 5 and 6 with a Denver Instruments UB10 pH meter and pH probes calibrated to pH 4, 7 and 10 before use. The pH was allowed to stabilise for approximately 30 seconds before measurements were read. Soil pH was determined by mixing fresh sediment with 40 ml of deionised water and measuring the pH after 1 hour (Thomas, 1996). Porewater Eh was measured in chapter 3 on an Orion 420A with a probe tested in a standard redox solution (200 mV at 25^{o}C, Jenway) prior to taking measurements. For each sample the Eh was left to stabilise for 60 seconds before the Eh measurement was recorded.

A2. Mineralogical characterisation

A2.1. X-ray diffraction (XRD)

X-ray diffraction (XRD) was used to identify the crystallographic structure of sediments and the mineral products of microbial reduction. Sediments were first dried and crushed to a fine powder. Reduced minerals were kept in a sealed anaerobic container prior to analysis and aqueous mineral samples were analysed as wet samples to prevent changes to the mineralogy through drying out. XRD analysis was performed on a Philips PW 1050 (chapter 3) or a Bruker D8Advance (chapters 4, 5 and 6) with the help of John Waters. Further information is available at: http://www.seaes.manchester.ac.uk/research/facilities/agu/equipment/xrd/.

Minerals were identified with the help of technician John Waters *via* comparison to a known database of standards. X-ray diffraction can only be used to identify minerals with an ordered crystal structure that are present in significant concentrations. Those

that are amorphous or semi-amorphous can be hard to detect. Similarly minerals that are present at < 5% in mixed samples may not be detected above the background noise (Dutrow and Clark, 2012).

A2.2. X-ray fluorescence (XRF)

X-ray fluorescence is a non destructive technique used to determine elemental concentrations in both solid and liquid samples (Jenkins, 1988; Beckhoff et al., 2006). In this project x-ray fluorescence (XRF) was used to determine the elemental composition of sediments prior to use in microcosm experiments (chapters 3 and 5). From freshly collected sediment 15 grams of soil was dried at 110 ^{o}C, ground to ~50 µm. At this point, 12g of ground soil was then mixed with 3g of binding wax in an agate mixing pot and a 40 mm diameter pellet was pressed at 10 tons. Samples were analysed on a Thermo ARL 9400 (chapter 3) or an Axios sequential x-ray fluorescence spectrometer (chapters 4, 5 and 6) with the help of Paul Lythgoe. Results were obtained for major and trace elements in weight percent. Further information available at:
http://www.seaes.manchester.ac.uk/research/facilities/agu/equipment/xrfinstrument/.
Two programs were run to determine both major and trace elemental composition.

A2.3. Environmental Scanning Electron Microscopy (ESEM)

Images in chapters 5 and 6 were taken using an environmental scanning electron microscope (ESEM) available in the William Research Centre. With help from John Fellowes the Phillips XL30 ESEM-FEG was used in ‘wet’ mode to allow the imaging

of uncoated samples and biological material that was undoubtedly present in our samples. The ESEM was equipped with an EDAX Gemini EDS system for elemental mapping and imaging and two different detection modes of electron detection were used: secondary electron detection and backscatter electron detection. In secondary electron detection mode the detector measured low energy electrons ejected from surface atoms to give a topographic image where peaks appeared bright and troughs dull as more or less electrons were able to exit the sample. In the backscatter electron detection mode main beam electrons were detected that were reflected back due to interactions with the nuclei of atoms in the sample. Elements with a higher atomic number backscatter more electrons than those with a lower atomic number and so appear brighter in the image (Figure A1a, A1b and A1c). In this project backscatter detection mode was used to identify Sr^{2+} rich areas in a sediment sample (Figure A1a, A1b and A1c; chapter 5) before EDAX and secondary electron detection was used to image and identify the elemental composition of the Sr rich area(s) (Figure A1d and A1e; chapters 5 and 6).

Samples were prepared simply by extracting ~0.2 g of sediment and placing this on a sample holder to dry. The sample holder was then placed directly in the ESEM machine. The beam energy was increased to allow EDAX detection of different elements on the sample surface and for Sr^{2+} the electron beam energy was increased to 30 keV and both directed at a specific spot on the sample (spot analysis) and scanned across the sample to produce and element map.

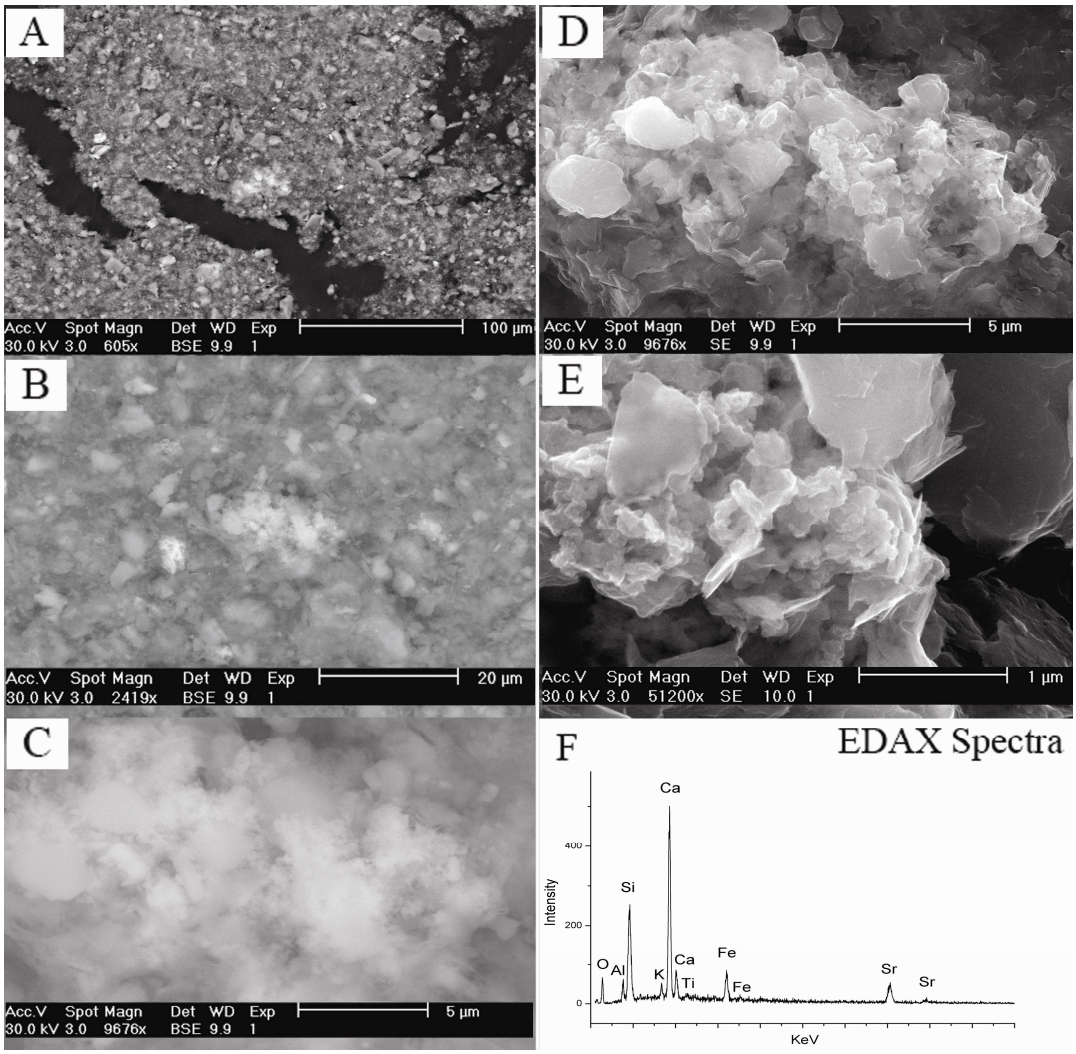

Figure A1. Images obtained using the Phillips XL30 environmental scanning electron microscope showing imaging of sediment in backscatter electron detection mode at magnification A) x 605, B) x 2419 and C) x 9676, secondary electron images at magnification D) x 9676 and E) x 51200 and F) an EDAX scan of the centre of image E.

A3. Geochemical modelling

Geochemical modelling of the end point of a number of aqueous systems was achieved using PHREEQC-2 using the Laurence Livermore National Laboratory (LLNL) database with the following input parameters:

Inputs for bicarbonate unamended systems				
	0.3 mM Na nitrate + 10 mM Na acetate	**10 mM Na nitrate + 10 mM Na acetate**	**25 mM Na nitrate + 20 mM Na acetate**	**100 mM Na nitrate + 70 mM Na acetate**
pH	6.5	7.5	7.8	6.5
Temp	21.0 ^{0}C	21.0 ^{0}C	21.0 ^{0}C	21.0 ^{0}C
Pe	-0.1667	-0.1667	-0.1667	-0.1667
Sr	1.14 x10^{-3} M	1.14 x10^{-3} M	1.14 x10^{-3} M	1.14 x10^{-3} M
Mg	0.794 x10^{-3} M	0.794 x10^{-3} M	0.794 x10^{-3} M	0.794 x10^{-3} M
K	0.0885 x10^{-3} M	0.0885 x10^{-3} M	0.0885 x10^{-3} M	0.0885 x10^{-3} M
Cl	1.05 x10^{-3} M	1.05 x10^{-3} M	1.05 x10^{-3} M	1.05 x10^{-3} M
Si	0.342 x10^{-3} M	0.342 x10^{-3} M	0.342 x10^{-3} M	0.342 x10^{-3} M
Na	11.1 x10^{-3} M	20.5 x10^{-3} M	45.5 x10^{-3} M	170 x10^{-3} M
C(+4)	2.57 x10^{-3} M	21.7 x10^{-3} M	41.6 x10^{-3} M	144 x10^{-3} M
S(+6)	0.395 x10^{-3} M	0.395 x10^{-3} M	0.395 x10^{-3} M	0.395 x10^{-3} M
Ca	1.67 x10^{-3} M	1.67 x10^{-3} M	1.67 x10^{-3} M	1.67 x10^{-3} M
Fe (2+)	2.50 x10^{-3} M	2.50 x10^{-3} M	2.50 x10^{-3} M	2.50 x10^{-3} M
N(+5)	0.0 x10^{-3} M	0.0 x10^{-3} M	0.0 x10^{-3} M	0.0 x10^{-3} M

Table A8: Parameters for geochemical modelling of unbuffered solutions.

Inputs for bicarbonate amended systems				
	0.3 mM Na nitrate + 10 mM Na acetate	**10 mM Na nitrate + 10 mM Na acetate**	**25 mM Na nitrate + 20 mM Na acetate**	**100 mM Na nitrate + 70 mM Na acetate**
pH	6.5	7.5	7.8	6.5
Temp	21.0 ^{0}C	21.0 ^{0}C	21.0 ^{0}C	21.0 ^{0}C
Pe	-0.1667	-0.1667	-0.1667	-0.1667
Sr	1.14 x10^{-3} M	1.14 x10^{-3} M	1.14 x10^{-3} M	1.14 x10^{-3} M
Mg	0.794 x10^{-3} M	0.794 x10^{-3} M	0.794 x10^{-3} M	0.794 x10^{-3} M
K	0.0885 x10^{-3} M	0.0885 x10^{-3} M	0.0885 x10^{-3} M	0.0885 x10^{-3} M
Cl	1.05 x10^{-3} M	1.05 x10^{-3} M	1.05 x10^{-3} M	1.05 x10^{-3} M
Si	0.342 x10^{-3} M	0.342 x10^{-3} M	0.342 x10^{-3} M	0.342 x10^{-3} M
Na	13.6 x10^{-3} M	23.3 x10^{-3} M	48.3 x10^{-3} M	173.5 x10^{-3} M
C(+4)	13.6 x10^{-3} M	24.5 x10^{-3} M	44.5 x10^{-3} M	144.5 x10^{-3} M
S(+6)	0.395 x10^{-3} M	0.395 x10^{-3} M	0.395 x10^{-3} M	0.395 x10^{-3} M
Ca	1.67 x10^{-3} M	1.67 x10^{-3} M	1.67 x10^{-3} M	1.67 x10^{-3} M
Fe (2+)	2.50 x10^{-3} M	2.50 x10^{-3} M	2.50 x10^{-3} M	2.50 x10^{-3} M
N(+5)	0.0 x10^{-3} M	0.0 x10^{-3} M	0.0 x10^{-3} M	0.0 x10^{-3} M

Table A9: Parameters for geochemical modelling of bicarbonate amended solutions.

Sr^{2+} was included in the model at varying concentrations to assess the saturation index of $SrCO_3$ under the geochemical conditions described above. Geochemical modelling was used to indicate supersaturation with regard to predicted mineral precipitates in microcosm experiments and to support interpretation of experimental data.

A4. XAS techniques

X-ray absorption spectroscopy is a non-destructive technique that can be used to determine the oxidation state, inter-atomic distances and nearest neighbouring atoms of an element ((Koningsburger and Prins, 1988). XAS was used in this project to determine the speciation of Sr^{2+} in sediment samples at beamline BM26A at the European Synchrotron Radiation Facility (ESRF), France and to determine the speciation of ^{99}Tc on Fe(II) bearing mineral phases at B18 at the DIAMOND synchrotron, UK.

Strontium XAS data collection

Samples prepared for XAS analysis were aerobic and anaerobic sediments (chapter 5) containing between 200 and 1000 ppm Sr^{2+} on solids. In the case of anaerobic samples the sample was packed into the sample holder under an argon atmosphere and sealed and frozen for transport. Standards were prepared: $SrCl_2$ to represent free Sr^{2+}, $SrCO_3$ powder, natural ground calcite and natural ground aragonite. At the synchrotron samples were transferred from the freezer to the sample chamber and cooled to - 80 K with a liquid nitrogen cryostat (see Nikitenko et al., 2008) during data collection. Sr K-edge spectra (16115.26 keV) were collected in fluorescence mode using a 9 element solid state Ge detector. Between 4 and 8 scans were taken to reduce the signal to noise ratio and result in a cleaner spectrum and 1000 ppm Sr^{2+} on solid sediment samples produced good quality data with 3 or 4 scans.

Technetium XAS data collection

Samples were prepared by sorbing ^{99}Tc to pre-reduced Fe(II) bearing mineral phases, leaving for ~ 2 weeks and then transferring the solid phase anearbically to the sample

chamber and freezing. Samples were then transported to the beam line and ~ 40 scans were taken at ambient temperature. For samples analysed in Chapter 6, Tc K-edge spectra (21047.3 keV) were collected in fluorescence mode using a 9 element solid state Ge detector.

Data analysis

Multiple scans μ(E) were combined and averaged in Athena version 0.8.061 (Ravel and Newville, 2005) and normalised XANES data plotted. Linear combination fitting is sometimes possible between pure end members where a mixed spectrum was suspected however was not applicable in this case. Background subtraction for EXAFS analysis was performed using PySpline v1.1 (Tenderholt et al., 2007). EXAFS data were fitted using DLexcurv v1.0 (Tomic et al., 2005) using full curve wave theory (Gurman et al., 1984) by defining a theoretical model which was informed by the relevant literature (e.g. O'Day et al., 2000; Finch et al., 2003) and comparing the model to the experimental data. Shells of backscatterers were added around the central absorber atom and by refining an energy correction Ef (the Fermi Energy; which for final fits typically varied between -3.8 and -2.6), the absorber-scatterer distance, and the Debye-Waller factor for each shell. Model iterations were performed until a least squares residual was minimised. Shells were only included in the model fit if the overall least square residual (the R-factor; Binsted et al., 1992) was improved by > 5 %.

Identification of Sr^{2+} species was challenged by the existence of Sr^{2+} in more than one speciation, sorbed and mineral bound Sr^{2+}. The raw data obtained from a synchrotron gives an average spectrum and where two species are present together it is necessary to extrapolated to estimate how much of each is present. This is possible using the program excurv but is always an approximation. Where a species is present at very low

concentrations it can be masked by the spectrum from the dominant phases. For this reason XAS can only give information about the state and speciation of the majority of an element in a sample. For ^{99}Tc the XANES spectrum changes distinctly when Tc(VII) is reduced to Tc(IV) whereas with Sr^{2+} there are no changes in valance state and XANES was used only to determine the co-ordination of Sr^{2+} in combination with EXAFS modelling.

A5. Microbial analysis

A5.1 Microbial community analysis by 16S gene sequencing

Amplification of 16S rRNA gene sequences

DNA was extracted from samples using a PowerSoil DNA Isolation Kit (MO BIO, USA). Copies of the 16S rRNA gene (approximately 1490 b.p. fragment) was amplified from samples using the broad-specificity primers 8F (Eden et al. 1991) and 1492R (Lane et al. 1985). PCR reactions were performed in thin-walled tubes using a BioRad iCycler (BioRad, UK). The PCR amplification protocol used with the 8F and 1492R primers was: initial denaturation at 94 ºC for 4 minutes, melting at 94 ºC for 30 seconds, annealing at 57 ºC for 30 seconds, elongation at 72 ºC for 1 minute; 35 cycles, followed by a final extension step at 72 ºC for 10 minutes. The purity of the amplified products was determined by electrophoresis in a tris-borate-EDTA (TBE) gel. DNA was stained with ethidium bromide and viewed under short-wave UV light using a BioRad Geldoc 2000 system (BioRad, UK).

Cloning

PCR products were purified using a QIAquick PCR purification kit (Qiagen, UK) and ligated directly into a cloning vector containing topoisomerase I-charged vector arms

(Agilent Technologies, UK) prior to transformation into *E. coli* competent cells expressing Cre recombinase (Agilent Technologies, UK). White transformants that grew on LB agar containing ampicillin and X-Gal were screened for an insert using PCR. Primers were complementary to the flanking regions of the PCR insertion site of the cloning vector. The PCR method was: an initial denaturation at 94 ºC for 4 minutes, melting at 94 ºC for 30 seconds, annealing at 55 ºC for 30 seconds, extension at 72 ºC for 1 minute; 35 cycles, followed by a final extension step at 72 ºC for 5 minutes. The resulting PCR products were purified using an ExoSap protocol, and 2 µl of ExoSap mix (0.058 µl Exonuclease I, 0.5 µl Shrimp Alkaline Phosphatase, and 1.442 µl QH_2O) was added to 5 µl of PCR product and incubated at 37 ºC for 30 minutes followed by 80 ºC for 15 minutes.

DNA sequencing and phylogenetic analysis

Nucleotide sequences were determined by the dideoxynucleotide method. An ABI Prism BigDye Terminator Cycle Sequencing Kit was used in combination with an ABI Prism 877 Integrated Thermal Cycler and ABI Prism 377 DNA Sequencer (Perkin Elmer Applied Biosystems, UK). Sequences (typically 900 base pairs in length) were analysed against the NCBI (USA) database using the BLAST program packages and matched to known 16S rRNA gene sequences.

A5.2 Isolation and identification of a pure species

Isolation of a single colony

The species was grown in liquid agar media with the recipe provided in Table 10. A loop was dipped into the liquid agar culture during log phase growth and streaked onto an agar plate in the pattern shown (Figure A2) in order to isolate a single microbial

colony. A single colony was then lifted from this plate and streaked out for growth on a second agar plate. The species was confirmed as pure using gram staining, microscopy and 16S gene analysis. The isolated species were frozen at -80 ^{o}C in 50 % glycerol and lodged in the national culture library.

Ingredient	**Plates**	**Liquid**
Bacto Tryptone	10.0g	10.0g
Yeast extract	5.0g	5.0g
NaCl	10.0g	10.0g
Bacto Agar	15.0g	NONE
Deionized water to total volume	1000 ml	1000 ml

Table A10: recipe for Luria-bertani Media.

Figure A2. Streaking of enrichment media containing *Serratia Liquifaciens* to isolate a single colony.

A5.3 Microcosm work

Microcosms are a useful tool for simplifying dynamic anaerobic sediment systems and maintaining controlled conditions in which to study bioreduction mechanisms and changing microbial communities. There are limitations to microcosm techniques that must be taken into account when considering the results of microcosm experiments. Firstly the porewater to sediment ratio 10:1 is skewed in order to aid sampling and the

lack of flow allows for the accumulation of species in solution that may in the field be diluted or transported away. For example, where the mechanism of pH increase described in Chapter 3 was identified as denitrification the magnitude of pH increase observed in sediment microcosms may not represent what might be observed in a dynamic flowing system. Similarly, in a natural system groundwater flow can cause recharge from further upstream and the existence of moving reduction fronts. To better understand how processes observed in microcosm systems may reflect field situation flow through column may be used. Column experiments would allow for a more representative sediment to porewater ratio and groundwater recharge.

A6 References

Begg, J.D.C., Burke, I.T., Morris, K. (2007). The behaviour of technetium during microbial reduction in amended soils from Dounreay, UK. *Science of the Total Environment*, 373, 297-304.

Bendschneider, K., Robinson, R.J., (1952). A new spectrophotometric method for the de- termination of nitrite in sea water. *Journal of Marine Research,* 11, 87-96.

Binsted, N., Strange, R.W., Hasnain, S.S. (1992). Constrained and restrained refinement in EXAFS data analysis with curved wave theory. *Biochemistry*, 31, 12117–12125.

Boss, C.B., Fredeen, K.J. (1997). Concepts, Instrumentation and Techniques in Inductively Coupled Plasma Optical Emissions Spectroscopy. Second Edition. Perkin-Elmer.

Burke, I.T., Boothman, C., Lloyd, J.R., Livens, F.R., Charnock, J.M., McBeth, J.M., Mortimer, R.J.G., Morris, K. (2006). Reoxidation behavior of technetium, iron, and sulfur in estuarine sediments. *Environmental Science & Technology*, 40, 3529-3535.

Burke, I.T., Boothman, C., Lloyd, J.R., Mortimer, R.J.G., Livens, F.R., Morris, K. (2005). Effects of progressive anoxia on the solubility of technetium in sediments. *Environmental Science & Technology*, 39, 4109-4116.

Cullity, B.D. (1956). Elements of x-ray diffraction. Addison-wesley publication company Inc, Massachusetts, USA.

Dodd, J., Large, D.J., Fortey, N.J., Milodowski, A.E., Kemp, S. (2000). A petrographic investigation of two sequential extraction techniques applied to anaerobic canal bed mud. *Environmental Geochemical Health*, 22, 281-296.

Dutrow, B.L., Clark, C.M., (2012). Geochemical Instrumentation and Analysis. Available at: http://serc.carleton.edu/research_education/geochemsheets/techniques/XRD.html. Last accessed: March 22nd 2012.

Finch, A.A., Allison, N., Sutton, S.R., Newville, M. (2003). Strontium in coral aragonite: 1. Characterization of Sr coordination by extended absorption X-ray fine structure. *Geochimica El Cosmochimic Acta*, 67, 1189-1194.

Fredrickson, J.K., Zachara, J.M., Balkwill, D.L., Kennedy, D., Li, S.M.W., Kostandarithes, H.M. (2004). Geomicrobiology of high-level nuclear waste-contaminated vadose sediments at the Hanford Site, Washington State. Applied and Environmental Microbiology, 70, 4230-4241.

Goto, K., Taguchi, S., Fukue, Y., Ohta, K., Watanabe, H. (1977). Spectrophotometric determination of manganese with 1-(2-pyridylazo)-2-naphthol and a non-ionic surfactant. *Talanta*, 24, 752-753.

Gurman, S.J., Binsted, N., Ross, I. (1984). A rapid, exact curved-wave theory for EXAFS calculations. *Journal of Physics C: Solid State Physics*, 17, 143–151.

Hall, P.O., Aller, R.C. (1992). Rapid, Small-Volume, Flow-Injection Analysis for Sigma-Co2 and Nh4+ in Marine and Fresh-Waters. *Limnology and Oceanography*, 37, 1113-1119.

Harris, D.C. (1948). Quantitative chemical analysis- 3rd Edition. W.H. Freeman and Company, USA.

Harris, S.J., Mortimer, R.J.G. (2002). Determination of nitrate in small water samples (100 mu L) by the cadmium-copper reduction method: A manual technique with application to the interstitial waters of marine sediments. *International Journal of Environmental Analytical Chemistry*, 82, 369-376.

Jackson, P., Haddad, P.R. (1990). Ion chromatography: principles and applications. Amsterdam: Elsevier.

Jenkins, R. (1988). X-ray fluorescence spectrometry. John Wiley and Sons: New York.

Keith-Roach, M.J., Morris, K., Dahlgaard, H. (2003). An investigation into technetium binding in sediments. *Marine Chemistry*, 81, 149-162.

Koningsberger, D., Prins, R. (1988). X-Ray Absorption - principles, applications, techniques of EXAFS, SEXAFS and XANES. Toronto, John Wiley and Sons.

Law, G.T.W., Geissler, A., Boothman, C., Burke, I.T., Livens, F.R., Lloyd, J.R., Morris, K. (2010). Role of Nitrate in Conditioning Aquifer Sediments for Technetium Bioreduction. *Environmental Science & Technology*, 44, 150-155.

Nikitenko, S., A.M. Beale, Van der Eerden, A.M.J., Jacques, S.D.M, Leynaud, O., O'Brien, M.G., Detollenaere, D., Kaptein, R. Weckhysen, B.M., (2008). Implementation of a combined SAXS/WAXS/QEXAFS set-up for time-resolved in situ experiments. *Journal of Synchrotron Radiation*, 15, 632-640.

O'Day, P.A., Newville, M., Neuhoff, P.S., Sahai, N., Carroll, S.A., (2000). X-ray absorption spectroscopy of strontium(II) coordination - I. Static and thermal disorder in crystalline, hydrated, and precipitated solids and in aqueous solution. *Journal of Colloid Interface Science*, 222, 184-197.

Poulton, S.W., Canfield, D.E. (2005). Development of a sequential extraction procedure for iron: implications for iron partitioning in continentally derived particulates. *Chemical Geology*, 214, 209-221.

Ravel, B., Newville, M. (2005). Athena, Artemis, Hephaestus: data analysis for X-ray absorption spectroscopy using IFEFFIT. *Journal of Synchrotron Radiation*, 12, 537-541.

Tenderholt, A., Hedman, B., Hodgson, K.O. (2007). PySpline: A modern, cross-platform program for the processing of raw averaged XAS edge and EXAFS data. In X-Ray Absorption Fine Structure-XAFS13, pp. 105-107.

Tessier, A., Campbell, P.G.C., Bisson, M. (1979). Sequential extraction procedure for the speciation of particulate trace-metals. *Analytical Chemistry*, 51, 844-851.

Thomas, GW. (1996). Soil pH and acidity. In: Sperks (ed) Methods of soil analysis, part 3 – Chemical methods. Soil Science Society of America. Madison, WI.

Tomic, S., Searle, B.G., Wander, A., Harrison, N.M., Dent, A.J., Mosselmans, J.F, Inglesfield, J.E. (2005). New tools for the analysis of EXAFS: the DL_EXCURV package, CCLRC technical report DL-TR-2005-00, ISSN 1362-0207, Daresbury SRS 2005.

Weber, K.A., Picardal, F.W., Roden, E.E. (2001). Microbially catalyzed nitrate dependent oxidation of biogenic solid-phase Fe(II) compounds. *Environmental Science & Technology*, 35, 1644-1650.

Wildung, R.E., Li, S.W., Murray, C.J., Krupka, K.M., Xie, Y., Hess, N.J., Roden, E.E. (2004). Technetium reduction in sediments of a shallow aquifer exhibiting dissimilatory iron reduction potential. *Fems Microbiology Ecology*, 49, 151-162.

Wilkins, M.J., Livens, F.R., Vaughan, D.J., Beadle, I., Lloyd, J.R. (2007). The influence of microbial redox cycling on radionuclide mobility in the subsurface at a low-level radioactive waste storage site. *Geobiology*, 5, 293-301.

Parsons, T.R., Maita, Y., Lalli, C.M., (1984). A manual of chemical and biological methods for seawater analysis. Pergamon press Ltd, Oxford.

Appendix 2: Conference presentations and awards

Prizes and Awards

Best Oral Communication of Research.
DIAMOND Consortium Annual Conference 2011, Coventry, UK. *14th-15th December 2011.*

Best poster presentation.
Environmental Mineralogy Group meeting 2010, BGS Nottingham, UK. *19th April 2010*

Best Poster Presentation.
DIAMOND Consortium Annual Conference 2009, York, UK. *9th-10th September 2009*

Oral Presentations

2011

DIAMOND conference 2011, Coventry, UK. *14th-15th December*
Thorpe, CL; Law, GTW; Lloyd, JR; Burke, IT; Shaw, S; Morris, K. 'Behaviour of ^{90}Sr in nitrate impacted sediments.'

Goldschmidt 2011, Prague, Czech Republic. *14th – 19th August*
Thorpe, CL; Law, GTW; Lloyd, JR; Burke, IT; Shaw, S; Morris, K. 'Behaviour of ^{90}Sr in nitrate impacted sediments.'

DIAMOND work package-2 meeting, Loughborough University, UK. *6th April*
Thorpe, CL; Law, GTW; Lloyd, JR; Burke, IT; Shaw, S; Morris, K. Behaviour of ^{90}Sr and ^{99}Tc in nitrate impacted sediments.

2010

DIAMOND conference 2010, Manchester, UK. *15th-16th December*
Thorpe, CL; Law, GTW; Lloyd, JR; Burke, IT; Morris, K. Remediation of ^{90}Sr and ^{99}Tc at UK nuclear legacy sites.

Nuclear waste management conference, Cambridge, UK. *28th-29th September*
Thorpe, CL; Law, GTW; Lloyd, JR; Burke, IT; Morris, K. Remediation of ^{90}Sr and ^{99}Tc at UK nuclear legacy sites.

ERA11: 11th Meeting, Chester, UK. *15th- 17th September*
Thorpe, CL; Law, GTW; Lloyd, JR; Burke, IT; Morris, K. Remediation of ^{90}Sr and ^{99}Tc at UK nuclear legacy sites.

RSC Radiochemistry group: Young Researchers Meeting, London, UK. *14th April*

Thorpe, CL; Law, GTW; Lloyd, JR; Burke, IT; Morris, K. Remediation scenarios for UK nuclear legacy sites.

COGER conference, Liverpool, UK. *29th March*
Thorpe, CL; Law, GTW; Lloyd, JR; Burke, IT; Morris, K. Remediation scenarios for UK nuclear legacy sites

DIAMOND work package- 2 meeting, London, UK. *29th March*
Thorpe, CL; Law, GTW; Lloyd, JR; Burke, IT; Morris, K. Remediation scenarios for UK nuclear legacy sites.

2009

DIAMOND conference, York, UK. *9th-10th September*
Thorpe, CL; Law, GTW; Lloyd, JR; Burke, IT; Morris, K. Remediation scenarios for UK nuclear legacy sites.

COGER conference, Liverpool, UK. *6th- 8th April*
Thorpe, CL; Law, GTW; Lloyd, JR; Burke, IT; Morris, K. Remediation scenarios for UK nuclear legacy sites.

Poster presentations

Opening for the Research Centre for Radwaste and Decommissioning. *8th October 2011.*
Thorpe, CL; Law, GTW; Lloyd, JR; Burke, IT; Shaw, S; Morris, K. The behaviour of Sr^{2+} during bioreduction in nitrate impacted sediments.

DIAMOND conference 2011, Coventry, UK. *14th-15th December 2011.*
Thorpe, CL; Law, GTW; Lloyd, JR; Burke, IT; Shaw, S; Morris, K. 'Behaviour of ^{90}Sr in nitrate impacted sediments.'

Environmental Mineralogy Group Meeting, BGS Nottingham, UK. *19th April 2010*
Thorpe, CL; Law, GTW; Lloyd, JR; Burke, IT; Morris, K. Remediation of ^{90}Sr and ^{99}Tc at UK nuclear legacy sites.

DIAMOND conference 2010, Manchester, UK. *15th-16th December 2010*
Thorpe, CL; Law, GTW; Lloyd, JR; Burke, IT; Morris, K. Remediation of ^{90}Sr and ^{99}Tc at UK nuclear legacy sites.

DIAMOND conference, York, UK. *9th-10th September 2009*
Thorpe, CL; Law, GTW; Lloyd, JR; Burke, IT; Morris, K. Remediation scenarios for UK nuclear legacy sites.